An investigation of inflammatory responses and wound healing in heat shock protein B1-deficient mice.

Jonathan Crowe

A thesis submitted for the degree of Doctor of Philosophy to

Imperial College London Department of Medicine

June 2013

The Kennedy Institute of Rheumatology

Imperial College London

Abstract

The function of heat shock protein (hspB1) *in vivo* is still poorly understood, despite a large literature describing *in vitro* functions of the protein. This research has focussed on the role of hspB1 *in vivo*, an opportunity created by the commercial generation of hspB1-deficient mice (*hspB1*$^{del/del}$). Initial experiments demonstrated an increase in cytokine production in *hspB1*$^{del/del}$ murine embryonic fibroblasts. Two well established and characterised *in vivo* models of acute inflammation, the air-pouch model and the peritonitis model, were used to investigate the role of hspB1. Increased cellular infiltration and an increase in chemokine expression in response to inflammatory challenge was observed in *hspB1*$^{del/del}$ mice relative to wild-type mice. It was found that the majority of the cellular infiltrate consisted of neutrophils, and these cells had reduced viability in *hspB1*$^{del/del}$ compared to wild-type mice, despite the discovery that neither hspB1 protein nor mRNA could be detected in murine neutrophils. The work of Anna Aubareda, a post-doc in the laboratory, showed that hspB1 deficiency results in impaired cell proliferation. The observation of a phenotype of increased inflammation and decreased proliferation in *hspB1*$^{del/del}$ mice and cells led to an investigation into the role of hspB1 in wound-healing. It was discovered that *hspB1*$^{del/del}$ mice have significantly impaired healing in response to excisional wounding compared to wild-type mice. HspB1 protein expression is increased in the proliferating epithelium of wounds in wild-type mice. It was also shown that HspB1 deficiency results in increased chemokine production and neutrophil accumulation in wounds. This research proposes an important role for hspB1 in inflammatory responses and wound healing *in vivo*.

Declaration

This thesis is the result of my own work, with the exception of Figures 3.4 and 4.1, which were compiled using data generated by Dr. Anna Aubareda, which is acknowledged in the text. All other figures are of my own work. All work was performed at the Kennedy Institute of Rheumatology Cell Signalling Division, University of Oxford (Imperial College London up to 1st August 2012). This work was supported by Arthritis Research UK; and a studentship and funding for the generation of *hspB1*$^{del/del}$ mice from the Kennedy Institute of Rheumatology Trustees.

Copyright Declaration

Acknowledgements

My greatest thanks go to my parents, who encouraged my decision to undertake this endeavour and who have supported me all the way throughout. There are no greater parents a man could ask for and I love you both very much.

Thank you very much to my supervisor, Jonathan Dean. Your insight, advice, strategy and patience have guided me into becoming a much better scientist. I will carry all the lessons you have taught me forward into my career. Thank you to my lab mates throughout the years, Anna Aubareda, Francesco Marchese, and Gerhard Ruspi. Your help, assistance and advice were invaluable.

I have met so many great friends throughout my time at the KIR. Adam Cribbs and Timothy Smallie provided excellent extra-curricular company and I look forward to spending many more evenings with you gentlemen.

Thank you so much to Adam Cartwright, Matt Bunn, Will Gamester and Simon Taylor. It's been a pleasure and an honour to live with you these last few years. I thank you for all your support, friendship, camaraderie and for the best years I have had in my life. I hope there never comes a summer where we can't BBQ together.

Thank you to all my colleagues throughout the KIR, in cell signalling, cytokine biology, matrix biology and the myriad groups in the ground floor, past and present. Without the wealth of knowledge and expertise at the Kennedy Institute I would not have been able to undertake a great deal of my work, and I am extremely grateful.

Table of Contents

List of Figures

List of Tables

Chapter 2

List of abbreviations

AD	Alzheimer's disease
ARE	AU-rich element
ASC	Apoptosis associated speck-like protein containing caspase recruitment domain
ASK1	Apoptosis signal-regulating kinase-1
ATP	Adenosine triphosphate
AUF1	ARE/poly(U)-binding/degradation factor 1
BCA	Bicinchoninic acid
BSA	Bovine serum albumin
C/EBP	cytidine-cytidine-adenosine-adenosine-thymidine (CCAAT)-enhancer-binding protein
C/EBPα	CCAAT/enhancer binding protein α
CAF1	Chromatin assembly factor-1
cAMP	Cyclic adenosine monophosphate
CCL	Cysteine – Cysteine motif ligand
CD	Cluster of differentiation
cFLIP	Cellular FLICE-like inhibitory protein
cIAP	Baculoviral IAP repeat-containing protein
CMT	Charcot-Marie-Tooth disease
CMV	Cyotomegalovirus
COX	Cyclooxygenase
CR	Complement receptor

CREB	cAMP response-binding protein
CXCL	Cysteine – X – Cysteine motif ligand
CYLD	Cylindromatosis (turban tumour syndrome)
DAMP	Danger-associated molecular patterns
DAXX	Death-associated protein 6
dHMN	Distal hereditary motor neuropathies
DISC	Death-inducing signalling complex
DMEM	Dulbecco's modified Eagle's medium
DNA	Deoxyribonucleic acid
DPX	3, 3'-diaminobenzidine
DTT	Dithiothreitol
DUSP1	Dual specificity protein phosphatase 1 (MKP1)
ECL	Enhanced chemiluminescence
ECM	Extracellular matrix
EDTA	Ethylenediaminetetraacetic acid
EGTA	Ethyleneglycoltetraacetic acid
eIF4G	Eukaryotic translation initiation factor 4 gamma
ELISA	Enzyme-linked immunosorbent assay
ER	Endoplasmic reticulum
Erk	Extracellular-signal-regulated kinases
ERK	Extracellular signal-related kinases
FADD	Fas-associated protein with death domain
FCS	Fetal calf serum
FITC	Fluorescein isothiocyanate
FPCL	Fibroblast-populated collage lattice

FPCL	Fibroblast-populated collage lattice
FRT	Flp-recombinase
GAPDH	Glyceraldehyde 3-phosphate dehydrogenase
GM-CSF	Granulocyte-monocyte colony-stimulating factor
GM-CSF	Granulocyte-monocyte colony-stimulating factor
Gp130	Glycoprotein 130
GROα/KC	Growth regulated oncogene-alpha/keratinocyte-derived chemokine
HCC	Hepatocellular carcinoma
HEK	Human embryonic kidney
HOIL	Haeme-oxidised IRP2 ubiquitin ligase
HOIP	HIOL-1-interacting protein
HRP	Horseradish peroxidase
hsp	Heat shock protein
HUVEC	Human umbilical vein endothelial cells
ICAM1	Intercellular adhesion molecule 1
Ig	Immunoglobulin
IHC	Immunohistochemistry
IKK-β	Inhibitor of nuclear factor kappa-B kinase subunit beta
IL	Interleukin
IL-1R	IL-1 receptor
IL-1RAcP	IL-1R accessory protein
IP	Intra-peritoneal
IRAK	IL-1R-associated kinase
IRF	Interferon regulatory factor
IRI	Ischemia-reperfusion injury

IRI	Ischemia-reperfusion injury
IκBα	Nuclear factor of kappa light polypeptide gene enhancer in B-cells inhibitor, alpha
JAK	Janus kinase
JNK	C-Jun N-terminal kinases
LFA	Lymphocyte function-associated antigen
LPS	Lipopolysaccharide
LUBAC	Linear ubiquitin chain assembly complex
MAC1	Macrophage-1 antigen
MACS	Magnetic-activated cell sorting
Mal	MyD88-adaptor like protein
MAP3K/MAPKKK	MAPK kinase kinase
MAPK	Mitogen activated protein kinase
MAPKAPK	MAPK-activated protein kinase
MAPKK/MKK	Mitogen-activated protein kinase kinase
MCP	Monocyte chemotactic protein
M-CSF	Macrophage colony-stimulating factor
M-CSF	Macrophage colony-stimulating factor
MD-2	Lymphocyte antigen 96
MEF	Mouse embryonic fibroblast
MEK	MAPK ERK kinase
MIP	Macrophage inflammatory protein
MK2	MAP kinase-activated protein kinase 2
MNK	MAPK-interacting kinase
mRNA	Messenger ribonucleic acid

MSK	Mitogen and stress-activated kinase
MTT	3-(4,5-Dimethylthiazol-2-yl)-2,5-diphenyltetrazolium bromide
myD88	Myeloid differentiation primary response gene (88)
NALP3	NACHT, leucine-rich repeat (LRR) and PYD-containing protein 3
NEMO	NF-kappa-B essential modulator
NF-κB	Nuclear factor kappa-light-chain-enhancer of activated B cells
NLR	NOD-like receptors
NOD	Nucleotide-binding oligomerization domain
NSAID	Non-steroidal anti-inflammatory drug
OCT	Optimal cutting temperature compound
P38 MAPK	P38 mitogen-activated protein kinases
PABP1	Poly-A-binding protein 1
PAGE	Polyacrylamide gel electrophoresis
PAMP	Pathogen-associated molecular patterns
PARP	Poly (ADP-ribose) polymerase
PBS	Phosphate buffered saline
PCR	Polymerase chain reaction
PE	R-phycoerythrin
PG	Prostaglandin
PGDF	Platelet-derived growth factor
PI	Propidium iodide
PK	Protein kinase
PMSF	Phenylmethanesulfonylfluoride
PU.1	31 kda-transforming protein
PVDF	Polyvinylidene fluoride

qRT-PCR	Quantitative real-time reverse-transcription PCR
RA	Rheumatoid arthritis
RANTES	Regulated on Activation, Normal T cell Expressed and Secreted
RHIM	Rip homotypic interaction motif
RIP1	Receptor-interacting serine/threonine-protein kinase 1
RNAi	RNA interference
ROS	Reactive oxygen species
RSK	p90 ribosomal S6 kinase
SDS	Sodium dodecyl sulphate
siRNA	Short interfering RNA
SOCS	Suppressor of cytokine signalling
STAT	Signal transducer and activator of transcription
TAE	Tris-acetate-EDTA
TAK1	Transforming growth factor-β-activated kinase 1
TBS	Tris-buffered saline
TEMED	Tetramethylethylenediamine
TEPM	Thioglycollate-elicited peritoneal macrophages
TG	Thioglycollate
TIR	Toll-IL-1 receptor domain
TLR	Toll-like receptors
TNF	Tumour necrosis factor
TRADD	Tumor necrosis factor receptor type 1-associated DEATH domain protein
TRAF2	TNF receptor associated factor
TRAM	Translocating chain-associated membrane protein

TRIF	TIR domain-containing adaptor-inducing interferon-β
TTP	Tristetraprolin
UPR	Unfolded protein response
UTR	3'-untranslated region
VEGF	Vascular endothelial growth factor

Chapter 1

Introduction

1.1 Innate immunity and the acute inflammatory response.

Inflammation is a component of the response of tissues to damage, such a pathogen activity, cellular damage or irritation, which allows the restoration of the tissue to homeostasis. The classical signs of inflammation are pain, redness, swelling, heat and loss of function. Inflammation is considered as a mechanism of innate and adaptive/acquired immunity, which may be acute or chronic. Innate immunity represents the first line of defence that defends the host against infection and tissue damage in a non-specific manner. Cells involved in mounting an innate immune response recognise pathogens in a generic manner, that is to say, unlike the antigen-specific response of the acquired immune response. The innate immune response provides immediate defence, although it does not confer long-term protection. The adaptive immune system is responsible for the recognition of 'self' and 'non-self' antigens, initiation of responses that efficiently and maximally eliminate specific pathogens and compile and immunological memory of encountered 'non-self' antigens.

Acute inflammation represents the initial response to harm and is achieved by a responsive change in the gene expression by cells in resident tissues and the migration and infiltration of leukocytes, including neutrophils and macrophages, the site of the inflammatory stimuli. This results in sequence of biochemical events that propagates the inflammatory response and its eventual resolution, which is mediated by the resident and infiltrated cells. Prolonged or delayed resolution of the inflammatory response may result in chronic inflammation, leading to a shift in the number or type of inflammatory cells responding to the site of inflammation and can result in harm to the organism by destruction of tissue through uncontrolled inflammatory processes. Chronic inflammation is a component of auto-inflammatory diseases, such as rheumatoid arthritis and psoriasis, which are leading causes of morbidity and require long-term drug management.

1.2 Mediators of inflammation.

Inflammation is usually initiated by disruption of tissue integrity and/or pathogen invasion. A variety of mediators regulate the inflammatory response. These include plasma derived mediators, such as complement, bradykinin, thrombin and Factor XII, which are instrumental in the complement system, vasodilation and the coagulation system. Leukocytes also produce mediators in response to wounding. These include eicosanoids, histamine, degranulated lysosomal enzymes and cytokines. Cytokines are small proteins, peptides or glycoproteins that belong to a large group of molecules that regulate cell signalling. Cytokines bind to specific receptors and activate intracellular signalling which results in the induction of the expression of numerous proteins included in the inflammatory response.

1.2.1 Interleukin-1 (IL-1).

IL-1α and IL-1β are both the original members of the IL-1 family of cytokines, of which there are now 11 members. IL-1 induces gene expression in multiple different cell types, such as fibroblasts (Jeong, Kim et al. 2004; Alford, Glennie et al. 2007), epithelial cells, (Hoffmann, Thiefes et al. 2005), vascular endothelial cells and smooth muscle cells (Bandman, Coleman et al. 2002). IL-1α and IL-1β also induce their own gene expression by autocrine/paracrine signalling (Gaestel, Kotlyarov et al. 2009; Weber, Wasiliew et al. 2010). IL-1-induced gene expression occurs within 30 mins and can be sustained for hours. IL-1α precursor molecule is biologically active and most cells express constitutive levels of IL-1α (Dinarello 2009). IL-1α is not usually found in extracellular fluids, except in cases where it is secreted by dying cells and this represents a major cytokine released by necrotic cells that induces inflammation (Chen, Kono et al. 2007). IL-1α is primarily membrane-bound and signals through paracrine mechanisms (Kaplanski, Farnarier et al. 1994).

Inactive Pro-IL-1β is cleaved into active IL-1β by the caspase-1 component of the NALP3 inflammasome, which is also comprised of NALP3 and the adaptor protein ASC. The NALP3 inflammasome belongs to a family of intracellular NOD-like receptors (NLRs) that are activated in response to binding with pathogen-associated molecular patterns (PAMPs) (Meylan, Tschopp et al. 2006) and danger-associated molecular patterns (DAMPs) such as reactive oxygen species (ROS) (Dostert, Petrilli et al. 2008), hsp90 (Mayor, Martinon et al. 2007) and microbial and host DNA (Muruve, Petrilli et al. 2008). IL-1β is capable of inducing the expression of cyclooxygenase (COX)-2 in the hypothalamus, which results in the increased production of prostaglandin E_2 in the thermoregulatory centre of the brain, causing fever (Dinarello 2004). Il-1β also increases the expression of adhesion molecules of vascular mesenchymal and endothelial cells and the induction of chemokines, which together result in the infiltration of inflammatory leukocytes from the circulation and into tissues (Dinarello 2009). The production of IL-8 by fibroblasts (Alford, Glennie et al. 2007) and IL-6 production by vascular endothelial cells is particularly sensitive to IL-1-mediated induction (Dinarello 1996; Dinarello 2005).

1.2.2 Tumour necrosis factor (TNF) α.

The biological activity of TNFα was discovered in the 1960/70s (Kolb and Granger 1968; Carswell, Old et al. 1975) and the gene was cloned under different names in the 1980s (Gray, Aggarwal et al. 1984; Pennica, Nedwin et al. 1984). TNFα is one of the most rapidly produced pro-inflammatory cytokines *in vivo.* The major sources of TNFα are macrophages and monocytes, although T cells, neutrophils, mast cells and vascular endothelium are also sources under certain conditions. Together with IL-1, TNFα is a key mediator of the inflammatory response. TNFα is implicated in the progression of a number of diseases (Feldmann and Maini 2001). TNFα can induce apoptotic cell death and is capable of inducing

the expression of chemokines and adhesion molecules required for leukocyte recruitment to the site of inflammation (Doukas and Pober 1990; Schroder, Sticherling et al. 1990). The discovery of the clinical application of anti-TNFα antibodies to treat rheumatoid arthritis was made at my research institute (Elliott, Maini et al. 1993). These anti-TNFα biologics, such as infliximab and adalimumab, are used to treat RA that is resistant to conventional disease modifying anti-rheumatic drugs and NSAIDS, often in a combination therapy with these conventional drugs (Upchurch and Kay 2012).

1.2.3 Interleukin-6 (IL-6).

IL-6 is a pro-inflammatory cytokine that is produced by a large variety of cells in response to a broad range of stimuli. IL-6 is produced by cells involved in the innate immune response, such as macrophages, dendritic cells and mast cells, and well as by endothelial cells, fibroblasts and epithelial cells (Hirano 1998). IL-6 expression and production is regulated by changes in the activity of NF-κB and CCAAT/enhancer binding protein α (C/EBPα). IL-6 mRNA stability is stabilised by p38 MAPK activity (Zhao, Liu et al. 2008; Tudor, Marchese et al. 2009). IL-6 binds to a receptor complex comprised of IL-6Rα and glycoprotein 130 (gp130), which results in the activation of the Janus kinase (JAK) family of tyrosine kinases. Activated JAKs phosphorylate and activate signal transducer and activator of transcription (STAT) 1 and 3 (Akira 1997; Fielding, McLoughlin et al. 2008). IL-6 induces angiogenesis (Nakahara, Song et al. 2003), chemokine production and monocyte recruitment and fever (Fonseca, Santos et al. 2009).

Gp130 is ubiquitously expressed, although IL-6Rα is not. However, IL-6 is capable of regulating gene expression in cells that do not express IL-6Rα. Soluble IL-6R (sIL-6R) can complex with IL-6 and associate with membrane bound gp130. Innate immune cells, such as neutrophils and macrophages, are the main sources of sIL-6R (Horiuchi, Koyanagi et al.

1994). IL-6 signalling through STAT3 has been shown to down-regulate the production of the neutrophil attractant chemokine CXCL1 and increased neutrophil clearance in a murine model of peritoneal inflammation (Fielding, McLoughlin et al. 2008).

The concentration of IL-6 is elevated in the serum of patients with RA (Houssiau, Devogelaer et al. 1988)and Crohn's disease (Kishimoto 2010). Serum IL-6 levels are elevated in some, but not necessarily all RA patients. Serum IL-6 is a marker of on-going inflammation; however, IL-6 levels do not always correlate with other markers of chronic inflammation, such as IL-1 and TNFα in RA patients. Tocilizumab, a humanized anti-IL-6R antibody that blocks IL-6 binding to surface and soluble IL-6R, has been successfully used to treat the symptoms and arrest the on-going inflammation in RA patients and is the primary therapy used to treat patients who do not respond to anti-TNFα (Rincon 2012).

1.2.4 Interleukin-10 (IL-10).

IL-10 is an anti-inflammatory cytokine and plays a crucial role in limiting the immune response to pathogens and preventing damage to the host. IL-10 is broadly expressed by many immune cells, including macrophages, dendritic cells, mast cells, neutrophils, T cells and B cells (Saraiva and O'Garra 2010), macrophages (Fiorentino, Zlotnik et al. 1991), dendritic cells (Boonstra, Rajsbaum et al. 2006) and to a lesser extent in neutrophils (Hu, Paik et al. 2006) Induction of IL-10 often occurs together with pro-inflammatory cytokines, although pathways that induce IL-10 may actually negatively regulate these pro-inflammatory cytokines (Saraiva and O'Garra 2010). IL-10 binds to IL-10R1 and IL-10R2 and induces STAT3 and JAK1 activation. However, unlike STAT3 activation by other inflammatory mediators such as IL-6, IL-10-mediated STAT3 activation is sustained and enhances the expression of suppressor of cytokine signalling (SOCS) -3 and IL-1Ra and soluble p55 and p75 TNFR. IL-10 inhibits the expression of COX-2, which in turn regulates

the expression of matrix metalloproteinase through a prostaglandin E_2/cAMP pathway (Mertz, DeWitt et al. 1994). IL-10 activity potently inhibits the production of IL-1/LPS- and TNF-induced pro-inflammatory cytokines, as well as itself, in macrophages and monocytes. IL-10 also inhibits the secretion of CC and CXC chemokines.

1.2.5 Chemotactic Cytokines (Chemokines).

Chemokines are cytokines that have a crucial role in orchestrating the movement of circulating leukocytes to the sites of inflammation and/or injury (Charo and Ransohoff 2006). There are four distinct families of chemokines, segregated on the basis of differences in structure and function and the adopted nomenclature based on the arrangement of first cysteine residues in these molecules (Bacon, Baggiolini et al. 2002). The largest family is that of the CC chemokines, which are responsible for attracting mononuclear cells to the site of inflammation. The most well understood CC chemokine is monocyte chemoattractant-1 (MCP-1/CCL2). CC chemokines (CCLs) are potent chemoattractants for monocytes, macrophages, dendritic cells, T cells and basophils (Charo and Ransohoff 2006). Other CCLs include macrophage inflammatory protein-1α (MIP-1α/CCL3), MIP-1β/CCL4 and RANTES/CCL5. CCLs are ligands for CCR receptor family. CCL3 binds to CCR1, expressed on monocytes, eosinophils and basophils, while CCL2 binds to CCR2, expressed on monocytes, immature dendritic cells, endothelial cells fibroblasts and memory T cells (Luster 1998; Gerard and Rollins 2001; Charo and Ransohoff 2006).

Another group of chemokines are the CXC chemokines, so named due to the single amino acid residue between the first two cysteine residues of their amino acid sequence. IL-8 (CXCL8) in humans, and its functional murine orthologues GROα/KC (CXCL1) and MIP-2α (CXCL2), are the canonical prototypes (Charo and Ransohoff 2006; Kolaczkowska and Kubes 2013). CXCL1 is produced by endothelial cells, fibroblasts and neutrophils to a

greater extent than macrophages, whereas CXCL2 is predominantly produced by neutrophils and macrophages, with very little production by endothelial cells (Armstrong, Major et al. 2004). These chemokines signal via CXCR2 to activate and promote the adhesion of neutrophils (Kolaczkowska and Kubes 2013) and mast cells (Hallgren and Gurish 2007).

Leukocyte recruitment and extravasation follows a sequence of steps, commonly named as tethering, rolling, adhesion, crawling and transmigration. Leukocyte adhesion and tethering is initiated by changes to the surface of the vascular endothelium in response to stimulation by pro-inflammatory mediators that are produced by resident leukocytes when they are activated by pathogen recognition.

Activation and recruitment of neutrophils by CXC chemokines induces a conformational change in the in the structure of integrins expressed neutrophil cell surface, which results in higher affinity toward their respective immunoglobulin-like cell adhesion molecules (CAMs). Neutrophils have high expression levels of the integrins lymphocyte function-associated antigen 1 (LFA1, comprised of CD18/CD11α) and the complement receptor macrophage-1 antigen (CR3/MAC1, comprised of CD18/CD11β), which having undergone this conformational change, bind to the endothelial cell surface molecules intercellular adhesion molecule 1 (ICAM1), and is essential for neutrophil adhesion and migration.

1.2.6 Cyclooxygenase-2 (COX-2).

There are two functional forms of COX, COX-1 and COX-2. These enzymes are crucial for the synthesis of eicosanoids from free arachidonic acid. COX-1 was first purified in 1976 (Miyamoto, Ogino et al. 1976) and is constitutively expressed in many tissues (Kargman, Charleson et al. 1996). It is thought that COX-1 activity is important for the production of prostacyclin and PGE_2, which are cytoprotective and maintain the integrity of gastric mucosa (Allison, Howatson et al. 1992). COX-2 is not constitutively expressed but is induced by a

variety of stimuli, such as LPS, IL-1 and TNF (Williams, Mann et al. 1999). COX-2 is responsible for the increase in the production of prostaglandins, leukotrienes and thromboxanes that cause inflammation, pain and fever (Smith, DeWitt et al. 2000). Non-steroidal anti-inflammatory drugs that do not selectively inhibit COX-2 typically result in gastric mucosal damage, and in severe cases, gastric ulcers and bleeding, if the use of NSAID treatment is prolonged (Steinmeyer 2000). COX-2 selective inhibitors, also known as coxibs, were developed to prevent the production of prostaglandins synthesised by COX-2. Although these were heavily prescribed in the early 2000s, clinical trial data revealed that there was a significant increase in the rate of incidents such as non-fatal myocardial infarction, non-fatal stroke and death from one of these events (Antman, Bennett et al. 2007). The cause of these cardiovascular incidents has become a major subject of research (Cannon and Cannon 2012).

1.2.7 Lipopolysaccharide (LPS).

TNFα secretion is induced by activation of pattern recognition receptors (PRRs), such as the toll-like receptors (TLRs). These receptors recognise structural elements common to pathogens, such as lipopolysaccharides, peptidoglycans, and bacterial DNA. TLRs are expressed on the surface of epithelial cells and resident macrophages, dendritic cells and mast cells, activation of which leads to induction of pro-inflammatory cytokine expression.

LPS is ligand for TLR4, and in fact the discovery of the receptor was a result of research into identifying the cause of sensitivity to LPS (Poltorak, He et al. 1998). LPS is a component of the outer membrane of gram-negative bacteria and is crucial for the structural integrity of these bacteria. LPS is also known as endotoxin, (Rietschel, Kirikae et al. 1994) and is one of the most studied inflammatory stimuli. It is capable of causing excessive inflammation and endotoxic shock in high concentrations or if prolonged inflammatory signalling processes occur (Freudenberg, Tchaptchet et al. 2008). LPS consists of 3 components; lipid A, an

oligosaccharide core, and a distal O-antigen polysaccharide side chain. Lipid A has been identified and the endotoxic component (Raetz and Whitfield 2002).

1.2.8 Zymosan.

Zymosan is a particulate cell wall extract from yeast, *Saccharomyces cerevisiae*. It is composed of many polysaccharides, of which mannose and β-glucan are the major constituents (Di Carlo and Fiore 1958), and is a TLR-2/6 and dectin-1 ligand (Sato, Sano et al. 2003). Zymosan induces recruitment and respiratory burst of neutrophils (Paya, Terencio et al. ; Su, Raghuwanshi et al. 2005) and induces TNFα, IL-1 and IL-6 production by monocytes and macrophages (Sanguedolce, Capo et al. 1992) (Young, Ye et al.). Zymosan induces the the expression of IL-6 and IL-8 in human fibroblasts (Nomi, Kimura et al. 2010). Zymosan has also been shown to promote the production of IL-10 in macrophages (Elcombe, Naqvi et al. 2013).

1.3 Inflammation and wound healing.

A normal and regulated acute inflammatory response is a necessary component of the wound healing response. It has been shown, using various animal models and study of human skin wounds, that the inflammatory response during normal healing is characterised by a sequence of changing patterns of various leukocyte subsets (Martin 1997; Singer and Clark 1999; Eming, Krieg et al. 2007).

The immediate response to wounding involves the consequence of damage caused to local blood vessels. Platelets activate and aggregate to produce a fibrin clot to stop local haemorrhage and provide a provisional matrix through which infiltrating cells can migrate (Nurden, Nurden et al. 2008). These platelets are also a source of transforming growth factor (TGF) β, platelet derived growth factor (PDGF) and vascular endothelial growth factor

(VEGF) (Bahou and Gnatenko 2004).The inflammatory response to wounding involves the recruitment and infiltration of leukocytes to the wound site. This infiltration is induced by stimulation of local resident cells, such vascular endothelial cells and activated resident mast cells, by serum components and TLR activation which results in the of pro-inflammatory cytokines and chemokines (Gillitzer and Goebeler 2001; Noli and Miolo 2001; Shaw and Martin 2009). Excessive inflammation is associated with impaired wound healing, although the positive and negative consequences of the inflammatory response to the outcome of wound healing are controversial.

Neutrophils are activated and are the first inflammatory cells to arrive at the wound site (Kim, Liu et al. 2008). The main function of the neutrophil is to act as an effector cell to decontaminate the wound bed and kill invading pathogens. Neutrophils release highly active anti-microbial substances, such as ROS, proteases (including as neutrophil elastase and PR-3) and produce small amounts of pro-inflammatory cytokines. However, these factors can delay healing by causing damage to the developing structures required for the progression of wound healing. For example, neutrophil elastase can degrade almost every component of the extracellular matrix, which is exacerbated by the release of ROS that inactivate endogenous protease inhibitors (Weiss 1989). Considering that the extracellular matrix provides a supporting scaffold for proliferating and migrating cells, impairment to the integrity of this structure might have negative consequences for wound repair and closure.

It has been demonstrated that anti-Gr-1 antibody-mediated neutrophil depletion in mice results in accelerated wound re-epithelialisation (Dovi, He et al. 2003). In the same study, using genetically diabetic mice which show an excessive neutrophil infiltrate in response to wounding, wound closure was accelerated in response to systemic neutrophil depletion (Dovi, He et al. 2003). However, Gr-1 is also present on monocytes, and the study did not

investigate the extent of monocyte and macrophage depletion mediated by anti-Gr-1 antibody-mediated leukocyte depletion.

CXCL1 and CXCL2 are the agonists for CXCR2 and promote neutrophil infiltration. *CXCR2*$^{-/-}$ mice have impaired neutrophil recruitment and delayed wound healing (Devalaraja, Nanney et al. 2000). However, the authors also demonstrated impaired keratinocyte proliferation angiogenesis, which are CXCR2-dependent processes, in *CXCR2*$^{-/-}$ mice compared to wild-type mice (Devalaraja, Nanney et al. 2000).

Neutrophils are largely absent from wounds that heal very well. Fetal dermal wounding often heals in the absence of an inflammatory response (Adzick, Harrison et al. 1985; Longaker, Whitby et al. 1990), and results in the complete restoration of dermal architecture without scarring. Adult skin in a fetal environment undergoes an inflammatory response to wounding with scarring (Longaker, Whitby et al. 1994). Wound healing experiments using PU.1 null mice, which lack both macrophage and neutrophils, demonstrate scar-free wound healing, although in the same time frame as wild-type mice (Martin, D'Souza et al. 2003). These findings suggest that the reduction in the magnitude of the inflammatory response, particularly the infiltration of leukocytes, to wounding results in rapid and improved repair of wounds.

Neutrophil influx peaks at 1-2 days post-wounding, in the absence of excessive infection (Kim, Liu et al. 2008). Unless the stimuli for the recruitment of neutrophils persist, resident macrophages and blood monocytes are recruited and infiltrate to the site of wounding 2 - 4 days after injury (Eming, Krieg et al. 2007). Macrophage infiltration to the wound site is regulated by gradients of chemotactic factors, such as growth factors, pro-inflammatory cytokines and the chemokines CCL2 and CCL3 (DiPietro, Burdick et al. 1998; Werner and Grose 2003). As the monocytes extravasate from the blood into the wound site, they

differentiate into mature tissue macrophages (Gordon 2003; Mosser 2003). These pro-inflammatory , M1 macrophages produce cytokines such as IL-1, IL-6 and TNFα, amplifying the inflammatory response (Barrientos, Stojadinovic et al. 2008).

Macrophages represent the single most effective means of removing neutrophils form the site of injury. Macrophages induce apoptosis of neutrophils (Meszaros, Reichner et al. 2000). Macrophages phagocytose and remove the large load of apoptotic neutrophils. This process is called efferocytosis and is thought to be essential to resolve wound inflammation and complete repair (Savill, Wyllie et al. 1989; Acosta, del Barco et al. 2008; Khanna, Biswas et al. 2010). There is evidence to suggest that phagocytosis of neutrophils promotes the differentiation of macrophages into a M2-like anti-inflammatory, growth promoting and reparative lineage (Fadok, Bratton et al. 1998).

Chronic and non-healing wounds, such as those associated with clinical disorders such as venous insufficiency (Singer and Clark 1999), diabetes (Eming, Smola et al. 2002) and vasculitis (Wlaschek and Scharffetter-Kochanek 2005), often fail to progress through the normal phases of wound healing and remain in a chronic inflammatory state (Loots, Lamme et al. 1998). Increased TNFα expression is found systemically and the local issue of ulcerative wounds in human patients compared to a control age population without underlying pathology and wounds. Neutralisation of TNFα in wounds accelerates resolution of healing (Ashcroft, Jeong et al. 2012). Factors such as hypoxia, amplified pro-inflammatory cytokine expression, unbalanced protease activity, fragments of necrotic tissue and the presence of bacteria all induce a prolonged and continued influx of neutrophils and macrophages (Singer and Clark 1999). These inflammatory cells are instrumental in further amplifying the inflammatory response which results in the creation of a proteolytic and oxidative hostile microenvironment, which over-whelms local mechanisms tissue protection

(Barrick, Campbell et al. 1999). The development of strategies to mitigate excessive inflammation to enhance wound healing represents a promising target for therapeutic intervention.

1.4 Inflammatory cellular signalling

1.4.1 IL-1R and TLR signalling.

Cell signalling is initiated by ligand binding to a receptor and inducing a conformational change resulting in receptor activation. There are nine members of the IL-1 receptor 1 (IL-1RI) family. IL-1α or IL-1β bind to the IL-1RI receptor, which then recruits the co-receptor accessory protein (IL-1RAcP) and forms a complex. This in turn results in recruitment of myeloid differentiation primary response gene (88) (MyD88) via the toll-IL-1R domain (TIR) (Dinarello 2011). The recruitment of MyD88 leads to the association of interleukin-1 receptor-associated kinase (IRAK) 1, 2 and 4, likely through the death domains of these molecules. IRAK4 then phosphorylates IRAK1, which results in the dissociation of IRAK1 and IRAK4 from MyD88 (Brikos, Wait et al. 2007). This IRAK complex then interacts with TNFR-associated factor 6 (TRAF6), which is an E3 ubiquitin ligase (Deng, Wang et al. 2000). TRAF6 then undergoes autoubiquitination, through a process involving E2 ubiquitin conjugating enzymes Ubc13 and Uev1a, which results in K63-polyubiquitination of TRAF6. K63-TRAF6 can then recruit transforming growth factor β-activated protein kinase (TAK1) in a complex with TAK-1 binding protein (TAB) 1, 2 and 3. TAK1 is then activated, which then associates with the inhibitor of NF-κB (IκB) kinase (IKK) complex, containing the NF-κB essential modulator (NEMO) scaffold protein and IKKβ, which is the kinase responsible for IκBα phosphorylation and subsequent degradation which results in NF-κB activation. Phosphorylated IRAK 1 also undergoes K63-polyubiquitantion caused by the recruitment of E3 ubiquitin ligases Pellino-1 and Pellino-3b (Ordureau, Smith et al. 2008), resulting in

NEMO recruitment which binds to polyubiquitinated IRAK1 (Conze, Wu et al. 2008). Eventually, the ubiquitinated components of this signalling pathway are eventually degraded which results in termination of the signal (O'Neill 2008). Activation of TAK1 also phosphorylates and activates mitogen activated protein kinases kinases (MAPKKs), which propagate downstream signalling and phosphorylate MAPKs, which will be introduced later.

IL-1 also binds to the IL-1RII receptor, which is incapable of inducing downstream signalling, due to a lack of a TIR domain and the inability to dock with MyD88. IL-1-complexed IL-1RII is also capable of recruiting IL-1RAcP, sequestering the accessory protein for participating in IL-1RI-mediated signalling. This receptor acts as a decoy receptor and is mostly expressed on macrophages and B cells (Dinarello 2011). IL-1 receptor antagonist (IL-1Ra) competitively prevents the binding of IL-1 to IL-1RI and is used as in the treatment of rheumatoid arthritis, where it is used under the trade name Anakinra.

The downstream TIR domain common to the signalling pathways of IL-1R and TLRs ensures that many downstream signalling events as a result of the activation of these families of receptors are shared. LPS stimulation involves interactions with a complex of proteins including LPS binding protein, CD14, MD-2 and TLR4 itself. Stimulation results in TLR4 oligomerisation and interacts with TIR to recruit downstream signalling adaptors, such as MyD88 and MyD88-adaptor like protein (Mal), which results in activation of TAK1. LPS-activated TLR4 is capable of undergoing endocytosis where it recruits two more TIR domain adaptors, translocating chain-associated membrane protein (TRAM) and TIR domain-containing adaptor-inducing interferon-β (TRIF) leading to activation of interferon regulatory factor (IRF) 3 and induction of genes that contain interferon responsive elements (Kagan, Su et al. 2008). The C-Terminal region of TRIF also contains a Rip homotypic interaction motif (RHIM) which interacts with receptor-interlacing protein (RIP) 1. RIP1 is a serine/threonine

kinase and has been identified as an important component of TNFα-induced NF-κB activation. This capacity of TLR4 to signal from two locations is thought to be unique among TIR-containing receptors (O'Neill 2008). TLR2 will dimerise with TLR6, and this has been shown to be required for the coordination of pathogen recognition and macrophage activation by zymosan through TIR domain signalling (Ozinsky, Underhill et al. 2000). IRAK2 has also been shown to be essential for TLR2-induced TRAF6-mediated signalling. IRAK2 activity has been shown to peak at 8 h, in contrast to IRAK1 which peaked at 1 h post TLR2 stimulation. This suggested sequential control of IRAK1 in early-stage and IRAK2 in late-stage responses to TLR stimulation (Kawagoe, Sato et al. 2008).

1.4.2 TNFR Signalling.

Research on TNF has characterised the largest known family of cytokines, the TNF superfamily, which are ligands for and signal through interaction with the TNF receptor (TNFR) superfamily (Wiens and Glenney 2011). TNFRs bind to adaptor proteins in order to activate intercellular signalling pathways. TNFRs can be grouped depending on which adaptor proteins they recruit. TNFR1 is expressed on almost all cell types and recruits adaptor proteins with a death domain such as TNFR-associated death domain (TRADD) or Fas-associated protein with death domain (FADD) which are important for TNF-mediated cell death. TNFR2 is expressed on astrocytes, T cells, myocytes and thymyocytes and endothelial cells and does not recruit adaptor proteins with a death domain. TNFR2 instead recruits TRAF.

TNFR1 is activated by soluble TNF and membrane bound TNF. Depending on the microenviromental conditions TNFR1 activation can result in the induction of proliferation, apoptosis or necrosis. Activation of TNFR1 results in the formation of two different signalling complexes. The first, complex I, controls activation of downstream signalling that

results in the expression of genes that prevent the triggering of cellular death processes. The second complex, complex II or the death-inducing signalling complex (DISC) is formed after the internalisation of TNFR1 (Micheau and Tschopp 2003). Complex I recruits TRAF2, baculoviral IAP repeat-containing protein (cIAP) 1, cIAP2 and RIP1. After this integration RIP1 is rapidly modified with polyubiquitin chains, which results in recruitment and activation of the TAK1 and the IKK complex, resulting in activation of MAPKKs and NF-κB, respectively. TNFR1- induced TRAF2 activation also results in the recruitment of the linear ubiquitin chain assembly complex (LUBAC), comprised of haeme-oxidised IRP2 ubiquitin ligase (HOIL) 1, HIOL-1-interacting protein (HOIP) and Sharpin (Emmerich, Schmukle et al. 2011). LUBAC is an E3 ubiquitin ligase and binds ubiquitin chains to RIP1 and NEMO, enhancing NF-κB activation. TNFR1 activation may also result in an endocytotic process which results in a change the assortment of adaptor proteins that may occupy it (Schneider-Brachert, Tchikov et al. 2004). RIP1 may be de-ubiquitinated by cylindromatosis (turban tumor sundrome) (CYLD), resulting in negative regulation of NF-κB activation and instead frees RIP1 for recruitment by RIP kinase into a complex with TRADD, FADD and procaspase-8. This activity of this complex, known as DISC, is dependent upon NF-κB. If NF-κB is active, cellular FADD-like IL-1β-converting enzyme-inhibitory protein (cFLIP) translocates to DISC and prevents the activation of caspase 8. If NF-κB is absent, cFLIP remains absent from DISC resulting in activation of caspase-8, an initiator caspase required for the induction of the cell to enter apoptosis (Micheau and Tschopp 2003).

TNFR2 belongs to the second group in the TNFR superfamily and is only activated by mTNF (Grell 1995). Activation of TNFR2 results in TRAF2-mediated activation of TAK1 and IKK as for complex I for TNFR1. However, TNFR2 activation induces changes in the cellular localisation of TRAF2 resulting in K48-linked ubiquitantion and proteasomal degradation (Wu, Conze et al. 2005). This has important implications for the survival of the cell.

Although TNFR2 is not a death receptor in of itself, the degradation of TRAF2 inhibits the binding of cIAP1 and cIAP2 to the TNFR1 complex I, preventing activation of NF-κB, and thus enhancing the activity of DISC and apoptosis. Thus is it clear that not only the extent of TNFR activation, but also the proportions in which TNFR1 and TNFR2 are activated and the conditions other cellular stresses the cell might be exposed to, leads to a delicate balance between the pro-inflammatory and pro-apoptotic actions resulting from TNFα stimulation (Cabal-Hierro and Lazo 2012).

1.4.3 Mitogen-activated protein kinases (MAPK).

MAPKs are serine/threonine kinases that are responsible for signal transduction of extracellular stimuli in to cellular responses. All eukaryotic cells have multiple MAPK pathways, which together regulate gene expression, metabolism, apoptosis and differentiation, to name but a few processes (Cargnello and Roux 2011). The classical and most commonly studied MAPKs are extracellular signal-regulated kinases (ERK) 1 and 2, c-Jun animo N-terminal kinases (JNK) 1, 2 and 3 and the p38 isoforms (α,β,γ and δ). Each of these MAPK groups is controlled by a set of sequentially activating kinases; a MAP3K, a MAP kinase, (MKK) and finally the MAPK itself (Cargnello and Roux 2011). IL-1/TLR and/or TNFR activation results in the phosphorylation and activation MAP3Ks, which then phosphorylate MAPKKs, which then induce MAPK activity through phosphorylation within a conserved Thr-X-Tyr motif located within the kinase domain of MAPKs. Phosphorylation of these residues is essential for MAPK activity (Cargnello and Roux 2011). The wide assortment of functions induced by MAPK activation is regulated through phosphorylation of substrates, such as p90 ribosomal S6 kinases (RSKs), mitogen and stress-activated kinases (MSKs), MAPK-interacting kinases (MNKs) and MAPK-activated protein kinases (MK2, 3 and 5).

1.4.4 Extracellular signal-related kinases (ERK).

ERK1 was the first MAPK to be characterised. Both ERK1 and ERK2 were cloned by the early 1990s (Cooper, Bowen-Pope et al. 1982) (Boulton, Nye et al. 1991) and share 83% amino acid identity. ERKs are expressed in various levels in all tissues and are activated by growth factors, such as platelet-derived growth factor (PGDF) and epidermal growth factor (EGF) (Boulton, Yancopoulos et al. 1990), cytokine stimuli and osmotic stress (Raman, Chen et al. 2007).

The activation pathway of ERKs consist of the MAP3Ks A-Raf, B-Raf and Raf-1 and the MAPKKs MAPK ERK kinase (MEK) 1 and MEK2. Activated ERKs phosphorylate a large number of substrates, such as MNKs, monocyte enhancer factor 2, c-Fos, c-Myc and STAT3 among, others.

The ERKs play a role in the control of cell proliferation and is required for G1 to S-phase progression (Meloche and Pouyssegur 2007). ERKs phosphorylate and stabilise c-Fos, resulting association with c-Jun and the formation of transcriptionally active AP-1 complexes (Whitmarsh and Davis 1996). Active AP-1 is required for cyclin D1 expression. This protein interacts with cyclin-dependent kinases (CDKs) and permits G1 to S phase transition and cell cycle progression (Shaulian and Karin 2001). ERKs phosphorylate RSKs, MSKs and MNKs, which are important regulators of ERK-induced biological processes (Cargnello and Roux 2011).

1.4.5 c-Jun amino (N)-terminal kinases (JNK).

JNKs, also known as stress-activated protein kinases (SAPKs), were also discovered in the early 1990s (Kyriakis and Avruch 1990; Hibi, Lin et al. 1993; Kracht, Truong et al. 1994) and are phosphorylated on Thr and Tyr residues in response to stress stimuli (Kyriakis,

Brautigan et al. 1991). There are 3 known JNK isoforms, JNK1, JNK2 and JNK3, which share 85% amino acid homology. JNK1 and JNK2 are expressed win a wide range of tissues. JNK3 expression seems to be restricted to neuronal tissue, testis and cardiac monocytes (Bode and Dong 2007).

JNKs are activated in response to cellular stresses such as ionizing radiation, oxidative stress, DAMPs, cytokines, growth factors, serum sensitivity and heat shock (Bogoyevitch, Ngoei et al. 2010). Inflammatory stimulation results in the phosphorylation of JNK mediated through activation of MAP3Ks such as MEKK1-4, TAK1 and ASK1 (Kyriakis and Avruch 2001), which results in activation and phosphorylation of MAPKKs MKK4 and MKK7, which together phosphorylate JNKs (Lawler, Fleming et al. 1998).

Activated JNKs are capable of relocating from the cytoplasm to the nucleus of the cell (Mizukami, Yoshioka et al. 1997) where they phosphorylate the transcription factor c-Jun and positively regulate cell proliferation (Jaeschke, Karasarides et al. 2006) through regulating AP-1 activity (Sabapathy, Hochedlinger et al. 2004). JNK activation is required for cytochrome-c release from mitochondria in MEF exposed to UV-induced cell stress (Tournier, Hess et al. 2000), which results in caspase 9 and caspase 3 activation and apoptosis. JNK phosphorylates activating transcription factor (ATF) 2 which results in the promotion of CRE-dependent transcription (Gupta, Campbell et al. 1995). The limited availability of JNK specific inhibitors has prevented the full understanding of JNK-dependent signalling.

1.4.6 p38 MAPK.

The p38α isoform was identified simultaneously in 1994 by 3 research groups (Han, Lee et al. 1994; Lee, Laydon et al. 1994; Rouse, Cohen et al. 1994). There are 3 isoforms of p38 MAPK in addition to p38α; p38β, p38γ and p38δ. P38α and p38β are ubiquitously expressed

cells, whereas p38γ and p38δ have more restricted expression and may have specialised functions. p38α expression is generally greater than that of p38β, and as consequence most of the published literature of p38 MAPK refers to p38α. There exist specific p38α and p38β inhibitors, which have also aided in developing the understanding of these isoforms.

p38 MAPKs are strongly activated by oxidative stress, hypoxia, ischemia and inflammatory cytokines such as IL-1 and TNFα (Cuadrado and Nebreda 2010). As described previously, TRAF recruitment promotes activation of TAK1 which then phosphorylates the MAPKKs MKK3 and MKK6 which then phosphorylate a conserved Thr-Gly-Tyr motif in p38 MAPKs (Derijard, Raingeaud et al. 1995; Han, Lee et al. 1996; Cuadrado and Nebreda 2010).

Isoforms of p38 MAPKs are located in the cytoplasm and nuclei of cells and accumulate in the nuclei of cells under cell stress (Raingeaud, Gupta et al. 1995). p38 MAPK phosphorylates MK2, MK3 and MK5, which results in the sequestering of p38 MAPK in the cytosolic compartment (Gaestel 2006). Activated p38 MAPKs phosphorylate a large number of substrates in various cellular compartments, including cytoplasmic cPL2, MNK1/2, MK2/3, Bax and Tau, p53 and MSK1/2, amongst others (Cuadrado and Nebreda 2010).

p38 MAPK has a crucial role in immune and inflammatory responses. Activation of p38 MAPKs can result from stimulation of the cell by cytokines, chemokines and LPS. P38 MAPKs induce pro-inflammatory cytokine expression by modulating the activity of transcription factors such as NF-κB (Karin 2006), or modulating mRNA stability through regulation and MK2/3 (Ronkina, Kotlyarov et al. 2008).

The p38 MAPKs have also been shown to be important regulators of cell proliferation and survival. Activation of p38 MAPK has been shown to result in negative regulation of cell cycle progression at both the G_1-S and G_2-M transition points by a variety of mechanisms, including deceased expression of cyclins and increased CDK inhibitor expression (Thornton

and Rincon 2009). P38 MAPK activity has been shown induce apoptosis in response to cellular stresses by both transcriptional and post-transcriptional mechanisms (Cuenda and Rousseau 2007).

1.4.7 Mitogen and stress-activated kinases (MSKs).

MSK1 and MSK2 were discovered in the late 1990s as substrates for p38 MAPK-mediated phosphorylation (Deak, Clifton et al. 1998; New, Zhao et al. 1999) and have approximately 63% amino acid sequence homology. ERK1/2 and p38 MAPKs interact and phosphorylate MSKs at their Leu-Ala-Lys-Arg-Arg-Lys MAPK-binding domains (Tomas-Zuber, Mary et al. 2001).

MSKs have been implicated in negatively regulating inflammation. MSK1 and MSK2-deficient mice are hypersensitive to LPS challenge. MSKs phosphorylate cAMP response-binding protein (CREB), with greater efficacy than any other MAPKAP (Pierrat, Correia et al. 1998), which results in the expression of c-Fos, JunB. MSK1 also activates CRE-binding activating factor (ATF1). MSKs have been shown to bind to and phosphorylate the p65 subunit of NF-κB, which results in interaction with histone acetylation cofactors and enhances NF-κB gene expression (Zhong, Voll et al. 1998). MSK1 and MSK2-deficient fibroblasts have reduced IL-6 mRNA expression in response to TNF stimulation compared to wild-type cells (Vermeulen, De Wilde et al. 2003). This suggests that MSK activity is important for NF-κB-dependent transcription. MSKs have also been shown to phosphorylate and activate STAT3 (Wierenga, Vogelzang et al. 2003). MSK2 has also been shown to inhibit p53 activity in resting cells (Llanos, Cuadrado et al. 2009). A recent study has shown that activation of MSKs and CREB by zymosan induces IL-10 transcription via a dectin-1 specific pathway in macrophages and also results in low level of IL-12p40 production (Elcombe, Naqvi et al. 2013). The same study has shown that dectin-1 activation results in

the induction of genes associated with regulatory/M2 polarised macrophages (Elcombe, Naqvi et al. 2013), suggesting a role for MSK activation the control of macrophage inflammatory phenotype.

1.4.8 MAPK-activated protein kinase 2 (MK2).

MK2 was originally discovered as a substrate of ERKs that could phosphorylate heat-shock protein beta 1 (hspB1) (Stokoe, Engel et al. 1992), although it was later discovered that is activated by p38 MAPK in response to pro-inflammatory stimuli (Freshney, Rawlinson et al. 1994). MK3, which has 75% amino acid homology with MK2, has also been identified as a substrate for p38 MAPK-mediated phosphorylation (McLaughlin, Kumar et al. 1996). MK2 is located in the nuclei of resting cells, and is exported to the cytoplasm as a result of stressful cellular stimuli, such as IL-1R/TLR and TLR activation, oxidative stress and UV radiation (Freshney, Rawlinson et al. 1994; Rouse, Cohen et al. 1994; Guay, Lambert et al. 1997; Engel, Kotlyarov et al. 1998).

MK2 plays a role in control of the cell cycle. MK2 has been shown to phosphorylate and activate CDC25B and CDC25C in response to UV radiation stress (Manke, Nguyen et al. 2005), which results in phosphorylation of CDCs and initiation of mitosis (Aressy and Ducommun 2008). MK2 is capable of promoting arrest of cell division at the G_2/M checkpoint in response to DNA damage-inducing stress (Manke, Nguyen et al. 2005). Phosphorylated MK2 has been shown to phosphorylate and activate HDM2 resulting in degradation of p53, suggesting that MK2 may decrease the duration and extent of the p53 response to stress and DNA damage (Weber, Ludwig et al. 2005; Johansen, Vestergaard et al. 2009).

MK2 regulates the p38-MAPK inflammatory response by through post-transcriptional mechanisms. MK2 activity increases the production of TNF, IL-6, COX-2, chemokines and

other inflammatory mediators by promoting the stability of mRNA encoding for these proteins. The stability of these mRNAs is dependent on the presence of AU-rich elements (AREs) located on the 3'-untranslated regions (UTRs). Tristetraprolin (TTP) initiates ARE-containing mRNA decay by promoting removal of the poly A tail by a process called deadenylation (Lai, Carballo et al. 1999). MK2 activation results in phosphorylation of TTP, which results in inhibition of TTP-dependent degradation of LPS-induced TNFα mRNA expression (Chrestensen, Schroeder et al. 2004; Stoecklin, Stubbs et al. 2004; Brook, Tchen et al. 2006). Recent work in my lab has suggested that phosphorylation of TTP inhibits its ability to recruit CCR4 CAF1 deadenylase, preventing deadenylation of ARE-containing mRNAs (Marchese, Aubareda et al. 2010). This work also demonstrated that 14-3-3 does not have a role in the mechanism of TTP-mediated mRNA deadenylation, as was previously thought (Stoecklin, Stubbs et al. 2004), although it could still have a role in mediating TTP subcellular localisation (Marchese, Aubareda et al. 2010).

A recent study has showed that MK2-mediated signalling is crucial for wound healing. MK-deficient mice have severely delayed wound healing compared to wild-type mice (Thuraisingam, Xu et al. 2010). In the same study, cytokine and chemokine levels were reduced in the wounds of MK2-deficient mice, however, no difference in the numbers of neutrophils and macrophages infiltrating the wounds was observed in MK2-deficient mice compared to wild-type mice (Thuraisingam, Xu et al. 2010). The authors suggested that a lack of the inflammatory response correlated with diminished capacity for wound healing in MK2-deficient mice (Thuraisingam, Xu et al. 2010).

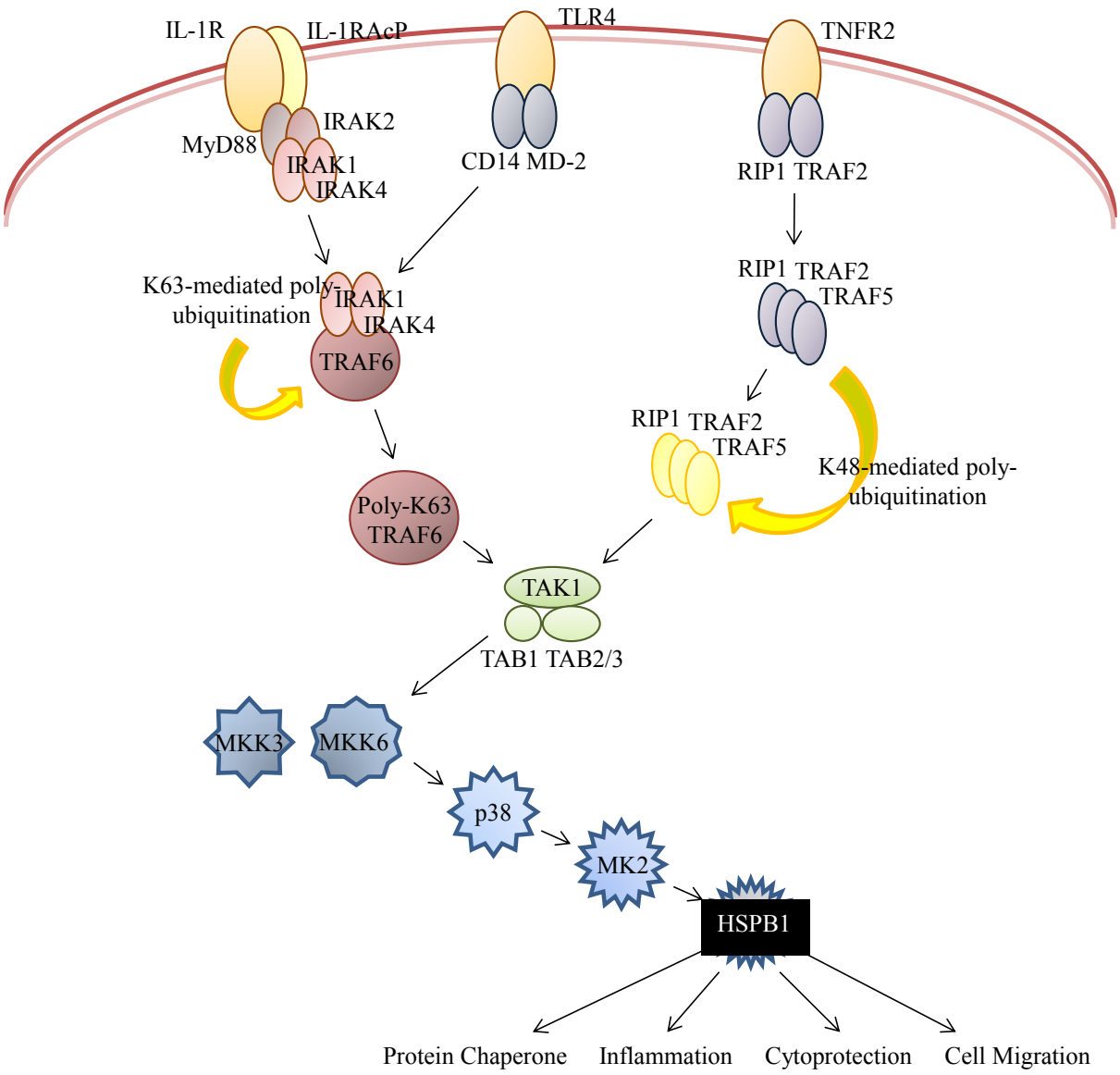

Figure 1.1 Schematic of pro-inflammatory signalling cascades resulting in activation of hspB1.

IL-1R, TLR and TNFR2 activation results in downstream signalling events that result formation of the TAK1 complex with TAB 1, 2 and 3. This results in TAK1 activation and phosphorylation of MKKs MKK3 and MMK6. These phosphorylate and activate p38 MAPK, which then phosphorylates and activates MK2. MK2 phosphorylates serine residues 15, 72 and 82 of hspB1, resulting in dimerisation and activation. Activated hspB1 has been shown to have a role as a inflammation, cytoprotetion, cell migration and acts as a protein chaperone.

1.5 Heat shock protein beta-1 (hspB1).

The cells of practically all organisms respond to stress stimuli by the rapid synthesis of a conserved group of proteins known as hsps. These proteins are ubiquitous, are expressed in all organisms, and are categorised by their different forms into families based on their molecular weights. The major families are hsp100/104, hsp90, hsp70, hsp60 and the small heat shock proteins, or shsps. (Kregel 2002) Many functional roles for hsps have been described, but the mechanisms for many of these roles are not entirely understood. Hsps have been shown to be induced by heat shock and a variety of other stresses, behave as molecular chaperones for other cellular proteins and have strong cytoprotective effects (Welch and Suhan 1986; Hightower 1991).

HspB1, also known as hsp27 in humans and hsp25 in mice, belongs to a family of small heat shock proteins (shsp). There are 10 proteins in this family which similar structure and have a monomer size typically in the range of 16-25 kDa. Examples include hspB1, αA-crystallin/hspB4 and αB-crystallin/hspB5 (Kappe, Franck et al. 2003). They all contain a highly conserved α-crystallin domain and have a less conserved N-terminal WDPF region (so called due to the sequence of amino acid residues (Lambert, Charette et al. 1999). These regions are thought to be important for the oligomerisation of hspB1. The C-terminal region is known as the 'flexible region' as it has little sequence homology within the shsp family, although it too has been suggested to be involved with hspB1 oligomerisation and to be important for hspB1 solubility (Lelj-Garolla and Mauk 2005).

Constitutive hspB1 expression is restricted to only a few cell types. HspB1 is strongly expressed in mouse skeletal muscle tissue with lower levels in epithelial cells. In adult mice, hspB1 was found to be expressed in the ear, skin (including panniculous carnosus and hair follicles), tongue, oesophagus, fallopian tubes and the interventricular septum of the heart,

but barely in any other cardiac compartments (Huang, Min et al. 2007). It is also expressed during mouse embryonic development, in particular in the cardiac tube and cerebral vasculature (Huang, Min et al. 2007). HspB1 is not expressed in lung, liver, pancreas, spleen, small intestine and colon (Huang, Min et al. 2007). HspB1 expression is induced in response to heat shock (Chretien and Landry 1988), oxidative stress (Okada, Otani et al. 2005), osmotic stress (Garmyn, Mammone et al. 2001). Previous work in my laboratory has been unable to detect hspB1 in mouse bone marrow derived macrophages, RAW 264.7 mouse macrophage-like cells, human monocytes, human neutrophils or T-cells (Brennan 2009). HspB1 was not detected in resting human monocytes, however, it is detectable in human monocytes differentiated into macrophages using either macrophage colony-stimulating factor (M-CSF) or granulocyte-monocyte colony-stimulating factor (GM-CSF) (Brennan 2009). HspB1 was detected in human endothelial cells, fibroblasts, HeLa cells (Alford, Glennie et al. 2007) and hypertrophic chondrocytes, but not resting or proliferating chondrocytes (Otsuka, Kubo et al. 1996; Vanmuylder, Evrard et al. 1997).

1.5.1 Phosphorylation of hspB1.

HspB1 is phosphorylated in response to heat shock (Chretien and Landry 1988), TNFα and IL-1-treatment (Kaur, Welch et al. 1989; Saklatvala, Kaur et al. 1991; Guesdon, Freshney et al. 1993), oxidative stress (Okada, Otani et al. 2005), osmotic stress (Garmyn, Mammone et al. 2001) and other cellular stresses (Kostenko and Moens 2009). Investigation of hspB1 phosphorylation *in vitro* led to the purification of the upstream kinase cascade, which is now known to be the p38 MAPK pathway (Freshney, Rawlinson et al. 1994). Human hspB1 is phosphorylated at three serine residues, Ser-15 (located on the WDPF domain), Ser-78 and Ser-82 (Landry, Lambert et al. 1992) by mitogen-activated protein kinase MK2 (Ahlers, Belka et al. 1994). HspB1 is also phosphorylated by MK3 *in vitro* (Clifton, Young et al.

1996) and MK5 in response to activation by cAMP/PKA (Gerits, Mikalsen et al. 2007). PKD has also been shown to phosphorylate hspB1 (Doppler, Storz et al. 2005; Stetler, Gao et al. 2012). However, it is thought that MK2 is the main kinase responsible for hspB1 phosphorylation. Murine hspB1 is phosphorylated by MK2 at serine residues 15 and 86 (Ser-86 in hsp25 being the equivalent of Ser-82 in hsp27 (Stokoe, Engel et al. 1992)). Phosphorylation of hspB1 has been postulated to modulate the structural and functional properties of the protein. Unphosphorylated hspB1 exists in the cytoplasm with an average mass of ~530-700 kDa, which equates to an oligomer comprised of approximately 24 subunits, which upon phosphorylation, dissociates into dimers and monomers (Lambert, Charette et al. 1999; Rogalla, Ehrnsperger et al. 1999; Lelj-Garolla and Mauk 2005).

1.5.2 The role of hspB1 as a protein chaperone.

Like the other hsps, hspB1 has chaperone-like properties and refolds denatured proteins, preventing their aggregation. The chaperone activity of hspB1 is ATP-independent (Knauf, Jakob et al. 1994), unlike the ATP-dependent chaperone activity of larger hsps, such as hsp70 and hsp90 (Young 2010; Neckers and Workman 2012). HspB1 has been shown to prevent aggregation of denatured α-glucosidase under thermal stress and to be required for correct refolding and reactivation of the enzyme following denaturation with urea (Jakob, Gaestel et al. 1993). It has been demonstrated that hspB1 can adopt a number of oligomerisation sates, and that larger oligomers are formed at higher temperatures (Lelj-Garolla and Mauk 2006). In addition, the chaperone activity of hspB1 is increased at higher temperatures, as indicated by inhibition of dithiothretiol-induced insulin aggregation, with a sharp increase in activity at 34-43^{o}C. This suggests that the protein chaperone function of hspB1 is increased as temperature is increased within a range that is relevant to physiological heat shock (Lelj-Garolla and Mauk 2006). Considering large oligomeric structures of hspB1 separate into

hspB1 dimers upon phosphorylation, it is thought that the protein chaperone function of hspB1 is dependent upon its oligomeric structure. It has been suggested that a part of the N-terminal region (amino acid residues 31-95) of hspB1 is involved in oligomerisation and chaperone function (Haslbeck, Ignatiou et al. 2004). It has been demonstrated that phosphorylation and dimerisation of hspB1 is not required to provide thermoresistance and the assisted refolding of denatured proteins (Knauf, Jakob et al. 1994). In fact, the ability of hspB1 to act as a protein chaperone has been shown to be decreased when hspB1 is phosphorylated (Rogalla, Ehrnsperger et al. 1999). It has been shown that during thermal stress hspB1 binds to the cap-binding mRNA translation initiation factor, eIF4G, which is critical for the translation of most cellular mRNAs (Cuesta, Laroia et al. 2000). This interaction was proposed to prevent eIF4G from initiating translation (Cuesta, Laroia et al. 2000). However, these findings have yet to be corroborated.

HspB1 has also been demonstrated to mediate ubiquitination of proteins and induce proteasomal degradation. It has been recently shown that phosphomimetic mutations of phosphorylation target serines to aspartic acid residues in hspB1 promotes degradation of AUF1 isoforms by proteasomes, thus promoting stabilisation of ARE-containing mRNAs (Li, Defren et al. 2013). These data would suggest that hspB1 phosphorylation stabilises the mRNA encoding for pro-inflammatory genes. HspB1 also induces the ubiquitination of cyclin-dependent kinase inhibitor $p27^{Kip1}$ and facilities cell cycle transition through G_1/S, enhancing cell proliferation (Parcellier, Brunet et al. 2006).

1.5.3 The regulation of the cytoskeleton by hspB1.

HspB1 has been suggested to act *in vitro* as an F-actin cap binding protein which inhibits actin polymerisation and maintains cytoskeletal integrity in response to stress (Landry and Huot 1995). Phosphorylation of hspB1 by p38 MAPK has been shown be required for actin

microfilament stability and increased rate of recovery of disrupted filaments (Guay, Lambert et al. 1997), however, this experiment used very high concentrations (10 μM and 25 μM) of SB203580 to achieve p38 MAPK-inhibition, which may introduce non-specific effects. The Induction of hspB1 in bovine arterial endothelial cells resulted in an increase in migration, whereas transfection with non-phosphorylatable hspB1 resulted in a decrease in migration (Piotrowicz, Hickey et al. 1998). It has been demonstrated that p38 MAPK activation and subsequent hspB1 phosphorylation is required for rearrangement of actin cytoskeleton and cell migration in human umbilical vein endothelial cells (HUVECs) treated with vascular endothelial growth factor (VEGF) (Rousseau, Houle et al. 1997). However, another study has shown that inhibition of cell migration by the chemotherapeutic agent cisplatin in HUVECs is not p38 MAPK-dependent (Montiel, Urso et al. 2009).

Wound contraction is a critical process for the healing of wounds, involving re-epithelialisation, connective tissue deposition and contraction, which is mediated by cells within the wound granulation tissue (Watts, Grillo et al. 1958; Martin 1997). The fibroblast-collagen matrix model provides a way to study the mechanisms of wound contraction, whereby mechanical loading is applied to the proliferating cells in culture (Grinnell 2000). Inhibition of hspB1/27 phosphorylation has been shown to result in delayed fibroblast-populated collage lattice (FPCL) contraction and the transient delay of wound contraction *in vivo* (Hirano, Rees et al. 2002). Another study has shown that over-expression of hspB1 results in enhanced fibroblast migration, elongation, adhesion and matrix contraction in a FPCL wound healing model (Hirano, Shelden et al. 2004).

Interpretation of the results supporting a role for hspB1 on cytoskeletal rearrangement must first take into consideration how the earliest experiments in this field were performed. One of the first publications suggesting a role for hspB1 inhibition of actin polymerisation were

performed using preparations of hspB1 purified from turkey gizzards (Miron, Vancompernolle et al. 1991). These preparations likely contained trace amounts of a potent inhibitor of actin polymerisation, cofilin, which has a molecular mass of 20-22 kDa (Panasenko, Kim et al. 2003). Purified hspB1 has since been shown to have little effect on the rate or extent of actin polymerisation (Panasenko, Kim et al. 2003).

1.5.4 The cytoprotective role of hspB1.

There is evidence that hspB1 is involved in the regulation of cell survival. HspB1 is cytoprotective against heat shock (Landry, Chretien et al. 1989) apoptosis inducing agents such as TNFα (Mehlen, Mehlen et al. 1995) and staurosporine (Mehlen, Schulze-Osthoff et al. 1996), oxidative stress agents, such as H_2O_2 (Huot, Houle et al. 1996) and anticancer drugs such as doxorubicin and cisplatin (Garrido, Ottavi et al. 1997). It has been demonstrated that hspB1 protects against TNFα and oxidative stress-induced cell death by its ability to increase the intracellular concentration of glutathione (Mehlen, Kretz-Remy et al. 1996). HspB1 has been shown to regulate 'intrinsic', mitochondria-dependent signalling by preventing cytochrome c release from the mitochondria, and binding procaspase-3 (Concannon, Orrenius et al. 2001). This prevents the activation of caspase-3, preventing formation of the apoptosome during caspase-dependent apoptotic stress events, such as accumulation of aggregated protein (Charette, Lavoie et al. 2000). HspB1 has also been shown to bind to apoptosis signal-retulating kinase-1 (ASK1) and DAXX, a FAS-associated protein (Charette and Landry 2000). 'Extrinsic' initiators of apoptosis, such as TNFα and reactive oxygen species, act as ligands at the FAS 'death' receptor. HspB1 binds to DAXX and prevents it from binding FAS at the cell surface membrane, an interaction that is required downstream FAS activation of pro-caspase-8, an initiator caspase for pro-caspase-3 (Charette and Landry 2000; Concannon, Orrenius et al. 2001; Gabai and Sherman 2002).

Overexpression of human hspB1 in mice has demonstrated that hspB1 protects against liver and kidney damage after liver ischemia-reperfusion injury (IRI) (Park, Chen et al. 2009). In addition, the overexpression of human hspB1 in mice showed decreased induction of several pro-inflammatory mRNAs, a decrease in neutrophil migration and a decrease number of cells undergoing apoptosis in the kidney after IRI (Park, Chen et al. 2009). Another study came to the opposite conclusion, showing that mice overexpressing human hspB1 had decreased renal function and increased renal expression of TNFα, ICAM1 and CCL2 mRNA and CXCL1 protein, although this study also shows that the overexpression of human hspB1 in murine renal tubular cells protects against H_2O_2-induced necrosis *in vitro* (Chen, Kim et al. 2009). PKD-mediated phosphorylation of hspB1 has been shown to be required for neuroprotection against transient focal cerebral ischemia in hspB1-overexpressing mice, (Stetler, Gao et al. 2012). However, these over-expression studies do not address the role of the murine hspB1 in mice. There is currently no agreed common mechanism that explains the function of hspB1 in cytoprotection.

1.5.5 HspB1 in disease.

The cytoprotective functions of hspB1 was been implicated in providing protection to cancer cells against the cellular stress induced by many chemotherapeutic drugs. High hsp27 expression has been shown to be associated with a poor clinical outcome in colon cancer (Bauer, Nitsche et al. 2012). Strategies to reduce hspB1 expression in cancer such as breast (Song, Ethier et al. 2004), colon (Garrido, Mehlen et al. 1996), ovarian (Song, Zhang et al. 2009), prostate (Andrieu, Taieb et al. 2010), bladder (Hadaschik, Jackson et al. 2008), and pancreatic (Xia, Liu et al. 2009) have been shown to reduce slow tumour growth and metastatic potential. Cell-cell contact has been show to promote the oligomerisation of hspB1 into large structures, regardless of phosphorylation state, which enhance its cytoprotective

activity. This has been suggested to a mechanism to describe the method by which hspB1 increases cell tumorigenicity (Bruey, Paul et al. 2000). There is limited data to suggest that hspB1 has a role in protecting the cell through autophagy. siRNA-mediated HspB1 depletion in A549 human alveolar epithelial cells inhibited prevented apoptosis and instead resulted in necrosis in response to heat shock (Lim, Duong et al. 2010).

HspB1 has been shown to play an important role in inhibiting ER stress-mediated apoptosis (Gupta, Deepti et al. 2010). Hepatocellular carcinoma (HCC) is a common solid malignancy and has a high degree of drug resistance (Wakamatsu, Nakahashi et al. 2007). Cisplatin is an anti-cancer drug that is one of the few drugs capable of treating HCC (Yoshikawa, Ono et al. 2008). The endoplasmic reticulum (ER) is an organelle that is required for the synthesis and maturation of proteins. ER stress can result in to disruption of ER functions and leads to the accumulation of misfolded proteins, and initiates the unfolded protein response (UPR), which promotes cell survival in the event of ER stress (Rutkowski and Kaufman 2004). Autophagy is a component of the UPR (Hoyer-Hansen and Jaattela 2007) and is a catabolic process required for the degradation and recycling of cellular components (Lum, DeBerardinis et al. 2005). Autophagy promotes cell survival under conditions of cell stress and nutrient starvation (Baehrecke 2005) and is one of the most important mechanisms enabling cancer survival and recurrence following long-term chemotherapy (Chen, Dai et al. 2011). siRNA mediated depletion of hspB1 suppresses ER stress and cisplatin-induced autophagy and apoptosis in HCC cells. This suggests that targeting of hspB1 regulation of the UPR might provide therapeutic benefits in the treatment of HCC (Chen, Dai et al. 2011). HspB1 inhibition by OGX-427, an antisense oligo therapy, has been shown to reduce tumour metastasis in a murine model of prostate cancer and castration resistant prostate cancer in patients in a phase I clinical trial (Shiota, Bishop et al. 2013) and is currently in six phase II clinical trials for the treatment of four cancer types.

Diseases such as distal hereditary motor neuropathies (dHMN) and Charcot-Marie-Tooth disease (CMT) involve motor and/or sensory neuronal abnormalities. As of 2012 fifteen different autosomal dominant mutations have been identifies in families with CMT and/or dHMN. The majority of these mutations are within the α-crystallin domain of hspB1. Mutations in the C-terminal domain of hspB1 present a more severe phenotype with earlier onset. The loss of the ability of hspB1 to clear aggregated neurofilaments due to increased and defective chaperone activity has been proposed to be the cause of these diseases (Almeida-Souza, Goethals et al. 2010; Rossor, Kalmar et al. 2012). An accumulation and impaired clearing of protein aggregates is also associated with Alzheimer's disease (AD) (Smith, Rosen et al. 2005). HspB1 expression has been found to be enhanced in neurons with amyloid beta fibril plaques, which are associated with the pathogenesis of AD. However, the association of hspB1 and amyloid beta actually increases the toxic effect, which has been suggested to be a result of hspB1 altering conformation of amyloid beta into a non-fibrile toxic form (Stege, Renkawek et al. 1999). Hyper-phosphorylated tau is a pathological hallmark and neurotoxic component of AD. Tau is a microtubule associated protein which has a role in the maintenance and stability of the microtubule network. Phosphorylation of tau releases it from the microtubule assembly, which can lead to neurofibil plaque formation. HspB1 interacts with and induces ubiquitination-independent degradation of pathological hyper-phosphorylated tau, which has been suggested a therapeutic basis for the treatment of AD (Shimura, Miura-Shimura et al. 2004).

Atherosclerosis is a chronic disease that underlies the pathology of cardiovascular disease and peripheral vascular disease and is a major cause of global mortality. It is a chronic inflammatory response in the arterial wall, caused by the accumulation of macrophages, low density lipoproteins and proliferation of vascular smooth muscle endothelial cells which form plaques within the arterial wall (Ghayour-Mobarhan, Saber et al. 2012). HspB1 expression

has been observed to be elevated in vascular tissue adjacent to atherosclerotic plaques compared to healthy reference tissue, although reduced hspB1 expression was observed in the lesion core. It has been suggested that the diminished hspB1 expression in the core is attributable to increased proteolytic activity in this area of the plaque (Wick 2006).

1.5.6 Extracellular hspB1.

Some studies have attempted to elucidate a role for extracellular hspB1 as a mediator of cellular processes. However the preparation of recombinant protein often results in contamination of the protein of interest with bacterial proteins, such as LPS or other contaminants. Hence, any such research where recombinant hspB1 is used as stimulus on cells must be considered with this in mind.

One such study has shown that treatment of human monocytes with recombinant human hspB1 resulted in a strong induction of IL-10 that p38 MAPK-dependent (De, Kodys et al. 2000). The authors proposed that this induction of IL-10 by recombinant hspB1 is independent of the effects of contaminating LPS, by demonstrating that the kinetics and extent of IL-10 production in response to a combination of Staphylococcal enterotoxin B (SEB) and muramyl dipeptide (MDP) (De, Kodys et al. 2000). The authors showed that this combination treatment resulted in significantly decreased IL-10 production compared to recombinant hspB1 treatment. Curiously, the authors did not determine the effect of LPS stimulation of IL-10 production in their experiment (De, Kodys et al. 2000). This, arguably, would have been a much more relevant experimental control. The authors proposed that treatment of monocytes resulted in p38 MAPK activation and increased hspB1 expression. This was determined by western blot (De, Kodys et al. 2000), a technique that would not have allowed the investigators the possibility of being able to differentiate between 2 μg/ml of recombinant hspB1 added and intracellular hspB1.

Another study has proposed a role for extracellular hspB1 in the suppression of the differentiation of monocytes into dendritic cells (Laudanski, De et al. 2007). Monocytes treated with recombinant hspB1, IL-4 and GM-CSF produced significantly greater levels of IL-10, M-CSF and IL-6 stimulated with IL-4 and GM-CSF alone. This effect was specific to recombinant human hsp27, as recombinant murine hsp25 did not mediate the same effect (Laudanski, De et al. 2007). The authors proposed that the regulation of the expression of these cytokines might affect monocyte/macrophage differentiation, and subsequently found that recombinant hspB1 and M-CSF derived macrophages had decreased phagocytic activity toward acetylated low-density lipoprotein, which is implicated in cardiovascular disease (Laudanski, De et al. 2007). The proposed mechanism for recombinant hpsB1 involved TLR and p38 MAPK signalling (Laudanski, De et al. 2007). The authors went the lengths to demonstrate that their observed recombinant hspB1-induced dysfunction of dendritic cell maturation was independent of the action of bacterial contaminants. Boiling and antibody-mediated neutralisation of hspB1 preparations rendered it inactive and did not induce the effects observed with functional recombinant hspB1 (Laudanski, De et al. 2007). However, the assays used to detect LPS were not very sensitive and the data directly confirming the absence of LPS and the activity of other proposed bacterial contaminants was not shown (Laudanski, De et al. 2007).

Another group showed that heterozygous heat shock factor (*hsf1*$^{+/-}$) mouse plasma, which contains 4 times higher extracellular hspB1 compared to plasma from wild-type mice, improved cardiac function and survival post-doxorubicin treatment in mice pre-treatd with *hsf1*$^{+/-}$ mouse plasma compared to mice pre-treated with normal mouse serum (Krishnamurthy, Kanagasabai et al. 2012). Mice treated with ehspB1-enriched serum or recombinant human hspB1 had elevated serum levels of IL-6 and TNFα, although the production of these cytokines was diminished post-doxorubicin treatment in these mice

control mice (Krishnamurthy, Kanagasabai et al. 2012). The authors acknowledged their previous findings, showing that deceased serum ehspB1 levels resulted in increased cardiomyocyte protection via a mechanism involving deceased p53-indcuced expression of the pro-apoptotic mediate bax (Vedam, Nishijima et al. 2010), contrasted with the recent findings (Krishnamurthy, Kanagasabai et al. 2012). The research in the field of the function of extracellular hspB1 is complicated by contradictory results from different groups, or even within the same group, and often poor control for the effects of contaminating bacterial products in recombinant ehspB1 preparations.

1.5.7 The role of hspB1 in inflammation.

A number of reports have shown that pro-inflammatory signalling is regulated by hspB1; however, different conclusions have been reached. HspB1 has been shown to be required for IL-1 induced activation of MK2 (Alford, Glennie et al. 2007). HspB1 depletion, using multiple siRNA oligo duplexes, has been shown to decrease IL-1 induced p38 and JNK activity, as well as inhibit the activity of upstream p38 MAPK activators (MKK3 and MKK6) and JNK activators (MKK 4 and MKK7) (Alford, Glennie et al. 2007). HspB1 was shown to be required for maximal activation of TAK1 by IL-1 and activation of JNK by TNFα in HeLa cells (Alford, Glennie et al. 2007). IL-1 induced ERK activity is not regulated by hspB1 (Alford, Glennie et al. 2007). HspB1 is also involved in the NF-κB inflammatory pathway. HspB1 depletion results in an inhibition of IKKβ but does not regulate IκBα degradation in IL-1-stimulated human fibroblasts (Alford, Glennie et al. 2007). This suggests that hspB1 is required for the activation of IKKβ. Depletion of TAK1 or hspB1 did not block IκBα degradation, although this may be the result of residual IKKβ activity in the hspB1 depleted cells (Alford, Glennie et al. 2007).

A different study showed that hspB1 regulates IL-1β-induced NF-κB activation by augmenting IL-1β-induced TRAF6 ubiquitination and IKK activation in human embryonic kidney 293 (HEK293) cells (Wu, Liu et al. 2009). IL-1β stimulation was also shown to reduce endogenous hspB1/TRAF6 association in these cells (Wu, Liu et al. 2009). Inhibition of hspB1 phosphorylation by p38 inhibition or MK2 siRNA depletion using a single oligo duplex increases hspB1/TRAF6 association, resulting in increased TRAF6 ubiquitination, IKK phosphorylation and NF-κB activation in HeLa cells (Wu, Liu et al. 2009). Another report using a single siRNA-mediated depletion of hspB1 showed that TNFα-induced NF-κB activation and inflammatory gene expression in HUVEC was inhibited (Gorska, Liang et al. 2007). These results suggest that phosphorylation of hspB1 results in a negative feedback loop in the regulation of IL-1/TNFα-induced signalling. All three of the above mentioned studies suggest that depletion of hspB1 inhibits signalling or inflammatory gene expression but in each case the proposed mechanism differs.

A different study has shown that p38 and MK2 activation is required for ICAM1 and IL-8 expression in human lung vascular endothelial cells (Acosta, del Barco et al. 2008). Another study also demonstrated, using a single siRNA oligo duplex to deplete hspB1 protein, that hspB1 is not involved in the regulation of ICAM-1 and IL-8 by p38 and MK2 (Su, Ao et al. 2008). The results suggesting that hspB1 is not involved in p38/MK2 signalling (Su, Ao et al. 2008) do not correlate with those indicating that hspB1 is required for activation of TAK-1, p38 and MK2 (Alford, Glennie et al. 2007). Inhibition of p38 MAPK in HeLa cells disrupted the association of hspB1 with IKKβ, resulting in increased IKKβ activity (Park, Gaynor et al. 2003). This study indicated that hspB1 phosphorylation results in down regulation of IKKβ activity following stimulation with TNFα (Park, Gaynor et al. 2003). Yet another study demonstrated that siRNA-mediated depletion of hspB1 resulted in increased PGE2 and IL-8 production in TNFα stimulated keratinocytes, which was associated

with increased NF-κB activity (Sur, Lyte et al. 2008). The different cells used and the different protocols for siRNA transfection used in these experiments may account for the different results. These results also indicate that hspB1 may have a different role in the regulation of inflammatory gene expression in different cell types.

1.5.8 The *in vivo* function of hspB1 in mice.

Investigations on hspB1 knockout mice by another research group have shown that despite constitutive hspB1 expression in many tissues in wild type mice, there were no apparent morphological abnormalities in new-born or adult *hspB1*$^{-/-}$ mice (Huang, Min et al. 2007). HspB1 has been shown to act synergistically with hsp70 to provide thermoprotection, although hspB1 protein expression was not up-regulated in response to heat shock in mice tissues (Huang, Min et al. 2007). This contrasted with increased hsp70 protein expression in mouse tissues in response to heat shock (Huang, Min et al. 2007). These findings using *hspB1*$^{-/-}$ mice have developed the hypothesis that a multitude of heat shock proteins are required for cells to develop maximal resistance to thermal challenge. *HspB1*$^{-/-}$ mouse embryonic fibroblasts (MEF) did not have significant changes in sensitivity to apoptotic stimuli, including X-rays, etoposide, serum starvation or oxidative stress, compared to wild-type (Huang, L. et al., 2007). However, the method of genetic disruption of *hspB1* in the mice used in this study involved targeted insertion of a 3.5 kb fragment containing the lacZ reporter sequence. After recombination this insert only replaced the start codon, the first exon and a portion of the first intron of *hspB1*, which meant that the second and third exons were still intact (Huang, Min et al. 2007). This technique did not eliminate the possibility of expression of structurally altered but potentially active hspB1 expressed in these mice.

1.6 Project Aims.

The aim of the project outlined in this thesis was to investigate the role of hspB1 in inflammation through the use of *in vivo* physiologically relevant murine models. Previous work in my laboratory demonstrated, by depletion of hspB1 protein by RNAi, that hspB1 is required for IL-1- and TNFα-induced receptor-proximal and downstream signalling, and is required for the IL-1-induced expression of the pro-inflammatory mediators COX-2, IL-6 and IL-8 in HeLa cells (Alford, Glennie et al. 2007). We have commercially generated *hspB1* knockout *hspB1*$^{del/del}$ mice by Cre–recombinase/LoxP deletion, which we then backcrossed onto a C57BL/6 background. Despite being identified as a substrate of MK2 and a component of the p38 MAPK signalling pathway, there is disagreement about the role of hspB1 in inflammation and the function of hspB1 *in vivo* is still unknown. The availability of an established colony of *hspB1*$^{del/del}$ mice afforded us the opportunity to investigate the physiological role of hspB1 in the regulation of inflammation *in vivo* and avoid potential artefacts arising from transient protein depletion strategies or the existence of truncated hspB1. Based on previous work performed in my lab demonstrating that hspB1 is required for the IL-1 induced inflammatory response in HeLa cells, the aim of this project was to determine the role of hspB1 in the inflammatory response *in vivo* and *in vitro* using *hspB1*$^{del/del}$ mice and cells.

Chapter 2

Materials and Methods

2.1 Materials.

2.1.1 General Reagents.

Deionised water purified by reverse osmosis was used for all applications, unless otherwise stated.

Reagent	Supplier	Product Code
10x phosphate buffered saline (PBS)	VWR	427117K
4mm Biopsy Punch	Stiefel	0372
Agarose	Invitrogen	16500
Ammonia	VWR	10004703
Aprotonin	Sigma	A6279
Bovine serum albumin (BSA)	PAA	K41-001
Bromophenol Blue sodium salt	Sigma	B8026
Cell culture water, EP grade, sterile	PAA	515-012
Cell proliferation kit (MTT)	Roche	11 465 007 001
Coomassie Brilliant Blue G	Sigma	B1131
Dithiothreitol (DTT)	Alexis	280-001-G025
DMEM	Lonza	BE12-604F
Dulbecco's PBS without $Ca^{2+,}$ Mg^{2+}	PAA	H15-011
EDTA	VWR	20302.266

EGTA	Sigma	E4378
Fetal Bovine Serum (FBS)	Gibco	10500-064
FITC Annexin V apoptosis Detection Kit II	BD	556570
Glacial Acetic acid	VWR	20104.334
Glycerol	VWR	24388.260
Glycine	Sigma	G8898
H_2O_2	Sigma	21676-3
H_2SO_4	VWR	102761C
HCl	VWR	20252.335
Igepal	Sigma	CA-630
Isofurane-Vet™	Merial	AP/DRUGS/220/96
LPS from E.Coli serotype EH 100 (TLRgrade™)	Alexis	581-010-L002
MACS MS columns	Miltenyi Biotec	130-042-401
Methanol	VWR	20847.320
Microcystin– LR	Enzo	ALX-350-012-C100
Neutrophil isolation Kit	Miltenyi Biotec	130-097-658
Non-fat dried milk powder	Marvel	92964
Nuclease free water	Promega	P1195
Pentobarbitone	Animalcare	BN7352

Penicillin/Streptomycin	PAA	P11-010
Pepstatin A	Sigma	P5318
phenylmethanesulfonylfluoride (PMSF)	Sigma	P7626
Pierce® BCA protein assay kit	Thermo Scientific	23227
Protease Inhibitor Cocktail	Sigma	P3840
'Polysceen' PVDF transfer membrane	Perkin Elmer	NEF1005001PK
Qiashredder homogeniser kit	Qiagen	79656
Quadro-MACS magnetic separator	Miltenyi Biotec	130-090-976
Red blood cell lysing buffer	Sigma	R7757
Sodium Azide	Sigma	S2002
Sodium chloride	VWR	31535.292
Sodium citrate dehydrate	Sigma	C0909
Sodium dodecyl sulphate (SDS)	Sigma	L4390
Sodium fluoride	Sigma	S1504
Sodium orthovanadate	Sigma	S6508
Streptavidin HRP	R&D	890803
TEMED	Sigma	T9281
Thioglycollate medium, Brewer's modification	BD	211716

Tris HCl	Sigma	3253
triton X-100	Fischer Chemical	T/3751/08
Trizma base	Sigma	T1503
Trypan blue solution (0.4%)	Sigma	T8154
Zymosan A from *Saccharomyces cerevisiae*	Sigma	Z4250

Table 2.1.1 General Reagents

2.1.2 Antibodies.

Primary antibodies for western blot were prepared by diluting in 5% non-fat dried milk powder/0.05% Tween20/PBS. Horse radish peroxidase (HRP)-conjugated secondary antibodies were used for western blotting and were prepared in the absence of sodium azide, which is a potent inhibitor of HRP. Biotinylated secondary antibodies were used for immunohistochemistry.

Antibody	**Clone**	**Host/ Species**	**Supplier**	**Product Code**
Anti-Hsp70 [505]	Monoclonal	Mouse	Abcam	ab2787
Anti-Hsp90	Polyclonal	Rabbit	Abcam	ab13495
Anti-PARP (46D11)	Monoclonal	Rabbit	Cell Signalling	9532
Anti-neutrophil elastase	Polyclonal	Rabbit	Abcam	21595
Anti-mouse Ly-6C FITC	Monoclonal	Rat	BD	553104
Alexa Fluor® 488 anti-mouse CD31	Monoclonal	Rat	BioLegend	102513
Anti-mouse CD11b PE/Cy7	Polyclonal	Rat	BioLegend	101215
Anti-mouse F4/80	Polyclonal	Rat	BioLegend	123101
Anti-mouse COX-2	Polyclonal	Rabbit	Cayman	160126
P38 MAPK antibody	Polyclonal	Rabbit	Cell Signalling	9212
Phospho-p38 MAPK (Thr180/Tyr182)	Polyclonal	Rabbit	Cell Signalling	9211
Anti-mouse CD115 (c-fms) PE	Monoclonal	Rat	eBiosciences	12-1152-82
Anti-mouse F4/80 e450	Monoclonal	Rat	eBiosciences	48-4801-80

Anti-mouse Ly-6G (Gr-1) PE	Monoclonal	Rat	eBiosciences	12-5931-81
Anti-HspB1	Polyclonal	Rabbit	Enzo	ADI-SPA-801
Anti-ERK-1	Polyclonal	Rabbit	Santa Cruz	SC-94
Anti-actin antibody	Polyclonal	Rabbit	Sigma	A2066
Anti-a-tubulin	Monoclonal	Mouse	Sigma	T3526
Swine anti-rabbit immunoglobulins/HRP	Polyclonal	Swine	Dako	P0217
Rabbit anti-mouse immunoglobulins/HRP	Polyclonal	Rabbit	Dako	P0260
Biotinylated goat anti-rabbit IgG Antibody	Polyclonal	Goat	Vector	BA-1000
Biotinylated rabbit anti-rat IgG Antibody	Polyclonal	Rabbit	Vector	BA-4001

Table 2.1.2 Antibodies

2.1.3 PCR and RT-PCR reagents.

Reagent	Supplier	Product Code
Wizard SV Genomic DNA purification System	Promega	A2361
Roche (Expand Long Template)	Roche	11 681 842 001
RNeasy Mini Kit	Qiagen	74106
Proteinase K	Promega	V3021
GelRed Nuclei Acid Stain	Biotium	41003
High Capacity cDNA reverse transcription Kit	ABI	4368814
FailSafe PCR 2x PreMix Buffer D, Buffer J	Epicentre	FSP995D FSP995J
Ethidium Bromide	BDH	443922U
BIOTAQ DNA	Bioline	BIO-21039
2 Kb Plus DNA ladder	Invitrogen	10787-018

Table 2.1.3 PCR and RT-PCR reagents.

2.1.4 SDS-PAGE and western blot reagents.

Reagent	Supplier	Product Code
10x Plus Strong ReBlot	Millipore	2564
10x 0.25M Tris, 1.92M glycine, 1% SDS (SDS-PAGE running buffer)	National Diagnostics	EC-870
Precision Plus Protein Standards, All Blue	Bio-Rad	161-0373
Chemiluminescence detection kit (ECL)	GE Healthcare	RPN2209

Table 2.1.4 SDS-PAGE and western blot reagents

2.1.5 Enzyme-linked immunosorbent assay (ELISA) reagents.

ELISA KIT	Blocking solution and reagent diluent	Supplier	Product Code
Mouse IL-1α	1% BSA	R&D	DY400
Mouse IL-1β	1% BSA	R&D	DY401
Mouse IL-6 OptEIA	10% FCS	BD	555240
Mouse IL-10 OptEIA	10% FCS	BD	555252
Mouse IL-23 Ready-SET-GO!®	Supplied	eBioscience	88-7234
Mouse TNF OptEIA	10% FCS	BD	555268
Mouse CCL2	1% BSA	R&D	DY479
Mouse CCL3	1% BSA	R&D	DY450
Mouse CXCL2/MIP-2 DuoSet	1% BSA	R&D	DY452

Mouse CXCL1/KC DuoSet	1% BSA	R&D	DY453
Paremeter PGE_2	Supplied	R&D	KGE004B

Table 2.1.5 ELISA reagents

2.1.6 Immunohistochemistry (IHC) reagents.

Reagent	Supplier	Product Code
DPX mounting medium	Cell Path	SEA-0302-00A
Paraformaldehyde (Cell Stor^{TM})	Cellpath	BAF-6000-08A
Trichrome Stain (Masson)	Tcsbiosciences	HS773
Vectastain Elite ABComplex kit	Vector	PK-6100
Immedge hydrophobic pen	Vector	H-4000
3, 3'-diaminobenzidine (DAB) peroxidase substrate kit	Vector	SK-4100
OCT	VWR	25608-930
Acetone	Sigma	534064

Table 2.1.6 IHC reagents

2.1.7 Buffers:

50x Tris-Acetate-EDTA (TAE):

242 g Tris, 57.1 ml glacial acetic acid, 18.6 g EDTA pH 8.0 in brought to 1 L volume.

TBS:

20 mM Tris HCl, 137 mM NaCl, pH 7.6.

4x Sodium dodecyl sulphate-polyacrylamide gel electrophoresis (SDS-PAGE) sample buffer:

250 mM Tris pH 6.8, 35% glycerol, 8 % SDS, 0.2 mg/ml bromophenol blue. Prior to use, DTT was added for a final concentration of 50 mM.

Whole cell lysis buffer:

(50 mM Tris HCl pH 7.5, 240 mM NaCl, 3mM EDTA, 3 mM EGTA, 1% triton X-100, 0.5% igepal, 10% glycerol, 1 mM PMSF, 5.5 μg/ml aprotonin, 1 ng/ml pepstatin, 2 mM DTT, 1 mM sodium vanadate, 2 mM sodium fluoride, 1 nM microcystin)

Western blot transfer buffer:

25 mM Tris, 192 mM Glycine, 20% (v/v) methanol.

PVDF membrane blocking solution:

(5% (w/v) Marvel non-fat dried milk powder, 1xPBS/1xTBS, 0.05% Tween-20)

TBS was used if the membrane was to be probed for phosphorylated protein.

Coomassie blue staining solution:

0.1 % (w/v) Coomassie Brilliant Blue G, 0.05 % (v/v) ethanol, 8.5 % (v/v) H_3P0_4.

Coomassie destain:

70 % (v/v) methanol.

Mouse tissue homogenisation buffer:

150 mM NaCl, 50 mM Tris HCl.

Sodium citrate buffer:

10 mM Sodium citrate dehydrate, 0.05 % Tween 20, pH 6.0.

MTT assay solubilisation solution:

10% SDS, 0.01M HCl.

FACS Buffer:

2% FCS, 2mM EDTA, PBS.

6x DNA loading buffer:

30 % glycerol, 0.25 % bromophenol blue

2.2 Methods.

2.2.1 Mice.

Targeting vector construction and knock-out strategy was designed and performed by genOway (Lyon, France). The genomic region of interest containing the murine *hspB1* locus was isolated by PCR from 129Sv/Pas ES cell genomic DNA. PCR fragments were subcloned into the pCRXL-TOPO or pCR4-TOPO vector (Invitrogen, Carlsbad, California). The resulting sequenced clones (containing whole *hspB1* gene sequence from promoter region to sequence downstream of exon 3) were used to construct the targeting vector. Briefly, a 3.3 kb region comprising exons 1 to 3 was flanked by a Neo cassette (*FRT* site-PGK promoter-Neo cDNA-FRT site-*Lox*P site) and a distal *Lox*P site in order to allow the generation of constitutive or conditional knock-out lines by deleting the whole gene (exons 1 to 3) of the *hspB1* gene. Linearised targeting vector was transfected into 129SvPas ES cells (genOway, Lyon, France) according to genOway's electroporation procedures (ie 10^8 ES cells in presence of 100 µg of linearised plasmid, 260 V, 500 µF). Positive selection was started 48 h after electroporation, by addition of 200 µg/ml of G418 (150 µg/ml of active component, Life Technologies, Inc.). 111 resistant clones were isolated and amplified in 96-well plates. The set of plates containing ES cell clones amplified on gelatin were genotyped by PCR: by amplification of the targeted locus: sense (Neo cassette), 5'-TGACTAGGGGAGGAGTAGAAGGTGGC-3'); antisense 5'-TCTTGCTACAAGCCTGGGACTCTGG-3'). Recombination of the targeted locus was confirmed by Southern blot analysis using internal and external probes on both 3' and 5' ends. Two clones were identified as correctly targeted at the *hspB1* locus. Clones were microinjected into C57BL/6 blastocysts, and gave rise to male chimeras with a significant ES cell contribution (as determined by an agouti coat colour). Mice were bred to wild-type C57BL/6 mice (*hspB1*^{flox} mice) and to C57BL/6 mice expressing Cre-recombinase to

generate a germline deletion of *hspB1* (*hspB1*$^{+/del}$ mice). Animals were then validated by *Spe* I Southern blot analysis using a 3' external probe. This confirmed that the founders were heterozygous for the 9.8 kb wild-type fragment with *hspB1*^{flox} mice displaying a 3.1 kb targeted Neo-excised signal and *hspB1*$^{+/del}$ mice showing a 6.5 kb *hspB1*-deleted signal.

The C57BL/6 mouse strain has been the standard choice for the creation and investigation of transgenic and knock-out mice (Zurita, Chagoyen et al. 2011). There are two major strains of these mice; C57BL/6J and C57BL/6N. The original strain is C57BL/6 J, or 'Jax' derived by The Jackson Laboratory in 1921. C57BL/6N is a subline that originated at the NIH in 1951. The C57BL/6 mouse strain was the second mammal and the first inbred mouse strain whose genome was sequenced (Waterston, Lindblad-Toh et al. 2002). The International Knockout Mouse Consortium has made progress on using embryonic stem (ES) cells isolated from C57BL/6N mice to systematically knockout every mouse gene (Pettitt, Liang et al. 2009; Skarnes, Rosen et al. 2011).

HspB1$^{+/del}$ mice were backcrossed for 12 generations (n = 12) onto a C57BL/6J background (Charles River). Heterozygotes were intercrossed to generate homozygous *hspB1*$^{del/del}$ and *hspB1*$^{+/+}$ littermate mice, which were expanded by incrossing for use in experiments. All mice were maintained at 21 °C ± 2 °C on a 12 h light/dark cycle with feed and water *ad libitum*. All animal experiments were approved by the local Ethical Review Process Committee and the UK Home Office.

2.2.2 Genotyping.

Mouse genotyping was assessed by PCR reactions on DNA extracted from mouse tail tips. DNA extraction was performed using the Wizard SV Genomic DNA purification System according to the manufacturer's instructions. Each tail tip was digested with proteinase K at 55 ^{o}C for 16 h. The DNA was extracted using a silica gel micro-column centrifugation with 4

wash steps. The DNA was eluted in two steps with washes of 250 µl of distilled water each giving a total of 500 µl and stored at 4 ^{o}C.

Our commercially generated constitutive *hspB1*$^{+/del}$ mouse line was supplied with instructions on how to genotype the mice. From this colony we derived *hspB1*$^{del/del}$ and littermate control wild-type mice. The ability to correctly identify the genotype of individual mice and cells obtained from them was critical to every aspect of the research undertaken using them. At the start of my project I had to overcome the difficulty of successfully amplifying the PCR products identifying the CRE-excised *hspB1*^{del} knock-out allele and the *hspB1*$^{+}$ wild-type allele. The instructions for genotyping the mice described the use of the Expand Long Template PCR system (Roche) but this approach was unsuccessful. It was very difficult to reproducibly amplify the wild-type allele. The decision was made to optimise the components of the PCR reaction mix. Previous work in my laboratory involved the use of pre-mixed 'FailSafe' (Epicentre) PCR buffers containing all of the reagents required for PCR, with the exception of the template DNA and DNA polymerase. Epicentre FailSafe buffer D had previously been successfully used to amplify long PCR products. This buffer was incorporated into the protocol for PCR amplicon of the wild-type allele and resulted in successful amplification compared to the 'Expand' Roche kit (Fig. 2.1A). This result made it possible to identify the genotype of individual mice and cells (Fig 2.1B).

The PCR reactions were set up immediately following DNA isolation and performed as follows. 10 µl of eluted DNA was added to a PCR reaction mixture containing 25 µl of FailSafe PCR 2x PreMix Buffer, (buffer J for amplification of the hspB1$^{del/del}$ amplicon, buffer D for the amplification of the wild-type amplicon), 14.35 µl of nuclease free water, 0.25 µl (1.25 U) of BIOTAQ DNA polymerase, and 0.2 µl of both the forward and reverse

primers required for the amplification of the specific amplicon, giving a final volume of 50 µl of PCR reaction mix. Primers were obtained from Eurofins MWG Operon.

The following primers were used to amplify a 600 bp fragment of *hspB1*$^{del/del}$ allele (forward: 5' AAT TCT AGC ACC CAC CTG GCA TTC C – 3', and reverse: 5'- AGC AGG GAG AGA AAT TAG CAG ATT GGC – 3'). The PCR programme was as follows: DNA was denatured (96 ^{o}C for 2 min), followed by 35 cycles of amplification (96 ^{o}C for 30 sec, 60 ^{o}C for 30 sec, and 68 ^{o}C for 7 min) with a final elongation step (68 ^{o}C for 8 min). The following primers were to amplify a 3.8 Kb sequence from the wild-type allele (forward: 5'- CTG GTG CAT CTG AAG GCA GTT ACG G -3', and reverse: 5'- TCT TGC TAC AAG CCT GGG ACT CTG G -3'). The PCR programme was as follows: DNA was denatured (96 ^{o}C for 2 min), followed by to 35 cycles of amplification (96 ^{o}C for 30 sec, 65 ^{o}C for 30 sec, and 68 ^{o}C for 300 sec), with a final elongation step (68 ^{o}C for 8 min).

10 µl of 6x DNA loading buffer was added to each 50 µl PCR product. PCR products were loaded and resolved on 2% agarose gels stained with 1 µg/ml ethidium bromide or 1 µg/ml GelRed Nuclei Acid Stain for visualisation. 2 Kb Plus DNA ladder was used to determine the sizes of the PCR amplicon.

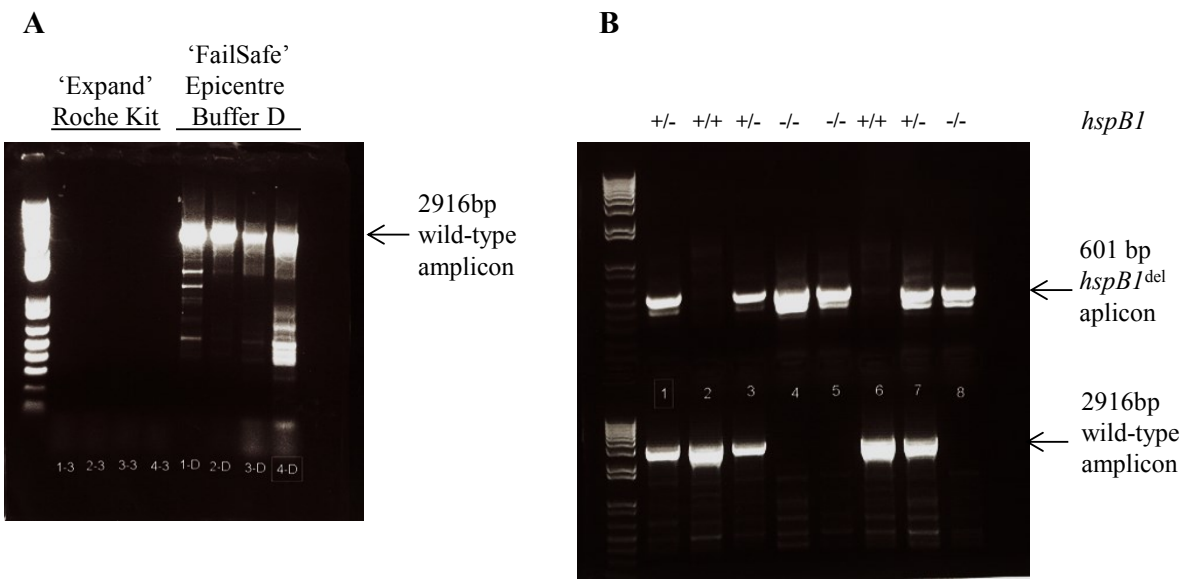

Figure 2.2.1 Successful amplification of wild-type PCR amplicon using Epicentre 'FailSafe buffer D' and an example of successful mouse genotyping for *hspB1*^{del} and wild-type PCR amplicons.

A, Four mouse tail genomic DNA samples, previously shown to be from wild-type mice, were used in a PCR amplification reaction using either 'Expand' PCR long template kit (Roche) or 'FailSafe' Buffer D. The successful amplification of the 2916 bp wild-type PCR amplicon is shown. B, successful mouse genotyping by PCR amplification of the 601 bp *hspB1*^{del} and 2916 bp wild-type alleles. A Gel Red-stained agarose gel showing PCR products for a litter of mice containing homozygous *hspB1*$^{del/del}$ (-/-), wild-type (+/+) and heterozygous *hspB1*$^{+/del}$ (+/-) is shown.

2.2.3 Timed matings and mouse embryo extraction.

Breeding pairs of 8 – 10 week old *hspB1*$^{+/-}$ mice were set up on day 0 and checked for cervical plugs early each morning following partnership. Discovery of a plug was designated as day 0.5. On day 12.5 the pregnant female mouse was sacrificed by CO_2 asphyxiation. All of the following procedures were performed under sterile conditions. The uterus from the mother was isolated, immersed in 30 ml of PBS and washed with a further 30 ml PBS. The uterus was then transferred to a Petri dish containing PBS. Embryos were excised, washed and the heart and liver removed and discarded. The majority of the head was removed and placed in a 1.5 ml eppendorf tube, 100 µl of PBS added and the tissue was homogenised by passing it through a 30 G blunt ended needle to allow efficient digestion for DNA extraction and genotyping. The remaining tissue was cut into small pieces using a scalpel and forceps. 2 ml of trypsin (prewarmed to 37 ^{o}C) was added to each dish and the tissue homogenised as before. This was incubated at 37 ^{o}C with 5% CO_2 for 15 min. 8 ml of complete medium (DMEM + 10% FCS + penicillin and streptomycin) pre-warmed to 37^{o}C was added to each dish. Cells were plated out using one 10 cm dish per embryo and incubated at 37 ^{o}C with 5% CO_2. These murine embryonic fibroblasts (MEF) were designated as 'passage 0'.

2.2.4 Primary MEF culture.

Upon reaching confluence, the media on the cells was aspirated away and the cells washed with 5 ml of serum free DMEM. The media was gently swirled over the cells and aspirated. 5 ml of trypsin was added to the cells and the dish swirled to ensure even coverage. The dish was then placed in an incubator at 37 ^{o}C with 5% CO_2 for 2 min. The dishes were then briefly removed, tapped gently on the side to dislodge the cells and incubated at 37 ^{o}C with 5% CO_2 for 3 min. Once the cells had detached 5 ml of complete medium was added. The cell suspension was transferred to a 20 ml Falcon tube. Lumps of tissue, if present, were allowed

to settle to the bottom of the tube and the suspension transferred to a fresh tube. The cells were centrifuged at 2000 g for 5 min, the supernatant was discarded and the cells were resuspended in 5 ml of complete medium. The viable cell count was determined using 0.4% trypan blue and a haemocytometer. Cells were resuspended and seeded at a density of $1.2x10^6$ cells per 10 cm dish. Cells were used at passage 2 (P2) or three (P3) for experiments and seeded at a density of $2x10^5$ cells per well in 6 well plates.

2.2.5 Isolation of mRNA, reverse transcription into cDNA and quantitative real time reverse-transcription polymerase chain reaction (qRT-PCR).

Cells were rinsed with PBS and total RNA was extracted using the RNeasy Mini Kit. 1 μg of total RNA was reverse transcribed into cDNA using random primers and High Capacity cDNA reverse transcription Kit. qRT-PCR was performed using Taqman Gene expression assays (COX-2 Mm0478374_m1, IL-6 Mm99999064_m1, CXCL1 Mm00433859_m1 and GAPDH Mm99999915_g1) in a *Corbett* Rotor-Gene 6000 real time PCR cycler (Qiagen). The standard curve method was used for the quantification of the results and gene expression was normalized to GAPDH. These techniques were performed by Anna Aubareda, a post doctorate researcher in my lab.

2.2.6 Cell lysis.

Cells were placed on ice and culture medium was removed, which was then centrifuged at 2000 g for 5 min to pellet insoluble fragments. The resulting supernatants were then transferred to fresh eppendorf tubes and stored at -20 ^oC. Cells were washed twice with 1ml of ice cold PBS and lysed in 200 μl of complete lysis buffer for 10 min on ice. The lysates were then scraped from the wells and centrifuged at 13,000 g for 10 min at 4 ^oC. The supernatant was transferred to a fresh eppendorf tube and the lysate and a sample of lysis

buffer stored at -20 ^{o}C. PMSF was added immediately before use and the complete lysis buffer vortexed to ensure complete solubilisation.

2.2.7 Bradford assay.

Protein concentration in the samples was determined by Bradford assay (Bradford 1976). A small aliquot of lysate was added to 1ml of Bradford reagent and vortexed to mix. Lysis buffer was used as a blank. BSA was used to generate a standard curve. Absorbance at 595 nm was measured using a Biophotometer (Eppendorf) and protein concentrations were calculated.

2.2.8 Gel preparation.

Gels were prepared according to standard techniques (Garfin 1990) using tris-buffered polyacrylamide gels containing SDS with a stacking gel. A greater concentration of acrylamide was used if the proteins of interest were of a low molecular weight.

2.2.9 Protein sample preparation.

Lysates were thawed at room temperature and prepared in 4x SDS-PAGE sample buffer, which were then heated at 90 ^{o}C for 10 min.

2.2.10 SDS - polyacrylamide gel electrophoresis (SDS-PAGE).

Mini-gels were electrophoresed using Ultra-Pure 10X Electrophoresis Running Buffer diluted to 1X and run at 30 mA per gel with Bio Rad PowerPac Basic. 5 µl Precision Plus Protein Standards, All Blue was used as a molecular weight marker.

2.2.11 Transfer.

6 pieces of 3 mm paper and one sheet of PVDF membrane were cut to 5 cm x 8 cm. PVDF membrane was soaked in methanol for 2 min. The membrane was then rinsed twice with distilled water. The paper and membrane were then immersed in transfer buffer. A Bio-Rad Trans-Blot Cell western electroblotting tank was filled 2/3 full with transfer buffer and a 4 ^{o}C cooling element placed inside.

The transfer sandwich was assembled, containing the soaked 3 mm paper, the rehydrated PVDF membrane, and the SDS polyacrylamide gel containing the electrophoresed proteins, carefully rolling over at each stage of the assembly with a clean 10 ml stripette to remove any bubbles between the gel and PVDF membrane. The transfer sandwich was secured within a cassette and placed in the transfer tank, which was then filled with transfer buffer. The proteins were transferred to the PVDF membrane by electrophoresis at 100 V for 1 h. After completion of the transfer the PVDF membrane was stained with Coomassie Brilliant Blue staining solution to visualise the protein and then washed with Coomassie destain solution.

2.2.12 Blocking and detection.

The following incubation steps were carried out with agitation on a shaking platform. The membrane was blocked with blocking solution for 1 h at room temperature. The membrane was then treated with primary antibody at the appropriate dilution in blocking solution with 0.01% sodium azide for 1 h at room temperature or overnight at 4 ^{o}C. The membrane was washed three times with PBS-T/TBS-T followed by three 10 min washes. The membrane was then incubated with the appropriate dilution of horseradish peroxidise-conjugated secondary antibody in blocking solution for 1 h at room temperature. The membrane was washed as before. Protein bound antibody was then visualised using enhanced chemiluminescence (ECL) detection kit.

2.2.13 Stripping PVDF membrane of antibodies.

The membrane was rehydrated in methanol for 2 min before being washed in distilled water as before. The membrane was incubated with 1xReBlot for 15 min with vigorous shaking. The membrane was washed as before and blocked for 30 min at room temperature with fresh blocking solution. The membrane was then re-probed with the appropriate primary and secondary antibodies.

2.2.14 Preparation of Zymosan.

0.5 g zymosan A from *Saccharomyces cerevisiae* was reconstituted in 20 ml PBS until fully resuspended, and aliquoted in 1 ml volumes into 1.5 ml sterile eppendorf tubes. These were then heated at 95 °C for 30 min in order to eliminate endogenous phospholipase A_2 activity, as recommended by (Dieter, Altin et al. 1987). The zymosan was then centrifuged at 10,000*g* for 5 min. The pellet was washed twice with PBS and resuspended in 1ml sterile PBS to yield a 25 mg/ml final stock concentration.

2.2.15 Air pouch model of acute inflammation.

A variation on the air-pouch model, as previously described (Edwards, Sedgwick et al. 1981), was used. Male mice 8-12 weeks of age were anaesthetised using isofluorane. An air pouch was created on the dorsal surface of the mouse. This was achieved by pinching the mouse skin mid-way on the back and lifting to form a tented sheet of tissue. The needle was inserted at the base of this flap and 5 ml of sterile air was injected. If done correctly the air should accumulate under the pinched sheet of skin. Four days later the air pouch was topped up by injecting 3 ml sterile air directly into the established air pouch without anaesthesia. The following day 100 μl 1 mg/ml zymosan was then injected into the air pouch without anaesthesia. After the desired stimulation time had expired the mice were culled by

asphyxiation in CO_2. The pouches were then injected with 2 ml PBS, massaged, and 1 ml of exudate removed. This exudate was then spun at 1500 g for 5 min to pellet the infiltrated cells. The supernatant was removed and stored at -20 ^{o}C for cytokine content analysis. The cells were resuspended in 1 ml 1x PBS. 10 µl of this re-suspension was mixed with 10 µl of 0.4% trypan blue solution and manually analysed for total cell count per ml using a haemocytometer. Humane procedures were used in all animal work, adhering to Home Office guidelines.

2.2.16 Peritoneal model of acute inflammation.

Male mice 8-12 weeks of age were injected intra-peritoneally (IP) with zymosan suspension. This was achieved by picking the mouse up by the scruff off the neck to impair resistance and biting, and inverting to expose the abdomen. A volume of 500 µl 1 mg/ml zymosan suspension was injected towards the hind-quarter of the mouse, either side of the abdominal midline, for a total of 1 ml/mouse. This location of injection was important, as it avoided potential disruption by the needle to the viscera and branches of the superior mesenteric vessels. At the desired time point the mice were culled by CO_2 asphyxiation. The peritoneal cavity was lavaged with 5 ml of ice-cold PBS, massaged and the exudate retrieved. Exudates were centrifuged at 1500 g, cells counted as described for the air pouch model, and cytokine concentrations in supernatants measured by ELISA.

2.2.17 Excisional cutaneous wound healing model.

The dorsal surfaces of anaesthetised female mice 8-12 weeks of age were shaved with clippers and disinfected by swabbing with 70 % ethanol. Four full thickness excisional wounds (4 mm diameter) were created on the dorsum of the mouse using a 4mm biopsy punch. The wounds were digitally imaged on days 0, 3, 5 and 7 post-wounding. Mice were culled on day 1, 3 or 7 post-wounding. Skin sections were surgically removed and fixed in 4

% paraformaldehyde and embedded in paraffin for histology. 5 µm thick sections were cut using an Accu-Cut SRM 200 Rotary Microtome (Sakura). Tissue sections were deparaffinised by heating at 60 ^{o}C for 30 min before being washed twice in xylene and twice in 95 % ethanol and stained with Masson's Trichrome or processed for IHC. The wound areas and distances between epithelial tongues in 3 day old wound histological sections were calculated using Image J software (Bethesda, MD).

2.2.18 Enzyme-Linked Immunosorbent Assay (ELISA).

ELISA was used to determine cytokine concentrations in MEF culture supernatants and air pouch exudates. The ELISA kits used are shown in table 2.1.5 and were used according to the manufacturer's instructions. Capture antibodies were diluted in PBS and seeded to a 96 well flat bottomed polystyrene microwell plate (Corning) overnight at 4 ^{o}C with gentle shaking.

2.2.19 Immunohistochemistry.

The preparation of surgically isolated wounded mouse skin presented a challenge. Established techniques within my research institute were unsatisfactory, as they involved the dissection of each individual wound, followed by fixation and embedding in paraffin. This often resulted in the skin rolling or folding, and made it impossible to determine the orientation of the tissue. The folded tissue made it impossible to accurately measure the size of the wound by microscopy. The tissue would also lose structural integrity and often display many cutting artifacts.

I developed a technique whereby the entire wounded dorsum was removed and pinned flat to cardboard using needles at the corners of the skin. The skin was mounted with the external surface of the skin facing the board to prevent the internal dermal matrix adhering to the board and being detached when the skin was removed. A notch was made in the skin at the

top right corner nearest the head of the mouse so that the orientation of the skin could be identified later. Care was taken not to stretch the skin and increase the size of the wounds during this procedure. The mounted skin was immersed and fixed in 4 % formalin as before. This resulted in skin that was fixed, flat and rigid before being processed for paraffin embedding. During paraffin embedding, the skin was cut into strips, horizontally relative to the orientation of the skin, directly through the centre of the wounds, using a scalpel. The skin strips were then placed in paraffin wax with the wound faces orientated to the face of the wax that would be exposed to the cutting blade. These techniques resulted in improved structural integrity of wound tissue during the cutting process, the ability to identify the orientation and identity of individual wounds and were highly reproducible.

Optimisation of the anti-hspB1 antibody for use in IHC resulted in the discovery that heat-induced antigen retrieval was best performed using citrate buffer pH 6.0 in a pressure cooker for 90 s. The slides were allowed to reach room temperature naturally in the buffer, to avoid shock cooling the tissues which would often cause the tissue to contract suddenly and cause structural artifacts. Slides were blocked with 10 % serum/PBS, raised against the host in which the secondary antibody was raised, for 1 h and incubated with 1:1000 hspB1 antibody overnight at 4 ^{o}C. Endogenous peroxidase was blocked by incubation in PBS / H_2O_2 (0.3 %) for 15 min. Slides were incubated with 1:400 biotinylated goat anti-rabbit IgG for 1 h and with streptavidin-biotin HRP macromolecular complex for 45 min. All incubations were performed in a humid chamber at room temperature. Slides were rinsed with PBS/ Tween-20 (0.05%) between incubations. Sections were developed with DAB substrate and counterstained with haematoxylin, cleared in acid alcohol, dehydrated through sequential washes in 50 %, 70 %, 95 % and 100 % ethanol and cleared by washing twice in xylene. Coverslips were mounted using a Tissue Tek – Glas G2 (Sakura) and DPX mounting

medium/ Images were captured using an Olympus BX-51 microscope and Olympus DP-71 camera using the DP Controller software.

2.2.20 Frozen histology of mouse carotid arteries.

Carotid arteries from wild-type mice and *hspB1*$^{del/del}$ mice were embedded in OCT and frozen at -80^{o}C. The tissue was sectioned onto slides on a cryostat cryotome at -20^{o}C and the tissue fixed and permeabalised with acetone pre-cooled to -20^{o}C. The tissue was then stained by IHC and imaged. No heat induced antigen retrieval techniques were used, as this would destroy the tissue.

2.2.21 Magnetic, indirect isolation of thioglycollate elected peritoneal neutrophils.

Male mice 8–12 weeks of age were injected IP with 1ml 4 % Thioglycollate/PBS. Neutrophils were allowed to accumulate for 4 h. The peritoneal cavity was lavaged with 10 ml ice cold PBS and the collected cells counted. The Neutrophil Isolation Kit was used to indirectly purify the peritoneal neutrophils. Briefly, the cells were counted and resuspended in 200 µl FACS buffer/5x10^{7} cells. The cells were then incubated with neutrophil biotin-antibody cocktail followed by anti-biotin microbeads, with washing, as per the manufacturer's instructions. The cells were then transferred into MACS MS columns attached to a QuadroMACS magnetic separator (Miltenyi Biotec). The non-magnetically labelled neutrophils were rinsed with buffer and collected as described by the manufacturer's instructions. The MACS MS tubes were then washed and plunged into a fresh collection tube to collect the remaining magnetically labelled leukocytes. The successful enrichment of neutrophils was confirmed by Ly-6G and CD-11b detection of the enriched neutrophils and magnetically labelled flushed leukocytes by flow cytometry.

2.2.22 Identification of neutrophil population and apoptotic cells by flow cytometry.

Cells were counted and re-suspended in PBS /1 % BSA. For identification of neutrophils, and detection of apoptosis, cells were stained with anti-mouse Ly-6G PE and FITC Annexin V apoptosis Detection Kit II, respectively. Samples were analysed using a BD FACSCanto II flow cytometer and BD FACSDiva software. Data analysis was performed using FlowJo software.

2.2.23 Cardiac puncture for collection of circulating blood cells.

Male mice 10 – 14 weeks of age were anaesthetised by IP injection of pentobarbitone and blood collected by cardiac puncture. The erythrocytes were removed using red blood cell lysing buffer according to the manufacturer's instructions.

2.2.24 Cell proliferation (MTT) assay.

250,000 cells were seeded to 96 well microplates in a final volume of 100 µl and incubated at 37 ^{o}C, 5 % CO^2 for 24 h. 10 µl 3-(4,5-dimethylthiazol-2-yl)-2,5-diphenyltetrazolium bromide (MTT) was added (0.5 mg/ml final concentration) and cells incubated for 4 h at 37 °C, 5 % CO_2. The formazan salt formed was solubilized by adding 100 µl MTT assay solubilisation solution and incubating at 37 °C for 16 h. A_{570} was measured using A_{690} as a reference.

2.2.25 Excision and homogenisation of wounds for cytokine analysis.

A technique to harvest and homogenise wounded tissue to isolate a lysate suitable for protein concentration measurements was adapted from a previous study (Armstrong, Major et al. 2004). It was difficult and time consuming to homogenise fresh tissue and it was a concern the cytokine concentration in the samples would deplete over time as the samples were kept on ice before they were processed. During the initial wound excision step some of the wound tissues were cut using surgical scissors within the eppendorf tubes used to store them in homogenisation buffer. This did not improve the effectiveness of homogenisation. The

decision was made to freeze the samples at -20 ^{o}C overnight. This reduced the mechanical integrity of the wound tissue and made the tissue easy to homogenise using mechanical disruption. After homogenisation the sample represented a viscous suspension of lysate and mouse hair and cellular debris. I decided to use centrifugal disruption to fully isolate an aqueous lysate. The samples were loaded into QIAShredder homogeniser microcentrifuge spin-columns and centrifuged at 13,000 g for 10 min at 4 ^{o}C. This resulted in a dark, solid pellet of hair and other debris, a salmon-pink aqueous lysate and a fatty surface precipitate.

Female mice were wounded as before and culled 6 h post-wounding. The wounded skin was excised and 2 wounded skin sections per mouse were added to 600 µl tissue homogenisation buffer and stored at -20 ^{o}C for 24 h to disrupt tissue integrity. The tissue was homogenised using a Fisher Scientific PowerGen 125 homogeniser. The element was washed with 95 % ethanol followed by water to reduce cross-sample contamination. The tissue homogenates were than centrifuged at 13,000 g for 10 min at 4 ^{o}C in QiaShredder columns to fully homogenise the tissue. The aqueous phase was removed and the protein concentration determined by BCA assay according to the manufacturer's instructions. Cytokine content was determined by ELISA. 2 ug/ml of wound homogenate protein was loaded/sample.

2.2.26 Statistical analysis.

All statistical analysis was performed using an unpaired student's *t*-test, unless otherwise stated.

Chapter 3

The function of hspB1 protein in inflammatory gene expression in embryonic fibroblasts and acute inflammation in the air pouch model in mice.

3.1 Introduction.

The function of hspB1 in inflammatory gene expression is unclear and the reasons for the discrepancies in the literature are unknown. Studies involving siRNA-mediated depletion of hspB1 have often come to opposite conclusions. The different cell types used and the employment of different siRNAs, each with different off-target profiles, make interpretation of these data difficult and demonstrate the need for a complete genetic knockout (Park, Gaynor et al. 2003; Alford, Glennie et al. 2007; Gorska, Liang et al. 2007; Sur, Lyte et al. 2008; Wu, Liu et al. 2009). The decision was made to generate an *hspB1*-deficient murine strain which would allow for the investigation of the physiological function of hspB1 in inflammation. Fibroblasts were chosen to investigate the function of hspB1 in inflammatory gene expression because hspB1 is expressed in these cells. Primary adult murine fibroblasts are difficult to culture, which led to the decision to use MEF. Treatment of MEF with IL-1 or TNFα results in the induction of several pro-inflammatory mediators such as COX-2, IL-6 and CXCL1. Macrophages express a range of cytokines in response to pro-inflammatory stimuli, but were not an ideal candidate cell for these experiments, as previous work has demonstrated that murine bone marrow derived macrophages do not express hspB1 (Alford, Glennie et al. 2007).

To investigate the role of hspB1 in acute inflammation *in vivo* it was decided to use the air pouch model which allows straightforward analysis of leukocyte trafficking and inflammatory gene expression. The creation of the air pouch, produced by the subcutaneous injection of air into the dorsum of the mouse, results in the growth of granulation tissue in the cavity lining with a structure and cellular composition resembling the joint synovial membrane (Edwards, Sedgwick et al. 1981). This procedure allows for the creation of readily available facsimile synovial tissue in mice. The model is used primarily as a technique to study the effect of a wide variety of agents on leukocyte trafficking *in vivo*. The commonly

believed mechanism for the air pouch model is that pro-inflammatory stimuli (typically TLR ligands) directly activate resident macrophages to produce TNFα and IL-1 (Tessier, Naccache et al. 1997). These cytokines, in turn, induce the production of other cytokines and chemokines by connective tissue cells (Arima, Nasu et al. 2000; Li, Farthing et al. 2000; Garcia-Ramallo, Marques et al. 2002) and induce the expression of adhesion molecules, such as ICAM-1, in vascular endothelium (Tessier, Naccache et al. 1998). Together these effects result in the egress of leukocytes (initially neutrophils) from capillaries to the site of inflammation. CXCL1 is thought to be the major neutrophil chemotactic stimulus in mouse models of acute inflammation (Garcia-Ramallo, Marques et al. 2002), and is a murine orthologue of human IL-8 (Hol, Wilhelmsen et al. 2010).

Zymosan was used as a pro-inflammatory stimulus in the air pouch model in which it is well characterised and has been used to determine the kinetics of inflammatory responses (Cabrera, Blanco et al. 2001). LPS is also a common pro-inflammatory stimulus for use in the air pouch model, but was not used as it was not covered by the project license under which the procedure was carried out.

3.2 Commercial development of an *hspB1* conditional knock-out (*hspB1*$^{del/del}$) mouse line.

The generation of floxed *hspB1* and heterozygous *hspB1* knock-out (*hspB1*$^{+/del}$) mice was perfomed by genOway, Lyon, France. Targeted deletion of the *hspB1* gene in mice was achieved by homologous recombination in 129Sv ES cells of all three exons of the *hspB1* gene with a targeting vector that introduced LoxP sites either side of the gene (Fig. 3.1A). This strategy resulted in creation of a floxed *hspB1* mouse line and allowed for the generation of constitutive or conditional *hspB1* knock-out mice from the same colony of mice by breeding with CMV-CRE or tissue specific CRE-expressing mice for *in vivo* CRE-mediated

excision of *hspB1*. This strategy reduced the risk of embryonic lethality associated with the creation of a constitutive knock-out. The ES cells were injected into blastocysts which were impregnated in pseudo-pregnant female C57BL/6 mice. Chimaeras were identified and crossed with C57BL/6 mice constitutively expressing CRE recombinase to generate heterozygous *hspB1*$^{+/del}$ mice. Successful introduction of LoxP sites and deletion of the *hspB1* gene was confirmed by Southern blotting by genOway (Fig. 3.1B). *HspB1*$^{+/del}$ mice were crossed to generate homozygous *hspB1*$^{del/del}$ mice that are viable, fertile and after 2 years show no obvious signs of disease, abnormalities, or increased morbidity compared to wild-type mice. A program of backcrossing the *hspB1*$^{+/del}$ mice onto a C57BL/6 background began with the offspring of the original chimera, which were considered to be 1st generation backcrossed (50% C57BL/6). This reduced the proportion of 129Sv genetic material from the original implanted stem cells with each successive generation and increased the contribution of genetic material from the C57BL/6 mouse strain, whilst preserving the *hspB1*^{del} allele (Fig. 3.1C).

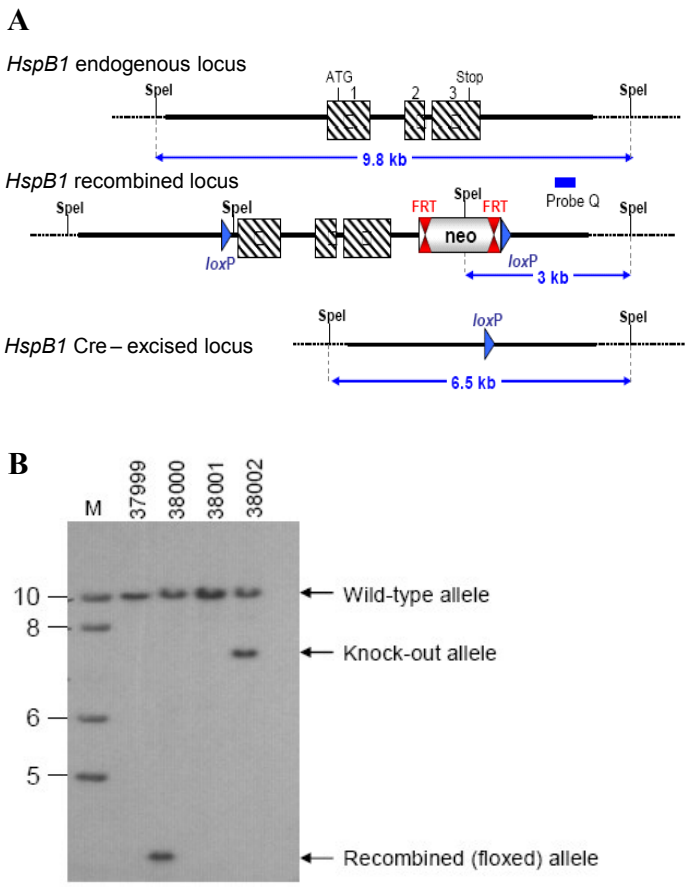

C

Backcross Generation	129/SV (%)	C57BL/6 (%)
1	50.00	50.00
2	25.00	75.00
3	12.50	87.50
4	6.25	93.75
5	3.13	96.88
6	1.56	98.44
7	0.78	99.22
8	0.39	99.61
9	0.20	99.80
10	0.10	99.90
11	0.05	99.95
12	0.02	99.98
13	0.01	99.99

Figure 3.1 Generation of *hspB1*$^{del/del}$ mice.

A, Schematic showing the size of *Spe* I fragments detected by Probe Q in Southern blot. *Spe* I sites separated by 9.8 kb flank the endogenous *hspB1* locus containing exons 1-3 (hashed boxes). Translational start (ATG) and stop codons are indicated. The introduction of an Flp-recombinase (FRT)-flanked neomycin cassette (NEO) and LoxP sites at 5' and 3' positions of exons 1-3 by homologous recombination introduces a new *Spe* I site, and Probe Q now recognises a 3kb fragment. The CRE-recombinase-excised locus produced by crossing floxed *hspB1* mice with a CMV-CRE deleter strain is indicated in which the endogenous *Spe* I sites are separated by 6.5 kb. B, Southern blot with Probe Q for four founder mice showing wild-type, knockout and recombined alleles of the expected sizes. M denotes DNA ladder (lengths in kb). C, table shows increasing C57BL/6 % genetic material in offspring after successive backcrosses. The Southern blot shown was performed by genOway.

3.3 The effect of hspB1 deficiency on basal and IL-1-induced COX-2 protein expression in murine embryonic fibroblasts (MEF).

To investigate the effect of complete hspB1 deficiency on inflammatory gene expression, wild-type and *hspB1*$^{del/del}$ MEF were left untreated, or treated with IL-1 for 4 h or 20 h. The cell culture medium was collected and centrifuged to remove cellular debris and stored for cytokine analysis. The cells were lysed with whole cell lysis buffer. A Bradford assay was carried out and the samples normalised for protein concentration and proteins were then separated by SDS-PAGE on a 12% polyacrylamide gel. COX-2, hspB1 and α-tubulin proteins (the latter as a loading control) were detected by western blot. Two identical experiments were performed using different batches of MEF.

Basal expression of COX-2 protein in resting *hspB1*$^{del/del}$ MEF appeared greater than that in wild-type MEF (Fig. 3.2A and B) but the difference in expression was small. IL-1 treatment weakly induced COX-2 protein expression in both *hspB1*$^{del/del}$ and wild-type cells compared to unstimulated cells in both batches of MEF (Fig. 3.2A, B). In one experiment there was slightly greater expression of IL-1-induced COX-2 protein in *hspB1*$^{del/del}$ MEF compared to wild-type cells (Fig. 3.2A). The other experiment showed no difference (Fig. 3.2B). The weak induction of COX-2 by IL-1 in MEF contrasts the strong induction of COX-2 by IL-1 in human fibroblasts (Ridley, Dean et al. 1998).

In a separate experiment I decided to investigate if MEF display stronger induction of COX-2 protein in response to a longer period of IL-1 treatment. For this, wild-type and *hspB1*$^{del/del}$ MEF were treated with IL-1 for 4 or 20 h, or left untreated. In wild-type MEF, COX-2 protein expression was not increased at 4 h post-IL-1, but was weakly increased at 20 h post-IL-1 compared to resting wild-type cells (Fig. 3.2C). Basal expression COX-2 protein and its induction following treatment with IL-1 for 4 h or 20 h appeared lower in *hspB1*$^{del/del}$ MEF

than that observed in the wild type cells (Fig. 3.2C). There appeared to be little induction by IL-1 of COX-2 protein in wild-type or *hspB1*$^{del/del}$ MEF. It was apparent that there was no regulation of COX-2 protein expression by hspB1 in MEF. These results were somewhat surprising, given the observation of strong inhibition of IL-1-induced COX-2 protein following hspB1 protein depletion in HeLa cells and human fibroblasts that was previously observed in my lab (Alford, Glennie et al. 2007).

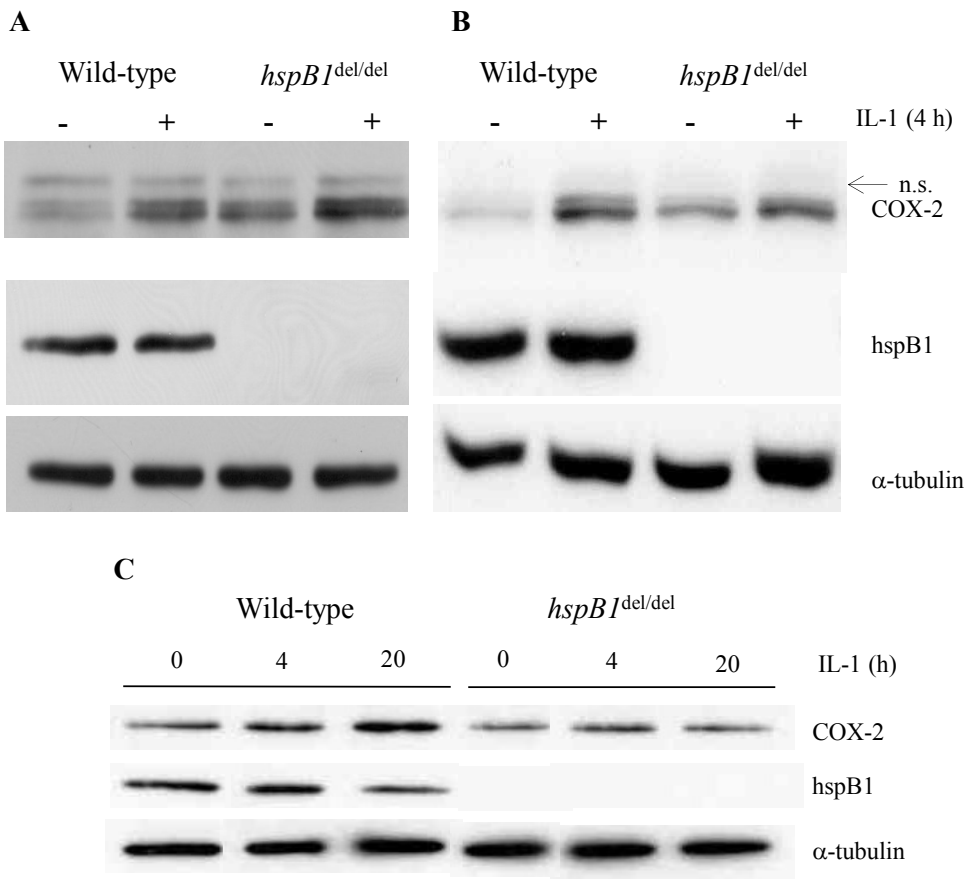

Figure 3.2 The effect of hspB1 deficiency on IL-1-induced COX-2 expression in MEF.

Heterozygous *hspB1*$^{+/del}$ male and female mice were set up as timed matings, 12.5 day embryos were isolated and MEF were prepared. The parents had been backcrossed onto a C57BL/6 background for 3 generations from the original chimera. MEF were used at passage 2 and seeded at a density of $2x10^5$ cells/well in a 6 well plate (A and B) or $4x10^4$ cells/well in a 12 well plate (C). MEF were treated with 20 ng/ml IL-1 for 4 h (A and B) or for 4 h and 20 h (C), or left untreated. Cells were lysed and protein concentration in the lysates measured by Bradford assay. Equal amounts of protein were separated by SDS-PAGE on a 12% polyacrylamide gel. COX-2, hspB1 and α-tubulin (as a loading control) proteins were detected by western blot. The results shown in (A) were performed by Dr. Francesco Marchese. n.s indicates non-specific band.

3.4 The effect of hspB1 deficiency on IL-1-induced IL-6 and CXCL1 protein expression in MEF.

I attempted to quantify the effect hspB1 deficiency on COX-2 expression by measuring PGE_2; however, I had little success with this owing to the difficulty in controlling the inherent variability of the PGE_2 ELISA kit used. The availability of robust ELISAs for IL-6 and CXCL1 meant that I would be able to determine any effects of hspB1 deficiency on expression of these cytokines even if it was small. The concentrations of IL-6 and CXCL1 protein in the cell culture supernatants from resting and IL-1-treated cells were measured by ELISA. Three different batches of MEF were used in these experiments.

A small amount of IL-6 protein was detected in the culture medium of resting wild-type and *hspB1*$^{del/del}$ MEF culture supernatants. There was a trend towards increased IL-6 expression in unstimulated *hspB*1$^{del/del}$ MEF and *hspB1*$^{del/del}$ MEF treated with IL-1 for 4 h compared to corresponding wild-type MEF (Fig. 3.3A). There was variability in the amount of IL-6 protein produced in individual experiments, and the induction of IL-6 protein by IL-1 was weak (Fig 3.3A), as seen for COX-2 protein (Fig. 3.2). This led to the decision to normalise the data to the IL-1-1 treated wild-type samples. When the values for IL-6 production were normalised to the IL-1-treated wild-type samples, there was a 2.2-fold increase in IL-6 protein production in resting *hspB1*$^{del/del}$ MEF compared to wild-type, and a 1.7-fold increase in IL-6 protein production in IL-1-stimulated *hspB1*$^{del/del}$ MEF compared to wild-type MEF (Fig 3.3B). This normalisation prevented statistical analysis of the data by unpaired Student's *t*-test. The increased expression of IL-6 in IL-1-treated *hspB1*$^{del/del}$ MEF compared to wild-type cells contrasts the observation that hspB1 depletion inhibits IL-1-induced expression of IL-6 protein in HeLa cells (Alford, Glennie et al. 2007).

There was variation in the amount of CXCL1 produced by MEF in individual experiments (Fig. 3.3C). The inducibility by IL-1 of CXCL1 in MEF was stronger than that of IL-6 (Fig 3.3A and C) but hspB1 deficiency did not appear to affect the expression of CXCL1 in either resting cells or MEF treated with IL-1 for 4 h (Fig. 3.4D). Although IL-6 expression was consistently found to be greater in *hspB1*$^{del/del}$ cells than in wild-type cells, the effect of hspB1 deficiency was weak.

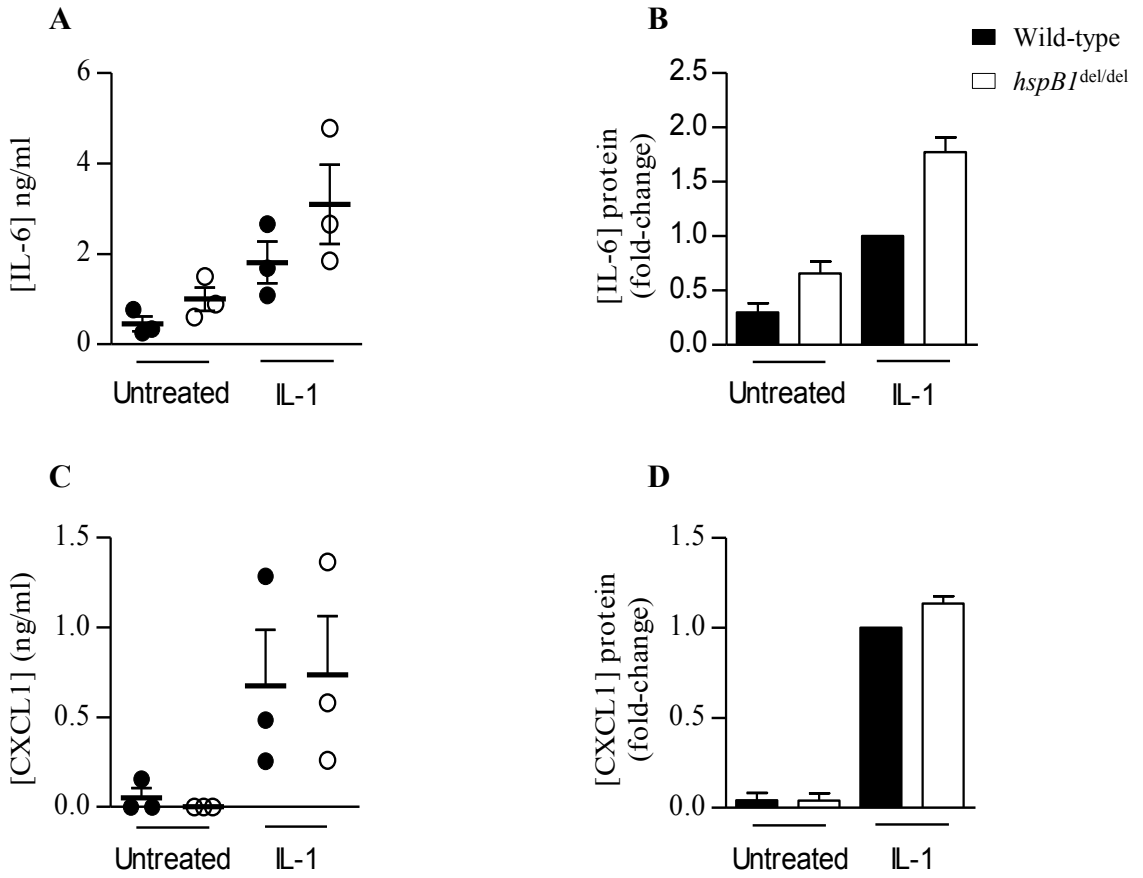

Figure 3.3 The effect of hspB1 deficiency on cytokine expression in MEF.

Wild-type or *hspB1*$^{del/del}$ MEF were seeded at 2x10^5 cells/well in 6 well plates and treated with IL-1 (20 ng/ml) for 4 h or left untreated. A, IL-6 and C, CXCL1 protein concentrations in MEF culture supernatants were measured by ELISA (points show means from n=3 experiments). Graphs B and D show mean fold-changes in cytokine protein concentrations (± SEM) relative to values for IL-1-treated wild-type MEF for IL-6 and CXCL1, respectively. Data show results from three separate experiments, each using different batches of wild-type and *hspB1*$^{del/del}$ MEF.

3.5 The effect of hspB1 deficiency on IL-1-induced expression of COX-2, IL-6 and CXCL1 mRNAs.

The expression of the corresponding mRNAs was also measured in the same experiments in which the effect of hspB1 deficiency on inflammatory mediator protein production was tested. MEF were left untreated, or treated with IL-1 as before, except that in these experiments cells were treated with IL-1 for 1, 2 and 4 h. RNA was extracted and reverse transcribed into cDNA. COX-2, IL-6 and CXCL1 mRNAs were measured by qRT-PCR using the standard curve method for quantification and mRNA values were normalised to those for glyceraldehyde-3 phosphate dehydrogenase (GAPDH) mRNA. Three identical experiments were performed with different batches of MEFs and the combined data are shown in Fig 3.4.

COX-2 mRNA expression was detected in untreated wild-type cells and only slightly increased following IL-1 stimulation, peaking at 2 h post-IL-1 (Fig. 3.4A), in agreement with the weak inducibility of COX-2 protein by IL-1 in MEF (Fig 3.2). COX-2 expression was approximately 2-fold greater in *hspB1*$^{del/del}$ MEF treated with IL-1 for 4 h compared to wild-type MEF (Fig. 3.4A). The mRNA results again clearly contrast those obtained in HeLa cells which showed inhibition of IL-1-induced COX-2 mRNA expression following hspB1 depletion (Alford, Glennie et al. 2007).

IL-6 mRNA expression peaked in wild-type and *hspB1*$^{del/del}$ cells at 2 h post-Il-1 and was sustained to 4 h post-IL-1 (Fig 3.4B). There was a tendency for increased IL-6 mRNA expression in *hspB1*$^{del/del}$ MEF but the differences in IL-6 mRNA expression in wild-type and *hspB1*$^{del/del}$ cells were within experimental error. IL-6 mRNA expression was very low in untreated *hspB1*$^{del/del}$ MEF and wild-type MEF (Fig. 3.4B) and IL-6 mRNA in resting cells did not appear to be regulated by hspB1 deficiency.

CXCL1 mRNA was barely detectable in resting cells and strongly induced by IL-1, peaking in *hspB1*$^{del/del}$ and wild-type MEF at 1 h post-IL-1 stimulation. Again, there was a trend towards increased CXCL1 mRNA expression in *hspB1*$^{del/del}$ MEF compared with wild-type MEF at all times post-IL-1 treatment (Fig. 3.4C) but the differences were not significant. The effect of hspB1 deficiency on the IL-1-induced expression of COX-2, IL-6 and CXCL1 mRNAs was small. Statistical analysis of the data could not be performed due to the fact that they had been normalised.

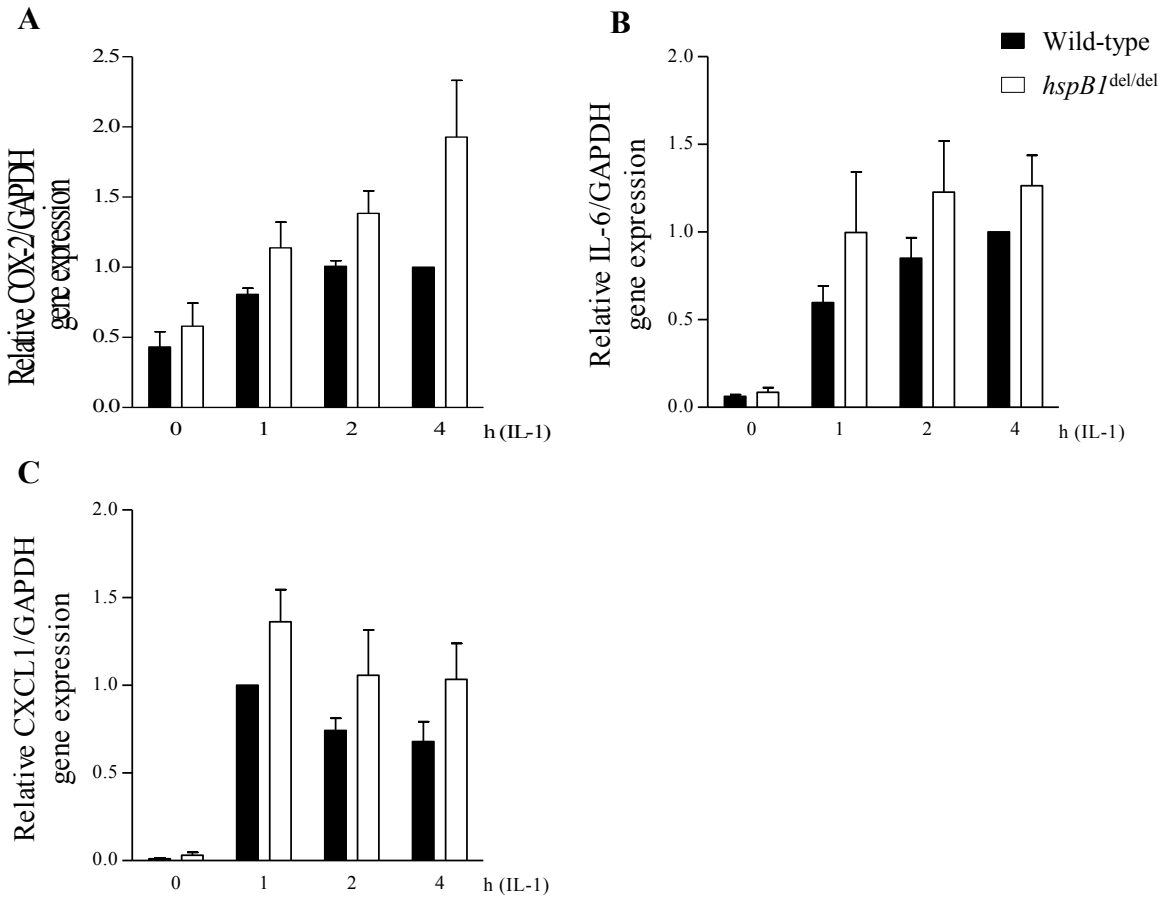

Figure 3.4 The effect of hspB1 deficiency on IL-1-induced COX-2, IL-6 and CXCL1 mRNA expression in MEF.

RNA was extracted from the same MEF used for the experiment shown in Fig. 3.3 in which cells were treated with IL-1 for 1, 2 or 4 h, or left untreated. 1 μg of total RNA was reverse-transcribed into cDNA. qRT-PCR was performed using Taqman Gene expression assays for COX-2, IL-6, CXCL1 and GAPDH mRNAs. The standard method curve was used for the quantification of the results and mRNA values were normalised to GAPDH as a control. COX-2, IL-6 and CXCL1 mRNA expression was normalised to values for wild-type cells treated with IL-1 for 4 h, 4 h and 1 h respectively. Data show fold-changes in expression from three separate experiments, each using different batches of wild-type and *hspB1*$^{del/del}$ MEF. Error bars represent mean ± SEM. mRNA measurements were performed by Dr. Anna Aubareda (n=3).

3.6 Investigation of the effect of hspB1 deficiency on the expression and IL-1-induced phosphorylation of p38 MAPK in MEF.

IL-1 signalling, downstream of TAK1 and including the activation and phosphorylation of p38 MAPK, was shown to be inhibited by hspB1 protein depletion in HeLa cells (Alford, Glennie et al. 2007). I assessed the effect of hspB1 deficiency in MEF on the activation of p38 MAPK, which lies downstream of TAK1 and which plays an essential role in inflammatory gene expression (Dean, Brook et al. 1999). These experiments were carried out to provide a test of the function of hspB1 protein in signalling in response to IL-1 stimulation in MEF.

MEF were treated with IL-1 for 30 mins or 4 h, or were left untreated. HspB1, p38 MAPK, phosphorylated p38 MAPK and α-tubulin proteins were detected by western blot (Fig. 3.5). There was a small increase in the amount of p38 MAPK protein detected in *hspB1*$^{del/del}$ MEF lysates compared to those from wild-type cells (Fig. 3.5A, B). At 30 mins and 4 h post-IL-1 treatment a slightly higher amount of phosphorylated p38 MAPK was detected in *hspB1*$^{del/del}$ MEF relative to wild-type MEF. (Fig. 3.5A, B). These findings contrast the inhibition of p38 MAPK activation observed previously following siRNA-mediated depletion of hspB1 in HeLa cells (Alford, Glennie et al. 2007).

The increased levels of p38 MAPK protein in IL-1-treated *hspB1*$^{del/del}$ MEF compared to wild-type MEF suggests a possible reason for the increased cytokine expression in hspB1-deficient MEF. The weak activation of p38 MAPK by IL-1 in MEF is consistent with the poor inducibility of inflammatory gene expression in these cells and confirmed that MEF were not the ideal cell type to investigate the effect of hspB1 deficiency on inflammatory gene expression.

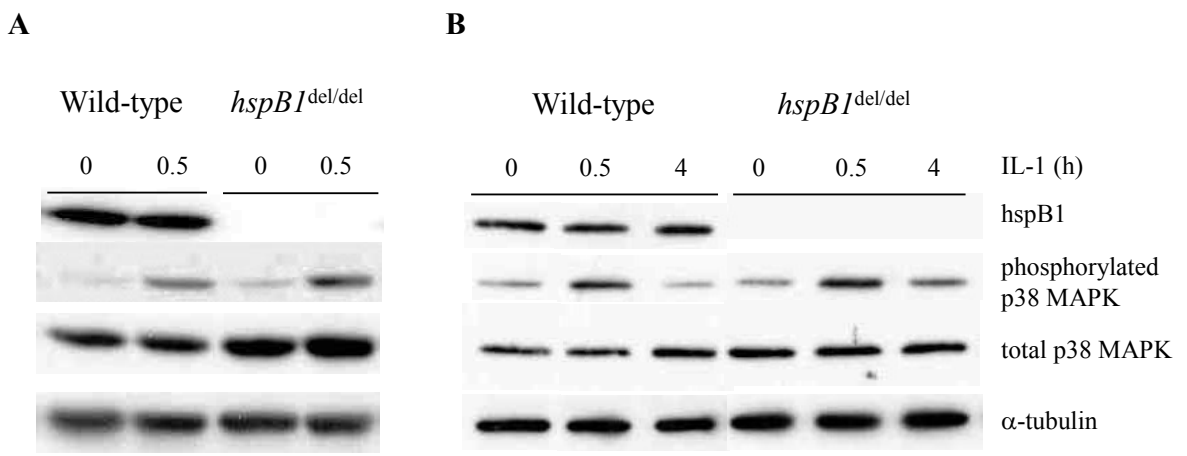

Figure 3.5 The effect of hspB1 deficiency on the expression and IL-1-induced phosphorylation of p38 MAPK in MEF.

Mouse embryos were isolated from 7th generation backcrossed parents. MEF were seeded at $2x10^5$ cells/well in 6 well plates and were treated with 20 ng/ml IL-1 for the times shown above. Cells were lysed and western blotting was used to detect hspB1, p38 MAPK, phosphorylated p38 MAPK (Thr180/Tyr182), hspB1 and α-tubulin proteins in MEF lysates from 2 separate experiments.

3.7 Investigation of the effect of hspB1 deficiency on the expression of hsp70 and hsp90 proteins in MEF.

Given the weak effects of hspB1 deficiency on inflammatory gene expression observed in MEF, and the differences to data obtained previously in HeLa cells and human fibroblasts (Alford, Glennie et al. 2007), the possibility of adaptation of the *hspB1*$^{del/del}$ MEF was considered. It was thought possible that complete removal of *hspB1* from the genome and subsequent growth of such cells for extended periods would cause the cells to adapt and overexpress another compensatory protein chaperone, such as the large heat shock proteins hsp70 and/or hsp90. The blot shown in Fig. 3.5 was re-probed for hsp70 and hsp90. This showed little difference in the expression of hsp70 and hsp90 proteins in *hspB1*$^{del/del}$ compared with wild-type MEF (Fig 3.6).

It was concluded that the responses to IL-1 was weak in MEF, making it hard to assess function of hspB1 in inflammatory gene expression in this system; therefore, I decided to use the air pouch model of acute inflammation. This is a far more physiological system to investigate the function of hspB1 in inflammatory gene expression than MEF.

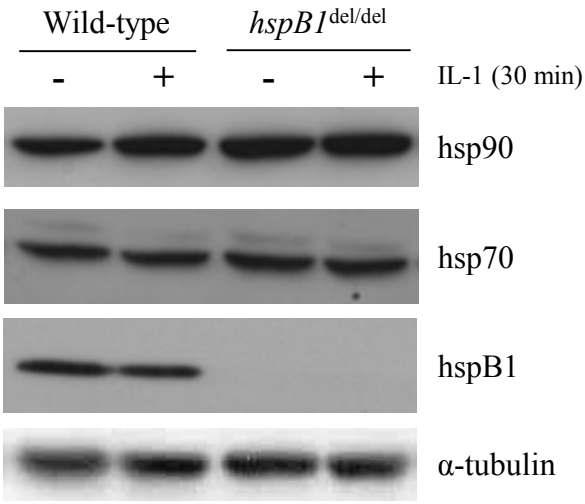

Figure 3.6 The effect of hspB1 deficiency on the expression of hsp70 and hsp90 proteins in MEF.

The blot shown in Fig. 3.5 was re-probed with antibodies against hsp90 and hsp70. Staining of hspB1 and α-tubulin performed in the previous experiment is shown for clarity.

3.8 An investigation into the function of hspB1 in acute inflammation.

The establishment of the *hspB1*$^{del/del}$ murine strain created the opportunity to investigate the role of hspB1 in inflammation *in vivo*. During the MEF experiments a program of backcrossing *hspB1*$^{+/del}$ mice onto a C57BL/6 background had been implemented. By the time MEF experiments were completed, the *hspB1*$^{+/del}$ mice had already been backcrossed for 7 generations. This meant that knockout mice with a 99.2 % C57BL/6 genetic contribution were ready for experiments and that preliminary *in vivo* data could be obtained. The initial goal was to determine the effect of hspB1 deficiency on cellular infiltration and the expression of chemokines responsible for the ingress of neutrophils. I also decided to determine if IL-6 protein expression was regulated by hspB1 in the air pouch model, as data from the MEF studies indicated that IL-6 production might be increased by hspB1 deficiency in fibroblasts.

7th generation backcrossed *hspB1*$^{+/del}$ parents were used to generate *hspB1*$^{del/del}$ and wild-type mice. Male mice of between 8 and 14 weeks of age were used for the air pouch experiment. Approximately half of all the mice used were littermates. A series of small experiments were carried out each using approximately 3 mice of each genotype. The mice were anaesthetised with isoflurane and injected with 5 ml air on day 1. On day 4 the air pouches were re-inflated by injection 1 ml air and on day 5 the mice were injected with 100 µl 1 mg/ml zymosan in PBS. After 4 h the mice were euthanised with CO_2 and the air pouches were injected with 2 ml PBS and massaged to ensure maximum cell retrieval. 1 ml of exudate was retrieved and centrifuged to pellet infiltrated cells. The supernatant was collected and the cell pellet re-suspended with 1 ml PBS. Cells were counted using a haemocytometer and cells/ml calculated (Fig. 3.7A) and the supernatant analysed for IL-6 (Fig. 3.7B) and CXCL1 (Fig. 3.7C) proteins by ELISA.

The data in Fig. 3.7 represents the results for all the mice used in the experiments. Not all *hspB1*$^{del/del}$ mice shown have a wild-type littermate control, and vice versa. There was variability in the number of cells migrating into the air pouch in *hspB1*$^{del/del}$ and wild-type mice. The mean number of cells migrating into each pouch in the *hspB1*$^{del/del}$ mice was 1.3-fold greater than the wild-type, however, the difference was not statistically significant. (Fig. 3.7A).

There was less variability in the concentration of IL-6 protein in air pouch exudates from wild-type mice compared to *hspB1*$^{del/del}$ mice. The mean amount of IL-6 produced in the *hspB1*$^{del/del}$ mice was 2.2-fold greater ($P \leq 0.05$) than that produced in wild-type mice (Fig. 3.7B). CXCL1 and TNFα protein concentrations were also measured in the air pouch exudates. It was thought that if CXCL1 and/or TNFα were regulated by hspB1, with a correlating regulation of cell migration, then a mechanism for the regulation of inflammation would present itself for investigation. CXCL1 protein expression was not regulated by hspB1 deficiency (Fig. 3.7C). There was very little difference in the means and large variability in CXCL1 protein production in *hspB1*$^{del/del}$ and wild-type mice. However, overall CXCL1 protein production in response to zymosan was low (< 1 ng/ml) (Fig. 3.7C). The concentration of TNFα in these exudates was too low to be detected (< 10-15 pg/ml, data not shown).

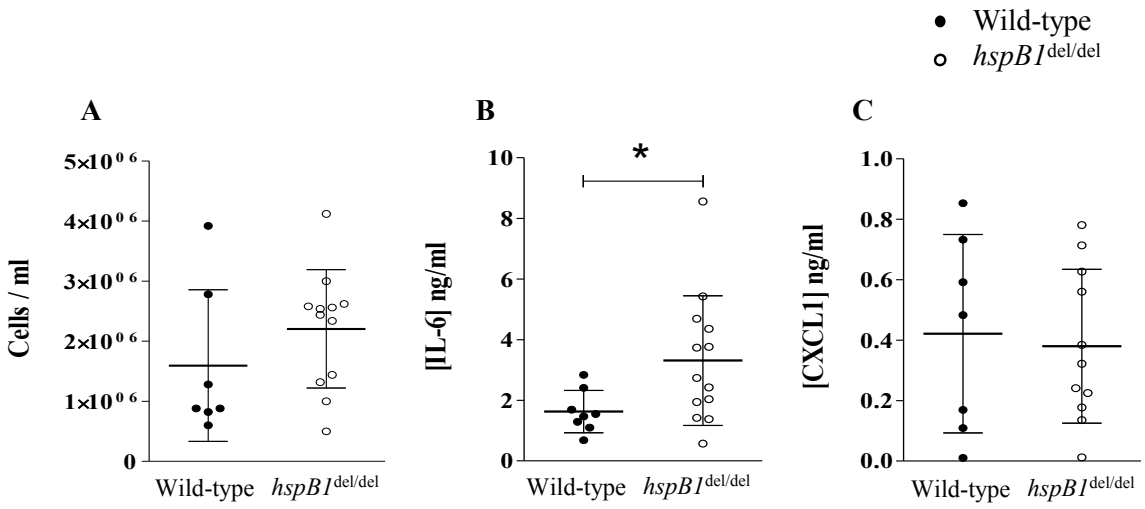

Figure 3.7 Preliminary experiments to investigate the effect of hspB1 deficiency on cellular infiltration and cytokine production in the zymosan-induced air pouch model of acute inflammation.

Eight to fourteen week old, male *hspB1*$^{del/del}$ and wild-type mice were used in the air pouch experiment and the exudate retrieved at t = 4 h and centrifuged to isolate cells. 100 µl 1 mg/ml zymosan was injected into 5 day old air pouches following 1ml air top-up on day 4. Infiltrating cells were counted using trypan blue staining and a haemocytometer and plotted as cells/ml of exudate (A). The supernatant was analysed for IL-6 (B) and CXCL1 (C) protein concentration by ELISA. Points represent mean values from individual mice. All graphs show mean ± SEM. * $P \leq 0.05$.

3.9 Consideration of the importance of littermate controls in the air pouch experiment.

The data from Fig. 3.7 were re-plotted to represent those that had strict littermate controls to isolate mice in which there was the least genetic variability. It was thought that this would provide a more rigorous method of investigating whether there really is a difference in cellular expression in wild-type and *hspB1*$^{del/del}$ mice or not. This revealed a statistically significant increase in cellular infiltration to the site of zymosan-induced local inflammation in *hspB1*$^{del/del}$ compared with wild-type littermate control mice ($P \leq 0.05$). There was close agreement in the number of cells migrating in the wild-type mice; however there was greater variability in *hspB1*$^{del/del}$ mice (Fig. 3.8A).

Mean IL-6 protein concentration in *hspB1*$^{del/del}$ mouse exudates was also greater than that in the littermate wild-type mice (Fig 3.8B). The wild-type IL-6 values were closely grouped, however, the variability of IL-6 concentrations in the *hspB1*$^{del/del}$ mice air pouch exudates, in addition to the low number of littermate mice used, prevented the increase in IL-6 production from being statistically significant (Fig. 3.8B). Despite the lack of a statistically significant difference in IL-6 production between wild-type and *hspB1*$^{del/del}$ mice, a trend towards increased IL-6 production was observed in *hspB1*$^{del/del}$ mice compared to wild-type mice. CXCL1 production was not affected by hspB1 deficiency in the littermate mice. The expression of CXCL1 appeared to be lower in the *hspB1*$^{del/del}$ mice compared to wild-type mice although the variability in both groups was high (Fig. 3.8C).

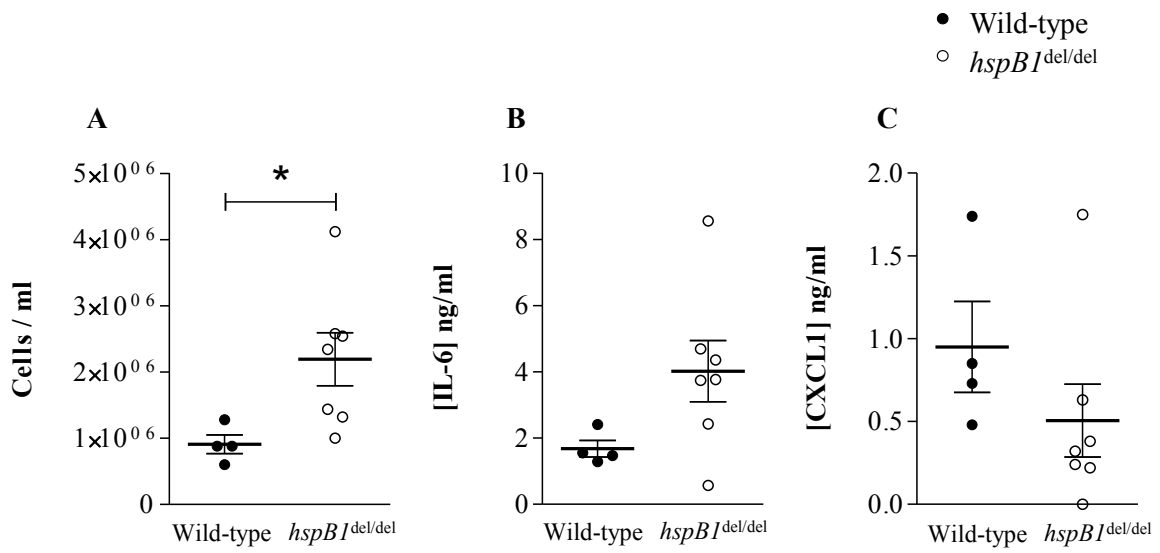

Figure 3.8 Consideration of the importance of littermate controls in preliminary experiments to investigate the effect of hspB1 deficiency on cellular infiltration and cytokine production in the zymosan-induced air pouch model of acute inflammation.

Data points in Fig 3.7 were re-plotted to display only littermate mice. Total cells/ml (A), IL-6 (B) and CXCL1 (C) protein concentrations from *hspB1*$^{del/del}$ and wild-type mice are shown. All graphs show mean ± SEM. *P ≤ 0.05.

The lack of significance on the effect of hspB1 deficiency on IL-6 protein expression in these air pouch experiments may be due to the small n number of mice used, the range of ages of mice used, and the fact that mice were used on different days with different stocks of zymosan. It was thought that removal of these variables might lead to better grouping of the data and provide a more rigorous way of investigating if hspB1 regulates IL-6 protein expression in the murine air pouch model.

3.10 Investigation of the effect of hspB1 deficiency on cytokine production in the air pouch model at different times post-zymosan.

The preliminary air pouch experiments were concluded as the original stock of zymosan was exhausted. The variation in the inflammatory responses to zymosan in the preliminary air pouch experiments prohibited many differences observed from being statistically significant when only 5-6 animals were used per genotype. In an attempt to control the variability of the results observed in earlier experiments, some improvements were devised to improve the reliability and accuracy of the experiment.

Firstly, a new large stock of Zymosan A was purchased, prepared and frozen at -20^{o}C in aliquots of sufficient volume for a single experiment. This ensured that for future air pouch experiments, the zymosan used would be of the same stock and would only have been thawed once.

Secondly, I noticed that the 'top-up' injection of 1 ml air on day 4 post air pouch creation was not always sufficient to give a consistent size of air pouch ready for injection on day 4. This was especially true of mice that were housed in large litters. I hypothesised that air was being forced from the pouch during the course of the experiment. A simple solution was to inject 3 ml of air on day 4, and to use a 30$^{1/2}$ gauge needle (the smallest available). This volume of air and size of needle caused no pain reflex or obvious distress to the mouse during

administration of the air or afterwards. This improvement resulted in the creation of air pouches of consistent size when the mice were ready for zymosan injection. This change in procedure is noted in the Materials and Methods section, and was used for all subsequent air pouch experiments.

Thirdly, the way the mice were bred was changed. During the time taken to undertake the initial air pouch experiments, *hspB1*$^{del+}$ mice were backcrossed for 12 generations. These *hspB1*$^{del/+}$ mice were then crossed as before to generate wild-type and *hspB1*$^{del/del}$ littermates. These mice were then bred with *hspB1*$^{+/+}$ or *hspB1*$^{del/del}$ mice from separate litters to produce *wild-type* x *wild-type* and *hspB1*$^{del/del}$ x *hspB1*$^{del/del}$ breeding pairs, producing litters consisting only of the respective genotype of the parents. Synchronisation of breeding allowed for the generation of large litters of mice of a single genotype that could be much more accurately age-matched. Although this strategy removed the means to produce strict littermate wild-type controls for the *hspB1*$^{del/del}$ mice, it was decided that being able to generate more mice at a faster rate and improve the ability to age-match the mice to wild-type controls was of greater benefit. The backcrossing strategy also meant that at mice within the colony that were used for experiments and further breeding were 99.99% pure Jackson C57BL/6, so the need for strict littermate controls was reduced.

Although increased cell migration was observed in the original air pouch experiment at 4 h zymosan stimulation (Fig 3.8A), TNFα concentrations were below the limit of detection at this time point and the concentrations of CXCL1 were also very low (Fig 3.8C). I hypothesised that the concentration of these cytokines would be greater in the early phase of the acute inflammatory response, as their production is a pre-requisite for leukocyte infiltration. I decided to determine if the concentrations of TNFα or CXCL1 were greater at earlier time points than those measured at 4 h post-zymosan stimulation. If this were the case then this would then allow for measurement of protein concentration of these cytokines in

mouse air pouch exudates and greater insight into the mechanism of increased cell migration in *hspB1*$^{del/del}$ mice compared with wild-type mice. I also decided to measure CXCL2 (MIP2α), as it is also a potent chemotactic agent for neutrophils in mice with high sequence homology to CXCL1 (Wolpe, Sherry et al. 1989; Iida and Grotendorst 1990). CXCL2 concentration has also been shown to peak at 1 h in a murine air pouch model (Tessier, Naccache et al. 1997; Schramm, Liu et al. 2000). IL-10, an anti-inflammatory cytokine produced by macrophages, was also measured as a test for regulation of macrophage function or numbers by hspB1 deficiency.

The concentrations of CXCL1, CXCL2, IL-6, IL-10 and TNFα proteins in exudate supernatants from mice challenged with zymosan for different times were measured by ELISA. The concentration of CXCL1 protein at 4 h post-zymosan was very low (Fig 3.9A), and the concentrations of CXCL2 and TNFα were below the level of detection at this time point (data not shown).

CXCL1 and CXCL2 protein production peaked at 1 h and was increased by 2.0-fold ($P \leq 0.05$) and 1.7-fold ($P \leq 0.05$), respectively, in *hspB1*$^{del/del}$ mice compared to wild-type controls (Fig. 3.9A and B). The concentrations of CXCL1 and CXCL2 were low at 2 h post-zymosan and there was no difference in the concentration of these cytokines in *hspB1*$^{del/del}$ mice compared to wild-type at these timepoints (Fig 3.9A and B).

IL-6 protein production peaked in *hspB1*$^{del/del}$ mice at 4 h post-zymosan and was significantly increased (3.2-fold; $P \leq 0.01$) relative to wild-type at this time point (Fig. 3.9C).There was an increase in mean IL-10 production in *hspB1*$^{del/del}$ mice (2.5 fold; $P \leq 0.01$) compared to wild-type 1 h post-zymosan (Fig 3.9D). IL-10 protein production peaked at 4 h post-zymosan; however there was no difference in IL-10 production in *hspB1*$^{del/del}$ mice compared to wild-type mice at this time point (Fig 3.9D). The protein concentration of IL-6 and IL-10 16 h

post-zymosan was very low (Fig 3.9C and D). The concentration of TNFα protein was increased in *hspB1*$^{del/del}$ mice (2.7-fold, $P \leq 0.05$) compared to wild-type at 1 h post-zymosan (Fig. 3.9E). These cytokines could not be detected at any time post-injection with PBS vehicle control (data not shown).

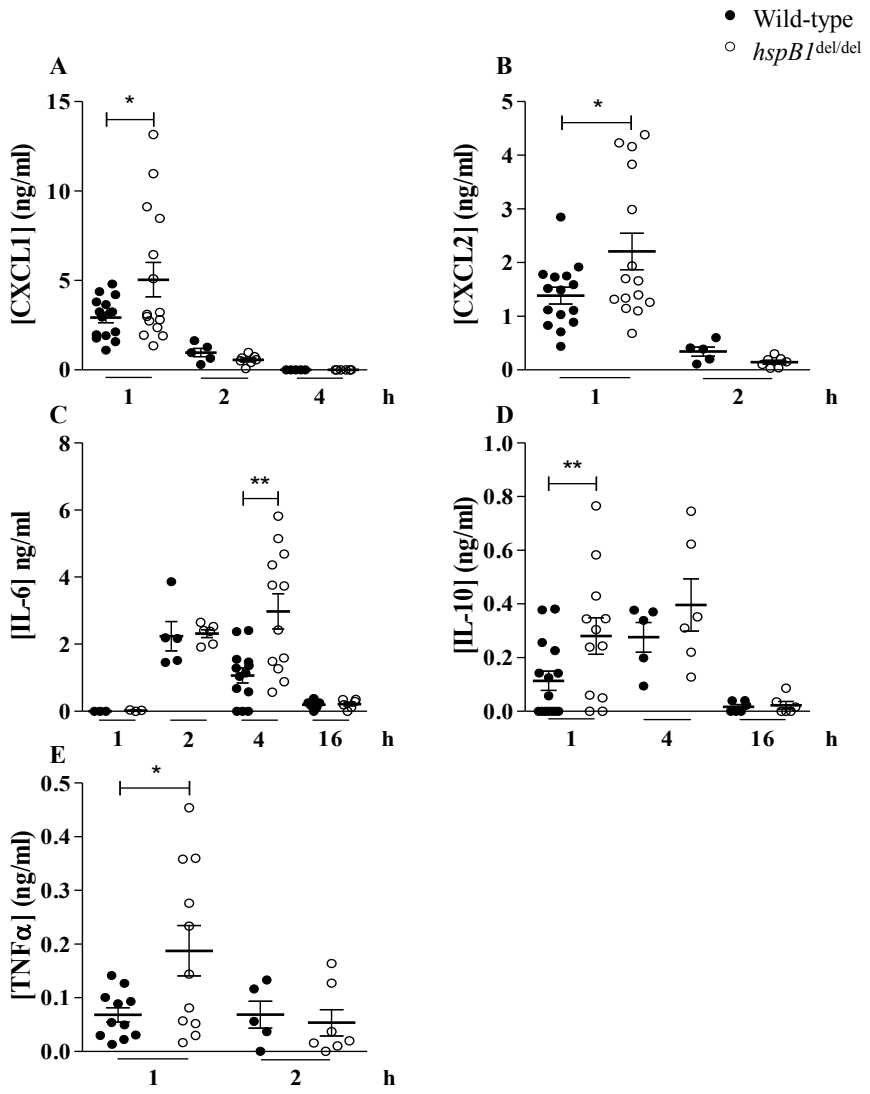

Figure 3.9 The effect of hspB1 deficiency on cytokine production in air pouches at different times post-zymosan treatment.

CXCL1 (A), CXCL2 (B), IL-6 (C), IL-10 (D) and TNFα (E) protein concentration in air pouch exudates were measured at 1 h (n = 3-15 from three experiments), 2 h (n = 5-7 from one experiment, 4 h (n = 5-13 from two experiments) and 16 h (n = 5-7 from one experiment) post-zymosan by ELISA. All graphs show mean ± SEM; *P ≤ 0.05, **P ≤ 0.01. Statistical analysis was performed using Student's *t*-tests, with Welch's correction for unequal variance where necessary.

3.11 HspB1 deficiency increases neutrophil migration in zymosan-treated air pouches.

The cells infiltrating the air pouch at different times after treatment with zymosan were counted. Cellular infiltration was very low at 1 h and commenced in wild-type mice at 2 h and peaked at 4 h post-zymosan (Fig. 3.10A). A statistically significant increase in infiltrating cells at 2 h (2.0-fold; $P \leq 0.01$) and 4 h (2.3-fold; $P \leq 0.01$) post-zymosan was observed in *hspB1*$^{del/del}$ mice relative to wild-type mice, with the peak of cellular infiltration occurring at 4 h (Fig. 3.10A). The numbers of infiltrating cells at 16 h post-zymosan were the same as those observed at 4 h in wild-type mice. There was no increase in the number of infiltrating cells at 16 h post zymosan in *hspB1*$^{del/del}$ mice compared to wild-type mice. No cellular infiltration was detected in mice injected with PBS as a vehicle control (Fig. 3.10A).

Flow cytometry analysis with Ly-6G (Gr-1) staining confirmed that at 4 h post-zymosan neutrophils comprised > 90 % of the cellular infiltrate in both wild-type and *hspB1*$^{del/del}$ mice (Fig. 3.10B), excluding the possibility that the increased cell counts in hspB1-deficient animals are due to infiltration by some other cell type. At 16 h post-zymosan, when monocyte infiltration normally commences in this model (Garcia-Ramallo, Marques et al. 2002), there was no effect of hspB1 deficiency on the proportions of infiltrating neutrophils or monocytes/macrophages as assessed by flow cytometry (Fig. 3.10C).

There was concern that the increased neutrophil infiltration observed in air pouches of *hspB1*$^{del/del}$ mice relative to wild-type mice might simply be due to an increase in the number of total circulating neutrophils caused by hspB1 deficiency. To address this, blood was collected by cardiac puncture and the red blood cells removed using red cell lysis buffer, according to the manufacturer's instructions. The leukocytes were stained for Ly-6G and CD11b to identify neutrophils by flow cytometry as before. There was no difference in the numbers of circulating neutrophils in wild-type and *hspB1*$^{del/del}$ mice (Fig 3.10D).

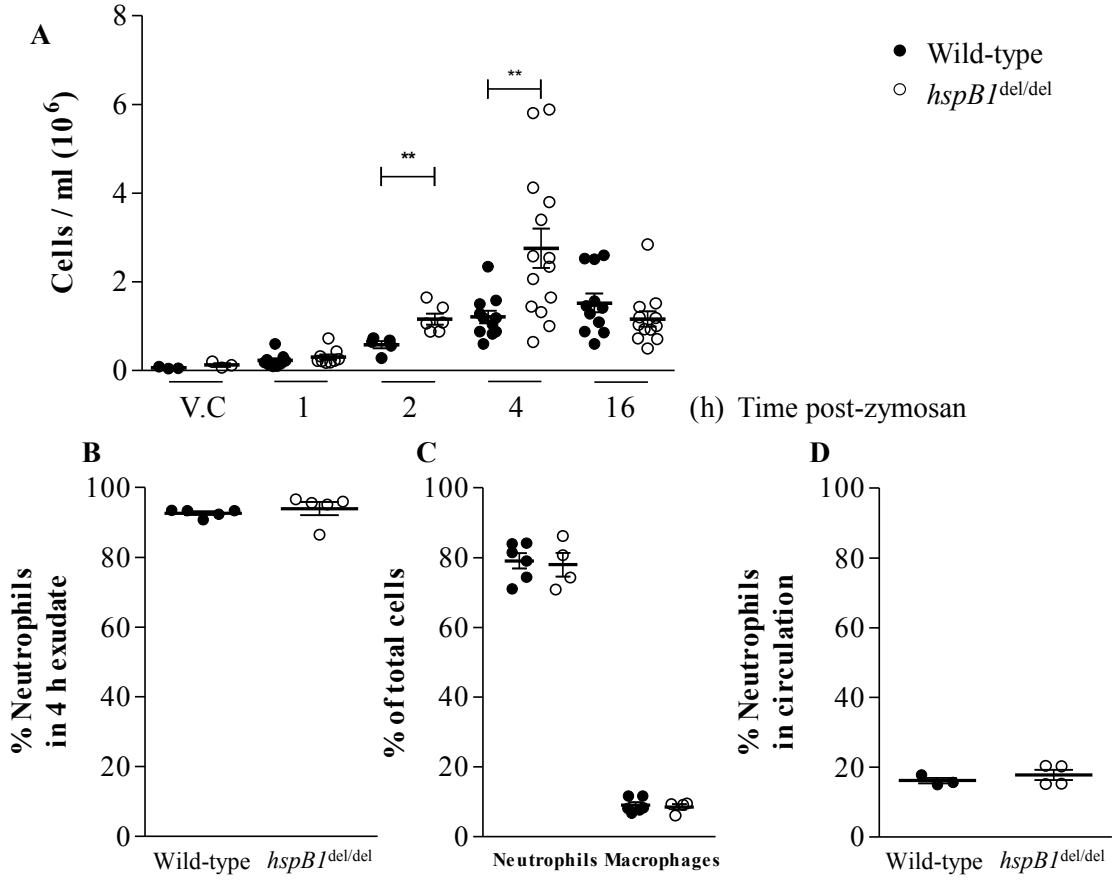

Figure 3.10 The effect of hspB1 deficiency on cellular infiltration in the zymosan-induced air pouch model of acute inflammation.

Air pouches were created on the dorsal surfaces of 10 – 12 week old, 12 generation backcrossed wild-type and *hspB1*$^{del/del}$ mice and were injected with 100 µl of 1 mg/ml zymosan. Exudates were retrieved at the indicated times. A, plot of number of infiltrating cells (n = 5-6 mice per group for 2 h post-zymosan; n = 9-14 from two experiments each for all other times). B, graph of population of neutrophils as a percentage of total infiltrating cells at 4h post-zymosan identified by gating for the Ly-6G^{hi} CD11b^{hi} population (n = 5). C, plots showing neutrophil and macrophage populations in infiltrates at 16 h post-zymosan determined by flow cytometry; neutrophil gate (Ly-6G^{hi}, CD11b^{hi}); macrophage gate (Ly-6G^{lo}, CD11b^{lo}); (n=6). D, Plot of neutrophils in peripheral blood of unchallenged mice identified as in (B); (n=3-4). All graphs show mean $\pm$ SEM. ** $P \leq 0.01$.

Statistical analysis was performed using Student's *t*-test with Welch's correction for unequal variance where necessary.

3.12 HspB1 deficiency results in increased numbers of neutrophils undergoing apoptosis in zymosan-treated air pouches.

The rapid decline in numbers of *hspB1*$^{del/del}$ cells at 16 h and following the peak of cellular infiltration at 4 h post-zymosan in *hspB1*$^{del/del}$ mice suggested that in addition to increased migration of cells to the site of inflammation, the neutrophils from *hspB1*$^{del/del}$ mice may undergo increased apoptosis relative to wild-type neutrophils. I used Propidium iodide (PI) and Annexin V staining as this technique is frequently used to determine if cells are viable, apoptotic, or necrotic through differences in plasma membrane integrity and permeability.

To determine if infiltrating neutrophils from *hspB1*$^{del/del}$ mice were less viable than those from wild-type mice, the zymosan-induced air pouch experiment was repeated. At 4 h post-stimulation the infiltrating cells were retrieved and apoptosis detected by staining with annexin V and PI and measured by flow cytometry. This showed a reduced proportion ($P \leq 0.05$) of viable, annexin V^{lo}/PI^{lo}, *hspB1*$^{del/del}$ cells (46 $\pm$ 5% (Fig. 3.11A, C)) compared with wild-type cells (66 $\pm$ 4% (Fig. 3.11A, B)), consistent with reduced viability of the hspB1-deficient cells. The proportion of annexin V^{hi}/PI^{hi} cells from *hspB1*$^{del/del}$ mice (41 $\pm$ 5% (Fig. 3.11A, C) was increased ($P \leq 0.01$) relative to that from wild-type animals (19 $\pm$ 4% (Fig. 3.11A, B) indicating an increased proportion of apoptotic hspB1-deficient cells. Less than 10 % of cells were identified as being in early apoptosis (Fig. 3.11A). These cells stained weakly for PI but positive for annexin V.

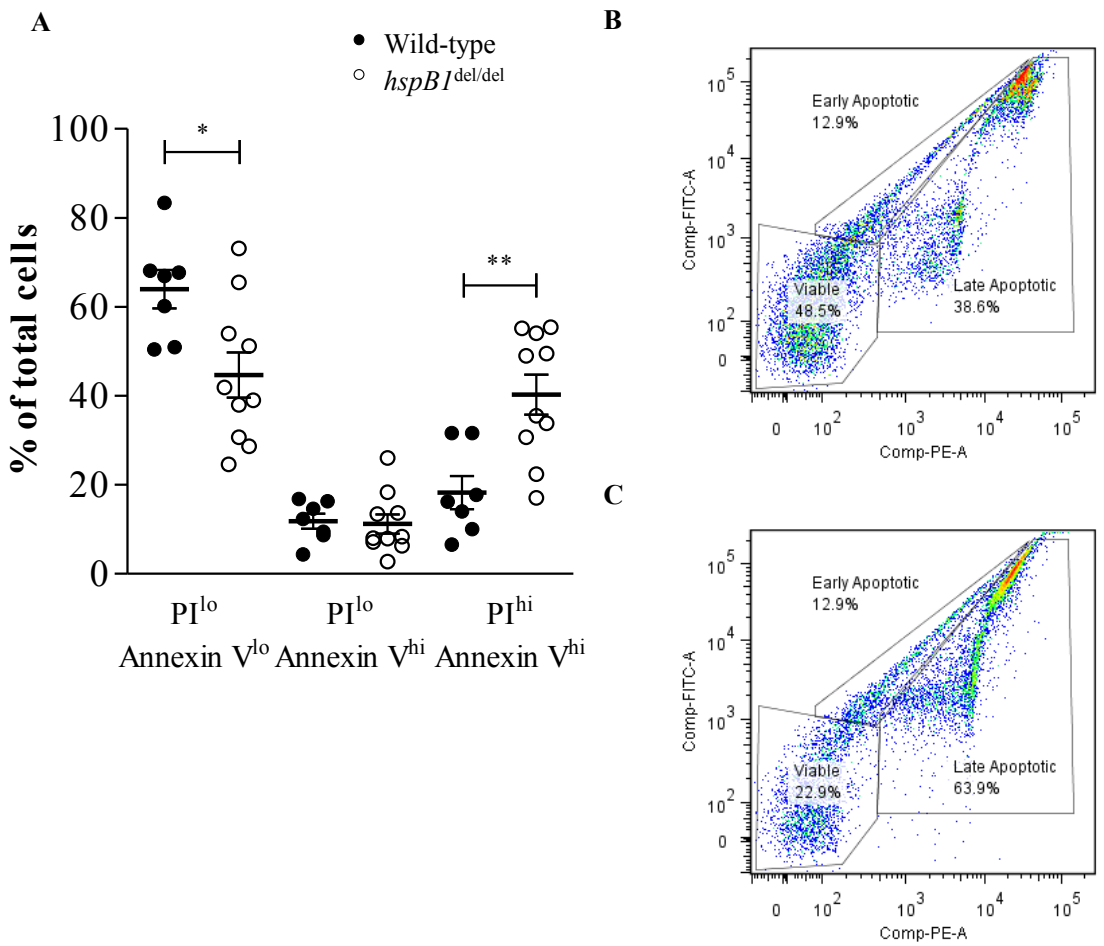

Figure 3.11 The effect of hspB1 deficiency on neutrophil viability and apoptosis in the zymosan-induced air pouch model of acute inflammation.

A, Cell viability and apoptosis of cellular infiltrates at 4 h post-zymosan were assessed by flow cytometry with annexin V and PI staining (n = 8-10 from two experiments). Three cell populations were observed and gated for (annexin V^{lo}, PI^{lo}; annexin V^{hi}, PI^{lo}; annexin V^{hi}, PI^{hi}), representative plots with gating strategies are shown for B, wild-type and C, *hspB1*$^{del/del}$ mice. Bars show mean ± SEM. *P ≤ 0.05, **P ≤ 0.01.

3.13 Discussion

Previous research done in my lab showed that hspB1 depletion inhibits IL-1-induced COX-2, IL-6 and IL-8 protein and mRNA expression in HeLa cells and COX-2 protein and mRNA in primary human dermal fibroblasts (Alford, Glennie et al. 2007). The results from our investigations in MEF showed that, in contrast to HeLa cells and primary human fibroblasts, the effect of deletion of the *hspB1* gene on IL-1-induced COX-2 and IL-6 protein and mRNA expression was small and expression tended to increase rather than decrease (Fig. 3.2, 3.3A, 3.4A, 3.4B). Basal expression of COX-2 protein also appeared to be increased in *hspB1*$^{del/del}$ MEF compared to wild-type MEF (Fig 3.2). The poor induction by IL-1 of COX-2 and IL-6 in MEF was unanticipated, as was the trend towards an opposite effect of hspB1 depletion on COX-2 and IL-6 expression observed in experiments in human cells (Alford, Glennie et al. 2007).

COX-2 and IL-6 mRNAs are known to be stabilised upon p38 MAPK activation (Dean, Brook et al. 1999; Wery-Zennaro, Zugaza et al. 2000). There was a small increase in p38 MAPK expression and IL-1-induced p38 MAPK phosphorylation in *hspB1*$^{del/del}$ MEF compared to wild-type cells (Fig. 3.5) which may partly account for the trend towards increased IL-1-induced COX-2 and IL-6 mRNA expression observed in these cells. However, the increase in p38 MAPK protein expression and phosphorylation in *hspB1*$^{del/del}$ MEF compared to wild-type cells is small and again contrasts previous findings in my lab showing that hspB1 protein depletion inhibits p38 MAPK activation in HeLa cells (Alford, Glennie et al. 2007). CXCL1 protein and mRNA expression were not regulated by hspB1 in MEF 4h post-IL-1 (Fig. 3.3C, Fig. 3.4C).

The data from MEF are in contrast to those of previous studies performed in our lab in human cells, which showed that hspB1 is required for the induction of COX-2, IL-6 and IL-8 protein

by IL-1 (Alford, Glennie et al. 2007). The different results obtained may well be a result of the different methods by which hspB1 depletion/elimination was achieved. Previous work by Alford et al. involved the use of siRNA-mediated transient and partial depletion of hspB1 expression in human cells and cell lines, whereas the current study involves the use of mice and cells that harbour genetic and constitutive deletion of the hspB1 gene and therefore completely lack expression of hspB1 protein.

An alternative explanation may be that the apparent increase in the IL-1 induced inflammatory response in *hspB1*$^{del/del}$ MEFs is an artefact of CRE toxicity. It has been shown that mammalian genomes contain 'cryptic' or 'pseudo' loxP sites (Schmidt-Supprian and Rajewsky 2007). The sequence of these sites can deviate considerably from the loxP site, whilst still serving as functional recognition sites for Cre (Thyagarajan, Guimaraes et al. 2000). It has been estimated these are present in the mouse genome at a frequency of 1.2 per megabase (Semprini, Troup et al. 2007). Although the affinity of Cre for these cryptic recognition sites is lower than for the loxP site, it is possible that DNA damage could occur from Cre-mediated recombination between endogenous Cre-recognition sites (Thyagarajan, Guimaraes et al. 2000). This 'Cre toxicity' phenomenon would be of particular concern in experiments performed using MEF isolated from mice that had not been backcrossed onto a C57BL/6 for many generations. However, this hypothesis was unlikely to be true as MEF derived from 7th and 12th generation backcrossed mice displayed the same phenotype as MEF derived from 3rd generation backcrossed mice.

There are other possible reasons why different results were obtained for the murine knockout or the knockdown of the human protein using RNAi. One possibility is that there is a genuine difference in the function of the hspB1 in murine and human cells. This could occur because the signalling pathways in murine and human cells may differ. Alternatively, the results may indicate a cell type difference, again because different signalling mechanisms may exist in

murine embryonic fibroblasts, human dermal fibroblasts and HeLa cells. Yet another possibility is that the results obtained with RNAi in human cells were due to off-target effects of the siRNAs used. However, it is highly unlikely that the multiple siRNAs used by Alford et al. would all produce the same type of off-target effect. There was little difference in the expression of hsp70 and hsp90 proteins in *hspB1*$^{del/del}$ and wild-type MEF (Fig 3.6). Over-expression of a compensatory protein would be unlikely in the situation where siRNA is used to deplete hspB1 protein, due to the transient and partial nature of the siRNA-mediated protein depletion.

The C57BL/6 strain of mice was selected for use in the zymosan-induced air pouch model as these mice exhibit a strong inflammatory response in this model , as measured by leukocyte counts in the exudate, when compared to other mouse strains (Delano, Montesinos et al. 2005). The strategy used to breed the mice was improved after the preliminary experiments, which resulted in the production of entire litters of wild-type or *hspB1*^{deldel} mice. Improvements to the air pouch procedure increased the accuracy and reproducibility of the experiment. The decision to only use male mice was based on evidence that leukocyte infiltration in female C57BL/6 mice has been shown to be ~50 % less compared to male C57BL/6 mice (Delano, Montesinos et al. 2005). Based on these findings, and the desire to control as many of the variables of the experiment as possible, it was decided that only male mice would be used for the air pouch model of acute inflammation.

The kinetics for the progression of inflammation in the air pouch model suggest that TNFα is secreted by zymosan-activated resident macrophages which then induces IL-6 production by fibroblasts in air pouch granulation tissue. Resident macrophages and infiltrating neutrophils are also sources of IL-6. I showed that *hspB1* deficiency caused a significant increase in cell migration and increased IL-6 production in response to zymosan stimulation for 4 h in *hspB1*$^{del/del}$ mice compared to littermate wild-type mice (Fig. 3.6A, 3.7B). The air pouch

technique was improved and an increase in IL-6 production in *hspB1*$^{del/del}$ mouse air pouches compared to wild-type was observed which was discernible and statistically significant compared to the preliminary results (Fig. 3.7B, 3.8B, 3.9C). The increased IL-6 protein production in *hspB1*$^{del/del}$ mice air pouches compared to wild-type mice reinforces the trend toward IL-6 regulation by hspB1 in MEF. This may explain why the increase in IL-6 production in hspB1-deficient mice *in vivo* was stronger than in hspB1-deficient MEF. An alternative explanation would be that *in vivo* IL-6 is expressed by other cell types in addition to fibroblasts.

Many studies measure the expression of cytokines within the air pouch exudate at the same time point where the peak of cellular infiltrate is observed. IL-1-induced CXCL1 production was not regulated by hspB1 deficiency 4 h post-zymosan *in vivo* (Fig. 3. 7C, 3. 8C, 3.9 A). CXCL1 and CXCL2 are thought to be the chemokines responsible for driving the neutrophil infiltration into the air pouch in response to pro-inflammatory stimuli. Mice that lack the expression of CXCL1 have poor leukocyte migration in response to inflammatory stimuli in subcutaneous air pouches (Terkeltaub, Baird et al. 1998). The concentrations of CXCL1 and TNFα were greater in mouse air pouches treated with zymosan for 2 h compared to 4 h zymosan (Fig. 3.9). These observations led to the decision to investigate the concentrations of these and other cytokines, at a very early time point that still allowed for accurate termination of the experiment at the chosen end point. A 1 h post-zymosan end point was chosen. I discovered that hspB1-deficient mice had increased expression of TNFα, IL-10 and the neutrophil chemotactic cytokines CXCL1 and CXCL2 1 h post-zymosan treatment compared to wild-type (Fig. 3.9), and the increased TNFα and chemokine expression provides, in part, a mechanism for the increased infiltration of neutrophils 4 h post-zymosan in *hspB1*$^{del/del}$ mice compared to wild-type mice.

The observed early peak in the production of these cytokines suggested that zymosan had a direct effect on their expression in a cell type that responds to zymosan treatment. Macrophages are capable of producing all of these cytokines. The increased concentration of TNFα and IL-10 in *hspB1*$^{del/del}$ mice compared to wild-type at 1 h post-zymosan suggested the involvement of resident macrophages in granulation tissue. Fibroblasts are capable of producing CXCL1 and CXCL2; however, fibroblasts are unlikely to be the cell type responsible for the regulation of CXCL1 protein by hspB1, as production of this chemokine was not increased in hspB1-deficient MEF. However, it is worth considering that the MEF used is these experiments were only treated with IL-1. There is the possibility that adult fibroblast may respond differently to IL-1 and other stimuli. The regulation of endothelial cell adhesion molecule expression by hspB1 was not investigated but would be an interesting avenue of investigation for the future. The precise contribution of macrophages to CXCL1, CXCL2 and IL-6 production in this model is unclear. The early peak in the production of the chemokines is to my knowledge a novel discovery and suggests that zymosan is capable of directly inducing the production of these chemokines in the air pouch. It is also possible that the expression of CXC chemokines in this model was a very rapid indirect response to zymosan stimulation. The cell type responsible and the mechanism for the very early regulation by hspB1 on CXCL1 and CXCL2 production in the zymosan-induced air pouch model is not clear, and warrants further investigation.

We found that hspB1 depletion did not result in a difference in the population of macrophages at 16 h and neutrophils at 4 and 16 h in the cellular infiltrate in air pouch exudates in response to zymosan (Fig 3.10B, C). The rapid decline in numbers of *hspB1*$^{del/del}$ cells following the peak of cellular infiltration and the lack of difference between wild-type and *hspB1*$^{del/del}$ phenotypes at 16 h suggested that in addition to increased migration of cells to the site of inflammation, the neutrophils from *hspB1*$^{del/del}$ mice were undergoing increased

clearance from the site of inflammation to relative to wild-type cells (Fig 3.10A). I observed decreased viability and increased apoptosis in neutrophils extracted from *hspB1*$^{del/del}$ mice compared to wild-type (Fig. 3.11). This may explain the reduction in the number of infiltrated leukocytes in *hspB1*$^{del/del}$ mice at 16 h compared to 4 h post-zymosan.

The effect of genetic deletion of *hspB1* on inflammatory gene expression in *hspB1*$^{del/del}$ mice *in vivo* and MEF was the opposite to that observed following siRNA-mediated depletion of the protein in HeLa cells and human dermal fibroblasts. The kinetics of cytokine expression induced by zymosan and the types of cytokines regulated by hspB1 suggested that macrophages might be the major cell type responsible for the differences in inflammation caused by hspB1 deficiency. To investigate the contribution of macrophages in the acute inflammatory response *in vivo*, I decided to investigate 1) the effect of hspB1 deficiency on the response to zymosan in a model of peritoneal inflammation, which would also afford the opportunity to reinforce the conclusions from the air pouch model, and 2) the function of hspB1 in the production of inflammatory cytokines in macrophages isolated from the peritoneal cavity in mice.

Chapter 4

The effect of hspB1 deficiency on peritoneal inflammation and inflammatory gene expression in peritoneal macrophages.

4.1 Introduction.

During the investigation into the effect of hspB1 deficiency on pro-inflammatory cytokine expression in MEF, it was observed that it took a longer time for *hspB1*$^{del/del}$ MEF to reach the same final confluence at each passage compared to wild-type MEF. This observation had implications for the results described in the last chapter on the regulation by hspB1 of inflammatory gene expression in MEF and murine air pouches. If *hspB1*$^{del/del}$ MEF proliferated at a slower rate than wild-type cells, then it would be expected that there would be fewer *hspB1*$^{del/del}$ cells than wild-type at the time point of stimulation. This would result in less cytokine production, and the effects of cell confluence on signalling might complicate the results. The magnitude of any increase in pro-inflammatory cytokine production in *hspB1*$^{del/del}$ MEF compared to wild-type in response to IL-1 stimulation may have been under-estimated if there were fewer *hspB1*$^{del/del}$ MEF than wild-type cells when IL-1 was added. It was therefore decided to investigate if hspB1 deficiency resulted in a reduced rate of cell proliferation.

Confidence in the role of hspB1 in pro-inflammatory cytokine expression in the air pouch model was reduced by the fact that the data were so variable and many *hspB1*$^{del/del}$ mice displayed comparable numbers of infiltrating cells and cytokine levels to those in wild-type mice. It was decided to investigate the effects of hspB1 deficiency on acute inflammation in another *in vivo* model to determine if a more consistent increase in cellular infiltration and inflammatory gene expression could be observed. The injection of zymosan into the peritoneal cavity of mice has been shown to produce acute inflammation, including leukocyte infiltration and production of inflammatory mediators (Doherty, Poubelle et al. 1985) and is widely used as a self-resolving model to characterise peritoneal inflammation in mice (Rao, Currie et al. 1994; Ajuebor, Gibbs et al. 1998; Cash, White et al. 2009). Importantly, the zymosan-induced peritonitis model does not rely on the creation of a sterile

air pouch and the prior formation of granulation tissue, but instead allows for the direct effects on inflammatory processes to be measured. Thus, in this model the effects of hspB1 deficiency on cell proliferation and consequential development of the granulation tissue in air pouches would be avoided. Zymosan was chosen as the stimulus in the peritonitis model, as this would allow for direct comparison of the effects of hspB1 deficiency in this model to its effects in the air pouch model of acute inflammation.

The use of the peritonitis model also provided the opportunity to investigate the function of hspB1 deficiency in cytokine production in peritoneal macrophages. In chapter 3, I observed an increase the expression of TNFα, IL-6, IL-10 and neutrophil-chemoattractant proteins CXCL1 and CXCL2 in *hspB1*$^{del/del}$ mice relative to wild-type mice in the air pouch model. Macrophages are resident within tissue lining of both the air pouches and peritoneal cavities and are thought to contribute to the production of cytokines in response to inflammatory challenge in these models. I decided to investigate the effect of hspB1 deficiency on cytokine expression in macrophages *in vitro* to understand the contribution of these cells to the production of cytokines in acute inflammation *in vivo*. Murine bone marrow-derived macrophages were not suitable for these investigations, as a previous study in my lab had shown that these cells do not express hspB1 protein (Alford, Glennie et al. 2007). Intraperitoneal injection of thioglycollate (TG) broth is a method commonly used to recruit leukocytes to the peritoneal cavity of mice (Spitalny 1981; Den Otter, De Groot et al. 1982; Leijh, van Zwet et al. 1984). TG is thought not to act as an inflammatory stimulus or result in the activation of TG-elicited peritoneal macrophages (TEPM) (Leijh, van Zwet et al. 1984). TEPM were isolated from the peritoneal cavities of wild-type and *hspB1*$^{del/del}$ mice and were used to investigate the role of hspB1 in inflammatory gene expression in *ex-vivo* macrophage cultures.

4.2 The effect of hspB1 deficiency on proliferation of MEF.

Having observed fewer *hspB1*$^{del/del}$ MEF than wild-type cells during culture, it was decided to quantify the numbers of viable cells in wild-type and hspB1-deficient MEF cultures and to investigate if hspB1 regulates apoptosis or proliferation of these cells. These experiments were performed by Dr. Anna Aubareda. MEF were seeded at equal densities and allowed to proliferate for 5 days. The number of viable cells was determined by MTT assay at various times after seeding. The number of *hspB1*$^{del/del}$ cells was reduced compared to wild-type at d 3-5 (Fig. 4.1A). I have already demonstrated decreased cell viability and increased apoptosis in *hspB1*$^{del/del}$ neutrophils compared to wild-type (Fig 3.13). The cytoprotective function of hspB1 has been well characterised in previous studies (Benn, Perrelet et al. 2002; Paul, Manero et al. 2002; de Graauw, Tijdens et al. 2005). It was possible that a greater proportion of *hspB1*$^{del/del}$ MEF were less viable or undergoing spontaneous apoptosis compared to wild-type cells. The terminal deoxynucleotidyl transferase dUTP nick end labelling (TUNEL) assay method was used to detect the amount of cells with DNA fragmentation which results from apoptotic signalling, however, this showed that only approximately 2 % of *hspB1*$^{del/del}$ and wild-type cells were undergoing apoptosis (Fig 4.1C). Another possibility was that hspB1 deficiency resulted in cell senescence. However, senescence-associated-β-galactosidase (SA-β-gal) detection confirmed similar proportions of senescent *hspB1*$^{del/del}$ and wild-type MEF (Fig. 4D). The number of proliferating cells was measured by incorporation of bromodeoxyuridine (BrdU) after 24 h exposure by *hspB1*$^{del/del}$ and wild-type MEF. This showed similar proportions of approximately 60 % proliferating cells in *hspB1*$^{del/del}$ and wild-type MEF at p 3, p5 and p8 (Fig 4.1D). A shorter exposure to BrdU for 2 h, which does not allow for sufficient time for all proliferating cells to uptake BrdU, showed a decrease in BrdU incorporation in *hspB1*$^{del/del}$ MEF compared to wild-type (Fig. 4.1E). BrdU is incorporated into newly synthesised DNA of replicating cells during the S phase of the cell cycle, a

process which is controlled, in part, by a family of cyclin-dependent kinases (CDKs). Expression of $p21^{waf1}$ $p27^{kip1}$, both CDK inhibitors responsible for arresting cells in the G1 phase of the cell cycle, was increased in *hspB1*$^{del/del}$ MEF compared to wild-type MEF, providing an explanation for the reduced proliferation rate of hspB1-deficient cells (Fig. 4.1F).

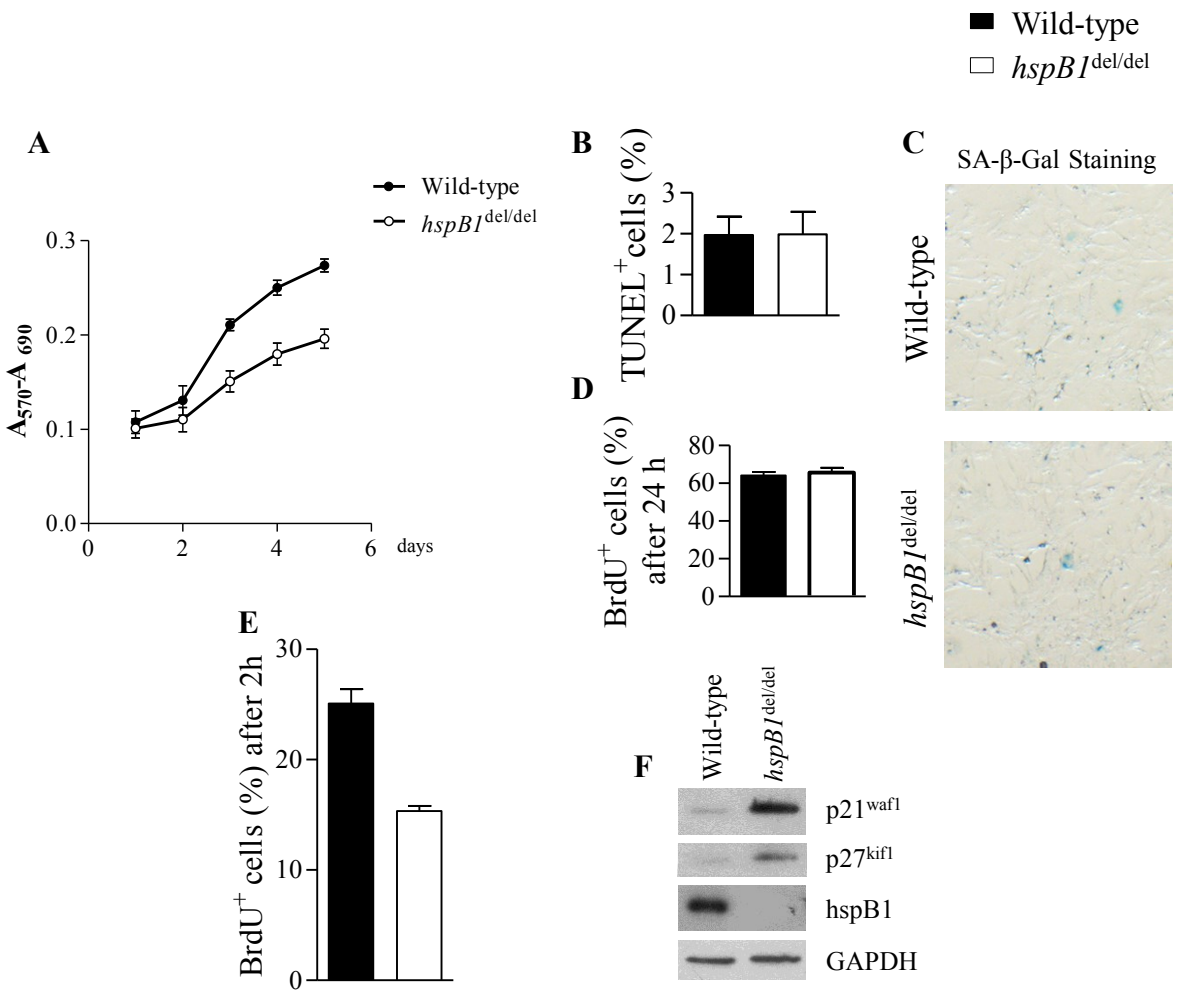

Figure 4.1 The effect of hspB1 deficiency on proliferation of MEF.

A, Growth curve analysis of wild-type and *hspB1*$^{del/del}$ MEF determined by MTT assay at different days post-seeding (means ± SEM; n = 3). B, Plot of mean (%) TUNEL^{+ve} MEF, detected by fluorescence staining (± SEM, n = 3). C, staining for SA-β-galactosidase activity (blue) in wild-type and *hspB1*$^{del/del}$ MEF are shown. D, Plot of mean (%) BrdU incorporation following a 24 h exposure (± SEM, n = 3). E, BrdU incorporation following a 2 h exposure. Plot of BrdU-positive cells (mean % ± SEM) from two independent experiments performed in triplicate are shown. F, western blot for p21^{waf1}, p27 ^{kip1}, hspB1 and GAPDH as a loading control. Experiments were performed by Dr. Anna Aubareda.

4.3 An investigation into distribution of hspB1 expression in murine carotid arteries.

The observation that the rate of proliferation of hspB1-deficient MEF was reduced compared to wild-type MEF had implications for the interpretation of the results from the air pouch experiments. The injection of air at the outset of the experiment creates the air pouch cavity and granulation tissue is allowed to develop in the lining of the air pouch during the course of the experiment. If fibroblasts within the *hspB1*$^{del/del}$ air pouch granulation tissue were proliferating at a slower rate than wild-type cells, then the granulation thickness and density would not be the same in *hspB1*$^{del/del}$ and wild-type mice at the time point of zymosan injection. Vascular endothelial cells express hspB1, which has been shown to play a role in modulating microfilament responses to oxidative stress (Huot, Houle et al. 1997). Hence, it was possible that hspB1 also promotes proliferation of these cells. The tissue was stained with anti-CD31 antibody to identify the vascular endothelium. (Fig 4.2A). Carotid artery tissue from *hspB1*$^{del/del}$ mice was used as a negative control for hspB1 staining (Fig. 4.2C). HspB1 protein staining correlated with the layer expressing CD31, confirming that vascular endothelial cells express hspB1 protein (Fig. 4.2B). HspB1 protein expression appeared to be restricted to tissues within the inside of the intima. HspB1 protein expression was not detected in vascular smooth muscle.

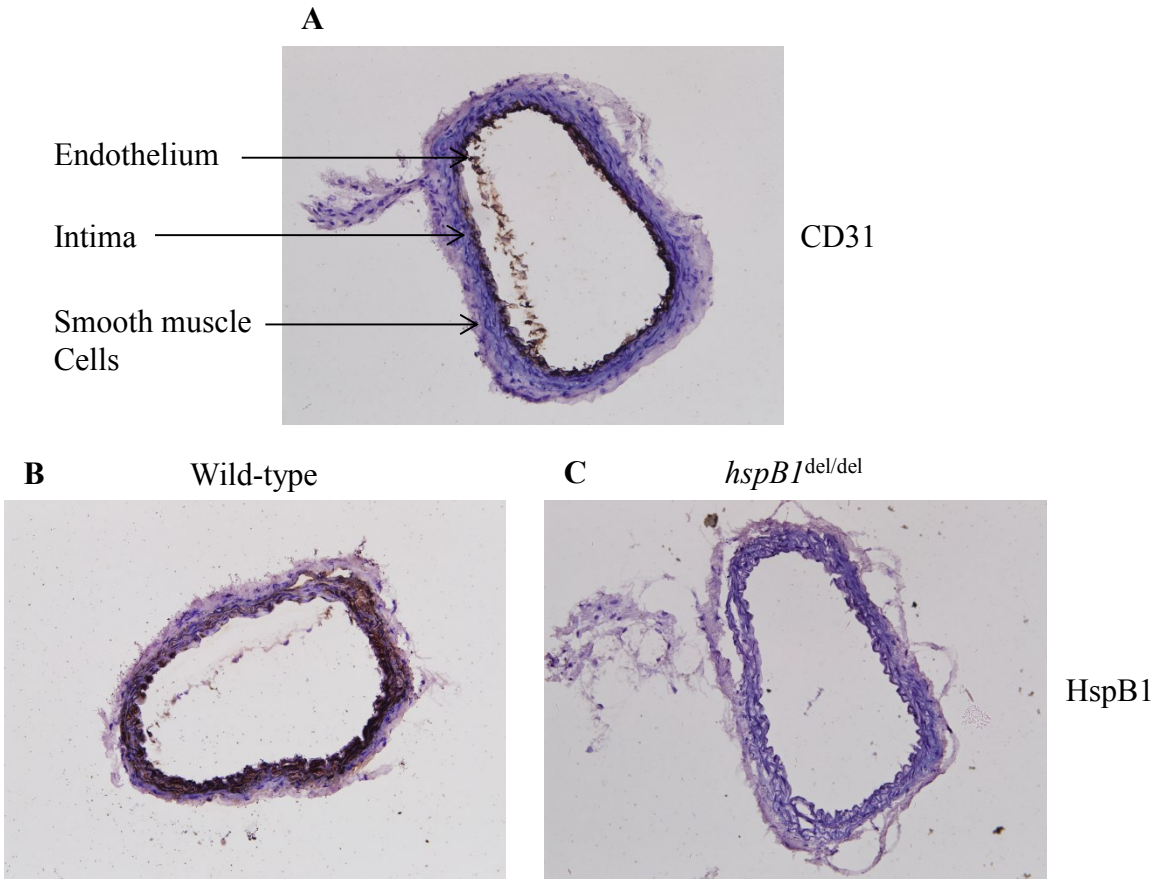

Figure 4.2 Vascular endothelial cells express hspB1 protein.

Mouse carotid arteries were frozen in OCT, sectioned on a cryostat cryotome and fixed in acetone pre-cooled to -20^{o}C. Brown colour indicates positive antigen staining. A, CD31 staining of wild-type mouse carotid artery to show expression in vascular endothelial cells. The location of the intima and vascular smooth muscle cells are also identified. B, HspB1 staining of wild-type and C, *hspB1*$^{del/del}$ mouse carotid arteries.

4.4 An investigation into the effect of hspB1 deficiency on the thickness and microvasculature density of murine air pouch skin.

Having identified that hspB1 protein is expressed in murine vascular endothelium, it was therefore considered relevant to assess the effect of hspB1 deficiency on the vascularity of the granulation tissue. A thinner and less dense granulation tissue could possibly contain fewer resident macrophages, and would therefore weaken the response to zymosan. This suggested that the effect of hspB1 deficiency on cytokine expression in the air pouch model may have been underestimated. I decided to determine the histological structure of wild-type and *hspB1*$^{del/del}$ air pouches. Skin tissue from d 5 air pouches from wild-type (Fig. 4.3C) and *hspB1*$^{del/del}$ (Fig 4.3D) mice was harvested and fixed in 4% formaldehyde and stained with Masson's Trichrome. The vessels were counted and the thickness of granulation tissue was measured by microscopy image capture with analysis by Image J. HspB1 deficiency did not result in a significant decrease in the thickness of the granulation tissue (Fig. 4.3A) or density of the microvasculature (Fig. 4.3B).

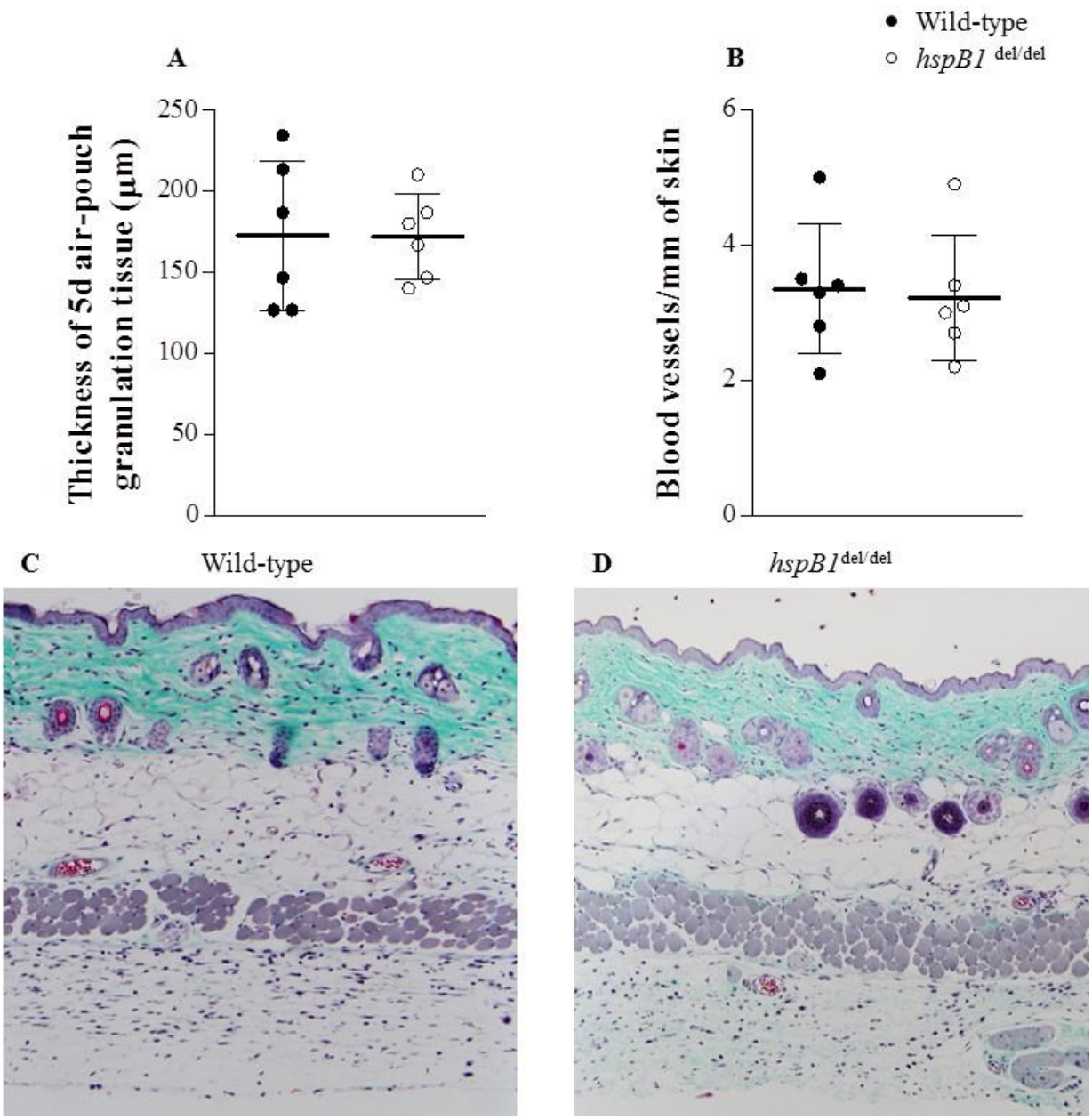

Figure 4.3 The effect of hspB1 deficiency on the thickness and microvasculature density of day 5 air pouch granulation tissue.

Skin from the dorsal surfaces of male wild-type and *hspB1*$^{del/del}$ mice was excised on d 5 after the creation of air pouch and re-inflation. Mean granulation tissue thickness from 10 representative fields / skin section (A) and the number of blood vessels / mm skin (B) were calculated by microscopy. Plots show mean ± S.D (n=6). Representative skin sections from d 5 air pouches from (C) wild-type and (D) *hspB1*$^{del/del}$ mice are shown.

These results indicated that despite the observation that hspB1 deficiency resulted in impaired proliferation of MEF *in vitro*, the thickness and vascularity of granulation tissue *in vivo* in air pouches of *hspB1*$^{del/del}$ mice is normal. However, there were many aspects of granulation tissue development that were not determined, such as fibroblast density and macrophage numbers. The Masson's trichrome stain allows for identification of blood vessels by the staining of red blood cells, however, the precise effect of hspB1 deficiency on newly forming micro-vessels was not determined. The observation of hspB1 expression in vascular endothelial cells questioned if hspB1 also had a role in regulation in the proliferation of these cells. These complications suggested that a more straightforward approach to investigate the effect of hspB1 deficiency on leukocyte trafficking and associated chemokine expression would be to inject zymosan directly into the peritoneal cavity.

4.5 The effect of hspB1 deficiency in a peritonitis model of acute inflammation *in vivo.*

10 - 12 week old male wild-type and *hspB1*$^{del/del}$ mice were injected intraperitoneally with 500 µl ml 1 mg/ml zymosan. The peritoneal cavity was lavaged after 4 or 24 h with 5 ml ice-cold PBS. The infiltrating cells were stained with trypan blue and manually counted using a haemocytometer. In agreement with the air pouch model data, intraperitoneal injection of zymosan resulted in a statistically significant 2.1-fold ($P \leq 0.01$) increase in infiltrating cells at 4 h post-zymosan in *hspB1*$^{del/del}$ mice compared to wild-type controls (Fig. 4.3A). In contrast to the air pouch model, the numbers of infiltrating cells at 4 h post-zymosan were much more closely grouped and statistical significance was reached with a small number of mice (Fig. 4.3A). Cellular infiltration in *hspB1*$^{del/del}$ mice returned to the same level as wild-type mice after 24 h (Fig. 4.3A). As seen in the air pouch model, cellular infiltrates at 4 h post-zymosan in wild-type and *hspB1*$^{del/del}$ mice contained similar proportions of neutrophils (Fig. 4.3B). There was also a trend towards a smaller proportion of neutrophils and a greater proportion of macrophages in the peritoneal lavage from wild-type mice compared to *hspB1*$^{del/del}$ mice at 24 h post-zymosan injection (Fig. 4.3C). The increase in cell infiltration at 4 h post-zymosan in *hspB1*$^{del/del}$ mice compared to wild-type mice in the peritonitis model was comparable to that observed in the air pouch model, although the data grouping was improved in the peritonitis model.

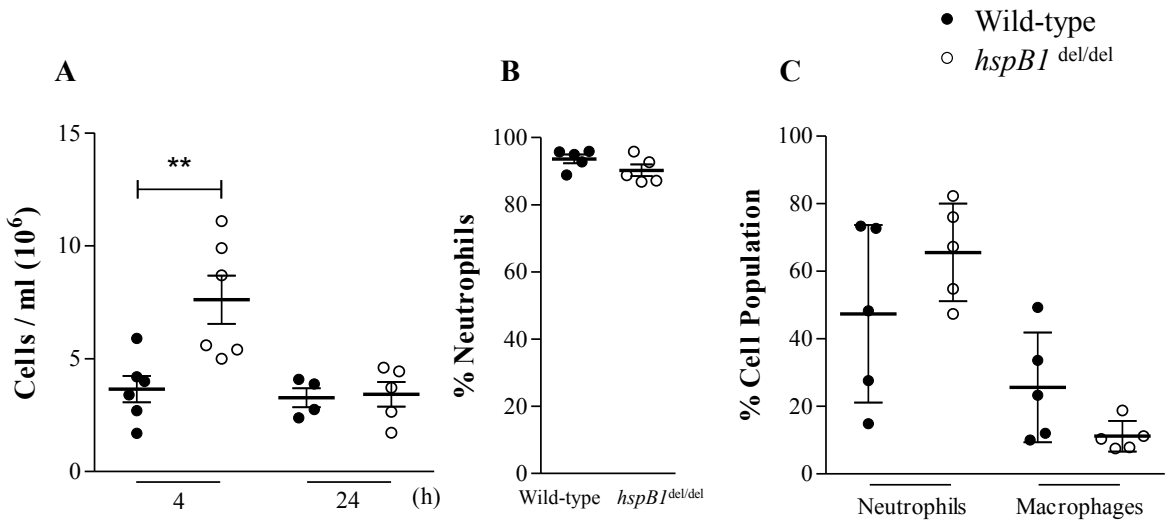

Figure 4.4 The effect of hspB1 deficiency on cellular infiltration in the peritonitis model of acute inflammation.

1 ml of zymosan (1 mg/ml) was injected into the peritoneal cavities of 10 – 12 week-old male wild-type and *hspB1*$^{del/del}$ mice**.** A, plot of the number of infiltrating cells with time of zymosan treatment indicated (n = 4 - 6). B, graph of population of neutrophils as a percentage of total infiltrating cells at 4 h post-zymosan identified by gating for the Ly-6G^{hi} CD11b^{hi} population (n = 5). C, plots showing neutrophil and macrophage populations in infiltrates at 24 h post-zymosan determined by flow cytometry; neutrophil gate (Ly-6G^{hi}, CD11b^{hi}); macrophage gate (Ly-6G^{lo}, CD11b^{lo}); (n=5). ** $P \leq 0.01$. Graphs show means ± SEM.

4.6 The effect of hspB1 deficiency on cytokine production in the zymosan-induced model of peritonitis.

I decided to measure the expression of pro-inflammatory cytokines, at the time points where their expression was observed to be increased in *hspB1*$^{del/del}$ mice compared to wild-type mice in the air pouch model. The aim of this was to determine if the variability of the inflammatory response in *hspB1*$^{del/del}$ mice to zymosan would be less in the peritonitis model and if a more distinct difference between groups of data for wild-type and *hspB1*$^{del/del}$ mice could be observed.

The peritoneal lavage fluid protein concentrations of CXCL1, CXCL2 and TNFα at 1 h, and IL-6, IL-10 in at 4 h post-zymosan were measured. These time points were chosen as the production of the cytokines measured was regulated by hspB1 at these times post-zymosan in the air pouch model. I also decided to measure the concentration of CCL2 (MCP-1), which is an important chemokine for monocyte recruitment.

The production of CXCL1 and CXCL2 protein at 1 h post-zymosan was significantly increased by 2.3-fold ($P \leq 0.001$) and 1.6-fold ($P \leq 0.05$) respectively, in *hspB1*$^{del/del}$ mice compared to wild-type (Fig. 4.4A and 4.4B), in agreement with the air pouch model. In contrast to air pouch system, the concentration of TNFα protein at 1 h post-zymosan was very low or undetectable and appeared to be unaffected by hspB1 deficiency (Fig. 4.4C). IL-6 protein expression was higher than in the air pouch model and was not regulated by hspB1 at 4 h post-zymosan (Fig. 4.4D). HspB1 deficiency did not result in a change in expression of IL-10 protein, a potent anti-inflammatory cytokine (Fig 4.4E), or CCL2 (Fig 4.4F) at 4 h post-zymosan.

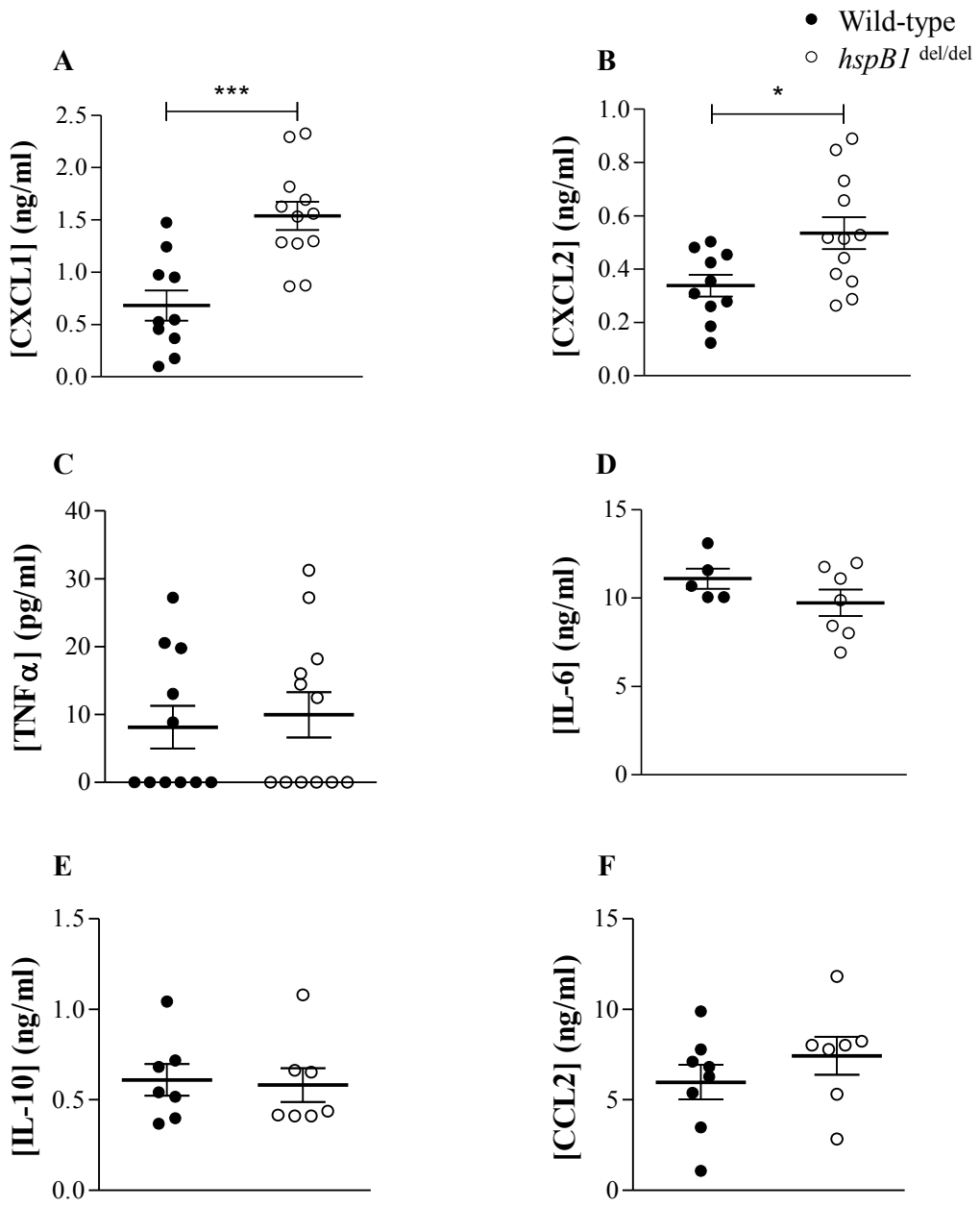

Figure 4.5 The effect of hspB1 deficiency on cytokine production in the zymosan-induced model of peritonitis.

1 ml of zymosan (1 mg/ml) was injected into the peritoneal cavities of 10 – 12 week-old male wild-type and *hspB1*$^{del/del}$ mice**.** Protein concentrations of CXCL1 (A), CXCL2 (B), TNFα (C), at 1 h (n = 5-12) and IL-6 (D), IL-10 (E) and CCL2 (F) at 4 h post-zymosan in peritoneal lavages are shown (n = 5-7). Graphs show mean ± SEM. * $P \leq 0.05$, *** $p \leq 0.001$.

4.7 HspB1 deficiency results in a reduction in viability and an increase in apoptosis in infiltrating neutrophils in zymosan-challenged peritoneal cavities.

The expression of IL-6 and TNFα protein and neutrophil apoptosis was increased in *hspB1*$^{del/del}$ mice compared to wild-type mice 4 h post-zymosan in the air pouch model (Fig. 3. 9, 3.10). IL-6 and TNFα have been shown to inhibit spontaneous apoptosis of neutrophils (McNamee, Bellier et al. 2005). I decided to investigate if the viability of neutrophils infiltrating into the peritoneal cavity at 4 h post-zymosan was affected by the lack of regulation of these cytokines by hspB1 at this time point. Cells infiltrating into the peritoneal cavity at 4 h post-zymosan in the experiment shown in Fig. 4.3 were retrieved and apoptosis detected by staining with annexin V and PI and measured by flow cytometry as before. This showed a trend towards a reduced proportion of viable ($P = 0.1682$), annexin V^{lo}/PI^{lo}, *hspB1*$^{del/del}$ cells (51.1 ± 4.4 %) compared to wild-type cells (62.7 ± 4.4 %), consistent with reduced viability of the hspB1-deficient cells observed in the air pouch model. The proportion of annexin V^{hi}/PI^{hi} cells from *hspB1*$^{del/del}$ mice (38.5 ± 5.3 %) was increased ($P \leq 0.01$) relative to that from wild-type animals (13.3 ± 3.4 %) indicating increased apoptosis of the hspB1-deficient cells. The proportion of cells which stained weakly for PI but positive for annexin V in wild-type mice (10.5 ± 2.1 %) was not significantly greater compared to *hspB1*$^{del/del}$ mice (7.6 ± 1.5 %). Overall these results were very similar to previous observations made using the air pouch model.

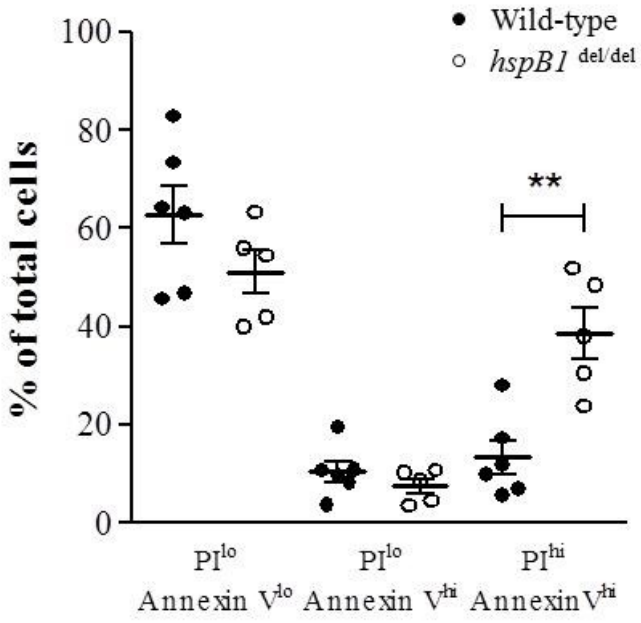

Figure 4.6 The effect of hspB1 deficiency on the viability and apoptosis of neutrophils in the zymosan-induced peritonitis model.

Cellular infiltrates in peritoneal lavages at 4 h post-zymosan were analysed for cell viability and apoptosis by flow cytometry with annexin V and PI staining (n = 5 - 6). Three cell populations were observed and gated (annexin V^{lo}, PI^{lo}; annexin V^{hi}, PI^{lo}; annexin V^{hi}, PI^{hi}). Bars show mean ± SEM; **P ≤ 0.01.

4.8 Investigation of hspB1 expression in murine neutrophils.

To investigate if the increased numbers of neutrophils undergoing apoptosis in *hspB1*$^{del/del}$ mice compared to wild-type mice in the two *in vivo* models of inflammation used was due to an intracellular defect in cytoprotective function resulting from hspB1 deficiency, it was decided to determine if hspB1 protein expression could be detected in neutrophils from wild-type mice. Cells were recruited by injection of wild-type mice with TG and were isolated 4 h later and washed. Neutrophils were purified in supernatants from magnetic beads coated with a cocktail of biotin-conjugated monoclonal antibodies raised against antigens that are not expressed on neutrophils. Purified cellular infiltrates were stained with Ly-6G and CD-11b to identify neutrophils and analysis by flow cytometry showed that the neutrophil population was enriched to a purity of 85.2% compared to 36.9% neutrophil purity of un-purified cells. The cells were lysed using whole cell lysis buffer and lysate containing 40 µg of protein was analysed for hspB1 and α-tubulin protein expression by western blot, together with 3 µg of wild-type MEF lysate as a positive control. HspB1 protein could not be detected in the neutrophil lysate but was readily detected in the MEF control lysate (Fig. 4.6). This observation suggested that it is unlikely that hspB1 protein is expressed in neutrophils and further suggests that hspB1 promotes neutrophil viability by a direct extracellular effect of the protein, or by indirect effects arising from other cells which do express hspB1.

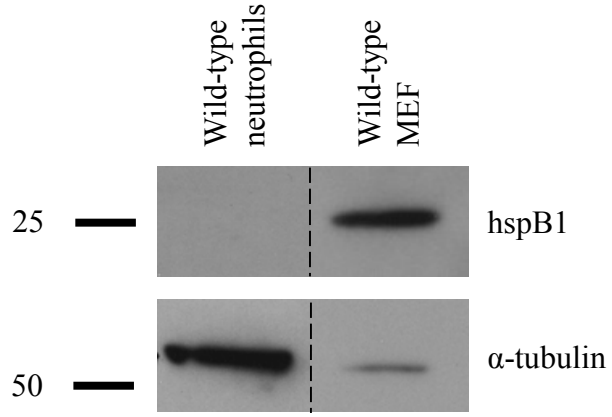

Figure 4.7 HspB1 protein cannot be detected in murine neutrophil lysates by western blot.

10 – 14 week old male mice were injected IP with 1 ml 4 % TG/PBS. After 4 h the peritoneal cavity was lavaged with 10 ml ice-cold PBS. The neutrophil isolation kit (Miltenyi Biotec) was used to purify the peritoneal neutrophils. The successful enrichment of neutrophils (85.2%) was confirmed by Ly-6G and CD-11b detection by flow cytometry. Cells were lysed and 40 µg of wild-type neutrophil lysate was loaded. 3 µg wild-type MEF lysate loaded as a positive control for hspB1 protein expression. HspB1 and α-tubulin proteins (the latter as a loading control) were detected by western blot. Dotted lines delineate lanes which were cropped from the original western blot.

4.9 Expression of hspB1 in wild-type peritoneal macrophages.

Having found that hspB1 protein could not be detected in neutrophils I decided to investigate if it is expressed in another myeloid cell type important for inflammatory cytokine expression, namely macrophages. If wild-type macrophages did not express hspB1 protein, it would be unlikely that it would have an intracellular role in regulation of cellular signalling or cytokine expression in these cells. If hspB1 protein could be detected in these cells this would allow the intracellular effects of hspB1 deficiency on cytokine expression by macrophages to be investigated.

Brewer's modified TG recruits macrophages, with peak numbers of macrophages observed 3 – 4 d post TG injection (Den Otter, De Groot et al. 1982; Leijh, van Zwet et al. 1984). A 4 % TG broth was prepared in LPS free cell culture grade PBS and autoclaved. The 4 % TG was allowed to mature for 2 weeks, as this has been shown to result in a greater magnitude of macrophage recruitment compared to fresh TG. Male mice 12 weeks of age were injected IP with 1 ml 4 % TG/PBS. After 3 d the peritoneal cavity was lavaged with 10 ml ice-cold PBS. TEPM were lysed with whole cell lysis buffer. 100 μg of TEPM lysate from wild-type and *hspB1*$^{del/del}$ mice was loaded on an SDS-polyacrylamide gel. 1 μg/ml of wild-type MEF lysate was loaded as positive control for hspB1 protein. HspB1 and α-tubulin protein expression in the cell lysates was analysed by western blotting. HspB1 protein was detected in wild-type TEPM lysate but only at a very low level compared to that in wild-type MEF (Fig 4.8). HspB1 protein was not detected in *hspB1*$^{del/del}$ TEPM lysates as expected (Fig 4.7). The positive detection of hspB1 protein in peritoneal macrophages prompted analysis of the function of hspB1 in cytokine expression in peritoneal macrophages.

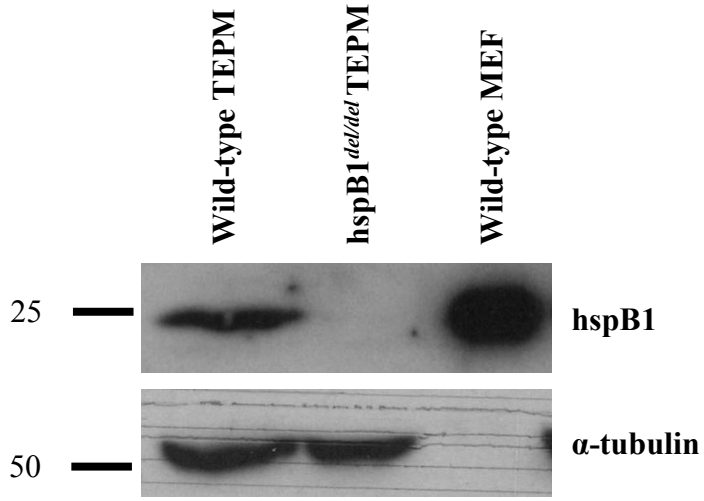

Figure 4.8 Detection of hspB1 protein expression in TEPM from wild-type mice.

Male mice 12 weeks of age were injected IP with 1 ml 4 % TG/PBS. After 3 d the peritoneal cavity was lavaged with 10 ml ice-cold PBS. TEPM were lysed immediately following isolation. TEPM and MEF lysates were analysed by western blot with anti-hspB1 and anti-α-tubulin antibodies as described previously. 100 μg of wild-type and *hspB1*$^{del/del}$ TEPM lysate was loaded. 1 μg of wild-type MEF lysate was loaded as a positive control for hspB1 protein expression. Western blots with molecular weight markers are shown for hspB1 and α-tubulin proteins.

4.10 The effect of hspB1 deficiency on pro-inflammatory cytokine expression in TEPM.

To investigate cytokine responses in macrophages relevant to the *in vivo* models used previously it was decided to use zymosan to stimulate the cells. The TLR-4 ligand, LPS, was also used as this is another potent and well-characterised agent that activates signalling and induces cytokine expression in these cells. TEPM were isolated from *hspB1*$^{del/del}$ and wild-type mice as described previously and cells counted and seeded in six-well plates. Preliminary experiments determined that 4 h was the optimal time point and 10 ng/ml LPS or 100 μg/ml zymosan were the optimal concentrations for the analysis of IL-6, CXCL1 and TNFα protein expression as determined by ELISA. Several experiments were performed using these conditions with several different batches of TEPM to determine the effect of hspB1 deficiency on cytokine protein expression.

4 h LPS treatment resulted in induction of TNFα and IL-6 protein, with a statistically significant increase in TNFα (2.1-fold; $P \leq 0.01$; Fig 4.8 A) and IL-6 (3.2-fold; $P \leq 0.01$; Fig 4.8 C) production in *hspB1*$^{del/del}$ TEPM compared to wild-type cells. As for zymosan, there was a statistically significant increase in zymosan-induced TNFα production (2.8-fold; $P \leq 0.05$; Fig. 4.8 B) in *hspB1*$^{del/del}$ TEPM compared to wild-type cells, although hspB1-dependent regulation of zymosan-induced IL-6 was not statistically significant ($P = 0.10$; Fig. 4.8 D). There was a trend towards increased CXCL1 production in response to LPS (Fig. 4.8 E) and zymosan (Fig. 4.8 F) in *hspB1*$^{del/del}$ TEPM compared to wild-type, however, these small increases were not statistically significant. No IL-10 protein was detected in TEPM supernatants at 4 h post-zymosan (data not shown). Only low concentrations of cytokines could be detected in untreated cells and basal cytokine expression was unaffected by hspB1 deficiency (Fig. 4.8).

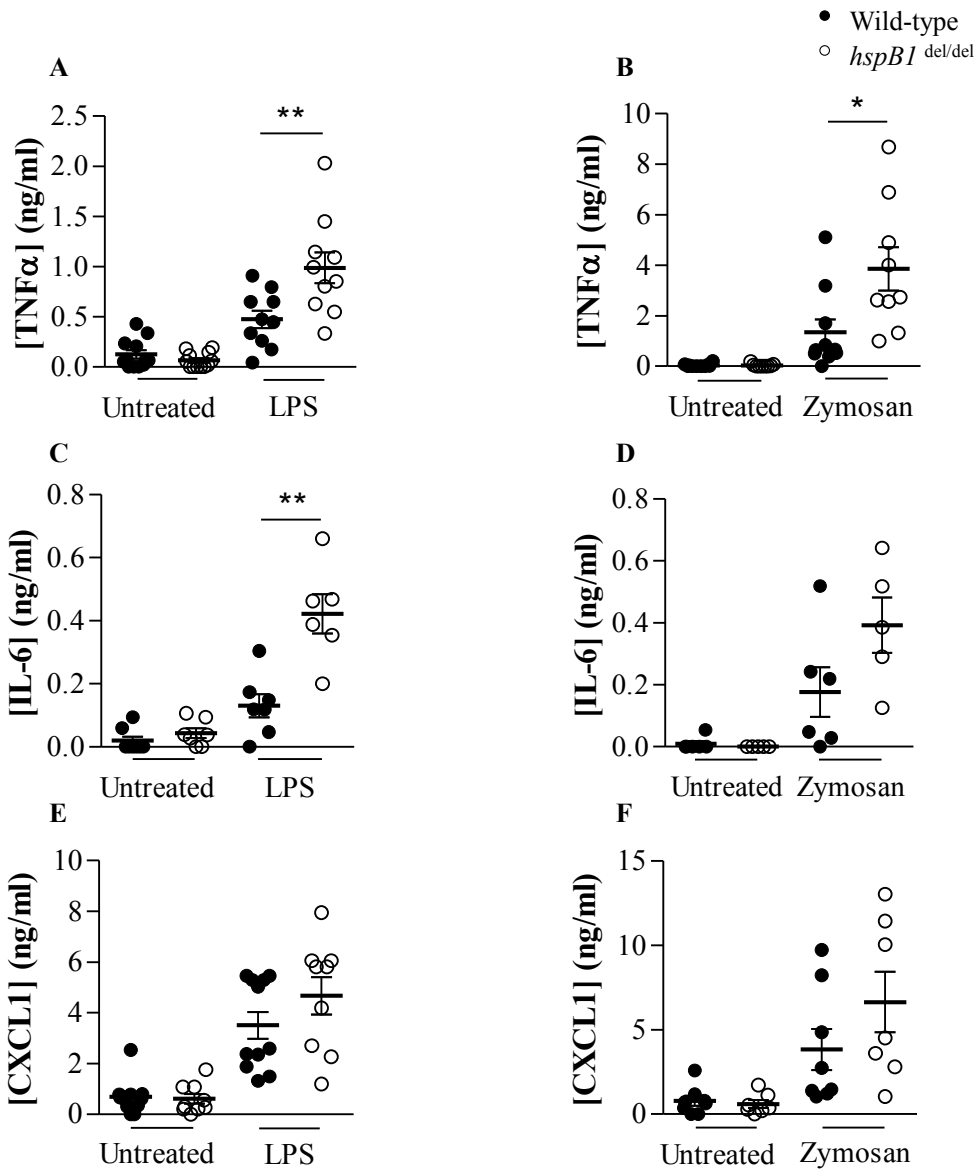

Figure 4.9 The effect of hspB1 deficiency on pro-inflammatory cytokine expression in TEPM.

TEPM were isolated and 1 x 10^6 cells/well were seeded in six-well plates, incubated overnight, washed with PBS, and treated with 10 ng/ml LPS or 100 µg/ml zymosan in 2 ml compete medium for 4 h. Plots show concentrations of TNFα (A, B; n = 9-13), IL-6 (C, D; n = 7-8) and CXCL1 (E, F; n = 7-11) proteins in supernatants of TEPM treated with LPS or zymosan (as indicated) determined by ELISA. Graphs show mean ± SEM; * $P \leq 0.05$, ** $P \leq 0.01$.

4.11 Experiment to investigate the effect of hspB1 deficiency on TEPM viability during cell culture.

It was possible that the differences in cytokine expression in wild-type and hspB1-deficient TEPM were due to differences in cell viability. I decided to perform a MTT assay on *hspB1*$^{del/del}$ and wild-type TEPM after overnight incubation (at the time point at which cells were stimulated in previous experiments). TEPM were isolated as before and seeded at 350,000, 175,000 or 35,000 cells/well in a 96 well plate. 35,000 cells/well in a 96 well plate format is approximately the same cell density as 1x10^6 TEPM in a 6 well plate format. There was an increase in A_{570}-A_{690} readings for *hspB1*$^{del/del}$ TEPM relative to wild-type TEPM at 350,000 (1.9-fold), 175,000 (2.1-fold) and 35,000 (2.0-fold) cells/well (Fig. 4.9A).

TEPM were also seeded at 1 x 10^6 cells/well in a six-well format as before. The cells were incubated overnight, washed and stimulated with 10 ng/ml LPS for 4 h or left untreated. The supernatants were removed and the cells lysed with whole cell lysis buffer. The protein concentrations of the cell lysates were determined by BCA assay. The concentrations of IL-6 and TNFα proteins in the TEPM supernatants were also measured by ELISA. As before, there was an increase in the concentration of IL-6 (4.3-fold, Fig. 4.9B) and TNFα (2.3-fold, Fig. 4.9C) in LPS stimulated *hspB1*$^{del/del}$ TEPM compared to wild-type. There was a 1.7-fold increase in the concentration of protein in untreated and LPS treated *hspB1*$^{del/del}$ TEPM compared to wild-type (Fig. 4.9D). I decided to investigate the effect of hspB1 deficiency of TEPM survival. 40 µg of TEPM cell lysate was probed by western blot for PARP and α-tubulin, the latter as a loading control. There was no difference in the amount of PARP, or indication of cleaved PARP, in TEPM stimulated with LPS or left untreated from hspB1$^{del/del}$ mice compared to corresponding wild-type cells (Fig 4.9E). Thus hspB1 deficiency does not appear to affect apoptosis in peritoneal macrophages but rather, increases the adherence,

proliferation or metabolic activity of these cells to a commensurate degree compared to its effects on LPS or zymosan-induced cytokine expression.

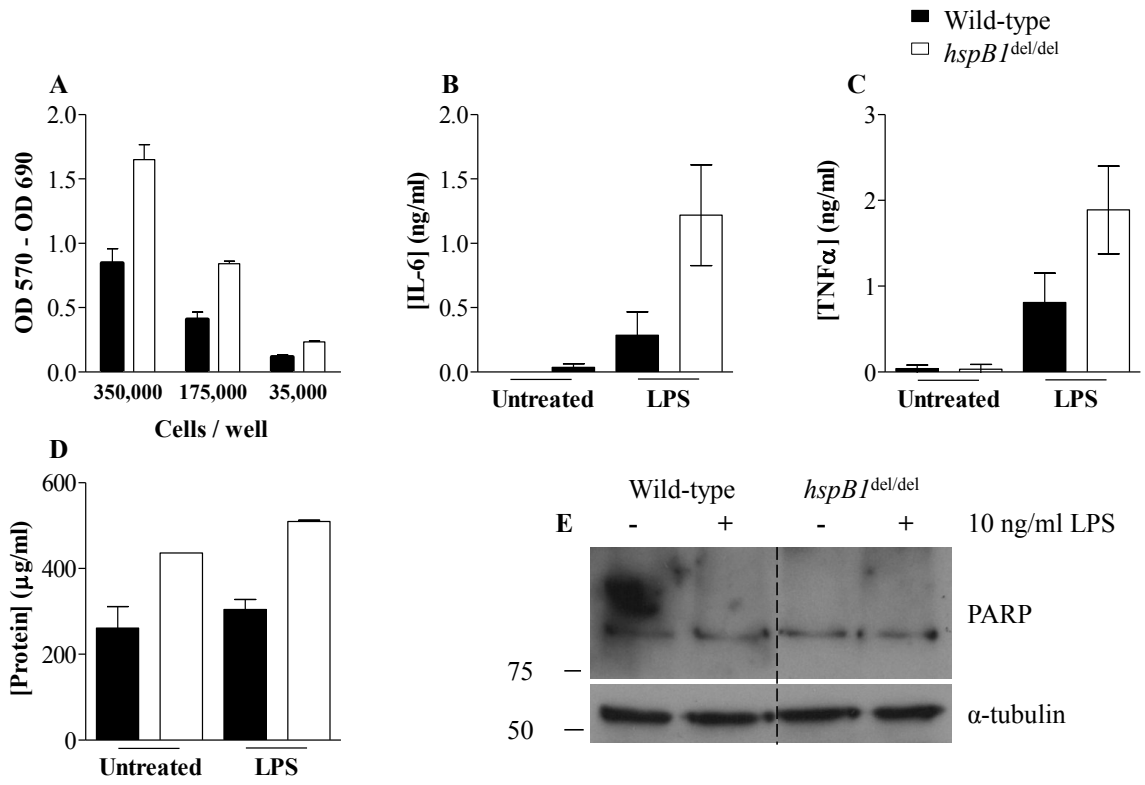

Figure 4.10 The effect of hspB1 deficiency on viability/metabolic activity, total cellular protein and pro-inflammatory cytokine expression in TEPM.

(A), TEPM were isolated as before and seeded in triplicate at 350,000, 175,000 or 35,000 cells/well in a 96 well plates. The viability of TEPM after overnight incubation at 37^{o}C, 5 % CO^2 was determined by MTT assay (n = 4 wild-type and 2 *hspB1*$^{del/del}$ mice). TEPM were seeded at 1x10^6 cells/ well in a 6 well plate format. TEPM were stimulated with 10 ng/ml LPS for 4 h or left untreated. The concentrations of IL-6 (B) and TNFα (C) protein in the TEPM supernatant were determined by ELISA (n = 4 wild-type and 2 *hspB1*$^{del/del}$ mice). (D), the cells were lysed and the protein concentration of the lysate was measured by BCA assay (n = 2 wild-type and 1 *hspB1*$^{del/del}$ mice). Bars and plots show mean ± SD. (E), 40 µg of cell lysates were probed by western blot for PARP and α-tubulin, the latter as a loading control. Dotted lines delineate lanes which were cropped from the original western blot.

4.12 Investigation of hspB1 protein expression in purified TEPM.

Re-examination of hspB1 expression in TEPM was prompted by a lack of cytokine expression regulation by hspB1 in these cells. The expression of hspB1 protein in TEPM was very weak compared to hspB1 protein expression in MEF (Fig.4.7) and there was a possibility that the hspB1 protein detected was produced by a small number of contaminating cells which strongly express the protein in TEPM isolates. I decided to determine if monocytes/macrophages purified with anti-CD11b microbeads from TG-treated wild-type mice express hspB1 protein.

TEPM from *hspB1*$^{del/del}$ and wild-type mice were isolated as before and the monocytes/macrophages magnetically isolated using anti-CD11b antibody-conjugated magnetic microbeads (Miltenyi Biotec). The purified monocyte/macrophage pellet was lysed in complete lysis buffer and 100 µg of purified lysate was analysed for hspB1 protein by western blot. 3 µg of wild-type MEF lysate was used as a positive control. HspB1 could not be detected in these purified monocytes/macrophages, which contrasted with the analysis of unpurified TEPM lysate (Fig. 4.10).

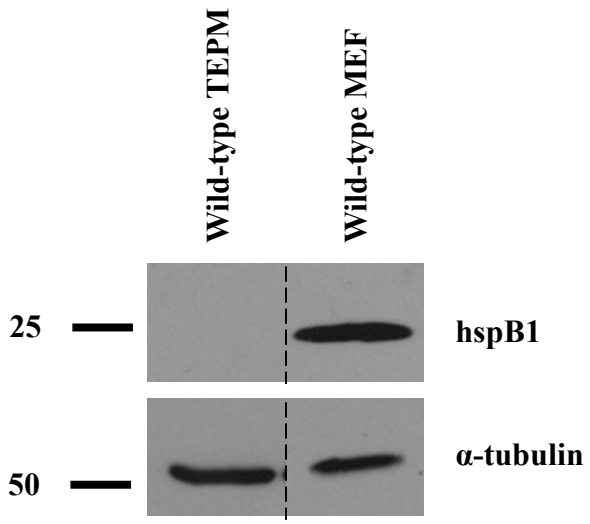

Figure 4.11 HspB1 protein expression cannot be detected in purified TEPM lysates by western blot.

TEPM were isolated as before and the monocytes/macrophages were purified by CD11b conjugated magnetic beads using a kit. These cells were lysed and prepared for western blot as described previously. 100 μg of wild-type purified monocyte/macrophage lysate was loaded. 3 μg of wild-type MEF lysate was loaded as a positive control. Western blots with molecular weight markers are shown for hspB1 and α-tubulin proteins. Dotted lines indicate lanes removed from the blot for clarity of presentation.

4.13 Discussion

The observation that hspB1 deficiency resulted in decreased MEF proliferation made interpretation of the air pouch data challenging. Previous studies have shown that the age of the air pouch had an impact on the thickness of the granulation tissue layer in rats (Sedgwick, Sin et al. 1983) and mice (Garcia-Ramallo, Marques et al. 2002). This growth of the granulation tissue could have been retarded in hspB1-deficient mice, which would reduce the number of cells exposed to zymosan. I investigated the architecture of the air pouch granulation tissue and found that hspB1 deficiency did not result in a difference in the thickness of air pouch lining granulation tissue or microvasculature density. This suggested that the phenotype of delayed proliferation observed in *hspB1*$^{del/del}$ MEF did not result in gross abnormalities in the formation of air pouches *in vivo*. Despite this observation, I sought clarification on the role of the effect of hspB1-depletion on the acute inflammatory response *in vivo*.

The effect of HspB1 deficiency on acute inflammation in the peritonitis model was similar to that observed in the air pouch model, shown by increased cell infiltration at 4 h post-zymosan treatment in *hspB1*$^{del/del}$ mice compared to wild-type mice. However, in the peritonitis model there was better grouping of the data for cellular infiltration and CXCL1 production and stronger statistical significance. CXCL1 and CXCL2 protein production was increased in *hspB1*$^{del/del}$ mice compared to wild-type mice at 1 h post-zymosan. These results supported the observation of increased CXCL1 and CXCL2 expression in the air pouch of hspB1-deficient mice compared to wild-type mice. HspB1 deficiency did not result in an increase in TNFα or IL-6 production at 1 h and 4 h post-zymosan respectively. This differs from the observations from the air pouch model. This suggests that different cell types may be responsible for IL-6 and TNFα protein production in the two models of acute inflammation.

TNFα expression was low in response to zymosan at 1h which challenged the established dogma of the importance of the initial macrophage response to inflammatory stimuli in this model. The expression of IL-6 in air pouches was the most strongly increased in *hspB1*$^{del/del}$ mice relative to wild-type mice, but it was not increased in the peritonitis model. I did not perform a vehicle control experiment in the peritonitis model, which limits the understanding of whether the inflammatory cytokines measured are upregulated in response to stimulation by zymosan in this model. The differences in the cytokine expression profile produced by hspB1 deficiency in the air pouch and peritonitis models may be due the presence of different cell types in the tissues exposed to zymosan. The peritoneum has a lining of mesothelial cells and its content of macrophages and fibroblasts is also likely to be different to that of the lining tissue of the air pouch.

The infiltrated neutrophils in the peritoneal cavity at 4 h post-zymosan were undergoing increased apoptosis in *hspB1*$^{del/del}$ mice compared to wild-type mice. This result was supported by the same result in the air pouch model. It is thought that the increased apoptosis of neutrophils in *hspB1*$^{del/del}$ mice explained the collapse of the total cell number after the peak at 4 h post-zymosan, which results in similar numbers of infiltrating cells in *hspB1*$^{del/del}$ and wild-type mice at the 16 h time point in the air pouch and 24 h time point in the peritonitis model.

I decided to investigate if hspB1 was expressed in neutrophils. TG was used to elicit neutrophils from the peritoneal cavities of mice. A 4 h time-point was employed to extract the maximum number of neutrophils, based on my observations of the time for peak neutrophil recruitment in response to zymosan in the air pouch and peritonitis models. I demonstrated that purified neutrophils extracted from wild-type mice do not express hspB1. This made it unlikely that hspB1 has a direct cytoprotective mechanism in neutrophils. It more likely that

the increased number of neutrophils into the site of zymosan-induced inflammation in *hspB1*$^{del/del}$ mice results in an increased concentration of reactive oxygen species and proteases by these cells, as well as the production of pro-inflammatory cytokines by neutrophils and other cells, resulting in an increased oxidative, proteolytic and pro-inflammatory environment which causes increased neutrophil apoptosis in these mice compared to wild-type.

I observed increased IL-6 and TNFα protein expression and a trend toward increased CXCL-1 protein production in LPS or zymosan stimulated TEPM from hspB1-deficient mice compared to wild-type cells. However, anti-CD11b microbead-isolated monocytes/macrophages from TEPM isolated from wild-type mice did not express hspB1 protein. I was concerned that the differences in pro-inflammatory cytokine expression observed were due to an increased number of *hspB1*$^{del/del}$ macrophages at the time of stimulation compared to wild-type macrophages rather than the regulation of cytokine expression by hspB1. MTT assays confirmed that there were either more hspB1$^{del/del}$ macrophages or these cells had increased metabolic activity compared to wild-type cells after overnight incubation. There was also a greater concentration of total protein in lysates of TEPM isolated from hspB1$^{del/del}$ mice compared to wild-type mice. There was no difference in the amount of cleaved PARP in LPS or untreated TEPM from $^{del/del}$ mice compared to the corresponding wild-type cells, suggesting that there was no difference in the viability of these cells.

The effects of hspB1 deficiency on MTT measurements on TEPM also correlated well with its effects on LPS or zymosan-induced cytokine expression in these cells. This suggests that hspB1 protein does not regulate cytokine expression in peritoneal macrophages, and is consistent with the lack of expression of hspB1 protein in purified TEPM. Another possibility

is that *hspB1*$^{del/del}$ TEPM had greater adherence to the cell culture wells compared to wild-type cells, which would suggest that the increases in pro-inflammatory cytokine protein concentration in TEPM from *hspB1*$^{del/del}$ mice was simply a consequence of there being more of these cells remaining in the wells in which they were seeded at the time of stimulation, compared to the number of wild-type cells. It is worth noting that the wild-type and *hspB1*$^{del/del}$ macrophage cytokine expression profiles, in terms of the effect of hspB1 deficiency and response to zymosan, correlate well with air-pouch data, suggesting that in contrast to *in vitro* cultures, cytokine expression in resident tissue macrophages is regulated by hspB1. The lack of expression of hspB1 in macrophages suggests that the difference in the properties of wild-type and *hspB1*$^{del/del}$ TEPM are due to either extracellular hspB1 or effects of some other cell types that are exerted on the macrophages.

MTT assays in MEF showed the opposite result observed in macrophages and suggested that cell numbers for hspB1-deficient MEF were decreased compared to wild-type MEF. The function of hspB1 in cell proliferation has remained unclear because many studies have been complicated by the anti-apoptotic function of the small heat shock protein. The only mechanism described so far for cell cycle control by hspB1 applies to conditions of cell stress (Parcellier, Brunet et al. 2006). Work done by Dr. Anna Aubareda, using BrdU incorporation assays and measurement of p21^{waf1} p27^{kip1} protein expression in MEF, found that entry into S phase is promoted by hspB1 and that it therefore controls cell proliferation directly. The characteristics of impaired proliferation of hspB1-deficient fibroblasts and increased acute inflammation in hspB1-deficient mice led to the decision to investigate the role of hspB1 in a physiological system where both of these factors are important. I decided to investigate the effect of hspB1 deficiency in a murine model of wound healing.

Chapter 5

Investigation of the function of hspB1 in wound healing.

5.1 Introduction.

The data described in chapters 3 and 4 show that hspB1 deficiency causes an increased inflammatory response to zymosan challenge *in vivo*. A trend towards increased inflammatory gene expression in response to IL-1 was also observed in MEF. In addition, hspB1 deficiency delays the progression of the cell cycle and reduces the rate of cell proliferation. Therefore, I decided to investigate the function of hspB1 in a physiological process that involves both inflammation and cellular proliferation. One such process is wound healing; a complex and dynamic process which restore tissue integrity and homeostasis following injury (Martin 1997). Wound healing involves three overlapping phases; inflammation, tissue formation and proliferation, and tissue remodelling (Singer and Clark 1999).

The results of increased inflammation *in vivo* and *in vitro*, and reduced proliferation *in vitro* observed in *hspB1*$^{del/del}$ mice and cells compared to their wild-type counterparts led us to establish the hypothesis that these characteristics would be deleterious to normal wound healing, and that wound healing in *hspB1*$^{del/del}$ mice would be impaired compared to wild-type mice. Many studies have made use of excisional wound healing models to examine the effects of gene disruption (Hubner, Brauchle et al. 1996; Grose and Werner 2003; Martin, D'Souza et al. 2003), age (Swift, Burns et al. 2001; Carter, Sykes et al. 2009), diseases (Singer and Clark 1999; Norgauer, Hildenbrand et al. 2002) and drug therapy (Fu, Li et al. 2005; Braund, Hook et al. 2009), to list only a few examples of the application of this model.

Female mice were used for this model, as all the male mice available for experiments were used for the air pouch and peritonitis models of acute inflammation. The wounding technique technique involves shaving and decontaminating the mouse dorsum and using a 4 mm skin biopsy punch to create 2 pairs of full thickness wounds. These wounds are allowed to develop

and heal for the desired time before the mice are culled and tissue collected and prepared for histology or homogenised for cytokine analysis.

5.2 Mouse skin histology.

Prior to performing wound healing experiments I decided to investigate the distribution of hspB1 protein expression in female murine skin. Skin sections from wild-type and *hspB1*$^{del/del}$ mice were stained with Masson's trichrome (Fig. 5.1A), with staining of subsequent sections with an anti-hspB1 antibody (Fig. 5.1B). This identified expression of hspB1 protein in stratum corneum, epidermis, hair follicles and muscle as reported previously (Fig. 5.1B) (Huang, Min et al. 2007). No staining could be detected for *hspB1*$^{del/del}$ skin with anti-hspB1 antibody when used at the same concentration and the structure of the tissue appeared normal compared to wild-type skin (Fig. 5.1C). HspB1 protein was detected in wild-type vasculature (Fig. 5.1D), identified by staining of red blood cells inside the vessels with Masson's trichrome (Fig. 5.1A). HspB1 protein was also detected at high power magnification in cells with fibroblast-like morphology in sudermal tissue (Fig. 5.1E).

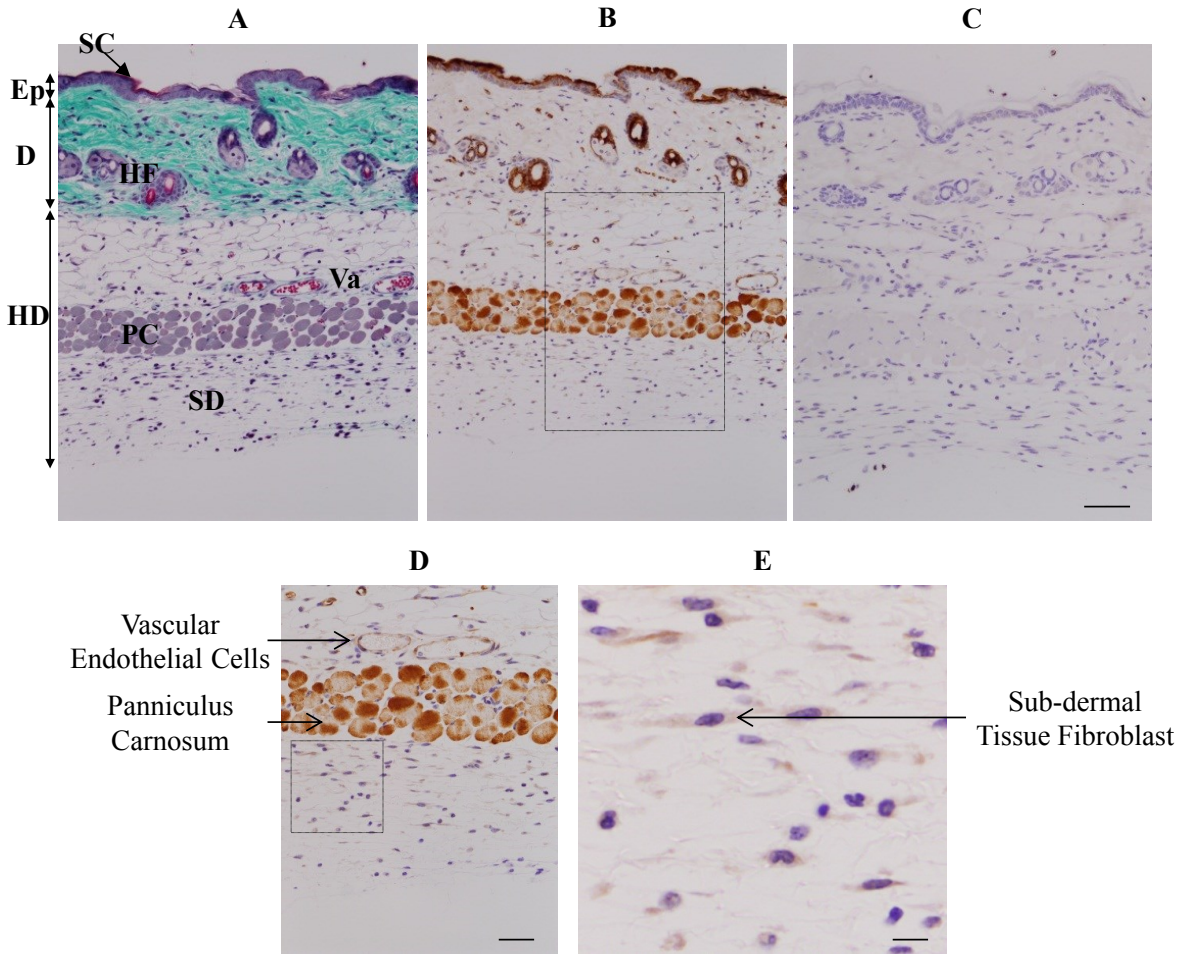

Figure 5.1 Detection of hspB1 protein expression in wild-type female murine skin by immunohistochemistry.

A, female wild-type skin was stained with Masson's trichrome. B, HspB1 protein was detected by IHC. Brown colour indicates positive antigen staining. C, hspB1 was not detected in skin sections from female *hspB1*$^{del/del}$ mice; bar = 100 µm. D, higher magnification image showing hspB1 staining in muscle and vasculature (as in B); bar = 50 µm, and (E), cells with fibroblast-like morphology in subdermal tissue (as for D); bar 10 µm. Arrows indicate tissue structures and cells Ep: epidermis, D: dermis, Hd: hypodermis, SC: stratum corneum, HF: fair follicle, Va: vasculature, PC: panniculus carnosus, SD: subdermis.

5.3 HspB1 deficiency results in delayed wound healing.

Excisional cutaneous wound healing was investigated in wild-type and *hspB1*$^{del/del}$ mice by creating wounds on the dorsal surface of mice using a 4 mm punch. Digital images of wounds were captured over a period of 7 days and wound areas measured. A 30 cm ruler was placed alongside the wounds during photography as a scale bar. There was a significant delay in the rate of wound healing in *hspB1*$^{del/del}$ mice compared to wild-type at 3 (1.3-fold; $P \leq 0.01$), 5 (1.5-fold; $P \leq 0.05$) and 7 (1.6-fold; $P \leq 0.05$) days post-wounding (Fig. 5.2A). Digital images of representative wounds over seven days post-injury are shown (Fig. 5.2B).

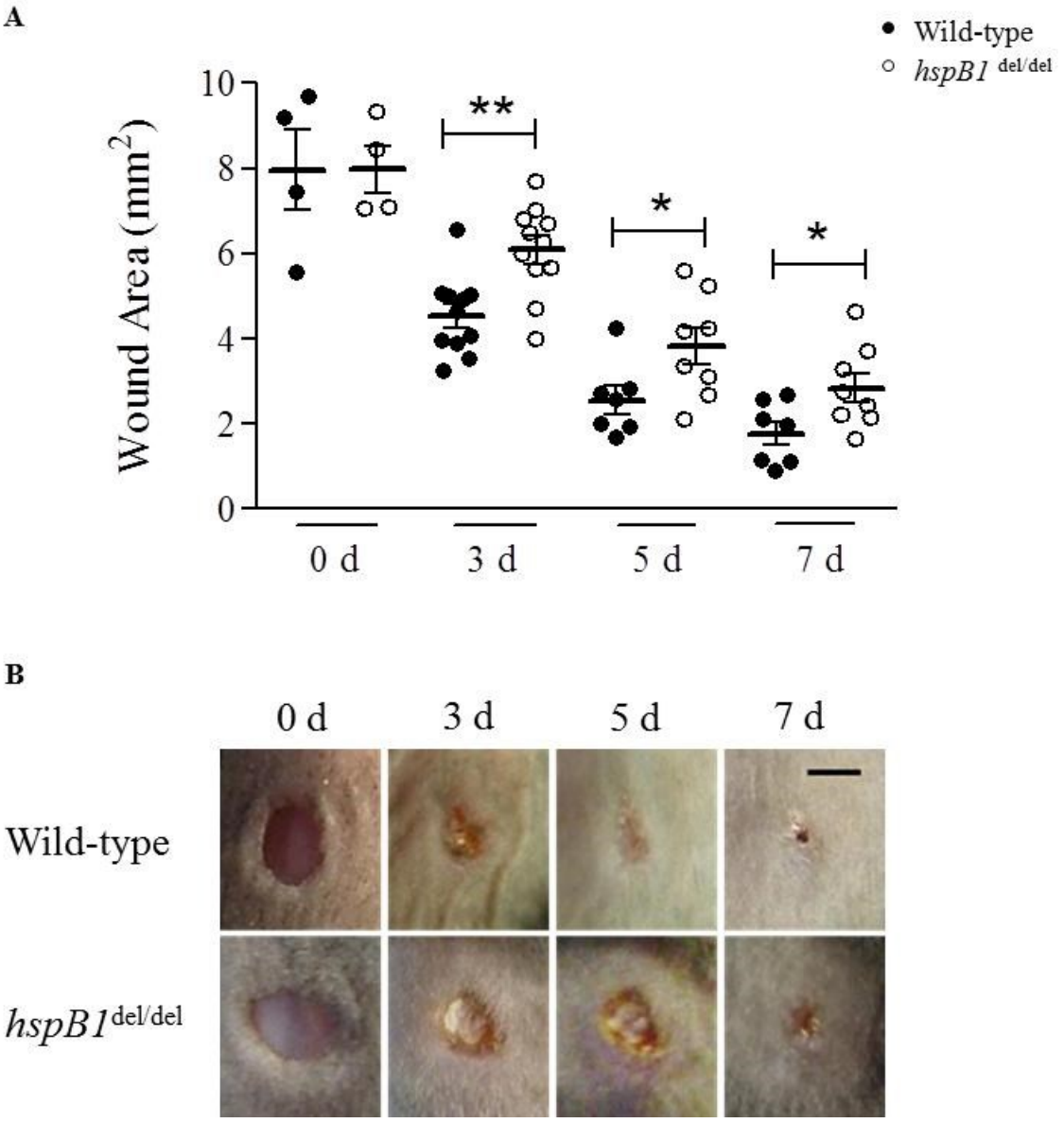

Figure 5.2 HspB1 deficiency impairs excisional cutaneous wound healing.

A, Four 4mm diameter wounds were created on the dorsal surface of 10-14 week-old female wild-type and *hspB1*$^{del/del}$ mice. Digital images were taken of each wound at 0, 3, 5 and 7 days post-wounding. 0 d (n = 3-4 mice); 3 d (n = 11 mice from three experiments), 5 d and 7 d (n = 7-8 mice from two experiments). Individual data points represent mean wound area of 4 wounds from 1 individual mouse. B, Digital images of wounds (representative of ≥ 14 wounds); bar = 2 mm. Graph shows mean wound areas ± SEM; * $P \leq 0.05$, ** $P \leq 0.01$.

5.4 Histological analysis of day 3 and day 7 wounds.

To investigate the function of hspB1 in wound healing in more detail, skin was taken from mice at 3 d and 7 d post-wounding. Skin samples were paraffin-embedded, sectioned and stained with Masson's trichrome to identify collagen, epithelium, and capillaries and with an anti-hspB1 antibody to detect hspB1 protein expression. At 3 d, Masson's trichrome staining of wild-type and *hspB1*$^{del/del}$ (Fig. 5.3A, 5.3C) skin showed discrete collagen staining at the periphery of the wound, scab formation and proliferating dermis and epithelial tongues. The cellular infiltrate in *hspB1*$^{del/del}$ mice (Fig 5.3C) was greater in density and more widespread compared to wild-type mice at 3 d (Fig 5.3A). The mean distance between epithelial tongues at 3 d was greater ($P \leq 0.05$) in the mutant animals indicating delayed re-epithelialisation (Fig. 5.3E). HspB1-expressing cells were present within the granulation tissue of wild-type mice at 3 d (Fig. 5.5A) that are not present in unwounded granulation tissue (Fig. 5. 1B). New vasculature was also observed in wild-type mice (Fig. 5.5A) and *hspB1*$^{del/del}$ mice (Fig. 5.5C), and hspB1 protein was strongly expressed by the vascular endothelium in the wild-type mice (Fig. 5.5A).

At 7 d, histological analysis showed that approximately half of wild-type wounds displayed near-complete healing, with the other half still having a relatively thick epithelial layer and incomplete collagen deposition. A representative image of a 7 d wild-type wound showing partially re-formed epidermis and advanced collagen distribution is shown (Fig. 5.3B). None of the 7 d *hspB1*$^{del/del}$ wounds displayed complete healing, and had relatively thick epithelial layers and incomplete collagen deposition (Fig. 5.3D). By d 7 there was widespread neovascularisation in wild-type and *hspB1*$^{del/del}$ mice. Large structures had developed within the wound area and wound margins, which stained strongly for hspB1 protein in wild-type mice (Fig. 5.5B). These show morphological similarities to neuronal nerve bundles. These

were present in some wild-type mouse wound sections at 7 d post wounding (Fig. 5.5D), but not all.

In wild-type mice, hspB1 protein staining was evident in epithelial tongues at 3 d (Fig. 5.3A), and fully formed epithelium at 7 d (Fig. 5.3B). HspB1 was also detected in stratum corneum, muscle, hair follicles, cells lining capillaries and in cells with fibroblast-like morphology in the dermis, at 3 d (Fig. 5.3A), and 7 d (Fig. 5.3B), as in unwounded skin (Fig. 5.1B). No hspB1 protein staining was seen in wounds from mutant mice (Fig. 5.3C and 5.3D), confirming the efficiency of the genetic deletion and specificity of anti-hspB1 protein staining by IHC. Fig. 5.4 shows additional representative images of the results shown in Fig. 5.3.

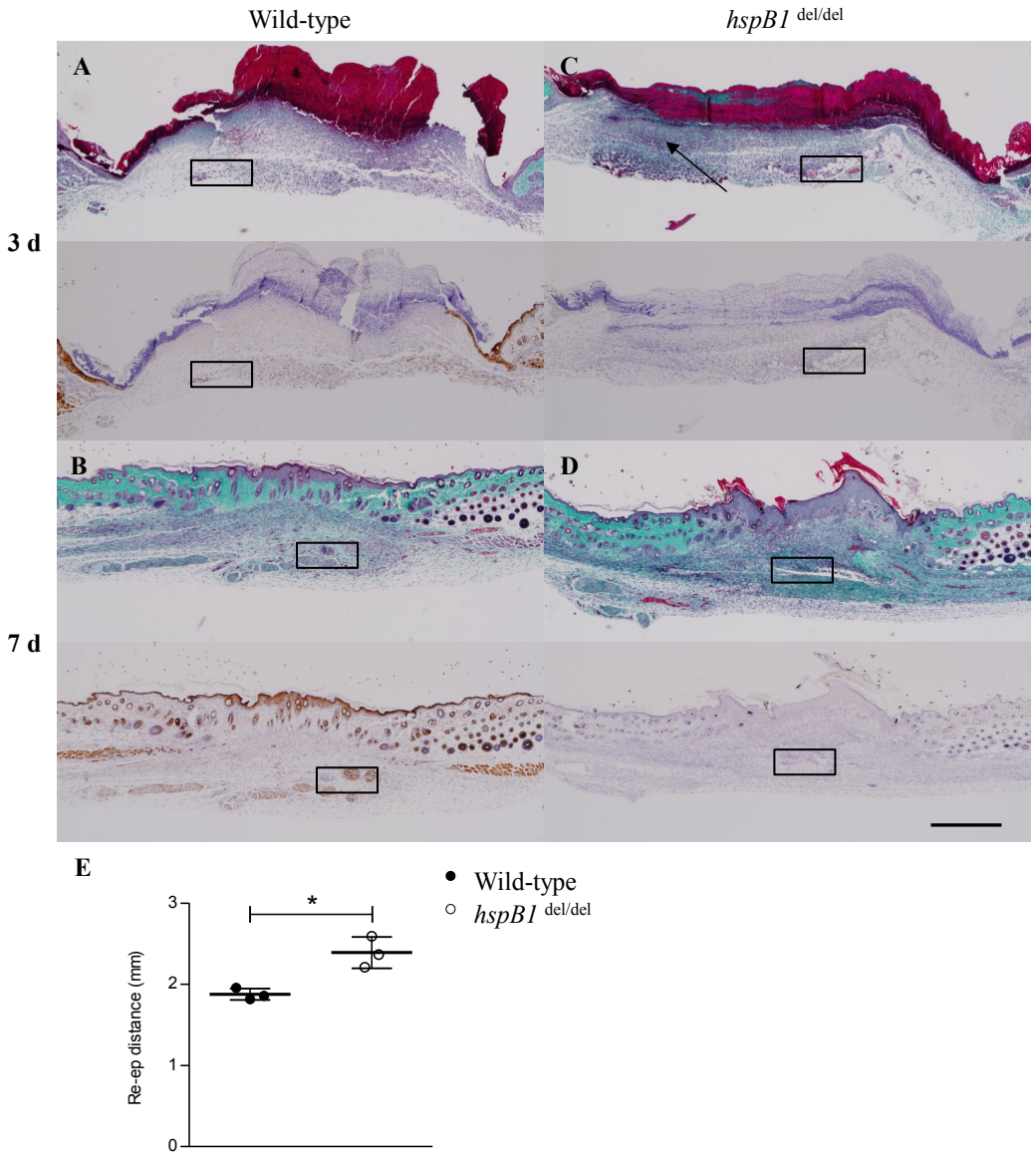

Figure 5.3 Delayed wound healing and re-epithelialisation in *hspB1*$^{del/del}$ mice.

11-14 week age-matched female wild-type and *hspB1*$^{del/del}$ mice were used. A, representative Masson's trichrome staining (top) and IHC for hspB1 (below) in wild-type 3 d and B, 7 d wounds. C, *hspB1*$^{del/del}$ wounds at 3 d and D, at 7 d. Brown colour indicates positive hspB1 antigen staining. Arrow indicates dense cellular infiltrate; Bar = 500 µm. E, Plot of mean distance ± SEM (n = 4 wounds per mouse, 3 mice per group) between re-epithelialisation margins in wild-type and *hspB1*$^{del/del}$ mice in 3 d wounds; * $P \leq 0.05$. Boxes indicate areas presented in at higher magnification in figure 5.5.

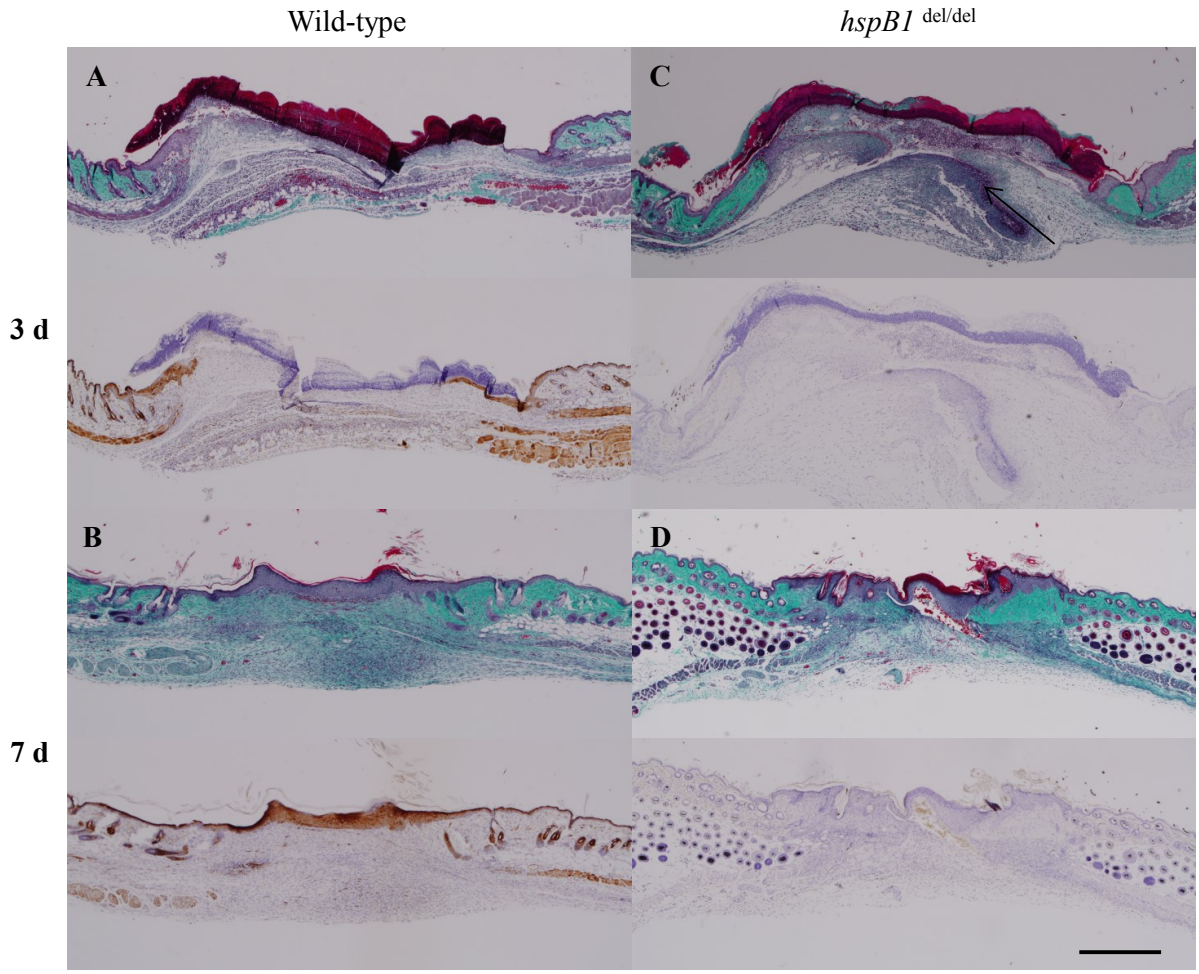

Figure 5.4 Further representative histological images showing delayed wound healing in *hspB1*$^{del/del}$ mice.

As shown in figure 5.3, A, representative Masson's trichrome staining (top) and IHC for hspB1 (below) in wild-type 3 d and B, 7 d wounds. C, *hspB1*$^{del/del}$ wounds at 3 d and D, at 7 d. Brown colour indicates positive hspB1 antigen staining. Arrow indicates dense cellular infiltrate; Bar = 500 µm.

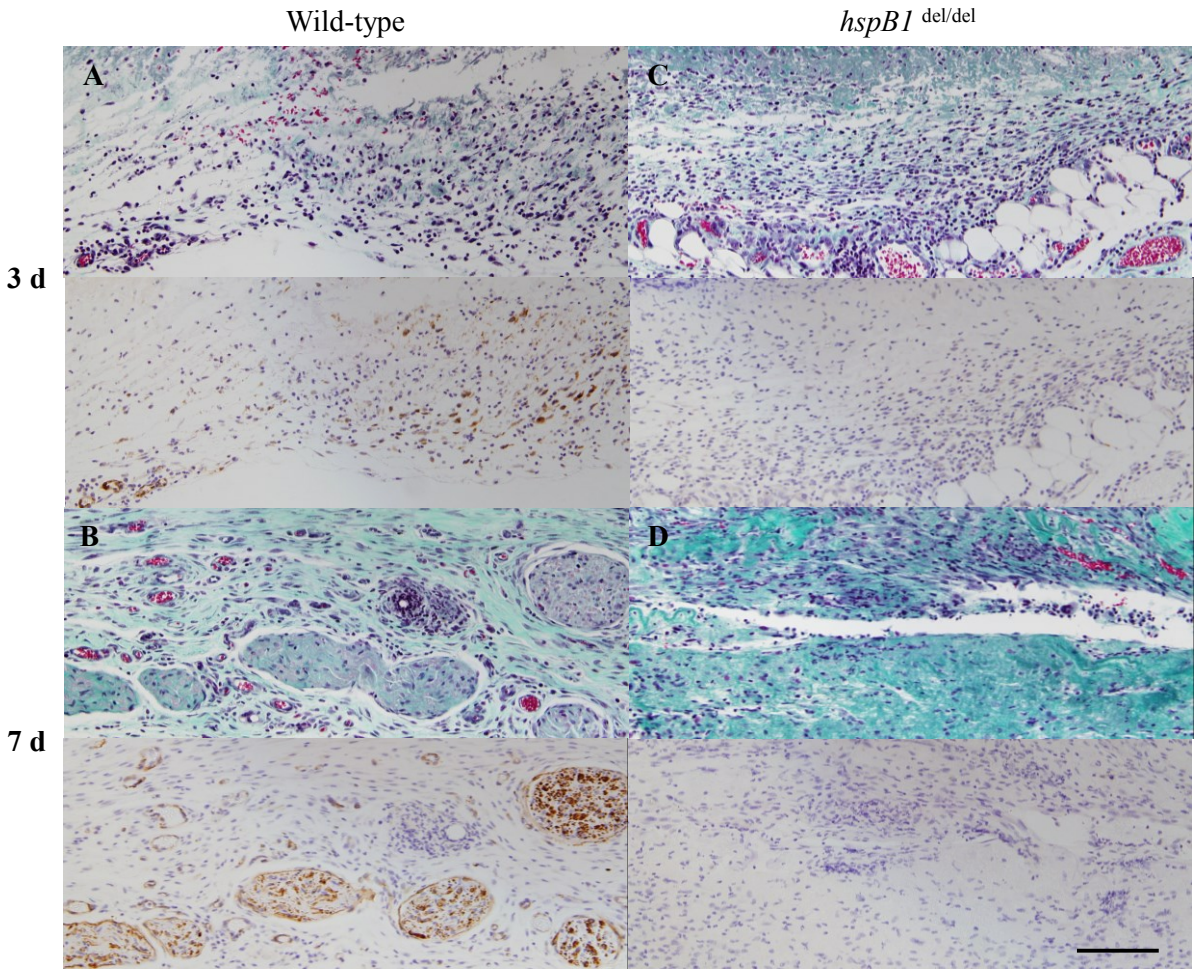

Figure 5.5 Detailed histological examinations of 3 d and 7 d wound granulation tissue in wild-type and *hspB1*$^{del/del}$ mice.

Higher magnification of wound granulation tissue from images, as presented in Fig. 5.3. A, representative Masson's trichrome staining (top) and IHC for hspB1 (below) in wild-type 3 d and B, 7 d wounds. C, *hspB1*$^{del/del}$ wounds at 3 d and D, at 7 d. Brown colour indicates positive hspB1 antigen staining. Bar = 100 µm.

5.5 Histological quantification of neutrophils in day 1 wounds.

Increased cellular infiltrate was observed in 3 d wounds in *hspB1*$^{del/del}$ mice compared to wild-type (Fig. 5.3). It was important to determine which leukocyte subsets comprised the inflammatory infiltrate in wounds, as this would give insight into how the inflammatory response to wounding progressed in *hspB1*$^{del/del}$ and wild-type mice.

I had already demonstrated that hspB1 deficient mice have increased neutrophil infiltration at early time-points using the air pouch and peritonitis models of acute inflammation. It was decided to investigate the number of infiltrating of neutrophils early in the inflammatory response to wounding in wild-type and *hspB1*$^{del/del}$ mice. The hypothesis was that the delayed wound healing observed in *hspB1*$^{del/del}$ mice compared to wild-type was attributable to increased infiltration of neutrophils during acute inflammation. Mice were wounded as before and the skin excised 24 h (1 d) post-wounding. The skin was analysed by immunohistochemistry for neutrophil elastase. Neutrophil infiltration was found to be increased in 1 d *hspB1*$^{del/del}$ wounds (Fig. 5.6B) relative to wild-type wounds (Fig. 5.6A) The average number of neutrophils within a 165 μm^2 field were counted by microscopy, which showed the increase to be significant ($P \leq 0.01$) (Fig. 5.6C). Staining 3 d wound tissue with anti-neutrophil elastase antibody failed to positively stain any cells.

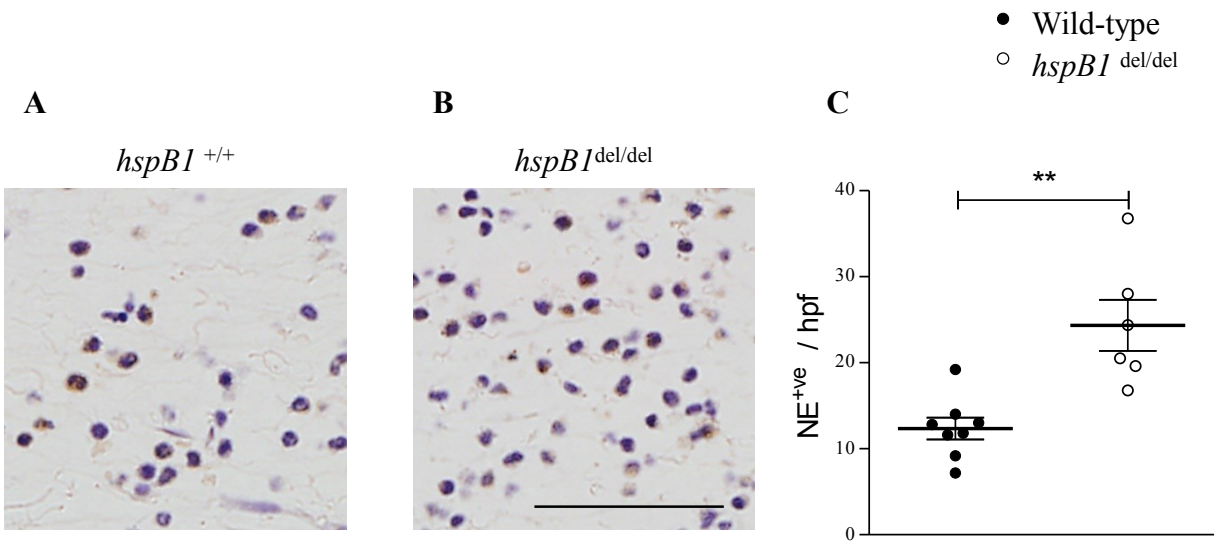

Figure 5.6 HspB1 deficiency results in increased neutrophil recruitment to the site of acute inflammation 1 d post-wounding.

Neutrophil infiltration in 1 d wounds assessed by IHC for neutrophil elastase (NE) in A, wild-type and B, *hspB1*$^{del/del}$ mice. C, Plot shows elastase positive neutrophils (NE+) per 165µm^2 high power field (hpf) (7 fields/wound; 2 wounds per mouse; n=4 mice). Brown colour indicates positive NE antigen staining. Bar = 50 µm. Graph shows mean ± SEM; ** $P \leq 0.01$.

There was a 1.9-fold increase ($P \leq 0.01$) in the number of neutrophils infiltrating the wound site in *hspB1*$^{del/del}$ mice compared to wild-type at 1 d (Fig. 5.6C). This observation supported the findings from the air pouch and peritoneal models of acute inflammation. These acute inflammation models also demonstrated that *hspB1*$^{del/del}$ mice were less viable and more apoptotic than wild-type neutrophils. This suggests that the increase in neutrophil infiltration to the wound site during acute inflammation would therefore result in a greater number of apoptotic cells within the wound. This apoptotic population of neutrophils would need to be cleared in order to facilitate the resolution of acute inflammation and allow for the progression of the wound healing response. The cells responsible for this are infiltrating macrophages. I decided to investigate these cells in the wound healing model.

5.6 Histological quantification of macrophages in 1 d and 3 d wounds.

I decided to investigate the effect of hspB1 deficiency on the ability of macrophages to enter to the wound, as deficiency in this ability might result in impaired removal of apoptotic neutrophils and impaired resolution of inflammation. However, an increased neutrophil influx might cause an increased chemotactic gradient for macrophage recruitment.

Paraffin embedded histological skin samples were analysed for F4/80 positive cells (mature macrophages) in 1 d and 3 d wound area tissue. There was a 0.6-fold decrease ($P \leq 0.01$) at 1 d (Fig. 5.7C) and a 0.14-fold decrease ($P \leq 0.05$) at 3 d (Fig. 5.7F) in the number of macrophages within the wound area of *hspB1*$^{del/del}$ mouse wounds compared wild-type wounds.

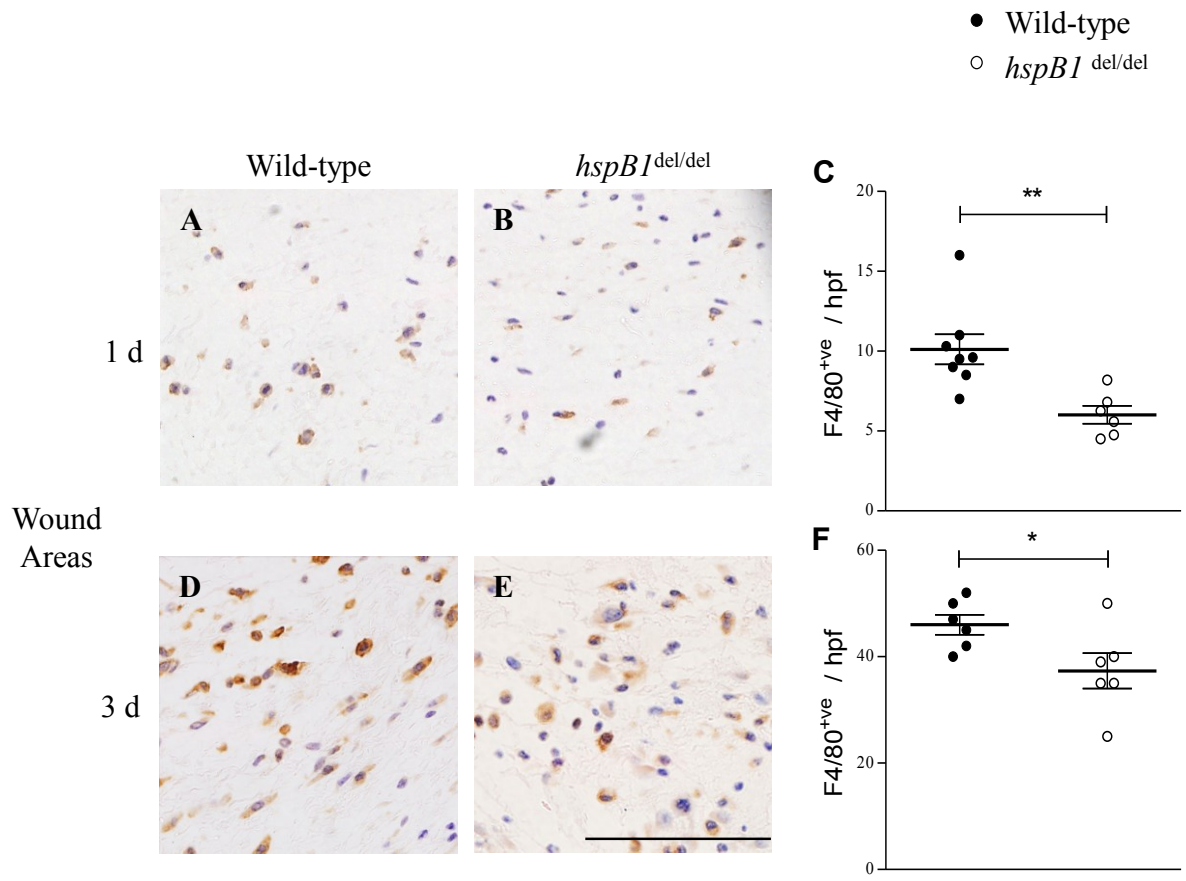

Figure 5.7 HspB1 deficiency resulted in decreased macrophage recruitment to the wound site at 1 d and 3 d post-wounding.

Macrophage infiltration was assessed by IHC for F4/80 in d1 wild-type (A) and *hspB1*$^{del/del}$ (B) wounds. C, plot shows F4/80 positive macrophages/hpf in d1 wounds. F4/80 positive cells were counted in d3 wild-type (D) and *hspB1*$^{del/del}$ (E) wounds. F, plot shows F4/80 positive macrophages/hpf in d3 wounds (7 fields/wound; 2 wounds per mouse; n = 4 mice). Brown colour indicates positive F4/80 antigen staining. Bar = 50 µm. All graphs show mean ± SEM; * $p \leq 0.05$ ** $P \leq 0.01$.

During the analysis of the wound areas I noticed that within the margins of the wounds there was a 1.5-fold increase ($P \leq 0.01$) in the number of macrophages in *hspB1*$^{del/del}$ mouse wound margins, compared to wild-type wounds (Fig. 5.8C) at 1 d. There was no difference in the number of macrophages within the wound margin of *hspB1*$^{del/del}$ and wild-type mouse wounds margins at 3 d. Representative images of wild-type (Fig 5.8G) and *hspB1*$^{del/del}$ (Fig 5.8H) wounds shown the identification of the wound margin as the location where the panniculus carnosus and dermis is disrupted.

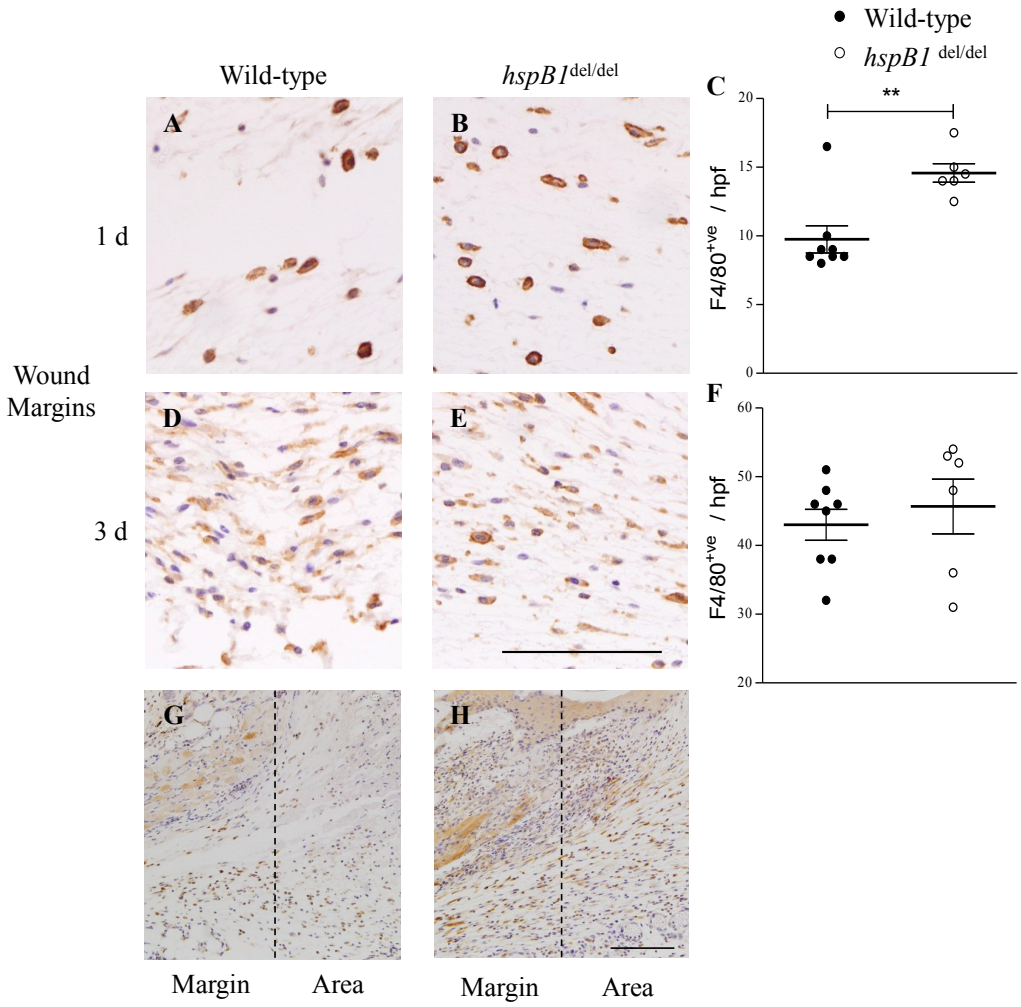

Figure 5.8 HspB1 deficiency results in an increased number of macrophages within the wound margin 1 d post-wounding.

Macrophage infiltration was assessed by IHC for F4/80 in wild-type (A) and *hspB1*$^{del/del}$ (B) 1 d wound margins. C, plot shows F4/80 positive macrophages/hpf in 1 d wound margins. F4/80 positive cells were counted in wild-type (D) and *hspB1*$^{del/del}$ (E) 3 d wounds margins; Bar = 50 µm. F, plot shows F4/80 positive macrophages/hpf in 3 d wound margins. (2 fields/wound margin 4 wound margins per mouse; n = 4 mice). Representative images of wound margins and wound areas in wild-type (G) and *hspB1*$^{del/del}$ (H) 3 d post-wounding; bar = 100 µm. Brown colour indicates positive F4/80 antigen staining. All graphs show mean ± SEM; ** $P \leq 0.01$.

5.7 The effect of hspB1 deficiency on the number of macrophages within wounded and distal skin tissue.

Macrophages were also counted in tissue distal to 1 d and 3 d wounds. Distal tissue was defined as unwounded skin from the dorsum of the mouse (Fig. 5.9C). This was considered pertinent as differences in macrophage numbers could be relevant to any differences in cytokine expression that I wished to investigate in the future. At 1 d, there was no difference in the number of macrophages within distal skin in *hspB1*$^{del/del}$ and wild-type mice (Fig. 5.9A). Macrophage numbers were reduced in wounds relative to distal tissue. At 3 d, there were reduced numbers of macrophages within the distal skin ($P \leq 0.05$) in *hspB1*$^{del/del}$ mice compared to wild-type mice (Fig. 5.9B). Macrophage counts from distal tissue, wounds and wound margins were re-plotted together and the graphs are shown in Fig. 5.9A.

When considering the implications of the number of macrophages within the wound area and the wound margins, it is important to note that wild-type mice had approximately the same number of macrophages within the wound area and margin on 1 d (Fig. 5.9A) and 3 d (Fig. 5.9B). However, there was a 2.4-fold increase ($P < 0.0001$) in the number of macrophages within the wound margin compared to the wound area at 1 d (Fig. 5.9A) in *hspB1*$^{del/del}$ mice. The greater density of macrophages within the wound margin compared to the wound area at d 1 in *hspB1*$^{del/del}$ mice suggests that there may be increased recruitment and extravasation of macrophages to the site of the wound compared to wild-type mice, but the macrophages have difficulty in migrating into the wound site. There may be an aberrant migratory capacity of *hspB1*$^{del/del}$ macrophages, compared to wild-type cells.

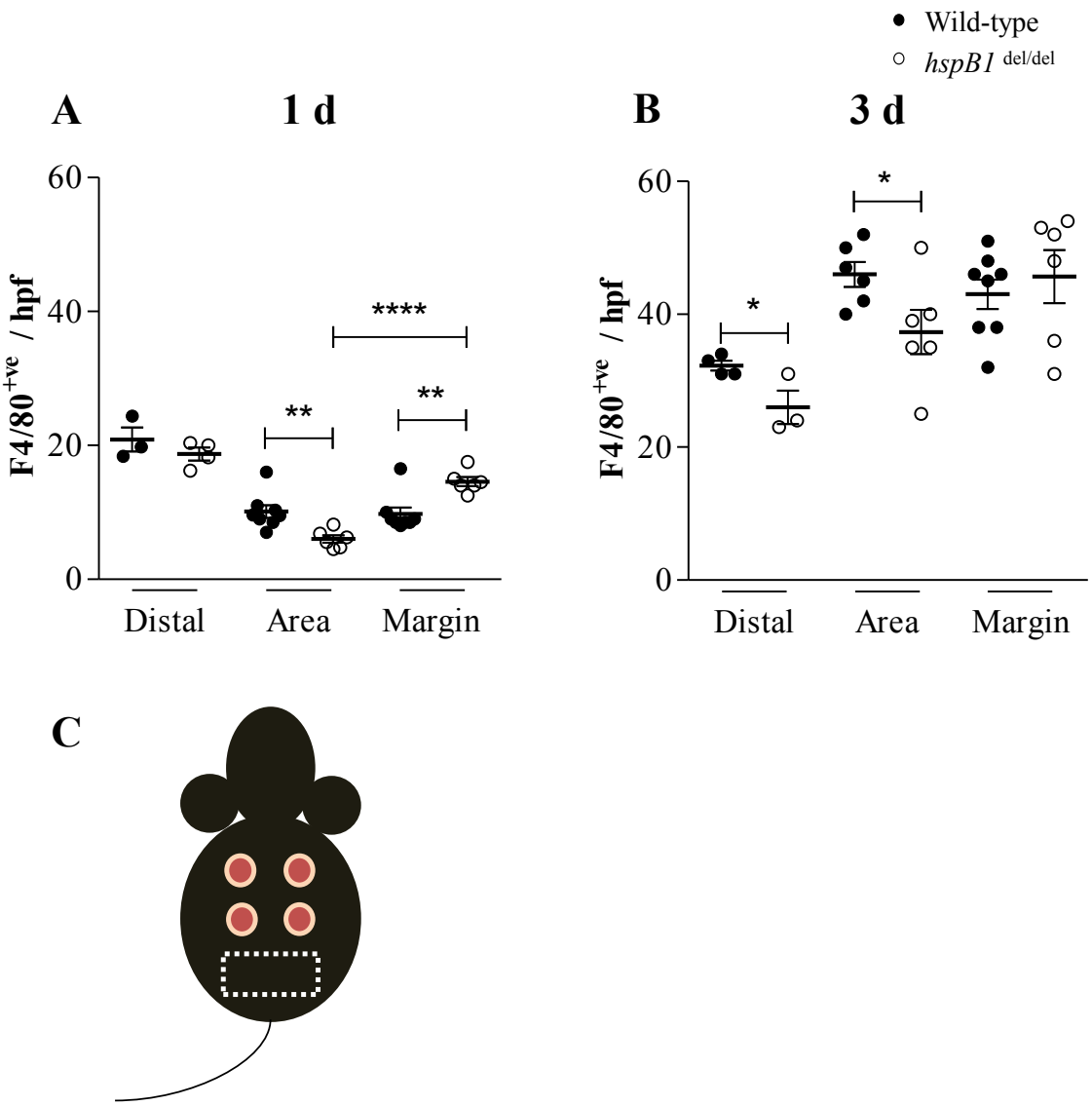

Figure 5.9 HspB1 deficiency results in decreased macrophage infiltration to the wound area in response to wounding.

Macrophages within the skin tissue distal to wounds (Distal), wound areas (Area) and wound margins (Margin) from wounded mouse skin sections were stained with anti-F4/80 antibody and counted at 1 d (A) and 3 d (B) post-wounding. The data for number of macrophages within the wound area and wound margins is re-plotted from Figures 5.5 and 5.6 so that comparison can be made with skin distal from wounds, indicated by dotted white line (C). All graphs show mean ± S.E.M; * $P \leq 0.05$, ** $P \leq 0.01$, **** $P \leq 0.0001$.

5.8 Quantification of the expression of pro-inflammatory cytokines in 6 h wound tissue.

The differences in the kinetics of leukocyte recruitment to the site of injury may be partly responsible for the delayed wound healing observed in *hspB1*$^{del/del}$ mice compared to wild-type mice. I have already demonstrated using the air pouch and peritonitis models of acute inflammation that hspB1 deficiency results in an increase in CXCL1 and IL-6 production during the early phases of acute inflammation *in vivo*. I have also shown that *hspB1*$^{del/del}$ mice displayed increased neutrophil infiltration in 1 d wound tissue compared to wild-type tissue. Monocyte chemotactic protein-1 (MCP-1, CCL2) is produced by keratinocytes and endothelial cells local to wounded tissue and is a major chemotactic stimulus for monocytes during the acute inflammatory response to wounding (DiPietro, Polverini et al. 1995; Engelhardt, Toksoy et al. 1998). Neutrophils are also a source of CCL2 (Yoshimura and Takahashi 2007). These pro-inflammatory cytokines are instrumental in inducing the acute inflammatory response to wounding. The decision was made to investigate whether the expression of these pro-inflammatory cytokines in response to wounding was regulated by hspB1.

I measured pro-inflammatory cytokine production 6 h post-wounding in tissue lysates from wounded and distal tissue from the dorsum of wounded mice. HspB1 deficiency resulted in a 2.5-fold increase ($P \leq 0.01$) in IL-6 (Fig. 5.10A), a 1.5-fold increase ($P \leq 0.05$) in CXCL1 (Fig. 5.10B) and a 1.6-fold increase ($P \leq 0.05$) in CCL2 protein expression (Fig. 5.10C). Wounding resulted in induction of the expression of these cytokines in wild-type and *hspB1*$^{del/del}$ mice, although CCL2 induction in wounded tissue compared to distal tissue was greater in *hspB1*$^{del/del}$ mice compared to wild-type mice.

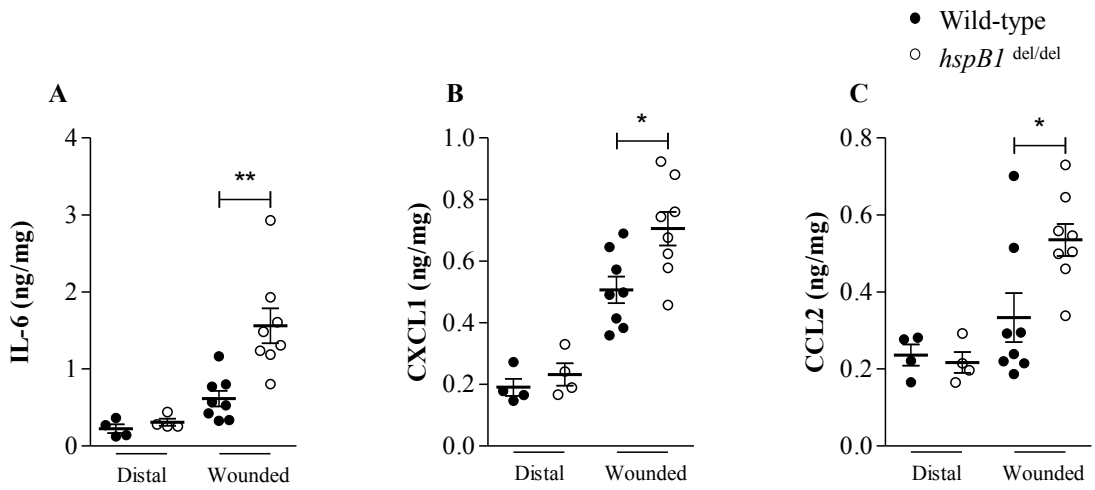

Figure 5.10 HspB1 deficiency results in increased pro-inflammatory cytokine production during the acute inflammatory response to excisional wounding.

Wounded and distal tissue from female mice was harvested 6 h post-wounding. The tissue was homogenised and cellular lysate prepared. The protein concentrations of the lysates were measured by BCA assay and lysates were adjusted to give the same protein concentration for all samples. The concentrations of IL-6 (A), CXCL1 (B) and CCL2 (C) proteins in normalised lysates were determined by ELISA (n=4 mice, 4 wounds per mouse, 2 wounds per data point). All graphs show mean amount of cytokine (ng)/total protein in lysate (mg) ± SEM; * $P < 0.05$, ** $P < 0.01$.

The increase in CXCL1 and IL-6 protein concentration in hspB1-deficient mouse wounds compared to wild-type is consistent with the results observed in the acute models of inflammation. The increase in CXCL1 protein concentration suggests one possible mechanism for the increased neutrophil recruitment to the wound site in hspB1-deficient mice compared to wild-type mice. CCL2 was also increased at 6 h post-wounding in *hspB1*$^{del/del}$ mice, which is consistent with the observation that there was a greater number of macrophages within the wound margins in these mice compared to wild-type mice.

5.9 The effect of hspB1 deficiency on the production of chemokines responsible for monocyte chemotaxis in response to wounding.

While the infiltration of neutrophils is extremely rapid, infiltration of monocytes that differentiate into macrophages is a slower process. Therefore, it was decided to investigate the effect of hspB1 depletion on CCL2 and CCL3 production at 1 d and 2 d post-wounding, and in unwounded tissue. CCL2 production was induced by wounding, peaking at 1 d post-wounding. CCL3 production was also induced by wounding and was sustained until 2 d (Fig. 5.11). There was no regulation of CCL2 or CCL3 by hspB1 deficiency at 1 d or 2 d post-wounding. The lack of regulation of CCL2 and CCL3 expression by hspB1 at 1 d and 2 d is consistent with the minimal changes in macrophage numbers in wild-type relative to *hspB1*$^{del/del}$ wounds at 3 d.

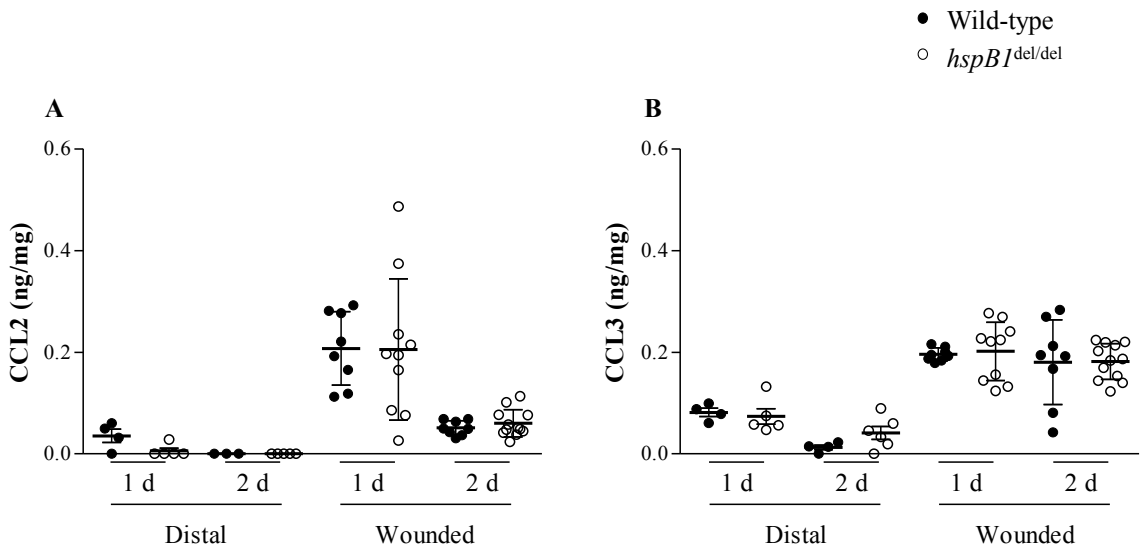

Figure 5.11 The effect of hspB1 deficiency on the production of CCL2 and CCL3 in response to wounding.

Skin wounds were surgically isolated, homogenised, and cells lysed. The concentrations of CCL2 (A) and CCL3 (B), 1 d and 2 d post-wounding in wounded and unwounded tissue lysates normalised for total protein were determined by ELISA (n = 4 – 5 mice, 4 wounds per mouse, 2 wounds per data point). All graphs show mean cytokine (ng / total protein (mg) ± SEM.

5.10 An investigation to determine if alterations in macrophage polarity are responsible for increased pro-inflammatory cytokine expression in *hspB1*$^{del/del}$ wounds compared to wild-type wounds.

The expression of monocyte chemo-attractants was not regulated by hspB1. I decided to determine if the polarisation of macrophages infiltrating to the site of wounding was influenced by hspB1 depletion, as a switch to an M1-like polarisation could account for the increase in cytokine production in wounded hspB1$^{del/del}$ mice compared to wild-type mice (Fig. 5.10).

Macrophages are capable of transitioning from a pro-inflammatory, M1 like, phenotype to a reparative, 'alternatively activated' or M2 like, phenotype within the wound environment (Stein, Keshav et al. 1992; Mosser 2003; Brancato and Albina 2011). The distinct phenotypes of M1 and M2 macrophages bears importance as the cytokine expression profiles of these two groups is very different, M1 producing predominantly pro-inflammatory cytokines and M2 producing anti-inflammatory cytokines, such as IL-10 (Martinez, Sica et al. 2008), and growth factors such as transforming growth factor beta (TGFβ) (Rappolee, Mark et al. 1988) and vascular endothelial growth factor (VEGF) (Nissen, Polverini et al. 1998). These growth factors are essential for resolving the inflammatory response and promoting cell proliferation, angiogenesis and re-epithelialisation in wounded tissue (Mosser and Edwards 2008).

M1 macrophages characteristically produce IL-23 and repress the expression of IL-10 (Krausgruber, Blazek et al. 2011). The structure of IL-23 is similar to that of IL-12 in that they both contain the p40 subunit. However, IL-23 is structurally distinct from IL-12 in that it contains a p19 subunit whereas IL-12 contains a p35 subunit. The ELISA system I used utilised an anti-mouse IL-23p19 capture antibody and gives accurate and precise measurement of IL-23 without the possibility of detection of IL-12. I measured the

concentration of TNFα, IL-1α and IL-1β proteins at 6 h and IL-23 protein at 1 d and 2 d as markers of M1 macrophage activity, and IL-10 protein 1 d and 2 d as a marker for M2 macrophage activity, in wounded and distal tissue from the dorsum of wounded mice.

The production of TNFα, IL-1α and IL-1β in wounded tissue was only slightly greater than that measured in distal tissue in wild-type and *hspB1*$^{del/del}$ mice. The concentration of TNFα protein in *hspB1*$^{del/del}$ wound tissue lysates was decreased 0.8-fold (P = 0.071) compared to wild-type tissue lysate (Fig. 5.12A). There was increased expression of IL-1α protein in wound tissue lysates from wild-type and *hspB1*$^{del/del}$ mice at 6h (Fig 5.12B) compared to the other cytokines measured at this time point (Fig. 5.10). However, there was no difference in the expression of IL-1α or IL-1β in hspB1-deficient mice compared to wild-type (Fig. 5.10B, C). There was no regulation by hspB1 of IL-23 (Fig. 5.12D) or IL-10 (Fig.5.12E) protein at 1 d or 2 d post-wounding. However, there was a decrease in IL-23 (Fig. 5.12D) and IL-10 (Fig 5.12E) in distal tissue for the dorsum of wounded *hspB1*$^{del/del}$ compared to wild-type mice 2 d post-wounding. These data are consistent with the observation of decreased macrophage numbers in distal tissue 3 d post-wounding in hspB1-deficient mice and suggest that the magnitude of expression of IL-10 and IL-23 is different in wounds and the surrounding tissue. These data also suggest that there is no difference in the polarity of macrophages at 1 d and 3 d in wild-type mice compared to *hspB1*$^{del/del}$ mice.

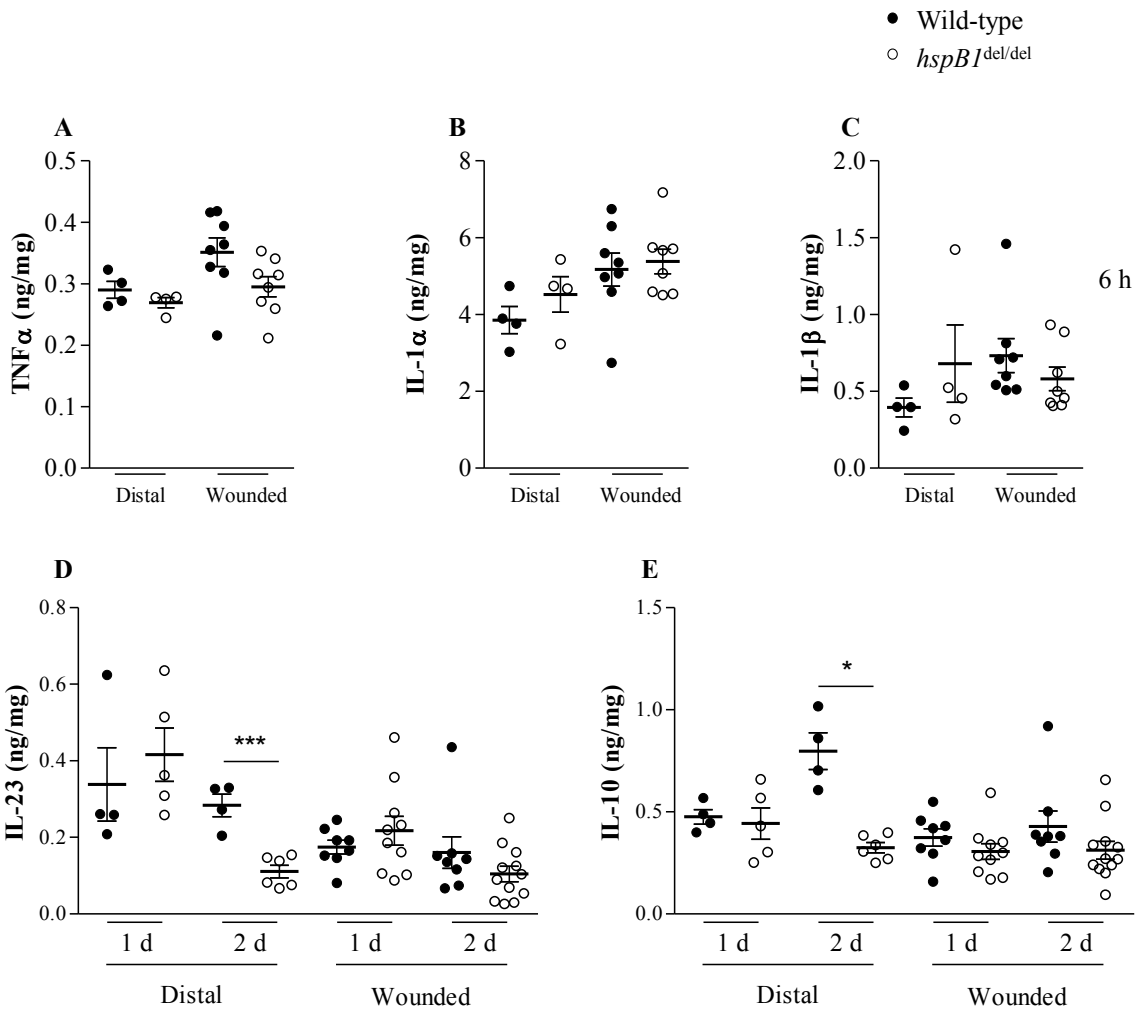

Figure 5.12 The effect of hspB1 deficiency on production of cytokines produced by M1 and M2 macrophages as markers of polarisation.

Wounds were surgically isolated, homogenised, and cells lysed. The concentrations of A, TNFα, B, IL-1α and C, IL-1β at 6 h, and D, IL-10 and, E IL-23 1 d and 2 d post-wounding in wounded and distal skin tissue lysates normalised for total protein were determined by ELISA (n = 4 – 5 mice, 4 wounds per mouse, 2 wounds per data point). All graphs show mean cytokine (ng / total protein (mg) ± SEM. * $P \leq 0.05$, *** $P \leq 0.005$

5.11 Discussion.

The wound healing model was selected as it would allow me to investigate the effect of hspB1 deficiency in a physiological model that involves both cell proliferation and acute inflammation. I observed that the rate of wound re-epithelialisation was delayed and acute inflammation, characterised by PMN infiltration and pro-inflammatory cytokine expression, was increased in *hspB1*$^{del/del}$ mice compared to wild-type mice. Strong expression of hspB1 protein was detected in cells in the migrating epithelium at the wound margin and in cells with fibroblast-like morphology in the wound bed in wild-type mice. The delayed wound healing in *hspB1*$^{del/del}$ mice at 3 d post-wounding is consistent with reduced proliferation of epidermal cells in hspB1-deficient mice. These results are supported by observations that hspB1 deficiency results in delayed cell proliferation in MEF, as described in chapter 3, and increased acute inflammation in the air pouch and peritonitis *in vivo* models, described in chapters 3 and 4, respectively. The lack of regulation of the production of TNFα, IL-1α and IL-1β by hspB1 suggests a lack of a role for hspB1 in macrophages in the acute inflammatory response to wounding. Although there was an increase in macrophage numbers in the wound margins in the early phase of the wound healing process (1 d), macrophages from *hspB1*$^{del/del}$ mice displayed deficient infiltration of the granulation tissue beneath the wound itself compared to wild-type cells. Infiltration of macrophages into both wild-type and *hspB1*$^{del/del}$ wound areas and margins was increased at 3 d relative to 1 d, as expected for normal murine wound healing but hspB1 deficiency caused little change in the cell numbers.

One might expect a degree of synergy of the increased pro-inflammatory and impaired proliferation characteristics in hspB1-deficient mice to result in a comparatively strong effect of hspB1 deficiency in the wound healing model. The delay in re-epithelialisation in *hspB1*$^{del/del}$ mice compared to wild-type is small compared to the comparisons in the size of

the wound area. In addition, the fold change in the difference in re-epithelialisation is not as great as the difference in the rate of MEF proliferation. This small difference in re-epithelialisation is typical in this model at 3 d (Seth, De la Garza et al. 2013; Vorstenbosch, Gallant-Behm et al. 2013). Re-epithelialisation is usually complete by 7 d post-wounding, unless another underlying pathology further delays the healing of the wound (Seth, De la Garza et al. 2013). Perhaps the extent of re-epithelialisation at a time point between the initiation of re-epithelialisation and completion, for example at d 5, 7 and 10, would show a greater difference in the rate re-epithelialisation in *hspB1*$^{del/del}$ and wild-type mice. One must also consider that the ways that these measurements are made are different; the calculations of the wound areas obviously involve squaring the radius, the result of which magnifies the degree of difference between the wild-type and *hspB1*$^{del/del}$ means compared to a set of data where the diameter between re-epithelialisation margins is measured. However, the overall results did not suggest a strong synergistic effect of exacerbated inflammation and delayed proliferation.

The resolution of the inflammatory phase of wound healing process is critical for the completion of the process. HspB1 deficiency results in increased neutrophil infiltration and pro-inflammatory cytokine production in two *in vivo* models of acute inflammation. Increased neutrophil infiltration was also observed in *hspB1*$^{del/del}$ mice compared to wild-type mice 1 d post-wounding and the associated increase in CXCL1 at 6 h post-wounding provides a possible mechanism for this, as for my results in the air pouch and peritonitis models of acute inflammation. The effects of hspB1 deficiency on neutrophil infiltration were followed by a delay in wound healing as measured by the area of the wound and distance between re-epithelisation frontiers at 3 d.

Neutrophils are well known to undergo rapid apoptosis, although I have not investigated the viability of neutrophils in response to wounding, the neutrophils are unlikely to be apoptotic upon arrival to the site of wounding considering that they were capable of responding to the inflammatory stimulus and undergoing transmigration to the site of inflammation. Therefore, they can be assumed to have contributed to the inflammatory response. These cells would then contribute to the apoptotic cellular load present within the wound. It is thus apparent that resident and infiltrating macrophages have a larger apoptotic cellular load to clear in *hspB1*$^{del/del}$ mice compared to wild-type mice. Macrophages actively ingest apoptotic neutrophils and previous studies have shown that this causes a shift in macrophage phenotype to an anti-inflammatory, proliferation inducing phenotype (Fadok, Bratton et al. 1998). I measured cytokines produced by M1 and M2 macrophages as markers of their polarisation, but observed no difference in the production of these cytokines in hspB1-deficient mice compared to wild-type mice, suggesting that hspB1 does not regulate macrophage cytokine production in wounds.

HspB1$^{del/del}$ wounds did, however, contain decreased numbers of macrophages compared to wild-type wounds at d 1 and d 3. Surprisingly, macrophage density was greater in the wound margins of *hspB1*$^{del/del}$ mice compared to wild-type at 1 d, suggesting that *hspB1*$^{del/del}$ macrophages have a diminished ability to migrate to the wound bed and allow for the progression of the wound response. There were more macrophages within the unwounded tissue compared to wounded tissue from wild-type and *hspB1*$^{del/del}$ mice at 1 d post-wounding. This is to be expected, as the excisional wound removes the granulation tissue in which the resident macrophages occupy. It is unclear if hspB1 directly affects macrophage migration in response to wounding, or if the results simply reflect a delay in the wound healing response caused by an earlier event. It is possible that the increased number of neutrophils observed

may be due to decreased uptake by macrophages in *hspB1*$^{del/del}$ mice compared to wild-type mice.

HspB1$^{del/del}$ wounded tissue lysates, at 6 h post-wounding, displayed significantly increased IL-6, CXCL1 and CCL2 expression compared to wild-type wounds. CCL2 and CCL3 would both be expected to provide chemotactic stimuli for macrophage recruitment. The increase in CCL2 production at 6 h post-wounding in hspB1-deficient mice is consistent with the increase in macrophage numbers in wound margins at 1 d. The lack of an effect of hspB1 deficiency on CCL2 and CCL3 expression at 1 d and 2 d post-wounding is consistent with the similar numbers of macrophages in wound areas and margins at 3 d in *hspB1*$^{del/del}$ mice compared to wild-type mice. HspB1 seems to limit the initial 'burst' of cytokine and chemokine production, early neutrophil infiltration of granulation tissue and macrophage infiltration of wound margins. At later times post-wounding hspB1 appears not to be involved in the production of any of the cytokines that I measured or in the subsequent infiltration of macrophages.

There was no evidence of neovascularisation in the wounded tissue at 1 d post-wounding. This suggests that macrophages migrate to the site of wounding from the established vasculature. Possible effects that hspB1 deficiency may result in are impairment in the ability of the macrophages to re-arrange their cytoskeleton for migration, the regulation of other chemokines that were not measured, and adhesion molecule expression.

At 7 d the collagen deposition within *hspB1*$^{del/del}$ wound areas was very dense and concentrated despite incomplete and delayed progression of wound healing compared to wild-type. Wild-type wounds that had healed completely showed collagen deposition throughout the dermis similar to that of unwounded skin, whereas this state of collagen deposition was not seen in wounds in hspB1-deficient mice at 7 d post-wounding. I did not

investigate the effect of collagen deposition directly, as my experiments did not include a time point where the wound was in a re-modelling phase.

To conclude, hspB1 deficiency in mice results in significantly impaired wound healing characterised by increased pro-inflammatory cytokine expression and neutrophil infiltration in the early phase of the wound healing process. We have also observed impaired proliferation of hspB1-deficient MEF and a greater distance between the borders of re-epithelialisation in *hspB1*$^{del/del}$ mice compared to wild-type mice. The strong expression of hspB1 expression in the advancing epithelium and infiltrating cells in the basal granulation tissue in wounds suggests an additional role for hspB1 in proliferation of these cells. The wound healing response is a complex series of temporally overlapping phases. My data show that hspB1 has a significant regulatory function in these processes may be important for the progression of the wound healing response.

Chapter 6

Discussion

The function of hspB1 in inflammation was previously unclear as the results from studies using RNA interference to deplete the protein were inconsistent (Park, Gaynor et al. 2003; Alford, Glennie et al. 2007; Sur, Lyte et al. 2008; Wu, Liu et al. 2009). The work in this thesis involved the use of a complete genetic knockout of the *hspB1* gene in mice to investigate the function of the protein *in vivo*. The results are not compromised by siRNA-mediated off-target effects or artefacts arising from trace levels of hspB1 expression. The data in this thesis suggests that hspB1 limits inflammatory gene expression. This is the opposite conclusion to that reached from research conducted in my group (Alford, Glennie et al. 2007) and by other laboratories (Gorska, Liang et al. 2007; Wu, Liu et al. 2009) using siRNA-mediated depletion of hspB1.

My data indicates that hspB1 regulates the production of pro-inflammatory cytokines early in the acute inflammatory response. The kinetics and expression of cytokines in MEF and TEPM *in vitro*, the air pouch and peritonitis models of acute inflammation and the wound healing model *in vivo*, suggests that hspB1 does not regulate cytokine production in macrophages. I consistently observed increased CXCL1 protein production and neutrophil infiltration in response to acute inflammation and injury *in vivo* in *hspB1*$^{del/del}$ mice compared to wild-type, although CXCL1 protein production was not regulated by hspB1 in MEF. It is possible that embryonic fibroblasts differ in inflammatory gene expression compared to adult fibroblasts.

I could not detect hspB1 expression in neutrophils isolated from wild-type mice, suggesting that it is unlikely that hspB1 directly regulates chemotaxis or inflammatory gene expression in these cells. The increased CXC chemokine expression in *hspB1*$^{del/del}$ mice provides a mechanism for the increased neutrophil recruitment in these mice compared to wild-type mice. It is likely that fibroblast/keratinocyte-like cells and/or vascular endothelial cells are the

responsible cell type for increased CXC chemokine production, which may be p38 MAPK-dependent.

The extent of hspB1 expression in leukocytes is still controversial. I was unable to detect expression of hspB1 in mouse neutrophils or TEPM, and others in my group have been unable to show hspB1 expression in human monocytes and murine bone marrow-derived macrophages (Alford, Glennie et al. 2007), although hspB1 expression was observed in M-CSF and GM-CSF-differentiated human macrophages. Others have shown hspB1 expression to be increased during human monocyte differentiation into macrophages and during macrophage polarisation (Fagone, Di Rosa et al. 2012). The expression of hspB1 in human macrophages could possibly be due to an *in vitro* artefact, although it is possible that there is a genuine species difference in hspB1 expression in human and mouse macrophages. I have not been able to eliminate the possibility of any effects of extracellular hspB1, which has been shown to block the differentiation of monocytes to dendritic cells (Laudanski, De et al. 2007) however, the observation that IL-1-induced IL-6 expression is increased in hspB1-deficient MEF suggests that hspB1 has an intracellular function in limiting inflammatory gene expression in cells such as fibroblasts. It would be interesting to investigate if a similar function exists in endothelial cells that produce various inflammatory cytokines and which also strongly express hspB1.

I did not investigate the effect of hspB1 on the viability of neutrophils infiltrating into the wounds, although results from the air pouch and peritonitis models both demonstrated reduced viability of neutrophils infiltrating to the site of acute inflammation in *hspB1*$^{del/del}$ mice, compared to wild-type. The data from these acute models are consistent with the inability to detect any elastase-positive neutrophils at 3 d post-wounding. Thus the increase in live neutrophil numbers in wounds of hspB1-deficient mice relative to wild-type mice is almost certainly transient. Neutrophils provide a chemo-attractant stimulus for monocytes

and produce CCL2. There was no difference in the amount of CCL2 at 1 d post-wounding in *hspB1*$^{del/del}$ and wild-type mice, however, if the neutrophils in *hspB1*$^{del/del}$ mice undergo apoptosis shortly after arriving to the site of the wound, this would explain why there is little effect of hspB1 deficiency on CCL2 expression or macrophage infiltration at 1 d post-wounding onwards. Efficient clearance of infiltrated neutrophils by macrophages is an important process for the resolution of acute inflammation after wounding. Activated neutrophils release reactive oxygen species (ROS), proteases (e.g. elastase) and collagenases (e.g. matrix metalloproteinase-9) (Dovi, Szpaderska et al. 2004). These have been shown to damage tissue and degrade the ECM during the inflammatory phase of wound healing, negatively influencing tissue repair and perhaps leading to overproduction of collagen to compensate for the weakened structural integrity of the ECM supporting scaffold. I observed a trend toward increased collagen deposition 7 d post-wounding in *hspB1*$^{del/del}$ wounds compared to wild-type wounds, and it would be interesting to quantify the effect of hspB1 deficiency on collagenesis and wound remodelling in the future by picro-sirius red staining at 5, 7 and 10 d post-wounding.

Macrophages promote the production and remodelling of ECM by releasing growth factors such as VEGF, PGDF and TGFβ (Barrientos, Stojadinovic et al. 2008). It is difficult to provide direct evidence for the contribution of macrophages to the wound healing process as they are not the sole source of these growth factors. Keratinocytes, neutrophils, fibroblasts, endothelial cells and platelets are also sources of one or more of these growth factors. I observed very similar numbers macrophages in the wound areas of *hspB1*$^{del/del}$ mice compared to wild-type mice 3 d post-wounding. This suggests that the macrophage-derived contribution to the expression of such growth factors might be similar in wild-type and *hspB1*$^{del/del}$ wounds. Nevertheless, it would be interesting to investigate if there is impaired production of

these growth factors in wounded hspB1-deficent mice, as this may provide an explanation for the poor wound healing outcome in these mice compared to wild-type mice.

I have demonstrated that vascular endothelial cells express hspB1. Neovascularisation was apparent in wounded tissue histology at 3 d and 7 d post-wounding. HspB1 activation is important for endothelial cell proliferation (McMullen, Bryant et al. 2005). If hspB1 regulates angiogenesis then this would result in a difference in the number of vessels available for leukocytes to migrate through in *hspB1*$^{del/del}$ and wild-type mice. The Masson's trichrome staining protocol, despite staining red blood cells a vivid pink colour, did not allow for the accurate identification of vessels. Staining of wound granulation tissue with anti-CD31 (Seth, De la Garza et al. 2013) or anti-factor VIII (Thuraisingam, Xu et al. 2010) antibodies would afford the ability to quantify the number of vessels in wounds. This would allow for the investigation of the effect of hspB1 deficiency on angiogenesis in response to wounding. It is possible that another factor involved in the regulation of cell migration is regulated by hspB1. HspB1 has been shown to maintain endothelial cell barrier integrity (Liu, Guevara et al. 2009; Liu, Milia et al. 2012). I did not investigate the effect of hspB1 deficiency on endothelial cell vascular adhesion molecule expression or inflammatory gene expression. These would be interesting lines of enquiry for future research.

The murine wound healing model has been criticised as a model of human wounding, as contraction plays a greater role in murine models than re-epithelialisation and granulation tissue formation, which are crucial for human wound healing (Davidson 1998). Recognition of this has led to models such as the rabbit dermal ulcer model (Ahn and Mustoe 1990; Mustoe, Pierce et al. 1991), which has the benefit of having the wounded tissue directly connected to the underlying cartilage. This provides the means to investigate the effect of applied growth factors/drugs or transgenic effects on granulation tissue formation and wound healing. A technique called splinting of full thickness excisional wounds, whereby the

excisional wound borders are bonded adhesively and sutured to a nylon ring, has been described in C57BL/6 mice (Galiano, Michaels et al. 2004). The authors observed that splinting did not affect the rate of re-epithelialisation and allows for the slower and gradual healing of the wound by granulation tissue formation, compared to rapid contractile wound healing in non-splinted wounds.

I have already observed strong expression of hspB1 in fibroblast-like cells in wild-type wound granulation tissue at 3 d and 7 d post-wounding. The wound splinting technique, when applied to the wound healing model described in chapter 5, would delay the contraction of the wound and allow for the investigation of the effect of hspB1 deficiency on wound granulation tissue formation in a gradually healing wound that more accurately models the healing of human wounds. Further investigation into the function of hspB1 in wound healing might be improved by the use of fluorescent antibody staining and microscopy, which would result in the ability to stain the tissue for multiple proteins of interest and observe any co-localisation of the expression of these proteins. For example, staining wound granulation tissue with BrdU (Seth, De la Garza et al. 2013) and hspB1 would give insight into the number of proliferating cells and the level of hspB1 expression in these cells.

Previous studies have shown the contribution of resident stem cells in the bulge region of hair follicles to injury repair, whereby these cells adopt an epidermal phenotype (Ito et al., 2005). We have demonstrated strong hspB1 expression in hair follicles in wild-type mice. The contribution of follicular stem cells to wound healing and possible regulation by hspB1 warrants further investigation.

I have not investigated the effect of hspB1 deficiency on TTP phosphorylation due to time limitations, although I considered if the lack of hspB1 as a substrate for phosphorylation by MK2 would result in a difference in the expression or activation of the shared MK2 substrate,

TTP, in hspB1-deficient mice compared to wild-type mice. We observed a trend toward COX-2, IL-6 and CXCL1 mRNA expression in hspB1-deficient MEF compared to wild-type, although we also did not investigate the extent of TTP expression in MEF, as these cells have vanishingly low expression of TTP. Furthermore, any such investigation would be hampered by the poor sensitivity of current anti-phosphorylated TTP antibodies available. TTP is strongly expressed in bone-marrow derived murine macrophages, and inhibition of TTP activity in these cells results in increased IL-1α, TNFα, IL-6, IL-10 (Tudor, Marchese et al. 2009) and CXCL1 (Datta, Biswas et al. 2008) mRNA stability. However, the observation that TEPM from wild-type mice do not express hspB1 suggests that TTP activity would not be affected in TEPM from hspB1-deficient mice.

HspB1 deficiency did not result in a reduction in protein production, as seen for inhibition of hsp90 (Sharma, Vabulas et al. 2012). The loss of the chaperone function and protein ubiquitination by hspB1 in *hspB1*$^{del/del}$ mice might result in the accumulation of proteins that otherwise might have been sequestered for degradation by the proteasome. HspB1 provides cellular resistance to thermal stress (Carper, Rocheleau et al. 1997) and is phosphorylation-independent (Knauf, Jakob et al. 1994). The effect of heat stress on hspB1-deficient mice has not been investigated in this thesis. All of the mice that were used were housed within a stable temperature range. Perhaps a dramatically increased inflammatory and apoptotic phenotype in *hspB1*$^{del/del}$ mice compared to wild-type mice would be observed in experiments repeated using mice housed at a higher than average temperature, which would drive increased hspB1 expression and function in wild-type mice.

Non-healing foot and leg ulcers are major pathologies that affect diabetics and patients on long-term glucocorticoid therapy. Chronic wounds are those which remain detained in the inflammatory stage for too long, which results in impaired production and promotion of the degradation of the ECM (Schonfelder, Abel et al. 2005). By definition, these wounds take

longer than three months to resolve and some may take far longer. These wounds represent a serious cause of morbidity, immobility, financial cost to the patient and healthcare system, and in extreme cases, can lead to lower extremity amputation (Snyder 2005). HspB1 accelerates wound healing, promotes re-epithelialisation and proliferation, and diminishes pro-inflammatory cytokine expression and neutrophil recruitment during the acute inflammatory response. The increase in the expression and/or activity of hspB1, whilst limiting the activity of TTP, might provide a novel therapeutic approach to treating chronic wounds.

While I have shown that hspB1 limits inflammatory cytokine expression *in vivo* and in embryonic fibroblasts, the precise molecular function of hspB1 in negatively regulating cytokine production is still unclear. The function of hspB1 is likely to be intracellular and may involve regulation of cell signalling via its ability to act as a chaperone but could equally well involve different direct chaperone effects on cytokines themselves or other proteins in the cell. The fact that many different proteins (p38 MAPK, p21, p27 and numerous cytokines) display increased expression in hspB1-depleted cells suggest that such effects could be mediated by the function of hspB1 in promoting ubiquitin-mediated degradation of client proteins as has recently been suggested for AUF1(Li, Defren et al. 2013). It would be very interesting to perform proteomic analysis of wild-type and hspB1-deficient cells and to identify the ubiquitin ligases that might be involved. One of the reasons why I did not attempt such as study was due to the fact that we were unable to reconstitute the *in vivo* effects of hspB1-depletion on cytokine expression in MEF. In these cells hspB1 appears not to regulate CXCL1 production and IL-6 expression was not regulated by hspB1 to the same extent as in vivo. To perform such studies it would be firstly necessary to identify a primary cell type that can be easily cultured from mouse tissue which displays strong hspB1-dependent effects on cytokine production. I attempted to isolate grow primary adult murine lung endothelial cells

but these proliferated poorly and it was impossible to grow hspB1-deficient cultures of these cells. Adult dermal fibroblasts might be a good choice, but obtaining sufficient numbers of cells for mechanistic analysis would be a challenge.

Chapter7

References

Acosta, J. B., D. G. del Barco, D. C. Vera, W. Savigne, P. Lopez-Saura, G. Guillen Nieto, et al. (2008). "The pro-inflammatory environment in recalcitrant diabetic foot wounds." Int Wound J **5**(4): 530-539.

Adzick, N. S., M. R. Harrison, P. L. Glick, J. H. Beckstead, R. L. Villa, H. Scheuenstuhl, et al. (1985). "Comparison of fetal, newborn, and adult wound healing by histologic, enzyme-histochemical, and hydroxyproline determinations." J Pediatr Surg **20**(4): 315-319.

Ahlers, A., C. Belka, M. Gaestel, N. Lamping, C. Sott, F. Herrmann, et al. (1994). "Interleukin-1-induced intracellular signaling pathways converge in the activation of mitogen-activated protein kinase and mitogen-activated protein kinase-activated protein kinase 2 and the subsequent phosphorylation of the 27-kilodalton heat shock protein in monocytic cells." Mol Pharmacol **46**(6): 1077-1083.

Ahn, S. T. and T. A. Mustoe (1990). "Effects of ischemia on ulcer wound healing: a new model in the rabbit ear." Ann Plast Surg **24**(1): 17-23.

Ajuebor, M. N., L. Gibbs, R. J. Flower, A. M. Das and M. Perretti (1998). "Investigation of the functional role played by the chemokine monocyte chemoattractant protein-1 in interleukin-1-induced murine peritonitis." Br J Pharmacol **125**(2): 319-326.

Akira, S. (1997). "IL-6-regulated transcription factors." Int J Biochem Cell Biol **29**(12): 1401-1418.

Alford, K. A., S. Glennie, B. R. Turrell, L. Rawlinson, J. Saklatvala and J. L. Dean (2007). "Heat shock protein 27 functions in inflammatory gene expression and transforming growth factor-beta-activated kinase-1 (TAK1)-mediated signaling." J Biol Chem **282**(9): 6232-6241.

Allison, M. C., A. G. Howatson, C. J. Torrance, F. D. Lee and R. I. Russell (1992). "Gastrointestinal damage associated with the use of nonsteroidal antiinflammatory drugs." N Engl J Med **327**(11): 749-754.

Almeida-Souza, L., S. Goethals, V. de Winter, I. Dierick, R. Gallardo, J. Van Durme, et al. (2010). "Increased monomerization of mutant HSPB1 leads to protein hyperactivity in Charcot-Marie-Tooth neuropathy." J Biol Chem **285**(17): 12778-12786.

Andrieu, C., D. Taieb, V. Baylot, S. Ettinger, P. Soubeyran, A. De-Thonel, et al. (2010). "Heat shock protein 27 confers resistance to androgen ablation and chemotherapy in prostate cancer cells through eIF4E." Oncogene **29**(13): 1883-1896.

Antman, E. M., J. S. Bennett, A. Daugherty, C. Furberg, H. Roberts and K. A. Taubert (2007). "Use of nonsteroidal antiinflammatory drugs: an update for clinicians: a scientific statement from the American Heart Association." Circulation **115**(12): 1634-1642.

Aressy, B. and B. Ducommun (2008). "Cell cycle control by the CDC25 phosphatases." Anticancer Agents Med Chem **8**(8): 818-824.

Arima, K., K. Nasu, H. Narahara, K. Fujisawa, N. Matsui and I. Miyakawa (2000). "Effects of lipopolysaccharide and cytokines on production of RANTES by cultured human endometrial stromal cells." Mol Hum Reprod **6**(3): 246-251.

Armstrong, D. A., J. A. Major, A. Chudyk and T. A. Hamilton (2004). "Neutrophil chemoattractant genes KC and MIP-2 are expressed in different cell populations at sites of surgical injury." J Leukoc Biol **75**(4): 641-648.

Ashcroft, G. S., M. J. Jeong, J. J. Ashworth, M. Hardman, W. Jin, N. Moutsopoulos, et al. (2012). "Tumor necrosis factor-alpha (TNF-alpha) is a therapeutic target for impaired cutaneous wound healing." Wound Repair Regen **20**(1): 38-49.

Bacon, K., M. Baggiolini, H. Broxmeyer, R. Horuk, I. Lindley, A. Mantovani, et al. (2002). "Chemokine/chemokine receptor nomenclature." J Interferon Cytokine Res **22**(10): 1067-1068.

Baehrecke, E. H. (2005). "Autophagy: dual roles in life and death?" Nat Rev Mol Cell Biol **6**(6): 505-510.

Bahou, W. F. and D. V. Gnatenko (2004). "Platelet transcriptome: the application of microarray analysis to platelets." Semin Thromb Hemost **30**(4): 473-484.

Bandman, O., R. T. Coleman, J. F. Loring, J. J. Seilhamer and B. G. Cocks (2002). "Complexity of inflammatory responses in endothelial cells and vascular smooth muscle cells determined by microarray analysis." Ann N Y Acad Sci **975**: 77-90.

Barrick, B., E. J. Campbell and C. A. Owen (1999). "Leukocyte proteinases in wound healing: roles in physiologic and pathologic processes." Wound Repair Regen **7**(6): 410-422.

Barrientos, S., O. Stojadinovic, M. S. Golinko, H. Brem and M. Tomic-Canic (2008). "Growth factors and cytokines in wound healing." Wound Repair Regen **16**(5): 585-601.

Bauer, K., U. Nitsche, J. Slotta-Huspenina, E. Drecoll, C. H. von Weyhern, R. Rosenberg, et al. (2012). "High HSP27 and HSP70 expression levels are independent adverse prognostic factors in primary resected colon cancer." Cell Oncol (Dordr) **35**(3): 197-205.

Benn, S. C., D. Perrelet, A. C. Kato, J. Scholz, I. Decosterd, R. J. Mannion, et al. (2002). "Hsp27 upregulation and phosphorylation is required for injured sensory and motor neuron survival." Neuron **36**(1): 45-56.

Bode, A. M. and Z. Dong (2007). "The functional contrariety of JNK." Mol Carcinog **46**(8): 591-598.

Bogoyevitch, M. A., K. R. Ngoei, T. T. Zhao, Y. Y. Yeap and D. C. Ng (2010). "c-Jun N-terminal kinase (JNK) signaling: recent advances and challenges." Biochim Biophys Acta **1804**(3): 463-475.

Boonstra, A., R. Rajsbaum, M. Holman, R. Marques, C. Asselin-Paturel, J. P. Pereira, et al. (2006). "Macrophages and myeloid dendritic cells, but not plasmacytoid dendritic cells, produce IL-10 in response to MyD88- and TRIF-dependent TLR signals, and TLR-independent signals." J Immunol **177**(11): 7551-7558.

Boulton, T. G., S. H. Nye, D. J. Robbins, N. Y. Ip, E. Radziejewska, S. D. Morgenbesser, et al. (1991). "ERKs: a family of protein-serine/threonine kinases that are activated and tyrosine phosphorylated in response to insulin and NGF." Cell **65**(4): 663-675.

Boulton, T. G., G. D. Yancopoulos, J. S. Gregory, C. Slaughter, C. Moomaw, J. Hsu, et al. (1990). "An insulin-stimulated protein kinase similar to yeast kinases involved in cell cycle control." Science **249**(4964): 64-67.

Bradford, M. M. (1976). "A rapid and sensitive method for the quantitation of microgram quantities of protein utilizing the principle of protein-dye binding." Anal Biochem **72**: 248-254.

Brancato, S. K. and J. E. Albina (2011). "Wound macrophages as key regulators of repair: origin, phenotype, and function." Am J Pathol **178**(1): 19-25.

Braund, R., S. M. Hook, N. Greenhill and N. J. Medlicott (2009). "Distribution of fibroblast growth factor-2 (FGF-2) within model excisional wounds following topical application." J Pharm Pharmacol **61**(2): 193-200.

Brennan, B. R. (2009). The Function of Heat Shock protein 27 in Interleukin-1 Signalling. London, Imperial College London. **PhD**.

Brikos, C., R. Wait, S. Begum, L. A. O'Neill and J. Saklatvala (2007). "Mass spectrometric analysis of the endogenous type I interleukin-1 (IL-1) receptor signaling complex formed after IL-1 binding identifies IL-1RAcP, MyD88, and IRAK-4 as the stable components." Mol Cell Proteomics **6**(9): 1551-1559.

Brook, M., C. R. Tchen, T. Santalucia, J. McIlrath, J. S. Arthur, J. Saklatvala, et al. (2006). "Posttranslational regulation of tristetraprolin subcellular localization and protein stability by p38 mitogen-activated protein kinase and extracellular signal-regulated kinase pathways." Mol Cell Biol **26**(6): 2408-2418.

Bruey, J. M., C. Paul, A. Fromentin, S. Hilpert, A. P. Arrigo, E. Solary, et al. (2000). "Differential regulation of HSP27 oligomerization in tumor cells grown in vitro and in vivo." Oncogene **19**(42): 4855-4863.

Cabal-Hierro, L. and P. S. Lazo (2012). "Signal transduction by tumor necrosis factor receptors." Cell Signal **24**(6): 1297-1305.

Cabrera, P. V., G. Blanco, M. J. Gravisaco, E. Alvarez and S. Hajos (2001). "Zymosan modulates CD44 isoform expression in a murine model of inflammation resembling rheumatoid arthritis synovitis." J Rheumatol **28**(5): 943-949.

Cannon, C. P. and P. J. Cannon (2012). "Physiology. COX-2 inhibitors and cardiovascular risk." Science **336**(6087): 1386-1387.

Cargnello, M. and P. P. Roux (2011). "Activation and function of the MAPKs and their substrates, the MAPK-activated protein kinases." Microbiol Mol Biol Rev **75**(1): 50-83.

Carper, S. W., T. A. Rocheleau, D. Cimino and F. K. Storm (1997). "Heat shock protein 27 stimulates recovery of RNA and protein synthesis following a heat shock." J Cell Biochem **66**(2): 153-164.

Carswell, E. A., L. J. Old, R. L. Kassel, S. Green, N. Fiore and B. Williamson (1975). "An endotoxin-induced serum factor that causes necrosis of tumors." Proc Natl Acad Sci U S A **72**(9): 3666-3670.

Carter, R., V. Sykes and D. Lanning (2009). "Scarless fetal mouse wound healing may initiate apoptosis through caspase 7 and cleavage of PARP." J Surg Res **156**(1): 74-79.

Cash, J. L., G. E. White and D. R. Greaves (2009). "Chapter 17. Zymosan-induced peritonitis as a simple experimental system for the study of inflammation." Methods Enzymol **461**: 379-396.

Charette, S. J. and J. Landry (2000). "The interaction of HSP27 with Daxx identifies a potential regulatory role of HSP27 in Fas-induced apoptosis." Ann N Y Acad Sci **926**: 126-131.

Charette, S. J., J. N. Lavoie, H. Lambert and J. Landry (2000). "Inhibition of Daxx-mediated apoptosis by heat shock protein 27." Mol Cell Biol **20**(20): 7602-7612.

Charo, I. F. and R. M. Ransohoff (2006). "The many roles of chemokines and chemokine receptors in inflammation." N Engl J Med **354**(6): 610-621.

Chen, C. J., H. Kono, D. Golenbock, G. Reed, S. Akira and K. L. Rock (2007). "Identification of a key pathway required for the sterile inflammatory response triggered by dying cells." Nat Med **13**(7): 851-856.

Chen, R., R. Y. Dai, C. Y. Duan, Y. P. Liu, S. K. Chen, D. M. Yan, et al. (2011). "Unfolded protein response suppresses cisplatin-induced apoptosis via autophagy regulation in human hepatocellular carcinoma cells." Folia Biol (Praha) **57**(3): 87-95.

Chen, S. W., M. Kim, J. H. Song, S. W. Park, D. Wells, K. Brown, et al. (2009). "Mice that overexpress human heat shock protein 27 have increased renal injury following ischemia reperfusion." Kidney Int **75**(5): 499-510.

Chrestensen, C. A., M. J. Schroeder, J. Shabanowitz, D. F. Hunt, J. W. Pelo, M. T. Worthington, et al. (2004). "MAPKAP kinase 2 phosphorylates tristetraprolin on in vivo sites including Ser178, a site required for 14-3-3 binding." J Biol Chem **279**(11): 10176-10184.

Chretien, P. and J. Landry (1988). "Enhanced constitutive expression of the 27-kDa heat shock proteins in heat-resistant variants from Chinese hamster cells." J Cell Physiol **137**(1): 157-166.

Clifton, A. D., P. R. Young and P. Cohen (1996). "A comparison of the substrate specificity of MAPKAP kinase-2 and MAPKAP kinase-3 and their activation by cytokines and cellular stress." FEBS Lett **392**(3): 209-214.

Concannon, C. G., S. Orrenius and A. Samali (2001). "Hsp27 inhibits cytochrome c-mediated caspase activation by sequestering both pro-caspase-3 and cytochrome c." Gene Expr **9**(4-5): 195-201.

Conze, D. B., C. J. Wu, J. A. Thomas, A. Landstrom and J. D. Ashwell (2008). "Lys63-linked polyubiquitination of IRAK-1 is required for interleukin-1 receptor- and toll-like receptor-mediated NF-kappaB activation." Mol Cell Biol **28**(10): 3538-3547.

Cooper, J. A., D. F. Bowen-Pope, E. Raines, R. Ross and T. Hunter (1982). "Similar effects of platelet-derived growth factor and epidermal growth factor on the phosphorylation of tyrosine in cellular proteins." Cell **31**(1): 263-273.

Cuadrado, A. and A. R. Nebreda (2010). "Mechanisms and functions of p38 MAPK signalling." Biochem J **429**(3): 403-417.

Cuenda, A. and S. Rousseau (2007). "p38 MAP-kinases pathway regulation, function and role in human diseases." Biochim Biophys Acta **1773**(8): 1358-1375.

Cuesta, R., G. Laroia and R. J. Schneider (2000). "Chaperone hsp27 inhibits translation during heat shock by binding eIF4G and facilitating dissociation of cap-initiation complexes." Genes Dev **14**(12): 1460-1470.

Datta, S., R. Biswas, M. Novotny, P. G. Pavicic, Jr., T. Herjan, P. Mandal, et al. (2008). "Tristetraprolin regulates CXCL1 (KC) mRNA stability." J Immunol **180**(4): 2545-2552.

Davidson, J. M. (1998). "Animal models for wound repair." Arch Dermatol Res **290 Suppl**: S1-11.

De, A. K., K. M. Kodys, B. S. Yeh and C. Miller-Graziano (2000). "Exaggerated human monocyte IL-10 concomitant to minimal TNF-alpha induction by heat-shock protein 27 (Hsp27) suggests Hsp27 is primarily an antiinflammatory stimulus." J Immunol **165**(7): 3951-3958.

de Graauw, M., I. Tijdens, R. Cramer, S. Corless, J. F. Timms and B. van de Water (2005). "Heat shock protein 27 is the major differentially phosphorylated protein involved in renal epithelial cellular stress response and controls focal adhesion organization and apoptosis." J Biol Chem **280**(33): 29885-29898.

Deak, M., A. D. Clifton, L. M. Lucocq and D. R. Alessi (1998). "Mitogen- and stress-activated protein kinase-1 (MSK1) is directly activated by MAPK and SAPK2/p38, and may mediate activation of CREB." EMBO J **17**(15): 4426-4441.

Dean, J. L., M. Brook, A. R. Clark and J. Saklatvala (1999). "p38 mitogen-activated protein kinase regulates cyclooxygenase-2 mRNA stability and transcription in lipopolysaccharide-treated human monocytes." J Biol Chem **274**(1): 264-269.

Delano, D. L., M. C. Montesinos, P. D'Eustachio, T. Wiltshire and B. N. Cronstein (2005). "An interaction between genetic factors and gender determines the magnitude of the inflammatory response in the mouse air pouch model of acute inflammation." Inflammation **29**(1): 1-7.

Den Otter, W., J. W. De Groot, C. D. Van Basten, L. H. Rademakers, R. A. De Weger and E. Pels (1982). "Brewer thioglycollate medium induces different exudates in guinea pigs and mice." Exp Mol Pathol **36**(3): 403-413.

Deng, L., C. Wang, E. Spencer, L. Yang, A. Braun, J. You, et al. (2000). "Activation of the IkappaB kinase complex by TRAF6 requires a dimeric ubiquitin-conjugating enzyme complex and a unique polyubiquitin chain." Cell **103**(2): 351-361.

Derijard, B., J. Raingeaud, T. Barrett, I. H. Wu, J. Han, R. J. Ulevitch, et al. (1995). "Independent human MAP-kinase signal transduction pathways defined by MEK and MKK isoforms." Science **267**(5198): 682-685.

Devalaraja, R. M., L. B. Nanney, J. Du, Q. Qian, Y. Yu, M. N. Devalaraja, et al. (2000). "Delayed wound healing in CXCR2 knockout mice." J Invest Dermatol **115**(2): 234-244.

Di Carlo, F. J. and J. V. Fiore (1958). "On the composition of zymosan." Science **127**(3301): 756-757.

Dieter, P., J. G. Altin, K. Decker and F. L. Bygrave (1987). "Possible involvement of eicosanoids in the zymosan and arachidonic-acid-induced oxygen uptake, glycogenolysis and Ca2+ mobilization in the perfused rat liver." Eur J Biochem **165**(2): 455-460.

Dinarello, C. A. (1996). "Biologic basis for interleukin-1 in disease." Blood **87**(6): 2095-2147.

Dinarello, C. A. (2004). "Infection, fever, and exogenous and endogenous pyrogens: some concepts have changed." J Endotoxin Res **10**(4): 201-222.

Dinarello, C. A. (2005). "Blocking IL-1 in systemic inflammation." J Exp Med **201**(9): 1355-1359.

Dinarello, C. A. (2009). "Immunological and inflammatory functions of the interleukin-1 family." Annu Rev Immunol **27**: 519-550.

Dinarello, C. A. (2011). "Interleukin-1 in the pathogenesis and treatment of inflammatory diseases." Blood **117**(14): 3720-3732.

DiPietro, L. A., M. Burdick, Q. E. Low, S. L. Kunkel and R. M. Strieter (1998). "MIP-1alpha as a critical macrophage chemoattractant in murine wound repair." J Clin Invest **101**(8): 1693-1698.

DiPietro, L. A., P. J. Polverini, S. M. Rahbe and E. J. Kovacs (1995). "Modulation of JE/MCP-1 expression in dermal wound repair." Am J Pathol **146**(4): 868-875.

Doherty, N. S., P. Poubelle, P. Borgeat, T. H. Beaver, G. L. Westrich and N. L. Schrader (1985). "Intraperitoneal injection of zymosan in mice induces pain, inflammation and the synthesis of peptidoleukotrienes and prostaglandin E2." Prostaglandins **30**(5): 769-789.

Doppler, H., P. Storz, J. Li, M. J. Comb and A. Toker (2005). "A phosphorylation state-specific antibody recognizes Hsp27, a novel substrate of protein kinase D." J Biol Chem **280**(15): 15013-15019.

Dostert, C., V. Petrilli, R. Van Bruggen, C. Steele, B. T. Mossman and J. Tschopp (2008). "Innate immune activation through Nalp3 inflammasome sensing of asbestos and silica." Science **320**(5876): 674-677.

Doukas, J. and J. S. Pober (1990). "IFN-gamma enhances endothelial activation induced by tumor necrosis factor but not IL-1." J Immunol **145**(6): 1727-1733.

Dovi, J. V., L. K. He and L. A. DiPietro (2003). "Accelerated wound closure in neutrophil-depleted mice." J Leukoc Biol **73**(4): 448-455.

Dovi, J. V., A. M. Szpaderska and L. A. DiPietro (2004). "Neutrophil function in the healing wound: adding insult to injury?" Thromb Haemost **92**(2): 275-280.

Edwards, J. C., A. D. Sedgwick and D. A. Willoughby (1981). "The formation of a structure with the features of synovial lining by subcutaneous injection of air: an in vivo tissue culture system." J Pathol **134**(2): 147-156.

Elcombe, S. E., S. Naqvi, M. W. Van Den Bosch, K. F. MacKenzie, F. Cianfanelli, G. D. Brown, et al. (2013). "Dectin-1 regulates IL-10 production via a MSK1/2 and CREB dependent pathway and promotes the induction of regulatory macrophage markers." PLoS One **8**(3): e60086.

Elliott, M. J., R. N. Maini, M. Feldmann, A. Long-Fox, P. Charles, P. Katsikis, et al. (1993). "Treatment of rheumatoid arthritis with chimeric monoclonal antibodies to tumor necrosis factor alpha." Arthritis Rheum **36**(12): 1681-1690.

Eming, S. A., T. Krieg and J. M. Davidson (2007). "Inflammation in wound repair: molecular and cellular mechanisms." J Invest Dermatol **127**(3): 514-525.

Eming, S. A., H. Smola and T. Krieg (2002). "Treatment of chronic wounds: state of the art and future concepts." Cells Tissues Organs **172**(2): 105-117.

Emmerich, C. H., A. C. Schmukle, T. L. Haas, B. Gerlach, S. M. Cordier, E. Rieser, et al. (2011). "The linear ubiquitin chain assembly complex forms part of the TNF-R1 signalling complex and is required for effective TNF-induced gene induction and prevents TNF-induced apoptosis." Adv Exp Med Biol **691**: 115-126.

Engel, K., A. Kotlyarov and M. Gaestel (1998). "Leptomycin B-sensitive nuclear export of MAPKAP kinase 2 is regulated by phosphorylation." EMBO J **17**(12): 3363-3371.

Engelhardt, E., A. Toksoy, M. Goebeler, S. Debus, E. B. Brocker and R. Gillitzer (1998). "Chemokines IL-8, GROalpha, MCP-1, IP-10, and Mig are sequentially and differentially expressed during phase-specific infiltration of leukocyte subsets in human wound healing." Am J Pathol **153**(6): 1849-1860.

Fadok, V. A., D. L. Bratton, A. Konowal, P. W. Freed, J. Y. Westcott and P. M. Henson (1998). "Macrophages that have ingested apoptotic cells in vitro inhibit proinflammatory cytokine production through autocrine/paracrine mechanisms involving TGF-beta, PGE2, and PAF." J Clin Invest **101**(4): 890-898.

Fagone, P., M. Di Rosa, M. Palumbo, C. De Gregorio, F. Nicoletti and L. Malaguarnera (2012). "Modulation of heat shock proteins during macrophage differentiation." Inflamm Res **61**(10): 1131-1139.

Feldmann, M. and R. N. Maini (2001). "Anti-TNF alpha therapy of rheumatoid arthritis: what have we learned?" Annu Rev Immunol **19**: 163-196.

Fielding, C. A., R. M. McLoughlin, L. McLeod, C. S. Colmont, M. Najdovska, D. Grail, et al. (2008). "IL-6 regulates neutrophil trafficking during acute inflammation via STAT3." J Immunol **181**(3): 2189-2195.

Fiorentino, D. F., A. Zlotnik, T. R. Mosmann, M. Howard and A. O'Garra (1991). "IL-10 inhibits cytokine production by activated macrophages." J Immunol **147**(11): 3815-3822.

Fonseca, J. E., M. J. Santos, H. Canhao and E. Choy (2009). "Interleukin-6 as a key player in systemic inflammation and joint destruction." Autoimmun Rev **8**(7): 538-542.

Freshney, N. W., L. Rawlinson, F. Guesdon, E. Jones, S. Cowley, J. Hsuan, et al. (1994). "Interleukin-1 activates a novel protein kinase cascade that results in the phosphorylation of Hsp27." Cell **78**(6): 1039-1049.

Freudenberg, M. A., S. Tchaptchet, S. Keck, G. Fejer, M. Huber, N. Schutze, et al. (2008). "Lipopolysaccharide sensing an important factor in the innate immune response to Gram-negative bacterial infections: benefits and hazards of LPS hypersensitivity." Immunobiology **213**(3-4): 193-203.

Fu, X., X. Li, B. Cheng, W. Chen and Z. Sheng (2005). "Engineered growth factors and cutaneous wound healing: success and possible questions in the past 10 years." Wound Repair Regen **13**(2): 122-130.

Gabai, V. L. and M. Y. Sherman (2002). "Invited review: Interplay between molecular chaperones and signaling pathways in survival of heat shock." J Appl Physiol **92**(4): 1743-1748.

Gaestel, M. (2006). "MAPKAP kinases - MKs - two's company, three's a crowd." Nat Rev Mol Cell Biol **7**(2): 120-130.

Gaestel, M., A. Kotlyarov and M. Kracht (2009). "Targeting innate immunity protein kinase signalling in inflammation." Nat Rev Drug Discov **8**(6): 480-499.

Galiano, R. D., J. t. Michaels, M. Dobryansky, J. P. Levine and G. C. Gurtner (2004). "Quantitative and reproducible murine model of excisional wound healing." Wound Repair Regen **12**(4): 485-492.

Garcia-Ramallo, E., T. Marques, N. Prats, J. Beleta, S. L. Kunkel and N. Godessart (2002). "Resident cell chemokine expression serves as the major mechanism for leukocyte recruitment during local inflammation." J Immunol **169**(11): 6467-6473.

Garfin, D. E. (1990). "One-dimensional gel electrophoresis." Methods Enzymol **182**: 425-441.

Garmyn, M., T. Mammone, A. Pupe, D. Gan, L. Declercq and D. Maes (2001). "Human keratinocytes respond to osmotic stress by p38 map kinase regulated induction of HSP70 and HSP27." J Invest Dermatol **117**(5): 1290-1295.

Garrido, C., P. Mehlen, A. Fromentin, A. Hammann, M. Assem, A. P. Arrigo, et al. (1996). "Inconstant association between 27-kDa heat-shock protein (Hsp27) content and doxorubicin resistance in human colon cancer cells. The doxorubicin-protecting effect of Hsp27." Eur J Biochem **237**(3): 653-659.

Garrido, C., P. Ottavi, A. Fromentin, A. Hammann, A. P. Arrigo, B. Chauffert, et al. (1997). "HSP27 as a mediator of confluence-dependent resistance to cell death induced by anticancer drugs." Cancer Res **57**(13): 2661-2667.

Gerard, C. and B. J. Rollins (2001). "Chemokines and disease." Nat Immunol **2**(2): 108-115.

Gerits, N., T. Mikalsen, S. Kostenko, A. Shiryaev, M. Johannessen and U. Moens (2007). "Modulation of F-actin rearrangement by the cyclic AMP/cAMP-dependent protein kinase (PKA) pathway is mediated by MAPK-activated protein kinase 5 and requires PKA-induced nuclear export of MK5." J Biol Chem **282**(51): 37232-37243.

Ghayour-Mobarhan, M., H. Saber and G. A. Ferns (2012). "The potential role of heat shock protein 27 in cardiovascular disease." Clin Chim Acta **413**(1-2): 15-24.

Gillitzer, R. and M. Goebeler (2001). "Chemokines in cutaneous wound healing." J Leukoc Biol **69**(4): 513-521.

Gordon, S. (2003). "Alternative activation of macrophages." Nat Rev Immunol **3**(1): 23-35.

Gorska, M. M., Q. Liang, S. J. Stafford, N. Goplen, N. Dharajiya, L. Guo, et al. (2007). "MK2 controls the level of negative feedback in the NF-kappaB pathway and is essential for vascular permeability and airway inflammation." J Exp Med **204**(7): 1637-1652.

Gray, P. W., B. B. Aggarwal, C. V. Benton, T. S. Bringman, W. J. Henzel, J. A. Jarrett, et al. (1984). "Cloning and expression of cDNA for human lymphotoxin, a lymphokine with tumour necrosis activity." Nature **312**(5996): 721-724.

Grell, M. (1995). "Tumor necrosis factor (TNF) receptors in cellular signaling of soluble and membrane-expressed TNF." J Inflamm **47**(1-2): 8-17.

Grinnell, F. (2000). "Fibroblast-collagen-matrix contraction: growth-factor signalling and mechanical loading." Trends Cell Biol **10**(9): 362-365.

Grose, R. and S. Werner (2003). "Wound healing studies in transgenic and knockout mice. A review." Methods Mol Med **78**: 191-216.

Guay, J., H. Lambert, G. Gingras-Breton, J. N. Lavoie, J. Huot and J. Landry (1997). "Regulation of actin filament dynamics by p38 map kinase-mediated phosphorylation of heat shock protein 27." J Cell Sci **110 (Pt 3)**: 357-368.

Guesdon, F., N. Freshney, R. J. Waller, L. Rawlinson and J. Saklatvala (1993). "Interleukin 1 and tumor necrosis factor stimulate two novel protein kinases that phosphorylate the heat shock protein hsp27 and beta-casein." J Biol Chem **268**(6): 4236-4243.

Gupta, S., D. Campbell, B. Derijard and R. J. Davis (1995). "Transcription factor ATF2 regulation by the JNK signal transduction pathway." Science **267**(5196): 389-393.

Gupta, S., A. Deepti, S. Deegan, F. Lisbona, C. Hetz and A. Samali (2010). "HSP72 protects cells from ER stress-induced apoptosis via enhancement of IRE1alpha-XBP1 signaling through a physical interaction." PLoS Biol **8**(7): e1000410.

Hadaschik, B. A., J. Jackson, L. Fazli, A. Zoubeidi, H. M. Burt, M. E. Gleave, et al. (2008). "Intravesically administered antisense oligonucleotides targeting heat-shock protein-27 inhibit the growth of non-muscle-invasive bladder cancer." BJU Int **102**(5): 610-616.

Hallgren, J. and M. F. Gurish (2007). "Pathways of murine mast cell development and trafficking: tracking the roots and routes of the mast cell." Immunol Rev **217**: 8-18.

Han, J., J. D. Lee, L. Bibbs and R. J. Ulevitch (1994). "A MAP kinase targeted by endotoxin and hyperosmolarity in mammalian cells." Science **265**(5173): 808-811.

Han, J., J. D. Lee, Y. Jiang, Z. Li, L. Feng and R. J. Ulevitch (1996). "Characterization of the structure and function of a novel MAP kinase kinase (MKK6)." J Biol Chem **271**(6): 2886-2891.

Haslbeck, M., A. Ignatiou, H. Saibil, S. Helmich, E. Frenzl, T. Stromer, et al. (2004). "A domain in the N-terminal part of Hsp26 is essential for chaperone function and oligomerization." J Mol Biol **343**(2): 445-455.

Hibi, M., A. Lin, T. Smeal, A. Minden and M. Karin (1993). "Identification of an oncoprotein- and UV-responsive protein kinase that binds and potentiates the c-Jun activation domain." Genes Dev **7**(11): 2135-2148.

Hightower, L. E. (1991). "Heat shock, stress proteins, chaperones, and proteotoxicity." Cell **66**(2): 191-197.

Hirano, S., R. S. Rees and R. R. Gilmont (2002). "MAP kinase pathways involving hsp27 regulate fibroblast-mediated wound contraction." J Surg Res **102**(2): 77-84.

Hirano, S., E. A. Shelden and R. R. Gilmont (2004). "HSP27 regulates fibroblast adhesion, motility, and matrix contraction." Cell Stress Chaperones **9**(1): 29-37.

Hirano, T. (1998). "Interleukin 6 and its receptor: ten years later." Int Rev Immunol **16**(3-4): 249-284.

Hoffmann, E., A. Thiefes, D. Buhrow, O. Dittrich-Breiholz, H. Schneider, K. Resch, et al. (2005). "MEK1-dependent delayed expression of Fos-related antigen-1 counteracts c-Fos and p65 NF-kappaB-mediated interleukin-8 transcription in response to cytokines or growth factors." J Biol Chem **280**(10): 9706-9718.

Hol, J., L. Wilhelmsen and G. Haraldsen (2010). "The murine IL-8 homologues KC, MIP-2, and LIX are found in endothelial cytoplasmic granules but not in Weibel-Palade bodies." J Leukoc Biol **87**(3): 501-508.

Horiuchi, S., Y. Koyanagi, Y. Zhou, H. Miyamoto, Y. Tanaka, M. Waki, et al. (1994). "Soluble interleukin-6 receptors released from T cell or granulocyte/macrophage cell lines and human peripheral blood mononuclear cells are generated through an alternative splicing mechanism." Eur J Immunol **24**(8): 1945-1948.

Houssiau, F. A., J. P. Devogelaer, J. Van Damme, C. N. de Deuxchaisnes and J. Van Snick (1988). "Interleukin-6 in synovial fluid and serum of patients with rheumatoid arthritis and other inflammatory arthritides." Arthritis Rheum **31**(6): 784-788.

Hoyer-Hansen, M. and M. Jaattela (2007). "Connecting endoplasmic reticulum stress to autophagy by unfolded protein response and calcium." Cell Death Differ **14**(9): 1576-1582.

Hu, X., P. K. Paik, J. Chen, A. Yarilina, L. Kockeritz, T. T. Lu, et al. (2006). "IFN-gamma suppresses IL-10 production and synergizes with TLR2 by regulating GSK3 and CREB/AP-1 proteins." Immunity **24**(5): 563-574.

Huang, L., J. N. Min, S. Masters, N. F. Mivechi and D. Moskophidis (2007). "Insights into function and regulation of small heat shock protein 25 (HSPB1) in a mouse model with targeted gene disruption." Genesis **45**(8): 487-501.

Hubner, G., M. Brauchle, H. Smola, M. Madlener, R. Fassler and S. Werner (1996). "Differential regulation of pro-inflammatory cytokines during wound healing in normal and glucocorticoid-treated mice." Cytokine **8**(7): 548-556.

Huot, J., F. Houle, F. Marceau and J. Landry (1997). "Oxidative stress-induced actin reorganization mediated by the p38 mitogen-activated protein kinase/heat shock protein 27 pathway in vascular endothelial cells." Circ Res **80**(3): 383-392.

Huot, J., F. Houle, D. R. Spitz and J. Landry (1996). "HSP27 phosphorylation-mediated resistance against actin fragmentation and cell death induced by oxidative stress." Cancer Res **56**(2): 273-279.

Iida, N. and G. R. Grotendorst (1990). "Cloning and sequencing of a new gro transcript from activated human monocytes: expression in leukocytes and wound tissue." Mol Cell Biol **10**(10): 5596-5599.

Jaeschke, A., M. Karasarides, J. J. Ventura, A. Ehrhardt, C. Zhang, R. A. Flavell, et al. (2006). "JNK2 is a positive regulator of the cJun transcription factor." Mol Cell **23**(6): 899-911.

Jakob, U., M. Gaestel, K. Engel and J. Buchner (1993). "Small heat shock proteins are molecular chaperones." J Biol Chem **268**(3): 1517-1520.

Jeong, J. G., J. M. Kim, H. Cho, W. Hahn, S. S. Yu and S. Kim (2004). "Effects of IL-1beta on gene expression in human rheumatoid synovial fibroblasts." Biochem Biophys Res Commun **324**(1): 3-7.

Johansen, C., C. Vestergaard, K. Kragballe, G. Kollias, M. Gaestel and L. Iversen (2009). "MK2 regulates the early stages of skin tumor promotion." Carcinogenesis **30**(12): 2100-2108.

Kagan, J. C., T. Su, T. Horng, A. Chow, S. Akira and R. Medzhitov (2008). "TRAM couples endocytosis of Toll-like receptor 4 to the induction of interferon-beta." Nat Immunol **9**(4): 361-368.

Kaplanski, G., C. Farnarier, S. Kaplanski, R. Porat, L. Shapiro, P. Bongrand, et al. (1994). "Interleukin-1 induces interleukin-8 secretion from endothelial cells by a juxtacrine mechanism." Blood **84**(12): 4242-4248.

Kappe, G., E. Franck, P. Verschuure, W. C. Boelens, J. A. Leunissen and W. W. de Jong (2003). "The human genome encodes 10 alpha-crystallin-related small heat shock proteins: HspB1-10." Cell Stress Chaperones **8**(1): 53-61.

Kargman, S., S. Charleson, M. Cartwright, J. Frank, D. Riendeau, J. Mancini, et al. (1996). "Characterization of Prostaglandin G/H Synthase 1 and 2 in rat, dog, monkey, and human gastrointestinal tracts." Gastroenterology **111**(2): 445-454.

Karin, M. (2006). "Nuclear factor-kappaB in cancer development and progression." Nature **441**(7092): 431-436.

Kaur, P., W. J. Welch and J. Saklatvala (1989). "Interleukin 1 and tumour necrosis factor increase phosphorylation of the small heat shock protein. Effects in fibroblasts, Hep G2 and U937 cells." FEBS Lett **258**(2): 269-273.

Kawagoe, T., S. Sato, K. Matsushita, H. Kato, K. Matsui, Y. Kumagai, et al. (2008). "Sequential control of Toll-like receptor-dependent responses by IRAK1 and IRAK2." Nat Immunol **9**(6): 684-691.

Khanna, S., S. Biswas, Y. Shang, E. Collard, A. Azad, C. Kauh, et al. (2010). "Macrophage dysfunction impairs resolution of inflammation in the wounds of diabetic mice." PLoS One **5**(3): e9539.

Kim, M. H., W. Liu, D. L. Borjesson, F. R. Curry, L. S. Miller, A. L. Cheung, et al. (2008). "Dynamics of neutrophil infiltration during cutaneous wound healing and infection using fluorescence imaging." J Invest Dermatol **128**(7): 1812-1820.

Kishimoto, T. (2010). "IL-6: from its discovery to clinical applications." Int Immunol **22**(5): 347-352.

Knauf, U., U. Jakob, K. Engel, J. Buchner and M. Gaestel (1994). "Stress- and mitogen-induced phosphorylation of the small heat shock protein Hsp25 by MAPKAP kinase 2 is not essential for chaperone properties and cellular thermoresistance." EMBO J **13**(1): 54-60.

Kolaczkowska, E. and P. Kubes (2013). "Neutrophil recruitment and function in health and inflammation." Nat Rev Immunol **13**(3): 159-175.

Kolb, W. P. and G. A. Granger (1968). "Lymphocyte in vitro cytotoxicity: characterization of human lymphotoxin." Proc Natl Acad Sci U S A **61**(4): 1250-1255.

Kostenko, S. and U. Moens (2009). "Heat shock protein 27 phosphorylation: kinases, phosphatases, functions and pathology." Cell Mol Life Sci **66**(20): 3289-3307.

Kracht, M., O. Truong, N. F. Totty, M. Shiroo and J. Saklatvala (1994). "Interleukin 1 alpha activates two forms of p54 alpha mitogen-activated protein kinase in rabbit liver." J Exp Med **180**(6): 2017-2025.

Krausgruber, T., K. Blazek, T. Smallie, S. Alzabin, H. Lockstone, N. Sahgal, et al. (2011). "IRF5 promotes inflammatory macrophage polarization and TH1-TH17 responses." Nat Immunol **12**(3): 231-238.

Kregel, K. C. (2002). "Heat shock proteins: modifying factors in physiological stress responses and acquired thermotolerance." J Appl Physiol **92**(5): 2177-2186.

Krishnamurthy, K., R. Kanagasabai, L. J. Druhan and G. Ilangovan (2012). "Heat shock protein 25-enriched plasma transfusion preconditions the heart against doxorubicin-induced dilated cardiomyopathy in mice." J Pharmacol Exp Ther **341**(3): 829-839.

Kyriakis, J. M. and J. Avruch (1990). "pp54 microtubule-associated protein 2 kinase. A novel serine/threonine protein kinase regulated by phosphorylation and stimulated by poly-L-lysine." J Biol Chem **265**(28): 17355-17363.

Kyriakis, J. M. and J. Avruch (2001). "Mammalian mitogen-activated protein kinase signal transduction pathways activated by stress and inflammation." Physiol Rev **81**(2): 807-869.

Kyriakis, J. M., D. L. Brautigan, T. S. Ingebritsen and J. Avruch (1991). "pp54 microtubule-associated protein-2 kinase requires both tyrosine and serine/threonine phosphorylation for activity." J Biol Chem **266**(16): 10043-10046.

Lai, W. S., E. Carballo, J. R. Strum, E. A. Kennington, R. S. Phillips and P. J. Blackshear (1999). "Evidence that tristetraprolin binds to AU-rich elements and promotes the deadenylation and destabilization of tumor necrosis factor alpha mRNA." Mol Cell Biol **19**(6): 4311-4323.

Lambert, H., S. J. Charette, A. F. Bernier, A. Guimond and J. Landry (1999). "HSP27 multimerization mediated by phosphorylation-sensitive intermolecular interactions at the amino terminus." J Biol Chem **274**(14): 9378-9385.

Landry, J., P. Chretien, H. Lambert, E. Hickey and L. A. Weber (1989). "Heat shock resistance conferred by expression of the human HSP27 gene in rodent cells." J Cell Biol **109**(1): 7-15.

Landry, J. and J. Huot (1995). "Modulation of actin dynamics during stress and physiological stimulation by a signaling pathway involving p38 MAP kinase and heat-shock protein 27." Biochem Cell Biol **73**(9-10): 703-707.

Landry, J., H. Lambert, M. Zhou, J. N. Lavoie, E. Hickey, L. A. Weber, et al. (1992). "Human HSP27 is phosphorylated at serines 78 and 82 by heat shock and mitogen-activated kinases that recognize the same amino acid motif as S6 kinase II." J Biol Chem **267**(2): 794-803.

Laudanski, K., A. De and C. Miller-Graziano (2007). "Exogenous heat shock protein 27 uniquely blocks differentiation of monocytes to dendritic cells." Eur J Immunol **37**(10): 2812-2824.

Lawler, S., Y. Fleming, M. Goedert and P. Cohen (1998). "Synergistic activation of SAPK1/JNK1 by two MAP kinase kinases in vitro." Curr Biol **8**(25): 1387-1390.

Lee, J. C., J. T. Laydon, P. C. McDonnell, T. F. Gallagher, S. Kumar, D. Green, et al. (1994). "A protein kinase involved in the regulation of inflammatory cytokine biosynthesis." Nature **372**(6508): 739-746.

Leijh, P. C., T. L. van Zwet, M. N. ter Kuile and R. van Furth (1984). "Effect of thioglycolate on phagocytic and microbicidal activities of peritoneal macrophages." Infect Immun **46**(2): 448-452.

Lelj-Garolla, B. and A. G. Mauk (2005). "Self-association of a small heat shock protein." J Mol Biol **345**(3): 631-642.

Lelj-Garolla, B. and A. G. Mauk (2006). "Self-association and chaperone activity of Hsp27 are thermally activated." J Biol Chem **281**(12): 8169-8174.

Li, J., P. M. Farthing and M. H. Thornhill (2000). "Oral and skin keratinocytes are stimulated to secrete monocyte chemoattractant protein-1 by tumour necrosis factor-alpha and interferon-gamma." J Oral Pathol Med **29**(9): 438-444.

Li, M. L., J. Defren and G. Brewer (2013). "Hsp27 and F-Box Protein beta-TrCP Promote Degradation of mRNA Decay Factor AUF1." Mol Cell Biol **33**(11): 2315-2326.

Lim, S. C., H. Q. Duong, J. E. Choi, K. R. Parajuli, H. S. Kang and S. I. Han (2010). "Implication of PI3K-dependent HSP27 and p53 expression in mild heat shock-triggered switch of metabolic stress-induced necrosis to apoptosis in A549 cells." Int J Oncol **36**(2): 387-393.

Liu, T., O. E. Guevara, R. R. Warburton, N. S. Hill, M. Gaestel and U. S. Kayyali (2009). "Modulation of HSP27 alters hypoxia-induced endothelial permeability and related signaling pathways." J Cell Physiol **220**(3): 600-610.

Liu, T., E. Milia, R. R. Warburton, N. S. Hill, M. Gaestel and U. S. Kayyali (2012). "Anthrax lethal toxin disrupts the endothelial permeability barrier through blocking p38 signaling." J Cell Physiol **227**(4): 1438-1445.

Llanos, S., A. Cuadrado and M. Serrano (2009). "MSK2 inhibits p53 activity in the absence of stress." Sci Signal **2**(89): ra57.

Longaker, M. T., D. J. Whitby, N. S. Adzick, T. M. Crombleholme, J. C. Langer, B. W. Duncan, et al. (1990). "Studies in fetal wound healing, VI. Second and early third trimester fetal wounds demonstrate rapid collagen deposition without scar formation." J Pediatr Surg **25**(1): 63-68; discussion 68-69.

Longaker, M. T., D. J. Whitby, M. W. Ferguson, H. P. Lorenz, M. R. Harrison and N. S. Adzick (1994). "Adult skin wounds in the fetal environment heal with scar formation." Ann Surg **219**(1): 65-72.

Loots, M. A., E. N. Lamme, J. Zeegelaar, J. R. Mekkes, J. D. Bos and E. Middelkoop (1998). "Differences in cellular infiltrate and extracellular matrix of chronic diabetic and venous ulcers versus acute wounds." J Invest Dermatol **111**(5): 850-857.

Lum, J. J., R. J. DeBerardinis and C. B. Thompson (2005). "Autophagy in metazoans: cell survival in the land of plenty." Nat Rev Mol Cell Biol **6**(6): 439-448.

Luster, A. D. (1998). "Chemokines--chemotactic cytokines that mediate inflammation." N Engl J Med **338**(7): 436-445.

Manke, I. A., A. Nguyen, D. Lim, M. Q. Stewart, A. E. Elia and M. B. Yaffe (2005). "MAPKAP kinase-2 is a cell cycle checkpoint kinase that regulates the G2/M transition and S phase progression in response to UV irradiation." Mol Cell **17**(1): 37-48.

Marchese, F. P., A. Aubareda, C. Tudor, J. Saklatvala, A. R. Clark and J. L. Dean (2010). "MAPKAP kinase 2 blocks tristetraprolin-directed mRNA decay by inhibiting CAF1 deadenylase recruitment." J Biol Chem **285**(36): 27590-27600.

Martin, P. (1997). "Wound healing--aiming for perfect skin regeneration." Science **276**(5309): 75-81.

Martin, P., D. D'Souza, J. Martin, R. Grose, L. Cooper, R. Maki, et al. (2003). "Wound healing in the PU.1 null mouse--tissue repair is not dependent on inflammatory cells." Curr Biol **13**(13): 1122-1128.

Martinez, F. O., A. Sica, A. Mantovani and M. Locati (2008). "Macrophage activation and polarization." Front Biosci **13**: 453-461.

Mayor, A., F. Martinon, T. De Smedt, V. Petrilli and J. Tschopp (2007). "A crucial function of SGT1 and HSP90 in inflammasome activity links mammalian and plant innate immune responses." Nat Immunol **8**(5): 497-503.

McLaughlin, M. M., S. Kumar, P. C. McDonnell, S. Van Horn, J. C. Lee, G. P. Livi, et al. (1996). "Identification of mitogen-activated protein (MAP) kinase-activated protein kinase-3, a novel substrate of CSBP p38 MAP kinase." J Biol Chem **271**(14): 8488-8492.

McMullen, M. E., P. W. Bryant, C. C. Glembotski, P. A. Vincent and K. M. Pumiglia (2005). "Activation of p38 has opposing effects on the proliferation and migration of endothelial cells." J Biol Chem **280**(22): 20995-21003.

McNamee, J. P., P. V. Bellier, B. C. Kutzner and R. C. Wilkins (2005). "Effect of pro-inflammatory cytokines on spontaneous apoptosis in leukocyte sub-sets within a whole blood culture." Cytokine **31**(2): 161-167.

Mehlen, P., C. Kretz-Remy, X. Preville and A. P. Arrigo (1996). "Human hsp27, Drosophila hsp27 and human alphaB-crystallin expression-mediated increase in glutathione is essential for the protective activity of these proteins against TNFalpha-induced cell death." EMBO J **15**(11): 2695-2706.

Mehlen, P., A. Mehlen, D. Guillet, X. Preville and A. P. Arrigo (1995). "Tumor necrosis factor-alpha induces changes in the phosphorylation, cellular localization, and oligomerization of human hsp27, a stress protein that confers cellular resistance to this cytokine." J Cell Biochem **58**(2): 248-259.

Mehlen, P., K. Schulze-Osthoff and A. P. Arrigo (1996). "Small stress proteins as novel regulators of apoptosis. Heat shock protein 27 blocks Fas/APO-1- and staurosporine-induced cell death." J Biol Chem **271**(28): 16510-16514.

Meloche, S. and J. Pouyssegur (2007). "The ERK1/2 mitogen-activated protein kinase pathway as a master regulator of the G1- to S-phase transition." Oncogene **26**(22): 3227-3239.

Mertz, P. M., D. L. DeWitt, W. G. Stetler-Stevenson and L. M. Wahl (1994). "Interleukin 10 suppression of monocyte prostaglandin H synthase-2. Mechanism of inhibition of

prostaglandin-dependent matrix metalloproteinase production." J Biol Chem **269**(33): 21322-21329.
Meszaros, A. J., J. S. Reichner and J. E. Albina (2000). "Macrophage-induced neutrophil apoptosis." J Immunol **165**(1): 435-441.
Meylan, E., J. Tschopp and M. Karin (2006). "Intracellular pattern recognition receptors in the host response." Nature **442**(7098): 39-44.
Micheau, O. and J. Tschopp (2003). "Induction of TNF receptor I-mediated apoptosis via two sequential signaling complexes." Cell **114**(2): 181-190.
Miron, T., K. Vancompernolle, J. Vandekerckhove, M. Wilchek and B. Geiger (1991). "A 25-kD inhibitor of actin polymerization is a low molecular mass heat shock protein." J Cell Biol **114**(2): 255-261.
Miyamoto, T., N. Ogino, S. Yamamoto and O. Hayaishi (1976). "Purification of prostaglandin endoperoxide synthetase from bovine vesicular gland microsomes." J Biol Chem **251**(9): 2629-2636.
Mizukami, Y., K. Yoshioka, S. Morimoto and K. Yoshida (1997). "A novel mechanism of JNK1 activation. Nuclear translocation and activation of JNK1 during ischemia and reperfusion." J Biol Chem **272**(26): 16657-16662.
Montiel, M., L. Urso, E. P. de la Blanca, S. Marsigliante and E. Jimenez (2009). "Cisplatin reduces endothelial cell migration via regulation of type 2-matrix metalloproteinase activity." Cell Physiol Biochem **23**(4-6): 441-448.
Mosser, D. M. (2003). "The many faces of macrophage activation." J Leukoc Biol **73**(2): 209-212.
Mosser, D. M. and J. P. Edwards (2008). "Exploring the full spectrum of macrophage activation." Nat Rev Immunol **8**(12): 958-969.
Muruve, D. A., V. Petrilli, A. K. Zaiss, L. R. White, S. A. Clark, P. J. Ross, et al. (2008). "The inflammasome recognizes cytosolic microbial and host DNA and triggers an innate immune response." Nature **452**(7183): 103-107.
Mustoe, T. A., G. F. Pierce, C. Morishima and T. F. Deuel (1991). "Growth factor-induced acceleration of tissue repair through direct and inductive activities in a rabbit dermal ulcer model." J Clin Invest **87**(2): 694-703.
Nakahara, H., J. Song, M. Sugimoto, K. Hagihara, T. Kishimoto, K. Yoshizaki, et al. (2003). "Anti-interleukin-6 receptor antibody therapy reduces vascular endothelial growth factor production in rheumatoid arthritis." Arthritis Rheum **48**(6): 1521-1529.
Neckers, L. and P. Workman (2012). "Hsp90 molecular chaperone inhibitors: are we there yet?" Clin Cancer Res **18**(1): 64-76.
New, L., M. Zhao, Y. Li, W. W. Bassett, Y. Feng, S. Ludwig, et al. (1999). "Cloning and characterization of RLPK, a novel RSK-related protein kinase." J Biol Chem **274**(2): 1026-1032.
Nissen, N. N., P. J. Polverini, A. E. Koch, M. V. Volin, R. L. Gamelli and L. A. DiPietro (1998). "Vascular endothelial growth factor mediates angiogenic activity during the proliferative phase of wound healing." Am J Pathol **152**(6): 1445-1452.
Noli, C. and A. Miolo (2001). "The mast cell in wound healing." Vet Dermatol **12**(6): 303-313.
Nomi, N., K. Kimura and T. Nishida (2010). "Release of interleukins 6 and 8 induced by zymosan and mediated by MAP kinase and NF-kappaB signaling pathways in human corneal fibroblasts." Invest Ophthalmol Vis Sci **51**(6): 2955-2959.
Norgauer, J., T. Hildenbrand, M. Idzko, E. Panther, E. Bandemir, M. Hartmann, et al. (2002). "Elevated expression of extracellular matrix metalloproteinase inducer (CD147) and membrane-type matrix metalloproteinases in venous leg ulcers." Br J Dermatol **147**(6): 1180-1186.
Nurden, A. T., P. Nurden, M. Sanchez, I. Andia and E. Anitua (2008). "Platelets and wound healing." Front Biosci **13**: 3532-3548.
O'Neill, L. A. (2008). "The interleukin-1 receptor/Toll-like receptor superfamily: 10 years of progress." Immunol Rev **226**: 10-18.
Okada, T., H. Otani, Y. Wu, S. Kyoi, C. Enoki, H. Fujiwara, et al. (2005). "Role of F-actin organization in p38 MAP kinase-mediated apoptosis and necrosis in neonatal rat

cardiomyocytes subjected to simulated ischemia and reoxygenation." Am J Physiol Heart Circ Physiol **289**(6): H2310-2318.

Ordureau, A., H. Smith, M. Windheim, M. Peggie, E. Carrick, N. Morrice, et al. (2008). "The IRAK-catalysed activation of the E3 ligase function of Pellino isoforms induces the Lys63-linked polyubiquitination of IRAK1." Biochem J **409**(1): 43-52.

Otsuka, G., T. Kubo, J. Imanishi and Y. Hirasawa (1996). "Expression of heat-shock-proteins in the differentiation process of chondrocytes." Nihon Geka Hokan **65**(2): 39-48.

Ozinsky, A., D. M. Underhill, J. D. Fontenot, A. M. Hajjar, K. D. Smith, C. B. Wilson, et al. (2000). "The repertoire for pattern recognition of pathogens by the innate immune system is defined by cooperation between toll-like receptors." Proc Natl Acad Sci U S A **97**(25): 13766-13771.

Panasenko, O. O., M. V. Kim, S. B. Marston and N. B. Gusev (2003). "Interaction of the small heat shock protein with molecular mass 25 kDa (hsp25) with actin." Eur J Biochem **270**(5): 892-901.

Parcellier, A., M. Brunet, E. Schmitt, E. Col, C. Didelot, A. Hammann, et al. (2006). "HSP27 favors ubiquitination and proteasomal degradation of p27Kip1 and helps S-phase re-entry in stressed cells." FASEB J **20**(8): 1179-1181.

Park, K. J., R. B. Gaynor and Y. T. Kwak (2003). "Heat shock protein 27 association with the I kappa B kinase complex regulates tumor necrosis factor alpha-induced NF-kappa B activation." J Biol Chem **278**(37): 35272-35278.

Park, S. W., S. W. Chen, M. Kim, V. D. D'Agati and H. T. Lee (2009). "Human heat shock protein 27-overexpressing mice are protected against acute kidney injury after hepatic ischemia and reperfusion." Am J Physiol Renal Physiol **297**(4): F885-894.

Paul, C., F. Manero, S. Gonin, C. Kretz-Remy, S. Virot and A. P. Arrigo (2002). "Hsp27 as a negative regulator of cytochrome C release." Mol Cell Biol **22**(3): 816-834.

Paya, M., M. C. Terencio, M. L. Ferrandiz and M. J. Alcaraz (1996). "Involvement of secretory phospholipase A2 activity in the zymosan rat air pouch model of inflammation." Br J Pharmacol **117**(8): 1773-1779.

Pennica, D., G. E. Nedwin, J. S. Hayflick, P. H. Seeburg, R. Derynck, M. A. Palladino, et al. (1984). "Human tumour necrosis factor: precursor structure, expression and homology to lymphotoxin." Nature **312**(5996): 724-729.

Pettitt, S. J., Q. Liang, X. Y. Rairdan, J. L. Moran, H. M. Prosser, D. R. Beier, et al. (2009). "Agouti C57BL/6N embryonic stem cells for mouse genetic resources." Nat Methods **6**(7): 493-495.

Pierrat, B., J. S. Correia, J. L. Mary, M. Tomas-Zuber and W. Lesslauer (1998). "RSK-B, a novel ribosomal S6 kinase family member, is a CREB kinase under dominant control of p38alpha mitogen-activated protein kinase (p38alphaMAPK)." J Biol Chem **273**(45): 29661-29671.

Piotrowicz, R. S., E. Hickey and E. G. Levin (1998). "Heat shock protein 27 kDa expression and phosphorylation regulates endothelial cell migration." FASEB J **12**(14): 1481-1490.

Poltorak, A., X. He, I. Smirnova, M. Y. Liu, C. Van Huffel, X. Du, et al. (1998). "Defective LPS signaling in C3H/HeJ and C57BL/10ScCr mice: mutations in Tlr4 gene." Science **282**(5396): 2085-2088.

Raetz, C. R. and C. Whitfield (2002). "Lipopolysaccharide endotoxins." Annu Rev Biochem **71**: 635-700.

Raingeaud, J., S. Gupta, J. S. Rogers, M. Dickens, J. Han, R. J. Ulevitch, et al. (1995). "Pro-inflammatory cytokines and environmental stress cause p38 mitogen-activated protein kinase activation by dual phosphorylation on tyrosine and threonine." J Biol Chem **270**(13): 7420-7426.

Raman, M., W. Chen and M. H. Cobb (2007). "Differential regulation and properties of MAPKs." Oncogene **26**(22): 3100-3112.

Rao, T. S., J. L. Currie, A. F. Shaffer and P. C. Isakson (1994). "In vivo characterization of zymosan-induced mouse peritoneal inflammation." J Pharmacol Exp Ther **269**(3): 917-925.

Rappolee, D. A., D. Mark, M. J. Banda and Z. Werb (1988). "Wound macrophages express TGF-alpha and other growth factors in vivo: analysis by mRNA phenotyping." Science **241**(4866): 708-712.

Ridley, S. H., J. L. Dean, S. J. Sarsfield, M. Brook, A. R. Clark and J. Saklatvala (1998). "A p38 MAP kinase inhibitor regulates stability of interleukin-1-induced cyclooxygenase-2 mRNA." FEBS Lett **439**(1-2): 75-80.

Rietschel, E. T., T. Kirikae, F. U. Schade, U. Mamat, G. Schmidt, H. Loppnow, et al. (1994). "Bacterial endotoxin: molecular relationships of structure to activity and function." FASEB J **8**(2): 217-225.

Rincon, M. (2012). "Interleukin-6: from an inflammatory marker to a target for inflammatory diseases." Trends Immunol **33**(11): 571-577.

Rogalla, T., M. Ehrnsperger, X. Preville, A. Kotlyarov, G. Lutsch, C. Ducasse, et al. (1999). "Regulation of Hsp27 oligomerization, chaperone function, and protective activity against oxidative stress/tumor necrosis factor alpha by phosphorylation." J Biol Chem **274**(27): 18947-18956.

Ronkina, N., A. Kotlyarov and M. Gaestel (2008). "MK2 and MK3--a pair of isoenzymes?" Front Biosci **13**: 5511-5521.

Rossor, A. M., B. Kalmar, L. Greensmith and M. M. Reilly (2012). "The distal hereditary motor neuropathies." J Neurol Neurosurg Psychiatry **83**(1): 6-14.

Rouse, J., P. Cohen, S. Trigon, M. Morange, A. Alonso-Llamazares, D. Zamanillo, et al. (1994). "A novel kinase cascade triggered by stress and heat shock that stimulates MAPKAP kinase-2 and phosphorylation of the small heat shock proteins." Cell **78**(6): 1027-1037.

Rousseau, S., F. Houle, J. Landry and J. Huot (1997). "p38 MAP kinase activation by vascular endothelial growth factor mediates actin reorganization and cell migration in human endothelial cells." Oncogene **15**(18): 2169-2177.

Rutkowski, D. T. and R. J. Kaufman (2004). "A trip to the ER: coping with stress." Trends Cell Biol **14**(1): 20-28.

Sabapathy, K., K. Hochedlinger, S. Y. Nam, A. Bauer, M. Karin and E. F. Wagner (2004). "Distinct roles for JNK1 and JNK2 in regulating JNK activity and c-Jun-dependent cell proliferation." Mol Cell **15**(5): 713-725.

Saklatvala, J., P. Kaur and F. Guesdon (1991). "Phosphorylation of the small heat-shock protein is regulated by interleukin 1, tumour necrosis factor, growth factors, bradykinin and ATP." Biochem J **277 (Pt 3)**: 635-642.

Sanguedolce, M. V., C. Capo, P. Bongrand and J. L. Mege (1992). "Zymosan-stimulated tumor necrosis factor-alpha production by human monocytes. Down-modulation by phorbol ester." J Immunol **148**(7): 2229-2236.

Saraiva, M. and A. O'Garra (2010). "The regulation of IL-10 production by immune cells." Nat Rev Immunol **10**(3): 170-181.

Sato, M., H. Sano, D. Iwaki, K. Kudo, M. Konishi, H. Takahashi, et al. (2003). "Direct binding of Toll-like receptor 2 to zymosan, and zymosan-induced NF-kappa B activation and TNF-alpha secretion are down-regulated by lung collectin surfactant protein A." J Immunol **171**(1): 417-425.

Savill, J. S., A. H. Wyllie, J. E. Henson, M. J. Walport, P. M. Henson and C. Haslett (1989). "Macrophage phagocytosis of aging neutrophils in inflammation. Programmed cell death in the neutrophil leads to its recognition by macrophages." J Clin Invest **83**(3): 865-875.

Schmidt-Supprian, M. and K. Rajewsky (2007). "Vagaries of conditional gene targeting." Nat Immunol **8**(7): 665-668.

Schneider-Brachert, W., V. Tchikov, J. Neumeyer, M. Jakob, S. Winoto-Morbach, J. Held-Feindt, et al. (2004). "Compartmentalization of TNF receptor 1 signaling: internalized TNF receptosomes as death signaling vesicles." Immunity **21**(3): 415-428.

Schonfelder, U., M. Abel, C. Wiegand, D. Klemm, P. Elsner and U. C. Hipler (2005). "Influence of selected wound dressings on PMN elastase in chronic wound fluid and their antioxidative potential in vitro." Biomaterials **26**(33): 6664-6673.

Schramm, R., Q. Liu and H. Thorlacius (2000). "Expression and function of MIP-2 are reduced by dexamethasone treatment in vivo." Br J Pharmacol **131**(2): 328-334.

Schroder, J. M., M. Sticherling, H. H. Henneicke, W. C. Preissner and E. Christophers (1990). "IL-1 alpha or tumor necrosis factor-alpha stimulate release of three NAP-1/IL-8-related neutrophil chemotactic proteins in human dermal fibroblasts." J Immunol **144**(6): 2223-2232.

Sedgwick, A. D., Y. M. Sin, J. C. Edwards and D. A. Willoughby (1983). "Increased inflammatory reactivity in newly formed lining tissue." J Pathol **141**(4): 483-495.

Semprini, S., T. J. Troup, N. Kotelevtseva, K. King, J. R. Davis, L. J. Mullins, et al. (2007). "Cryptic loxP sites in mammalian genomes: genome-wide distribution and relevance for the efficiency of BAC/PAC recombineering techniques." Nucleic Acids Res **35**(5): 1402-1410.

Seth, A. K., M. De la Garza, R. C. Fang, S. J. Hong and R. D. Galiano (2013). "Excisional wound healing is delayed in a murine model of chronic kidney disease." PLoS One **8**(3): e59979.

Sharma, K., R. M. Vabulas, B. Macek, S. Pinkert, J. Cox, M. Mann, et al. (2012). "Quantitative proteomics reveals that Hsp90 inhibition preferentially targets kinases and the DNA damage response." Mol Cell Proteomics **11**(3): M111 014654.

Shaulian, E. and M. Karin (2001). "AP-1 in cell proliferation and survival." Oncogene **20**(19): 2390-2400.

Shaw, T. J. and P. Martin (2009). "Wound repair at a glance." J Cell Sci **122**(Pt 18): 3209-3213.

Shimura, H., Y. Miura-Shimura and K. S. Kosik (2004). "Binding of tau to heat shock protein 27 leads to decreased concentration of hyperphosphorylated tau and enhanced cell survival." J Biol Chem **279**(17): 17957-17962.

Shiota, M., J. L. Bishop, K. M. Nip, A. Zardan, A. Takeuchi, T. Cordonnier, et al. (2013). "Hsp27 regulates epithelial mesenchymal transition, metastasis, and circulating tumor cells in prostate cancer." Cancer Res **73**(10): 3109-3119.

Singer, A. J. and R. A. Clark (1999). "Cutaneous wound healing." N Engl J Med **341**(10): 738-746.

Skarnes, W. C., B. Rosen, A. P. West, M. Koutsourakis, W. Bushell, V. Iyer, et al. (2011). "A conditional knockout resource for the genome-wide study of mouse gene function." Nature **474**(7351): 337-342.

Smith, R. C., K. M. Rosen, R. Pola and J. Magrane (2005). "Stress proteins in Alzheimer's disease." Int J Hyperthermia **21**(5): 421-431.

Smith, W. L., D. L. DeWitt and R. M. Garavito (2000). "Cyclooxygenases: structural, cellular, and molecular biology." Annu Rev Biochem **69**: 145-182.

Snyder, R. J. (2005). "Treatment of nonhealing ulcers with allografts." Clin Dermatol **23**(4): 388-395.

Song, H., S. P. Ethier, M. L. Dziubinski and J. Lin (2004). "Stat3 modulates heat shock 27kDa protein expression in breast epithelial cells." Biochem Biophys Res Commun **314**(1): 143-150.

Song, T. F., Z. F. Zhang, L. Liu, T. Yang, J. Jiang and P. Li (2009). "Small interfering RNA-mediated silencing of heat shock protein 27 (HSP27) Increases chemosensitivity to paclitaxel by increasing production of reactive oxygen species in human ovarian cancer cells (HO8910)." J Int Med Res **37**(5): 1375-1388.

Spitalny, G. L. (1981). "Dissociation of bactericidal activity from other functions of activated macrophages in exudates induced by thioglycolate medium." Infect Immun **34**(1): 274-284.

Stege, G. J., K. Renkawek, P. S. Overkamp, P. Verschuure, A. F. van Rijk, A. Reijnen-Aalbers, et al. (1999). "The molecular chaperone alphaB-crystallin enhances amyloid beta neurotoxicity." Biochem Biophys Res Commun **262**(1): 152-156.

Stein, M., S. Keshav, N. Harris and S. Gordon (1992). "Interleukin 4 potently enhances murine macrophage mannose receptor activity: a marker of alternative immunologic macrophage activation." J Exp Med **176**(1): 287-292.

Steinmeyer, J. (2000). "Pharmacological basis for the therapy of pain and inflammation with nonsteroidal anti-inflammatory drugs." Arthritis Res **2**(5): 379-385.

Stetler, R. A., Y. Gao, L. Zhang, Z. Weng, F. Zhang, X. Hu, et al. (2012). "Phosphorylation of HSP27 by protein kinase D is essential for mediating neuroprotection against ischemic neuronal injury." J Neurosci **32**(8): 2667-2682.

Stoecklin, G., T. Stubbs, N. Kedersha, S. Wax, W. F. Rigby, T. K. Blackwell, et al. (2004). "MK2-induced tristetraprolin:14-3-3 complexes prevent stress granule association and ARE-mRNA decay." EMBO J **23**(6): 1313-1324.

Stokoe, D., K. Engel, D. G. Campbell, P. Cohen and M. Gaestel (1992). "Identification of MAPKAP kinase 2 as a major enzyme responsible for the phosphorylation of the small mammalian heat shock proteins." FEBS Lett **313**(3): 307-313.

Su, X., L. Ao, N. Zou, Y. Song, X. Yang, G. Y. Cai, et al. (2008). "Post-transcriptional regulation of TNF-induced expression of ICAM-1 and IL-8 in human lung microvascular endothelial cells:

an obligatory role for the p38 MAPK-MK2 pathway dissociated with HSP27." Biochim Biophys Acta **1783**(9): 1623-1631.

Su, Y., S. K. Raghuwanshi, Y. Yu, L. B. Nanney, R. M. Richardson and A. Richmond (2005). "Altered CXCR2 signaling in beta-arrestin-2-deficient mouse models." J Immunol **175**(8): 5396-5402.

Sur, R., P. A. Lyte and M. D. Southall (2008). "Hsp27 regulates pro-inflammatory mediator release in keratinocytes by modulating NF-kappaB signaling." J Invest Dermatol **128**(5): 1116-1122.

Swift, M. E., A. L. Burns, K. L. Gray and L. A. DiPietro (2001). "Age-related alterations in the inflammatory response to dermal injury." J Invest Dermatol **117**(5): 1027-1035.

Terkeltaub, R., S. Baird, P. Sears, R. Santiago and W. Boisvert (1998). "The murine homolog of the interleukin-8 receptor CXCR-2 is essential for the occurrence of neutrophilic inflammation in the air pouch model of acute urate crystal-induced gouty synovitis." Arthritis Rheum **41**(5): 900-909.

Tessier, P. A., P. H. Naccache, I. Clark-Lewis, R. P. Gladue, K. S. Neote and S. R. McColl (1997). "Chemokine networks in vivo: involvement of C-X-C and C-C chemokines in neutrophil extravasation in vivo in response to TNF-alpha." J Immunol **159**(7): 3595-3602.

Tessier, P. A., P. H. Naccache, K. R. Diener, R. P. Gladue, K. S. Neote, I. Clark-Lewis, et al. (1998). "Induction of acute inflammation in vivo by staphylococcal superantigens. II. Critical role for chemokines, ICAM-1, and TNF-alpha." J Immunol **161**(3): 1204-1211.

Thornton, T. M. and M. Rincon (2009). "Non-classical p38 map kinase functions: cell cycle checkpoints and survival." Int J Biol Sci **5**(1): 44-51.

Thuraisingam, T., Y. Z. Xu, K. Eadie, M. Heravi, M. C. Guiot, R. Greemberg, et al. (2010). "MAPKAPK-2 signaling is critical for cutaneous wound healing." J Invest Dermatol **130**(1): 278-286.

Thyagarajan, B., M. J. Guimaraes, A. C. Groth and M. P. Calos (2000). "Mammalian genomes contain active recombinase recognition sites." Gene **244**(1-2): 47-54.

Tomas-Zuber, M., J. L. Mary, F. Lamour, D. Bur and W. Lesslauer (2001). "C-terminal elements control location, activation threshold, and p38 docking of ribosomal S6 kinase B (RSKB)." J Biol Chem **276**(8): 5892-5899.

Tournier, C., P. Hess, D. D. Yang, J. Xu, T. K. Turner, A. Nimnual, et al. (2000). "Requirement of JNK for stress-induced activation of the cytochrome c-mediated death pathway." Science **288**(5467): 870-874.

Tudor, C., F. P. Marchese, E. Hitti, A. Aubareda, L. Rawlinson, M. Gaestel, et al. (2009). "The p38 MAPK pathway inhibits tristetraprolin-directed decay of interleukin-10 and pro-inflammatory mediator mRNAs in murine macrophages." FEBS Lett **583**(12): 1933-1938.

Upchurch, K. S. and J. Kay (2012). "Evolution of treatment for rheumatoid arthritis." Rheumatology (Oxford) **51 Suppl 6**: vi28-36.

Vanmuylder, N., L. Evrard and N. Dourov (1997). "Strong expression of heat shock proteins in growth plate cartilage, an immunohistochemical study of HSP28, HSP70 and HSP110." Anat Embryol (Berl) **195**(4): 359-362.

Vedam, K., Y. Nishijima, L. J. Druhan, M. Khan, N. I. Moldovan, J. L. Zweier, et al. (2010). "Role of heat shock factor-1 activation in the doxorubicin-induced heart failure in mice." Am J Physiol Heart Circ Physiol **298**(6): H1832-1841.

Vermeulen, L., G. De Wilde, P. Van Damme, W. Vanden Berghe and G. Haegeman (2003). "Transcriptional activation of the NF-kappaB p65 subunit by mitogen- and stress-activated protein kinase-1 (MSK1)." EMBO J **22**(6): 1313-1324.

Vorstenbosch, J., C. Gallant-Behm, A. Trzeciak, S. Roy, T. Mustoe and A. Philip (2013). "Transgenic mice overexpressing CD109 in the epidermis display decreased inflammation and granulation tissue and improved collagen architecture during wound healing." Wound Repair Regen **21**(2): 235-246.

Wakamatsu, T., Y. Nakahashi, D. Hachimine, T. Seki and K. Okazaki (2007). "The combination of glycyrrhizin and lamivudine can reverse the cisplatin resistance in hepatocellular carcinoma cells through inhibition of multidrug resistance-associated proteins." Int J Oncol **31**(6): 1465-1472.

Waterston, R. H., K. Lindblad-Toh, E. Birney, J. Rogers, J. F. Abril, P. Agarwal, et al. (2002). "Initial sequencing and comparative analysis of the mouse genome." Nature **420**(6915): 520-562.

Watts, G. T., H. C. Grillo and J. Gross (1958). "Studies in Wound Healing: II. The Role of Granulation Tissue in Contraction." Ann Surg **148**(2): 153-160.

Weber, A., P. Wasiliew and M. Kracht (2010). "Interleukin-1 (IL-1) pathway." Sci Signal **3**(105): cm1.

Weber, H. O., R. L. Ludwig, D. Morrison, A. Kotlyarov, M. Gaestel and K. H. Vousden (2005). "HDM2 phosphorylation by MAPKAP kinase 2." Oncogene **24**(12): 1965-1972.

Weiss, S. J. (1989). "Tissue destruction by neutrophils." N Engl J Med **320**(6): 365-376.

Welch, W. J. and J. P. Suhan (1986). "Cellular and biochemical events in mammalian cells during and after recovery from physiological stress." J Cell Biol **103**(5): 2035-2052.

Werner, S. and R. Grose (2003). "Regulation of wound healing by growth factors and cytokines." Physiol Rev **83**(3): 835-870.

Wery-Zennaro, S., J. L. Zugaza, M. Letourneur, J. Bertoglio and J. Pierre (2000). "IL-4 regulation of IL-6 production involves Rac/Cdc42- and p38 MAPK-dependent pathways in keratinocytes." Oncogene **19**(12): 1596-1604.

Whitmarsh, A. J. and R. J. Davis (1996). "Transcription factor AP-1 regulation by mitogen-activated protein kinase signal transduction pathways." J Mol Med (Berl) **74**(10): 589-607.

Wick, G. (2006). "The heat is on: heat-shock proteins and atherosclerosis." Circulation **114**(9): 870-872.

Wiens, G. D. and G. W. Glenney (2011). "Origin and evolution of TNF and TNF receptor superfamilies." Dev Comp Immunol **35**(12): 1324-1335.

Wierenga, A. T., I. Vogelzang, B. J. Eggen and E. Vellenga (2003). "Erythropoietin-induced serine 727 phosphorylation of STAT3 in erythroid cells is mediated by a MEK-, ERK-, and MSK1-dependent pathway." Exp Hematol **31**(5): 398-405.

Williams, C. S., M. Mann and R. N. DuBois (1999). "The role of cyclooxygenases in inflammation, cancer, and development." Oncogene **18**(55): 7908-7916.

Wlaschek, M. and K. Scharffetter-Kochanek (2005). "Oxidative stress in chronic venous leg ulcers." Wound Repair Regen **13**(5): 452-461.

Wolpe, S. D., B. Sherry, D. Juers, G. Davatelis, R. W. Yurt and A. Cerami (1989). "Identification and characterization of macrophage inflammatory protein 2." Proc Natl Acad Sci U S A **86**(2): 612-616.

Wu, C. J., D. B. Conze, X. Li, S. X. Ying, J. A. Hanover and J. D. Ashwell (2005). "TNF-alpha induced c-IAP1/TRAF2 complex translocation to a Ubc6-containing compartment and TRAF2 ubiquitination." EMBO J **24**(10): 1886-1898.

Wu, Y., J. Liu, Z. Zhang, H. Huang, J. Shen, S. Zhang, et al. (2009). "HSP27 regulates IL-1 stimulated IKK activation through interacting with TRAF6 and affecting its ubiquitination." Cell Signal **21**(1): 143-150.

Xia, Y., Y. Liu, J. Wan, M. Wang, P. Rocchi, F. Qu, et al. (2009). "Novel triazole ribonucleoside down-regulates heat shock protein 27 and induces potent anticancer activity on drug-resistant pancreatic cancer." J Med Chem **52**(19): 6083-6096.

Yoshikawa, M., N. Ono, H. Yodono, T. Ichida and H. Nakamura (2008). "Phase II study of hepatic arterial infusion of a fine-powder formulation of cisplatin for advanced hepatocellular carcinoma." Hepatol Res **38**(5): 474-483.

Yoshimura, T. and M. Takahashi (2007). "IFN-gamma-mediated survival enables human neutrophils to produce MCP-1/CCL2 in response to activation by TLR ligands." J Immunol **179**(3): 1942-1949.

Young, J. C. (2010). "Mechanisms of the Hsp70 chaperone system." Biochem Cell Biol **88**(2): 291-300.

Young, S. H., J. Ye, D. G. Frazer, X. Shi and V. Castranova (2001). "Molecular mechanism of tumor necrosis factor-alpha production in 1-->3-beta-glucan (zymosan)-activated macrophages." J Biol Chem **276**(23): 20781-20787.

Zhao, W., M. Liu and K. L. Kirkwood (2008). "p38alpha stabilizes interleukin-6 mRNA via multiple AU-rich elements." J Biol Chem **283**(4): 1778-1785.

Zhong, H., R. E. Voll and S. Ghosh (1998). "Phosphorylation of NF-kappa B p65 by PKA stimulates transcriptional activity by promoting a novel bivalent interaction with the coactivator CBP/p300." Mol Cell **1**(5): 661-671.

Zurita, E., M. Chagoyen, M. Cantero, R. Alonso, A. Gonzalez-Neira, A. Lopez-Jimenez, et al. (2011). "Genetic polymorphisms among C57BL/6 mouse inbred strains." Transgenic Res **20**(3): 481-489.